2019 | Faculty of Medicine and Life Sciences

UHASSELT
KNOWLEDGE IN ACTION

Maastricht University

Doctoral dissertation submitted to obtain the degree of
Doctor of Biomedical Sciences, to be defended by

Niels Belmans

DOCTORAL DISSERTATION

Biological effects of ionizing radiation in medical imaging: a prospective study in children and adults following dental cone-beam computed tomography

BIOMED
BIOMEDICAL
RESEARCH INSTITUTE
UHASSELT

Promoter: Prof. Dr Ivo Lambrichts | UHasselt

Co-promoters: Prof. Dr Stéphane Lucas | Université de Namur
Dr Marjan Moreels | SCK-CEN

D/2019/2451/55

STUDIECENTRUM VOOR KERNENERGIE
CENTRE D'ETUDE DE L'ENERGIE NUCLEAIRE

Table of contents

Table of tables

Table of figures

List of abbreviations

2D	Two-dimensional
3D	Three-dimensional
4-HNE	trans-4-hydroxy-2-nonenal
53BP1	p53-binding protein 1
7-AAD	7-aminoactinomycin D
8-oxo-dG	7,8-dihydro-8-oxo-2'-deoxyguanosine
α	Alpha radiation
β	Beta radiation
γ	Gamma radiation
γH2AX	Phosphorylated histone 2AX on Serine 139
ω_R	Radiation weighting factor
ω_T	Tissue-weighting factor
AGEs	Advanced glycation end products
ALARA	As-low-as-reasonable-achievable
ANOVA	Analysis of variance
ATM	Ataxia telangiectasia mutated
ATR	Ataxia telangiectasia and Rad3-related protein
BER	Base excision repair
BM	Buccal mucosa
BMCs	Buccal mucosa cells
BRCA1	Breast cancer early onset 1
BRCT	Breast cancer 1 C-terminal
BrdU	5-bromo-2'-deoxyuridine
BuBu	Buccal buffer
CAT	Catalase
CBCT	Cone-beam computed tomography
CDK	Cyclin-dependent kinase
Chk	Checkpoint kinase
CT	Computed tomography
$CTDI_{vol}$	Volume computed tomography dose index
CVD	Cardiovascular disease
DAPI	4'-6-diamidino-2-phenylindole
DDR	DNA damage response
DF	Degrees of freedom
DFSCs	Dental follicle stem cells
DIMITRA	Dentomaxillofacial Paediatric Imaging: An Investigation Towards Low Dose Radiation Induced Risks
DLP	Dose-length product
DNA	Deoxyribonucleic acid
DNA-PK	DNA-dependent protein kinase
DPSCs	Dental pulp stem cells
DSBs	Double strand breaks
ED	Effective dose
ELISA	Enzyme-linked immunosorbent assay
ESR	Election spin resonance
FOV	Field of view
FRAP	Ferric reducing antioxidant power
FWO	Fonds Wetenschappelijk Onderzoek Vlaanderen
GSH	Reduced glutathione
GSH-Px	Glutathione peroxidase
GSSG	Glutathione disulphide
Gy	Gray
H_2O_2	Hydrogen peroxide
HLEG	European High-Level Expert Group on European Low Dose Risk Research
HPLC	High-performance liquid chromatography
HR	Homologous recombination

ICRP	International Commission on Radiological Protection
IGF	Insulin-like growth factor
IGFBP	Insulin-like growth factor binding protein
IL	Interleukin
IR	Ionizing radiation
IRIF	Ionizing radiation-induced foci
kV	Tube voltage
LC-MS	Liquid chromatography tandem mass spectrometry
LNT	Linear-no-threshold
mAs	Tube current-exposure time product
MC	Monte Carlo
MDA	Malonaldehyde
MDC1	Mediator of the DNA damage checkpoint 1
miRNA	Micro-RNA
MMR	Mismatch repair
MN	Micronucleus
MRN	Mre11/Rad50/NBs1 complex
MSCs	Mesenchymal stem cells
NER	Nucleotide excision repair
NF-κβ	Nuclear factor κβ
NHEJ	Non-homologous end-joining
O_2^-	Superoxide anion
OECD	Organisation for Economic Cooperation and Development
$OH^•$	Hydroxyl radical
OPERRA	Open Project for European Radiation Research Area
oxLDL	Oxidized low-density lipoproteins
PBS	Phosphate-buffered saline
PCR	Polymerase chain reaction
PDLSCs	Periodontal ligament stem cells
PFA	Paraformaldehyde
PIG	Pre-immunized goat serum
PIKK	Phosphatidylinositol 3-kinase like kinase
qPCR	Real-time polymerase chain reaction
REID	Risk of exposure-induced death
ROS	Reactive oxygen species
RT	Room temperature
SASP	Senescence-associated secretory phenotype
SCAPs	Stem cells from the apical papilla
SCK•CEN	Belgian Nuclear Research Centre
SEM	Standard error of the mean
SF	Saccomanno's fixative
SHEDs	Stem cells from human exfoliated deciduous teeth
SI	International System of the Units
SOD	Superoxide dismutase
SSBs	Single strand breaks
Sv	Sievert
TGFβ	Transforming growth factor β

Chapter 1:

Introduction

1.1 Ionizing radiation

1.1.1 What is ionizing radiation?

On earth people are continuously exposed to ionizing radiation (IR) from natural and/or man-made sources. IR can be defined as electromagnetic waves or particles that have enough energy to eject electrons from their orbit in an atom. This ejection causes the atom to become ionized, hence 'ionizing radiation'.[1, 2] IR originates from natural processes and from man-made sources. In nature, three main types of IR can be identified: alpha (α), beta (β) and gamma (γ) radiation. They occur naturally when unstable nuclei (e.g. cobalt-60) undergo spontaneous radioactive decay. During radioactive decay, unstable nuclei will emit energy in the form of IR, i.e. electromagnetic particles (α and/or β) or waves (γ), in order to become energetically more stable.[3] X-rays are the most common form of man-made IR. They are mostly identical to γ-radiation but their origin is different: γ-radiation comes from the natural process of radioactive decay, whereas X-rays are produced by man-made X-ray generators. Man-made IR sources include 1) the use of IR in medicine, such as X-rays in diagnostics and X-rays, protons and carbon ions in radiotherapy treatment, and nuclear medicine procedures using radioactive isotopes, 2) radiation exposure from the nuclear fuel cycle, such as uranium, which decays by emitting α, β, and γ radiation, and 3) exposure to radioactive fallout from nuclear weapons/accidents, such as the atomic bombs in Hiroshima and Nagasaki (1945) and the nuclear reactor accidents in Chernobyl (1986) and Fukushima (2011).[4]

α particles are subatomic particles consisting of two protons and two neutrons, which is in fact a helium core. They are relatively heavy, positively charged and energy-rich particles. β particles can be either negatively charged electrons or positively charged positrons. Their energy is intermediate between α particles and γ-rays/X-rays. γ-rays and X-rays are massless, electrically neutral, packets of energy, also known as photons.[2] Finally, besides the main types of IR discussed here, other types of natural and man-made IR exist (e.g. neutrons and accelerated ions).[5, 6]

1.1.2 Radiation doses and units

IR is ubiquitous and can have a major impact on human health. Therefore, it is important to know which energy or which radiation dose is absorbed by the human body and its organs. Furthermore, in order to study radiation-induced health effects, it is important to know the excessive risk associated with a certain radiation dose. To this end, several units are used in the International System of

Units (SI) to express radiation doses: the absorbed dose, the equivalent dose and the effective dose. Besides these three widely used dose units, others are used, which are related to specific fields. In medical diagnostics for example, the volume computed tomography dose index ($CTDI_{vol}$) and the dose-length product (DLP) are used alongside the previously mentioned ones (Table 1.1).[7-9]

The absorbed dose represents the amount of radiation energy that is absorbed per unit of mass of a substance. The SI unit is Gray (Gy). The *absorbed dose* does not take into account the radiation type nor its biological effect on tissues and organs.[10] The *equivalent dose* takes into account the radiation type and its effectiveness. It is calculated as the absorbed dose multiplied by a *radiation weighting factor* (ω_R), which is an estimate of the effectiveness per dose unit of a given radiation type compared to a standard (Table 1.2). The SI unit is Sievert (Sv).[7, 8] The *effective dose* is defined as the weighted sum of all tissue and organ equivalent doses multiplied by their respective *tissue-weighting factor* (ω_T), which is a relative measure of the risk of stochastic effects that could result from radiation exposure of a specific tissue (Table 1.3). It represents the health risk, i.e. the probability of carcinogenesis and/or genotoxic effects of IR. The SI unit is Sv.[8] Both ω_R and ω_T are recommended by the International Commission on Radiological Protection (ICRP).[10]

Table 1.1. Overview of different radiation dose units.[11]

Radiation dose	Unit	Symbol	Calculation	What does it mean?
Absorbed dose	Gray (Gy) (J•kg-1)	D	$D = \frac{\bar{\varepsilon}}{m_T}$	Represents the amount of radiation energy that is absorbed per unit of mass of a substance.
Equivalent dose	Sievert (Sv) (J•kg-1)	H_T	$H_T = \sum_R \omega_R D_{T,R}$	Takes into account the type of radiation as well as its effectiveness. When exposed to multiple radiation types, the equivalent doses of each radiation type must be calculated and then summated. [7, 8]
Effective dose	Sievert (Sv) (J•kg-1)	E	$E = \sum_T \omega_T H_T + \omega_{rem} H_{rem}$	Takes into account the equivalent doses in all specified tissues and organs of the body, which is multiplied by a tissue-specific weighting factor. Represents the health risk, i.e. the probability of cancer induction and/or genetic effects.[8]
Volume computed tomography dose index	Gray (Gy)	$CTDI_{vol}$	((1/3) x $radiation_{center}$ + (2/3) x $radiation_{periphery}$)/pitch	Quantifies the relative intensity of the radiation that is delivered to the patient during a computed tomography examination.[9]
Dose-length product	Gray•centimeter (Gy•cm)	DLP	$CTDI_{vol}$ x scan length	Used to calculate the total absorbed dose of radiation a patient is exposed to in a computed tomography examination and is therefore directly related to the stochastic risk.[9] Note: DLP is not equal to the effective dose.

$\bar{\varepsilon}$ = mean energy; m_T = mass of volume of interest; $D_{T,R}$ = D in a target tissue (T) due to radiation type 'R'; ω_R = radiation weighting factor; ω_T = tissue weighting factor; rem = remainder tissues

Table 1.2. ICRP recommended radiation weighting factors[10]	
Radiation type	ω_R*
Photons (X-rays, gamma rays)	1
Electrons and muons	1
Protons and charged ions	2
α particles, fission fragments, heavy ions	20
Neutrons	A continuous function of neutron energy
*:ω_R = radiation weighting factor ICRP = International Commission on Radiological Protection	

Table 1.3. ICRP recommended tissue weighting factors[10]		
Target organ	ω_T*	$\sum_T \omega_T$
Red bone-marrow, colon, lung, stomach, breast, remainder tissues**	0.12	0.72
Gonads	0.08	0.08
Bladder, oesophagus, liver, thyroid	0.04	0.16
Bone surface, brain, salivary glands, skin	0.01	0.04
Total		1.00
*:ω_T = tissue weighting factor; **: Remainder tissues include adrenals, extra-thoracic region, gallbladder, heart, kidneys, lymphatic nodes, muscles, oral mucosa, pancreas, prostate, small intestine, spleen, thymus, uterus/cervix. ICRP = International Commission on Radiological Protection		

1.2 The use of X-rays in medical diagnostics

1.2.1 Introduction to medical radiation exposure

The discovery of X-rays by Sir Wilhelm Conrad Roentgen in 1895 led to a revolution in the field of medicine. Soon after its discovery, X-ray machines were built that made it possible to study and/or treat internal structures of the body, without the need for dissection. Therefore, IR was increasingly used in medicine, leading to the medical fields of radiology and radiotherapy, and today IR is an indispensable tool for both medical diagnostics and therapy.[12] For most of the 20th century, radiography was limited to two-dimensional radiographs. This changed in 1972 with the introduction of computed tomography (CT) by Hounsfield. The evolutionary CT allowed for three-dimensional (3D) imaging, which led to more accurate diagnostics and new treatment strategies.[13] The introduction of CT further increased the use of IR in medical diagnostics and treatment.

The use of IR in medical diagnostics (e.g. CT and two-dimensional radiography) has increased globally from 280 per 1000 capita in 1988 to 488 per 1000 capita in 2008, an average increase of 74%. This remarkable increase in the amount of examinations using IR coincides with an increase in the global average annual effective dose (contributed by medical diagnostics) per caput. In 1988, the average effective dose per caput was 0.35 mSv, whereas in 2008, the average effective dose per caput was 0.62 mSv. An increase of 77% in IR exposure due to medical applications (excluding radiotherapy). Currently, medical applications of IR account for about 14% of the total annual exposure worldwide, which makes medical applications the largest man-made source of IR exposure to the general population.[12, 14] Data available from the European Commission show that in the 36 countries from which data are collected, radiography is by far the most frequently used in the clinic, followed by CT, fluoroscopy, and finally interventional radiology (Figure 1.1). Despite the high frequency of radiographs taken, the radiation burden due to CT is the highest in almost all countries of the European Union. It is estimated that CT examinations account for 55% of the annual effective dose in Europe. Radiography examinations account for 23% of the annual effective dose, followed by fluoroscopy (13%) and interventional radiology (9%).[15] On average, the radiation doses used in CT range from 15 mSv to 30 mSv, in adults and neonates respectively.[16] In radiography, the radiation doses range from 0.001 mSv to 0.1 mSv. In fluoroscopy examinations, the radiation doses vary between 0.4 mSv and 5 mSv.[17] Next, in interventional radiology, the cumulative air kerma ranges from 4 mGy to 3230 mGy at the patient entrance reference point.[18] These data explain why the average effective radiation dose due to CT examinations is much higher than that of radiographs, fluoroscopy and interventional radiology.[19]

In the following paragraphs, the focus will be on the use and potential health risks of two-dimensional radiography and CT, the two most frequently used medical imaging techniques with X-rays, as well as on the use and potential health risks of cone-beam computed tomography (CBCT), a relatively new CT-based imaging technique.

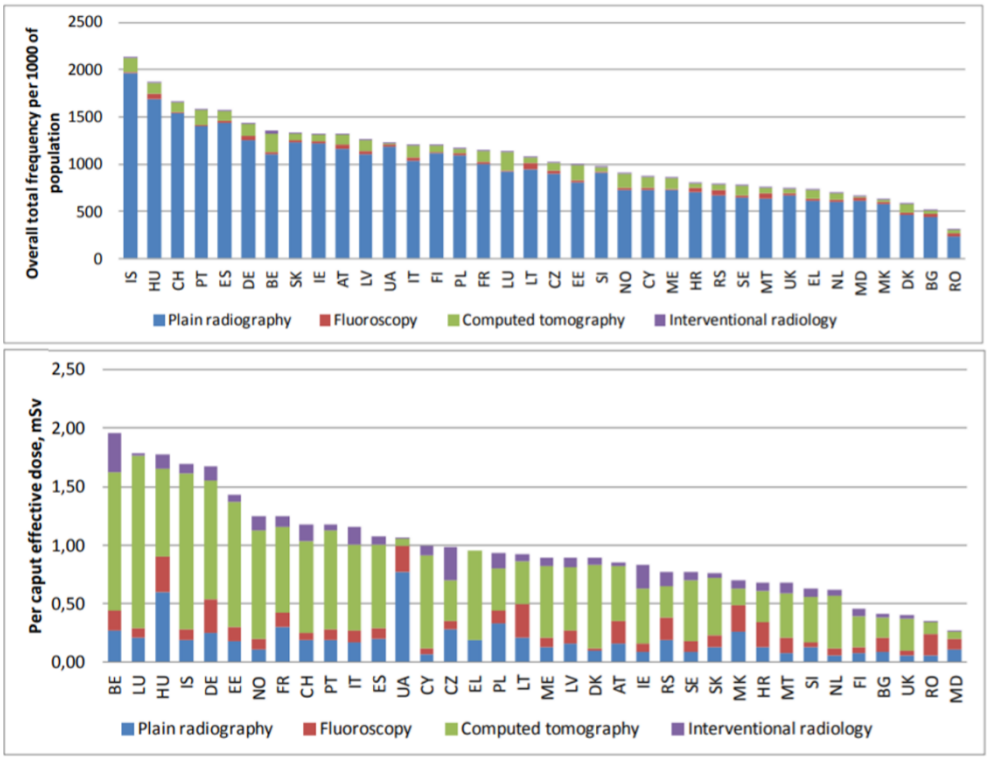

Figure 1.1. Overview of the frequency of medical diagnostic procedures per 1000 capita in the European Union (top panel) and of the effective dose per caput (bottom panel). Radiography are the most used in medical diagnostics, however the exposure due to computed tomography is by far the highest. Note that the radiation exposure in Belgium is highest among the participating countries. Data on the effective dose due to fluoroscopy and interventional radiology were not available for Greece (EL).[15]

1.2.2 Radiography, computed tomography, and cone beam computed tomography

1.2.2.1 Radiography

Radiographs have been widely used in medicine since shortly after the discovery of X-rays (Figure 1.2). Currently, radiographs are the most frequently used diagnostic imaging modality (Figure 1.1). X-ray radiographs are mostly used

for bone and dental examinations, orthopaedic evaluations, chiropractic examinations, and mammography.[19]

The average radiations doses associated with radiographs are very low and range from 0.001 mSv to 0.1 mSv. However, these doses could rapidly increase when multiple radiographs have to be taken. The average effective dose related to radiography has been steadily decreasing since the 1970s due to better X-ray equipment and improvement of radiation protection guidelines.[12, 19]

1.2.2.2 Computed tomography

Since its introduction in the 1970s, the use of CT has increased rapidly (Figure 1.2). In Belgium, for example, 180 examinations per 1000 capita were performed in 2008. In 2017, this number increased to 200 examinations per 1000 capita, meaning one in five inhabitants is subjected to a CT examination per year.[20] The Organisation for Economic Cooperation and Development (OECD) calculated that the use of CT scans in the OECD countries ranged from 37 per 1000 capita (Finland) to 231 per 1000 capita (Japan).[21] CT scans are mostly used for diagnosis, such as bone disorders, but CT can also be used to detect internal bleedings, localize tumours, to guide surgeons during surgery or radiotherapy treatment, and to monitor disease or treatment progression.[16]

As mentioned above, of all medical imaging procedures, the average effective dose due to CT examinations is by far the highest. The radiation dose varies between 15 mSv and 30 mSv. On average, this is about 150 times higher than doses used in radiography examinations. Furthermore, these doses are very dependent on the settings that are used during CT examinations. Radiation doses increase with increasing field of view (FOV), tube voltage (kV), and the tube current-exposure time product (mAs). Furthermore, multiple scans are often required during patient follow-up, which causes the radiation burden to increase rapidly.[16] The average effective dose related to CT examinations has been increasing, and is now about six times higher than in the early 1970s.[12]

1.2.2.3 Cone beam computed tomography

Introduced at the turn of the 21st century, CBCT is a relative new member of the family of medical diagnostic devices. CBCT is an innovative diagnostic imaging technique in the field of dentomaxillofacial radiology (Figure 1.2).[22, 23] Like CT devices, it allows for quick generation of detailed 3D images.[24, 25] CBCT was specifically designed to produce cross-sectional images of the dentomaxillofacial region. Due to its low cost and easy accessibility CBCT has evolved rapidly. Today, it is used for implant planning, endodontics, orthodontics and maxillofacial surgery.[26, 27] Exact numbers for the use of CBCT are currently not available. However, a recent Belgian survey found that one out of five Belgian

dentists has access to a CBCT device. It should be noted that only 9% of the general dental practitioners and 12% of the orthodontists have direct access to a CBCT device. On the other hand, over 60% of oral and maxillofacial surgeons and periodontologists have direct access to a CBCT device.[28]

The radiation doses associated with CBCT examinations are intermediate to those used by CT and radiography devices.[29-31] Typically, doses associated with CBCT range from 0.01 mSv to 1.1 mSv per examination. As with CT devices, these doses are highly dependent on the FOV, kV, and mAs.[32-36] Finally, the radiation dose also increases rapidly with repeated exposure from multiple examinations.

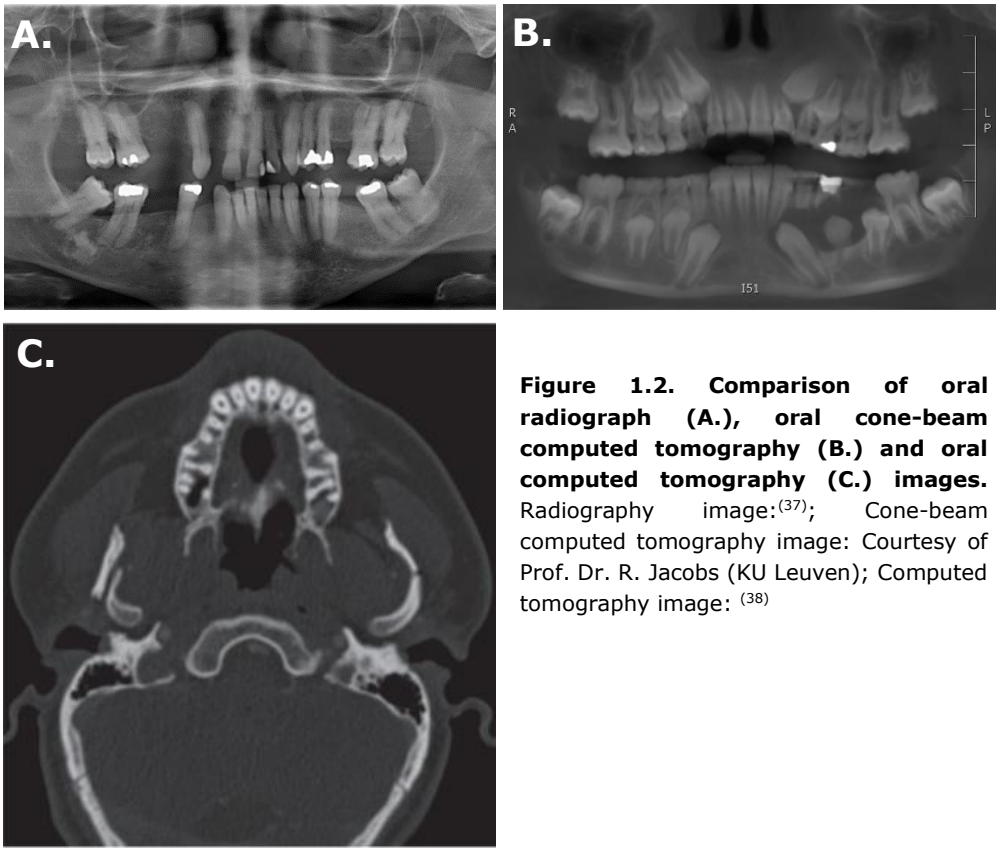

Figure 1.2. Comparison of oral radiograph (A.), oral cone-beam computed tomography (B.) and oral computed tomography (C.) images. Radiography image:[37]; Cone-beam computed tomography image: Courtesy of Prof. Dr. R. Jacobs (KU Leuven); Computed tomography image: [38]

1.2.3 Radiation protection in medical imaging

As will be discussed in the next section ('1.2.4 Health risks associated with medical diagnostic procedures'), the use of IR in medical diagnostics is potentially not without risk. These risks are expected to be even higher in children, since it is known that children are more radiosensitive than adults. This is because the tissues and organs in children are still growing and developing and fast-dividing

cells are more sensitive to IR. Furthermore, the longer life expectancy of children also plays a role. The longer you will live after IR exposure, the longer the time to develop potential adverse health effects.[39] To control and limit these risks, the principles of 'justification' and 'dose optimization' of radiation protection guidelines (see also '1.4 Radiation protection: guidelines and risk assessment') have been defined for use in medical diagnostics.

Justification implies that a diagnostic procedure should only be performed if its use results in more benefit than harm to the patient. Therefore it is important to consider whether it is absolutely necessary to perform the imaging procedure. The use of alternatives (e.g. magnetic resonance imaging) should always be considered.[40]

Dose optimization is directly linked to the 'as-low-as-reasonably-achievable' (ALARA) principle. It focusses on minimizing radiation exposure to the patient. Thus the IR dose that is used should be balanced between ALARA and the required image quality for the intended use.[40] The IR dose, as well as the image quality, mostly depend on the FOV, kV and mAs.[29, 36]

1.2.4 Health risks associated with medical diagnostic procedures

Exposure to IR is associated with (potential) health risks (see Chapter 1.3). Although the use of CT, radiography and CBCT has undeniable benefits for the patient, it is recognized that exposure to IR in medical diagnostics could have drawbacks as well. As discussed in Chapter 1.4, exposure to IR increases the risk of stochastic effects, or it can induce tissue reactions when the radiation dose is above a certain threshold. The radiation doses used in medical diagnostics are not high enough to cause tissue reactions, however there is a potential risk of inducing stochastic effects. Currently, there is no conclusive data about the risks associated with the low dose range. Therefore, understanding the health effects of radiation doses associated with medical diagnostics is one of the major challenges in radiation protection today.[41]

Radiation protection guidelines are important to protect the general public, especially young children, from excessive IR exposure. It is well-known that radiation sensitivity changes with age. Children are more radiosensitive than adults.[39, 42] Therefore, questions were posed about radiation-induced health effects, especially in children.[43-45] Most concern was raised about CT examinations, since the doses there are the highest.[46] However, recently concerns were expressed about the use of CBCT in children. The New York Times published the article "Radiation Worries for Children in Dentists' Chairs" in 2010 which clearly raised public awareness about radiation exposure to children.[47] In this section available epidemiological data of patients on medical diagnostic associated health risks will be discussed briefly.

1.2.4.1 Epidemiological data on medical diagnostic exposure

The rapid increase in frequency of CT in medical diagnostics has led to increased worries about the radiation dose. Therefore, several retrospective epidemiological studies were conducted.[48] It has been estimated that the risk of leukaemia increases following CT examinations in young children.[49-52] A positive correlation between radiation dose and development of brain tumours later in life was also described.[50-52] Huang *et al.* (2014) reported an association between pediatric head CT and the risk of both benign and malignant tumour incidence. They reported that the risk of developing a brain tumour increased 2.6-fold following head CT.[53] Mathews *et al*. (2013) reported a 24% greater cancer incidence in exposed children than in unexposed children.[51] Finally, it was estimated that in the United States, all CT scans taken annually could cause up to 4870 future cancers.[49] Although valuable, these studies are criticized for several reasons. Chief among them are the lack of individual dosimetrical data and a lack of exposure information. Additionally, concerns were raised about reverse causation.[54, 55]

The first epidemiological data concerning X-ray radiography dates back to 1958. It was reported that of the children who died of cancer before the age of ten, the number of them that received radiographs was higher than in controls.[56] After that, multiple studies have tried (and failed) to find a correlation between cancer development and exposure to ionizing radiation due to radiography examinations (reviewed in Mulvihill *et al.* (2017)).[48] Other studies, however, did find a positive correlation between cancer development and exposure to radiographs. In this context, exposure to radiographs has been linked to an increased risk for Ewing's disease, a rare sarcoma that usually occurs in/near bones.[57] Furthermore, it has been reported that there is increased risk of leukaemia and/or lymphoma.[58-63] One study also reported a correlation between radiography and the incidence of brain tumours.[64] Finally, there are some studies reporting an increased incidence of breast cancer following radiography.[65-67] Despite a great number of studies failing to find a correlation between radiography and cancer incidence, some of these studies indicate that even low doses such as those associated with radiography can induce detrimental health effects. Finally, these studies have also been criticized, mostly due to short follow-up periods and the lack of proper exposure parameters and individual dosimetrical data.

To the best of our knowledge there is no epidemiological data linking CBCT exposure to increased cancer incidence.

1.2.4.2 How to cope with limited data on health effects related to CBCT examinations?

Today, there are no epidemiological data showing a connection between CBCT examinations and increased cancer risk later in life. At best, some studies

provided risk estimates based on radiation doses and simulations.[68, 69] These studies estimate that in six cases per one million CBCT examinations, cancer will develop later in life. Pauwels *et al.* (2014) estimated, based on skin dosimetry, that in adults the incidence would be 2.7 cases per one million examinations, whereas for children this would be 9.8 cases per one million examinations.[69] Similar estimates were recently reported by Yeh *et al.* (2018).[68] Additionally, there are only a few prospective studies aimed at investigating potential adverse effects following CBCT examinations, whereas multiple studies were performed for CT and radiological examinations (see Appendices 1 - 3). To the best of our knowledge, only five have been conducted related to CBCT.[70-74] All of them found increases in cytotoxicity markers after CBCT examination, but only two of them found increases in genotoxicity markers (see Appendix 3). Thus, the available data is inconclusive at this time. Furthermore, these studies did not specifically study age-related differences.

To tackle these limitations, the overall aim of this thesis is to investigate the biological effects of CBCT examinations in different age categories. Cellular and subcellular changes following CBCT examinations in children and adults were studied in dental stem cells, buccal mucosal cells, and saliva samples. As this is a prospective study, that focusses mainly on acute changes, the emphasis is placed on the DNA damage response, the DNA repair kinetics, and the (anti-)oxidative stress response. This way, we hope to contribute to the current knowledge of potential health risks associated with medical diagnostic imaging, specifically CBCT examinations.

1.3 Cellular and subcellular effects following ionizing radiation exposure

Exposure to IR can have detrimental health effects. This has been clearly shown by epidemiological data (see '1.4 Radiation protection: guidelines and risk assessment'). Since the focus of this PhD thesis is on the cellular and subcellular effects of X-rays used in medical diagnostic imaging, the next part will give an overview of the interactions between X-rays and human cells/tissues.

1.3.1 Direct and indirect effects of ionizing radiation

X-rays transfer (part of) their energy to cells and biomolecules (e.g. deoxyribonucleic acid (DNA), proteins and lipids) that make up the tissues that they pass through. By transferring their energy directly to biomolecules, X-rays can cause chemical changes, such as ionizations. This is called the direct effect of IR.[75] Alternatively, IR can damage biomolecules indirectly by transferring its energy to water molecules. This leads to the radiolysis of water, which generates reactive oxygen species (ROS), thereby inducing oxidative stress (Figure 1.3).[76] ROS are very reactive radicals and can cause sufficient damage to biomolecules (e.g. DNA and proteins) to alter essential cellular functions.

Since more than 80% of a cell consists of water, most of the DNA damage caused by X-rays is indirect.[16, 77] IR can cause several types of DNA lesions, including single strand breaks (SSBs), double strand breaks (DSBs) and base alterations. DNA DSBs are considered the most harmful because they are more difficult to repair correctly.[78, 79] Inaccurate repair of DSBs could result in mutations, chromosome rearrangements, chromosome aberrations and loss of genetic information, which in turn can give rise to malignancies later in life.[80, 81]

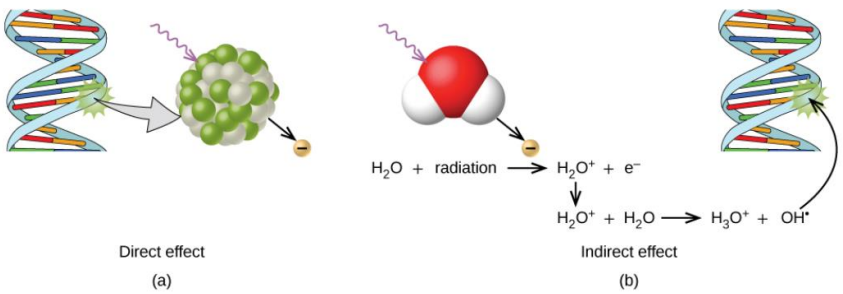

Figure 1.3. Biological effects of ionizing radiation. Ionizing radiation can (a) directly damage biomolecules by ionizing it or by breaking chemical bonds. Alternatively, it can (b) radiolyse water, generating reactive oxygen species, which in turn will react with biomolecules. This will result in indirect radiation-induced damage.[76]

1.3.2 Oxidative stress

1.3.2.1 Generation and effect of reactive oxygen species by ionizing radiation

IR can generate free radicals or ROS through radiolysis of water.[77] ROS generation takes place in three stages, all within nano- to microseconds: 1) the physical stage, 2) the pre-chemical or physico-chemical stage and 3) the chemical stage (Figure 1.4). During the physical stage, which occurs well within 10^{-12} seconds after the interaction with IR, the transferred energy from the IR leads to excitation and ionization of water molecules (H_2O^* and H_2O^+, respectively), as well as the formation of sub-excitation electrons (e^-). These three newly formed species then interact with each other and other nearby molecules. This happens during the pre-chemical or physico-chemical stage. This stage occurs between 10^{-15} and 10^{-12} seconds after IR exposure. An example of these reactions is the formation of the hydroxyl radical ($OH^\bullet$): $H_2O^+ + H_2O \rightarrow H_3O^+ + OH^\bullet$. Next, the chemical stage takes place between 10^{-12} and 10^{-6} seconds after the initial IR exposure. During this stage, the formed radicals will diffuse and react with surrounding molecules, leading up to the biological stage.[77, 82] During the biological stage, which takes place minutes or even years after the initial exposure, important biomolecules are damaged by the newly formed ROS. ROS can cause severe DNA damage by inducing DNA breaks, base damage, destruction of sugars, cross links and telomere dysfunction.[83] $OH^\bullet$ is the main actor, since it is very effective in breaking chemical bonds. This damage can either be repaired, in which case the cell survives, or the damage can be too extensive, which will lead to cell death. However, if the damage is not correctly repaired, mutations can occur. If these persist this could eventually lead to carcinogenesis.[77]

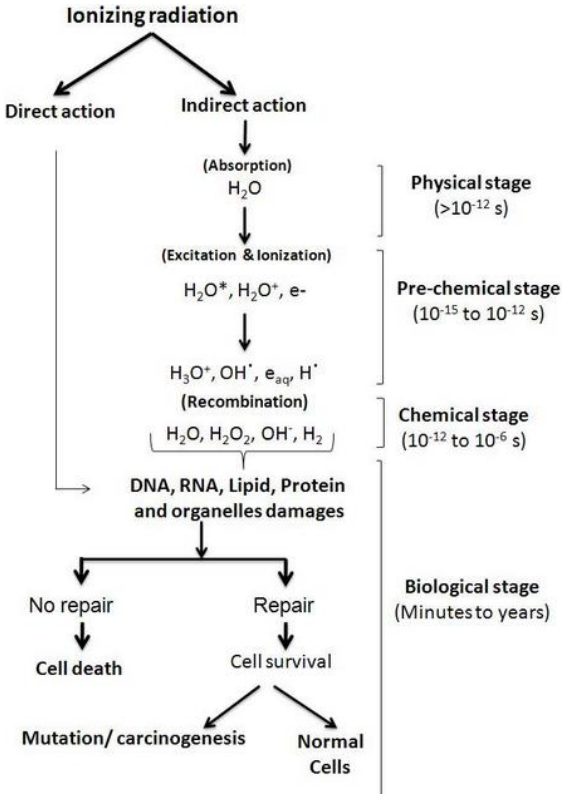

Figure 1.4. Overview of the direct and indirect actions of ionizing radiation. Ionizing radiation can directly damage important biomolecules such as the DNA. Alternatively, it can damage them indirectly via the generation of reactive radicals through the radiolysis of water molecules. The three phases of ROS formation are shown, namely the physical stage, the pre-chemical (or physico-chemical) stage and the chemical stage. Finally the biological stage occurs where the newly formed ROS interact with important biomolecules, leading to damage to these molecules. Depending on the efficient repair of this damage, cells may die or survive.[77]

$OH^\bullet$ is the most prevalent radical, as well as the most potent at breaking chemical bonds. It is highly reactive and causes harmful oxidations of cellular components.[84] Other important ROS are hydrogen peroxide (H_2O_2) and the superoxide anion ($O_2^{\bullet -}$). The latter is, like $OH^\bullet$, very reactive. The former, however, is less reactive. H_2O_2 is mildly oxidizing and mildly reducing, but it does not readily oxidize biological molecules (i.e. DNA, lipids and proteins). The main hazard of H_2O_2 is its ability to be converted into $OH^\bullet$, either by exposure to ultraviolet light, or by interaction with one of several transition metal ions, iron being the most important one. The latter will result in a Fenton reaction in which $OH^\bullet$ is formed.[85] ROS can cause oxidative damage to DNA, protein oxidation and lipid peroxidation.[83, 84] Luckily, cells harbour an antioxidant defence system against excessive ROS exposure. Only when the antioxidant defence system is

saturated, ROS will be able to cause cellular damage. This imbalance between oxidants and antioxidants in favour of the oxidants is called *oxidative stress*.[86]

1.3.2.2 Cellular defence mechanisms against oxidative stress

The antioxidant system is important for the redox homeostasis inside the cell. It allows low levels of ROS to be present because at low concentrations, ROS act as signalling molecules.[87] ROS can reversibly modulate several important intracellular pathways that ensure the integrity and fitness of the cell.[86, 88] It has been found that H_2O_2 for example is involved in microbial killing by macrophages and neutrophils.[89]. It is important to note that ROS that acts as signalling molecule mostly comes from intracellular sources and is not induced by IR. IR mostly induces $OH^{\bullet}$ in higher, localized concentrations, whereas endogenous ROS mostly comprises of $O_2^{\bullet-}$ and H_2O_2 in lower concentrations.[84] Endogenous sources of ROS include the electron transport chain in mitochondria, nicotinamide adenine dinucleotide phosphate oxidases, lipoxygenase, xanthine oxidase, cyclooxygenase, cytochrome P450 monooxygenase, and nitric oxide synthase. The delicate balance between signalling concentrations of ROS and harmful concentrations of ROS, or redox balance, is vital for a normal cellular function.[88] The redox balance is mostly maintained by an endogenous antioxidant system that consists of 1) enzymatic antioxidants, 2) hydrophilic antioxidants, and 3) lipophilic radical antioxidants. Hydro- and lipophilic antioxidants are also called non-enzymatic antioxidants. They all have in common that they counteract free radicals and neutralize oxidants.[90]

Enzymatic antioxidants include, amongst others, superoxide dismutases (SOD), catalase (CAT) and glutathione peroxidases (GSH-Px) (Figure 1.5). They are very effective against high levels of oxidative stress since they have the ability to decompose ROS.[91] SOD is the major defence system against $O_2^{\bullet-}$ and exists in three isoforms in humans: cytoplasmatic Copper/ZincSOD (SOD1), mitochondrial SOD (SOD2) and extracellular Copper/ZincSOD (SOD3). SOD dismutate $O_2^{\bullet-}$ to H_2O_2 and O_2.[92] They are the first line of defence against ROS and can be rapidly induced when oxidative stress is sensed.[86] CAT and GSH-Px both neutralize H_2O_2 through reduction of H_2O_2 into water. By removing H_2O_2, these enzymes prevent the formation of $OH^{\bullet}$, which is very reactive and damaging to biomolecules. GSH-Px are a family of enzymes that are homologous to the selenocysteine-containing mammalian GSH-Px1 enzyme. GSH-Px1 uses reduced glutathione (GSH) as a co-substrate in the reduction of H_2O_2 to water. During this reduction, GSH is oxidized to glutathione disulphide (GSSG). GSH is regenerated through the reduction of GSSG by glutathione reductase, which therefore also is important in the endogenous antioxidant system.[86, 93]

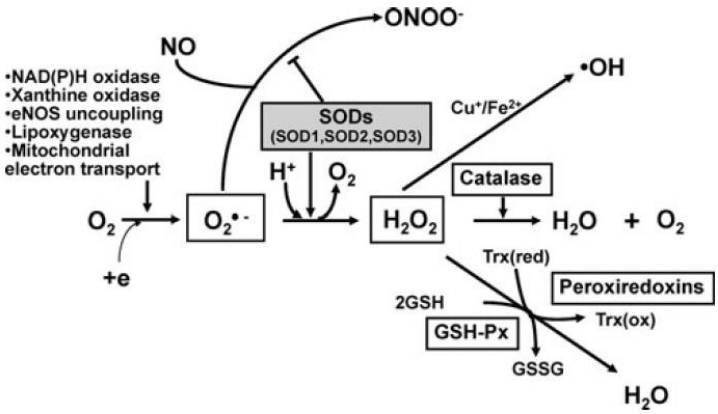

Figure 1.5. Generation and metabolism of reactive oxygen species by enzymatic antioxidants. Superoxide dismutases (SODs) convert superoxide anions ($O_2^{\bullet -}$) to H_2O_2, which in turn is reduced to water by catalase, glutathione peroxidases (GSH-Px) and peroxiredoxins. In the presence of transition metals, H_2O_2 can spontaneously be converted into the hydroxyl radical ($OH^{\bullet}$), which is extremely reactive. CAT, GSH-Px and peroxiredoxins are therefore important in reducing the number of $OH^{\bullet}$ molecules.[92] GSH = reduced glutathione; GSSG = oxidized glutathione

Non-enzymatic antioxidants are low molecular weight, hydro- or lipophilic molecules. Several vitamins are known to have antioxidant capabilities, which is why they are frequently studied as food supplements for radiation protection purposes. Vitamin A for example, which is produced in the liver, can bind to peroxides and prevent peroxidation of lipids.[94] Vitamin C, on the other hand, is effective in scavenging ROS, such as $O_2^{\bullet -}$, H_2O_2, and, $OH^{\bullet}$.[95] Besides vitamins, minerals are also dietary antioxidants. The most important minerals in this regards are selenium and zinc. They are components of important antioxidant enzymes (e.g. SOD and GSH-Px) and they are important for maintaining their enzyme activity.[96, 97] Except for vitamins and minerals, there are many cellular metabolites that exhibit an antioxidant function. Uric acid, for example is known to prevent lipid and protein peroxidation.[98] Finally, flavonoids also exhibit antioxidant activity. Their antioxidant activity depends on the arrangement of their functional groups. Examples of flavonoids are phenolic acids and carotenoids, which are mostly present in herbs, fruit, vegetables, seeds, and nuts.[86]

1.3.3 Oxidative stress measurements

Reactive radicals, such as ROS, have a very short half-life. This poses a major problem when one wants to measure these ROS directly. Luckily, indirect ways of assessing the impact of ROS exist.[99]

Currently, the only available technique that can be used to measure ROS directly is electron spin resonance (ESR).[100] However, this technique is too

insensitive to detect $O_2^{\bullet-}$ and $OH^{\bullet}$ radicals in living systems. This can be overcome by a process called 'trapping'. In 'trapping', a radical will react with a trap molecule (e.g. alpha-phenyl N-tertiary-butyl nitrone and 5,5-dimethyl-pyrroline N-oxide), which results in one or more stable products. These products are then measured. An example of 'trapping' is spin trapping. One major drawback is that the use of traps perturbs the system under investigation. For example, if you want to measure $OH^{\bullet}$ and the damage it is causing, than trapping $OH^{\bullet}$ molecules will decrease the damage caused.[99] Therefore it might be better to opt for indirect measurements of oxidative stress.

An indirect way of measuring ROS is through 'fingerprinting'. 'Fingerprinting' techniques do not measure the ROS itself, but the damage that they cause. For example, if ROS interact with a biomolecule and induce a biochemical change to that molecule (i.e. a fingerprint), than the presence of that fingerprint can be used to infer that ROS was generated. This approach uses biomarkers to monitor the effects of antioxidants on oxidative stress, or the induction of oxidative stress by certain agents.[101, 102] It should be noted that currently there is no single biomarker for oxidative stress that meets all the criteria of an 'ideal' biomarker of oxidative damage.[99] Examples of clinically used biomarkers for the chemical impact of ROS that are relevant in the context of this thesis, will be discussed next. Note that this overview is far from complete and is discussed in more detail elsewhere (e.g. Halliwell and Gutteridge (2015) and Frijhof *et al.* (2015)).[99, 103]

1.3.3.1 Oxidation of proteins

One approach to indirectly measure ROS, is to look at protein oxidation. Protein carbonyls are formed when the protein backbones are oxidatively cleaved. They can arise from several mechanisms, which explains their high concentration in comparison to other ROS biomarkers.[104] Protein carbonyls can be detected spectrophotometrically or by enzyme-linked immuno-sorbent assay (ELISA), Western blot, immunohisto- or immunocytochemistry, or high-performance liquid chromatography (HPLC).[103] They have been measured in blood and in plasma.[103, 105] Additionally, reactions between arginine and lysine residues and carbohydrates results in the formation of advanced glycation end products (AGEs). AGEs can be measured through the use of antibodies. They can be detected through ELISA, immunohisto- or immunocytochemistry, and Western blot. Furthermore they can also be measured by HPLC. AGEs also have a specific autofluorescence which can be used to detect them. They have been measured in plasma or serum samples. However, due to the heterogeneity of AGEs, there is no method that allows for measuring specific AGEs in a clinical setting.[103]

1.3.3.2 Oxidation of lipids

Oxidized low-density lipoproteins (oxLDL) have been used for years as a biomarker for cardiovascular disease (CVD).[106] OxLDL is mostly measured in plasma samples. They can be detected by immunological techniques using antibodies.[107] Linoleic and arachidonic acid are important targets for lipid peroxidation by ROS. Examples of lipid peroxidation products are trans-4-hydroxy-2-nonenal (4-HNE) and malonaldehyde (MDA). They can be detected by several methods. Antibodies have used to detect them via immunocyto- and immunohistochemistry but ELISA has been used as well.[108] 4-HNE has been measured in plasma and serum samples.[108, 109]

1.3.3.3 Oxidation of DNA

Oxidative DNA damage occurs continuously *in vivo*. This oxidative damage mostly takes place at the site of the purine guanine and is mostly caused by the $OH^{\bullet}$ radical.[99] Oxidized nucleotides are usually removed through nucleotide excision repair (NER) or base excision repair (BER). Therefore the damaged nucleotides are excreted into the extracellular space, after which they will leave the body through excretion in urine.[103] Oxidative DNA damage is important since it is widely accepted that it can contribute significantly to cancer development. It could lead to misrepair of DNA, which could cause mutations.[110, 111] Thus oxidative DNA damage could potentially be a biomarker that predicts cancer development later in life.[99]

The most commonly measured oxidatively modified DNA base is 7,8-dihydro-8-oxo-2'-deoxyguanosine (8-oxo-dG).[112, 113] It was first measured using HPLC-based assays with sensitive electrochemical detection.[114] Later, ELISA assays also became available for detecting 8-oxo-dG.[115, 116] Measuring 8-oxo-dG has several important advantages: 1) the availability of sensitive detection techniques, 2) it is formed by several ROS, including $O_2^{\bullet -}$ and $OH^{\bullet}$, and 3) it is a mutagenic lesion. The latter indicates that it will be perceived by cells and that mechanisms exist (i.e. NER/BER) to remove it. 8-oxo-dG has successfully been measured in blood, urine and saliva.[117-123]

1.3.3.4 Markers of antioxidant defence

In theory, oxidative stress occurs when there is an imbalance between the amount of oxidants and antioxidants. Therefore, it is likely that oxidative stress can also be caused by, or aggravated by, an impaired antioxidant defence. As antioxidants play an important role in ROS scavenging, it might be of interest to

monitor antioxidant levels and/or activity. Concentrations of enzymatic antioxidants (e.g. SOD1, CAT, and GSH-Px1) can be measured by ELISA or Western blot, but their activity can also be monitored in saliva and blood samples.[93, 124-130] Finally, antioxidants can also be monitored through gene expression assays.[93, 130]

1.3.3.5 Oxidative stress after low dose radiation exposure

The link between low dose IR exposure and oxidative stress markers has been studied before, mostly in blood samples.[131-133] Although, in recent years, saliva has been recognized as a potentially useful bio-fluid in radiation protection research, but has been scarcely investigated.[132, 134, 135] There are indications that salivary levels of monocyte chemoattractant protein 1, interleukin-8, and intracellular adhesion molecule 1 (all inflammation markers) are increased following whole-body irradiation in cancer patients.[136] However, a lot of work still needs to be done. Currently, no effects on salivary oxidative stress biomarkers have been described following low dose IR exposure. Therefore, we will, for the first time, monitor oxidative stress parameters (8-oxo-dG and antioxidant activity) in saliva samples from adults and children following CBCT examination.

1.3.4 Radiation-induced DNA damage and the DNA damage response

As described in '1.3.1 Direct and indirect effects of ionizing radiation', IR can directly or indirectly cause a wide range of DNA lesions. Such lesions include DNA breaks, both SSBs and DSBs, DNA cross links, base damage, base alterations and destruction of the sugar phosphate backbone. Most of this DNA damage is caused by ROS. Of the aforementioned lesions, DNA DSBs are considered the most harmful, if not properly repaired.[79] If improperly repaired, DNA DSBs could result in chromosome rearrangements, mutations, chromosome aberrations, loss of genetic information, and, cell death. DSBs could cause genetic instability which can be the onset for carcinogenesis.[80, 81] To cope with DNA damage, eukaryotes have developed an efficient signalling network known as the DNA damage response (DDR).[137] The DDR is a signalling cascade that responds to certain kinds of DNA damage in order to repair it, or to induce apoptosis.

The DDR provides a mechanism for signal transduction from DNA damage sensors to DNA damage mediators/transducers. These mediators/transducers target a series of downstream effectors that will determine the outcome of the IR-induced DNA damage. The main outcomes are 1) cell cycle arrest to provide time for DNA repair, which in over 99% of the time occurs accurately, but could also lead to misrepair, which could be the cause of mutations, or 2) cell cycle arrest with no DNA repair leading to cellular senescence, or 3) induction of programmed

cell death or apoptosis (Figure 1.6).[81, 138] Since DNA DSBs are considered the most cytotoxic DNA lesion induced by IR, the DDR to DNA DSBs will be discussed further in this section.

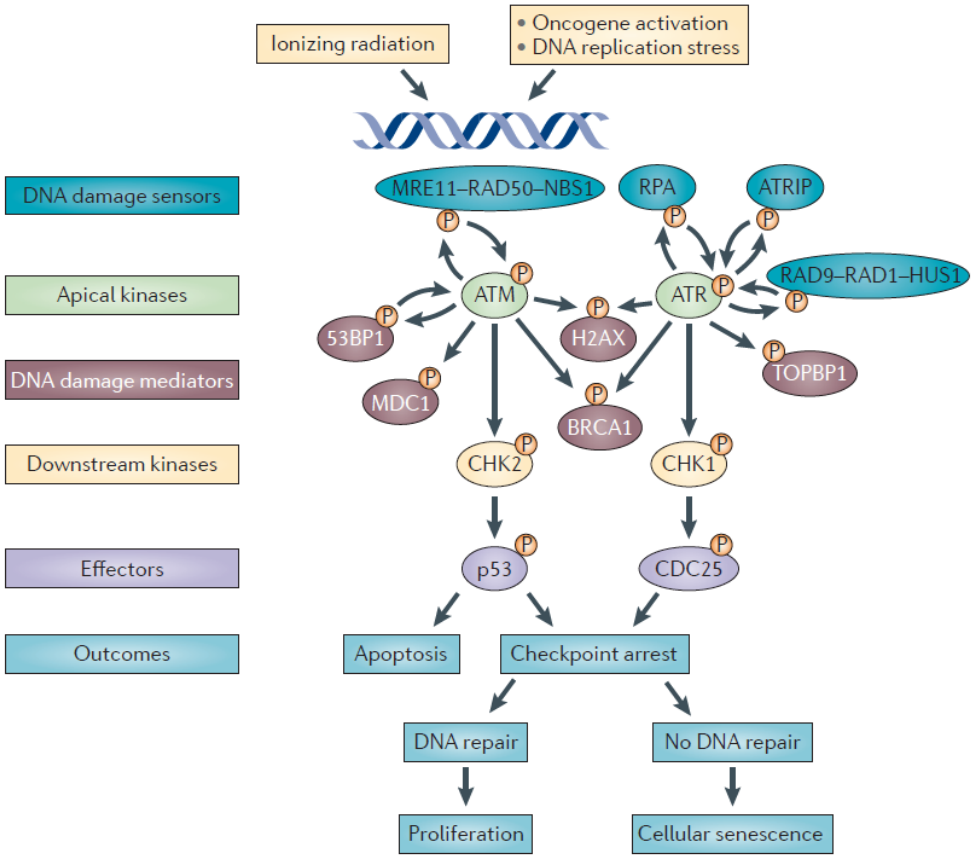

Figure 1.6. General overview of the DNA damage response. The presence of a DNA double strand break is detected by a DNA damage sensor, which transmits the signal downstream to a series of effector molecules through a signal transduction cascade of DNA damage mediators/transducers. These will activate signalling mechanisms for either cell cycle arrest and induction of DNA repair, or, when no repair occurs, cell death.[138]

1.3.4.1 DNA damage mediators

Radiation-induced DNA DSBs in eukaryotic cells are sensed quickly. However, which proteins fulfil the function of 'damage sensor' is debatable. The Mre11/Rad50/Nbs1 (MRN) complex, as well as Ku70/80 proteins, have been described as having DNA damage sensing capabilities.[139, 140] These sensors

activate several members of the phosphatidylinositol 3-kinase like kinase (PIKK) serine/threonine protein kinase family. This protein kinase family includes ataxia telangiectasia mutated (ATM), ataxia telangiectasia and Rad3-related protein (ATR), and DNA-dependent protein kinase (DNA-PK), which become active depending on the source of DNA damage and the timing.[141, 142] Both ATM and DNA-PK are essential for the detection of DSBs, whereas ATR is necessary for repair of single-stranded DNA regions that arise for example during replication fork stalling.[143] Thus, for the repair of DSBs ATM and DNA-PK are the main players. After activation, ATM has been shown to activate hundreds of proteins, including p53-binding protein 1 (53BP1) and histone 2AX (H2AX) (Figures 1.6). DNA-PK and ATR also has the ability to phosphorylate H2AX on serine 139 (γH2AX).[142, 144] γH2AX is one of the earliest DNA damage mediators that becomes activated following DNA DSB formation. Accumulation of γH2AX at the DSB site generates so called ionizing radiation-induced foci (IRIF) that provide a binding site for downstream mediators in the DDR, such as 53BP1.[145] It is of interest to know that visualization of both γH2AX and 53BP1 is increasingly being used to monitor DSB formation and repair.[78, 140, 146-148] After IRIF formation, γH2AX induces a positive feedback loop and serves as a binding site mainly for the breast cancer 1 C-terminal (BRCT) domains of the mediator of DNA damage checkpoint 1 (MDC1) protein.[149, 150] When MDC1 is positioned at the site of the DSB, this creates a dock for other DNA repair proteins. That way, the MRN-ATM complex is recruited to the DSB and ATM will phosphorylate other DNA damage mediators, such as 53BP1 and breast cancer early onset 1 (BRCA1). At this point, γH2AX serves as a signalling platform onto which all DDR proteins are concentrated. This concentration of DDR proteins allows for amplification of the original DNA damage signal.[151] The DNA damage mediators then transduce the DNA damage signal to downstream effectors of the DDR (e.g. Checkpoint kinase (Chk) 2 and p53 (Figure 1.6)[152]

1.3.4.2 DNA damage effectors

DNA damage sensors can activate DNA damage mediators, that in turn will transduce the DNA damage signal to DNA damage effectors, including cell cycle checkpoints (that allow for DNA damage repair), DNA repair pathways, and the removal of severely damaged cells.

Cell cycle checkpoints

The main function of cell cycle checkpoints in eukaryotic cells is to detect DNA damage, and allowing for this DNA damage to be repaired by slowing or stopping the cell cycle (i.e. cell cycle arrest). The cell cycle depends on multiple proteins, including cyclins, cyclin-dependent kinases (CDKs), and cyclin-dependent kinase inhibitors (CKIs), which regulate the progression through the

cell cycle.[153] Cyclins are the regulatory subunit of a heterodimer they form with CDKs. CDKs, in turn, are the heterodimer's catalytic subunit which will phosphorylate several downstream targets upon activation by binding to its respective cyclin. Through phosphorylation of target proteins, CDKs orchestrate the cell cycle progression. Finally, CKIs inhibit the catalytic activity of CDKs, resulting in cell cycle arrest. Several CKIs are therefore known as tumour suppressor proteins, e.g. p16 and p21. Generally, CKIs cause cell cycle arrest in the G_1 phase to allow for DNA damage repair.[154, 155]

The cell cycle has three major checkpoints, namely the G_1/S checkpoint, the intra-S phase checkpoint and the G_2/M checkpoint. At each of these checkpoints, the cell has to assess if the genetic material is suited for cell division or if DNA repair is needed. Activation of these checkpoints is regulated by CDKs and CKIs.[156]

The G_1/S checkpoint prevents cells from replicating when DNA DSBs are detected in the G_1 phase. This checkpoint is regulated by two pathways: 1) through tumour suppressor p53, and 2) the checkpoint kinases (Chk) 1/Chk2-Cdc25A-CDK2 pathway.[157] In short, activation of p53 in the nucleus will lead to the induction of p21, which causes the cell to remain in the G_1 phase by preventing transition to the S phase.[157, 158] The Chk1/Chk2-Cdc25A-CDK2 pathway involves the degradation of Cdc25A phosphatase, which results in rapid arrest of the cell cycle at the G_1/S checkpoint.[157, 158] Both pathways result in the inactivation of CDK2, which inhibits the release of G_1/S phase-promoting E2F transcription factor from its bond to the retinoblastoma protein (RB).[159, 160] When E2F is bound to RB, cell cycle progression is inhibited. Normally, when cell cycle progression is needed, CDK2 will phosphorylate RB, which results in the release of E2F and subsequent progression from the G_1 phase to the S phase. Thus, the cell cycle is halted in the G_1 phase if CDK2 is inhibited and E2F is not released from RB.[161]

In the S phase, damaged DNA inhibits replication of DNA. This is known as the intra-S phase checkpoint. It is regulated by two pathways: 1) the ATM/ATR-Chk1/Chk2-Cdc25A pathway, and 2) the ATM-NBS1-SMC1 pathway.[162] As with the G_1/S checkpoint, ATM/ATR phosphorylate Chk1 or Chk2, resulting in the phosphorylation and degradation of Cdc25A, which inhibits transition into the S phase.[157, 162] On the other hand, ATM can phosphorylate NBS1, which eventually leads to the activation of the intra-S phase checkpoint.[157]

Finally, there is the G_2/M phase checkpoint. This checkpoint prevents the cell from entering mitosis and thus transferring its (damaged) DNA to the next generation of cells.[157] It is important to note that most cells are found to be most sensitive to IR-induced DNA damage when they are in the G_2 or M phase.[163]

DNA damage repair pathways

IR can induce several types of DNA damage (as discussed above), all of which rely on different DNA repair pathways. Simple lesions, such as SSBs and base damage, can effectively be repaired through BER. Different 'excision' repair mechanisms exist, such as NER and mismatch repair (MMR). However, these pathways are less relevant in IR-induced DNA damage, since the most important DNA lesion induced by IR are DNA DSBs.[159] In the following paragraphs, the focus will be on two DNA repair pathways that are important in DSB repair: 1) non-homologous end-joining (NHEJ), and 2) homologous recombination (HR). The former is error-prone, but it is the most prominent pathway for DSB repair, whereas the latter is error-free but in order to work it needs an intact homologous template, which is not always present in severe DSBs.[159, 164]

NHEJ allows for DSB repair that can occur rapidly and throughout the entire cell cycle, in contrast to HR. After detection of a DSB, the Ku70/80 complex binds the ends of the DSB. This binding ultimately results in end processing of the DNA strands, after which the DSB termini are ligated (Figure 1.7). This results in complete repair of the DSB.[165] Although NHEJ efficiently repairs DSBs, it often results in a loss of genetic information because at each end of the DSB a few nucleotides are lost. However, NHEJ is the main DNA repair pathway in eukaryotes and can be performed throughout the cell cycle, mostly in the G_0 and G_1 phases.[142, 166]

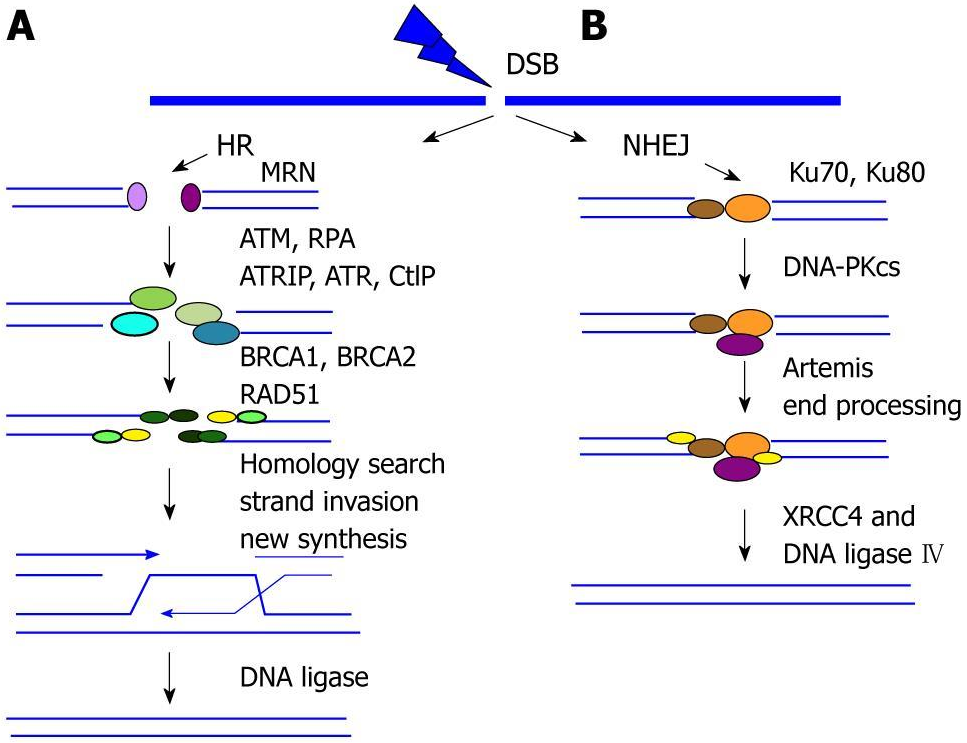

Figure 1.7. Error-free homologous recombination (HR) compared to error-prone non-homologous end joining (NHEJ). A. The DNA double strand breaks (DSBs) are recognized and DNA damage mediators are activated. This initiates a cascade leading to resection of the DNA strands. Next, a homologous strands is searched. When a homologous sequence is found, DNA polymerase extends the single-stranded DNA. Then, the exchange of damaged DNA strands occurs, resulting in the pairing of each damaged strand with its homologous template. Finally, the damaged strands are extended and ligated, which results in full repair of the DNA DSB. **B.** DNA DSBs are mainly repaired by error-prone NHEJ. When a DSB is detected, the Ku70/80 complex binds the ends of the DSB. This binding ultimately results in end processing of the DNA strands, after which the DSB termini are ligated.[167]

DNA DSB repair through HR is based on using an intact homologous DNA strand as a template for DSB repair. By using a template strand, HR results in error-free DSB repair, unlike NHEJ. However, the need for a template strand also implies that HR can only occur when sister-chromatids are present, i.e. during the late S phase and G_2 phase. The DNA DSBs are recognized and DNA damage mediators ATM and ATR are activated. This initiates a cascade leading to resection of the DNA strands. Next, the repair mechanisms search for a homologous DNA strand. When a homologous sequence is found, DNA polymerase extends the single-stranded DNA. Then, the exchange of damaged DNA strands occurs, resulting in the pairing of each damaged strand with its homologous template.

Finally, the damaged strands are extended and ligated, which results in full repair of the DNA DSB. (Figure 1.7).[156, 165, 168]

When DNA DSB are sensed, the cell has to decide via which of these mechanisms the damage will be repaired. How they decide between NHEJ and HR is not well understood so far. The cell cycle phase at the time of the DSB plays a role, since HR can only occur in the late S- and G_2 phases. Furthermore, 53BP1 and BRCA1 are thought to play a key role in deciding between NHEJ and HR.[169, 170]

Removal of severely damaged, non-functioning cells

If a cell is too damaged, or its genomic integrity cannot be guaranteed, cells will be removed. As with DNA repair, several pathways for the removal of cells exist. The four main modes of cell removal that can be induced by severe DNA damage are senescence, apoptosis, necrosis, and autophagy (Figure 1.8).[171]

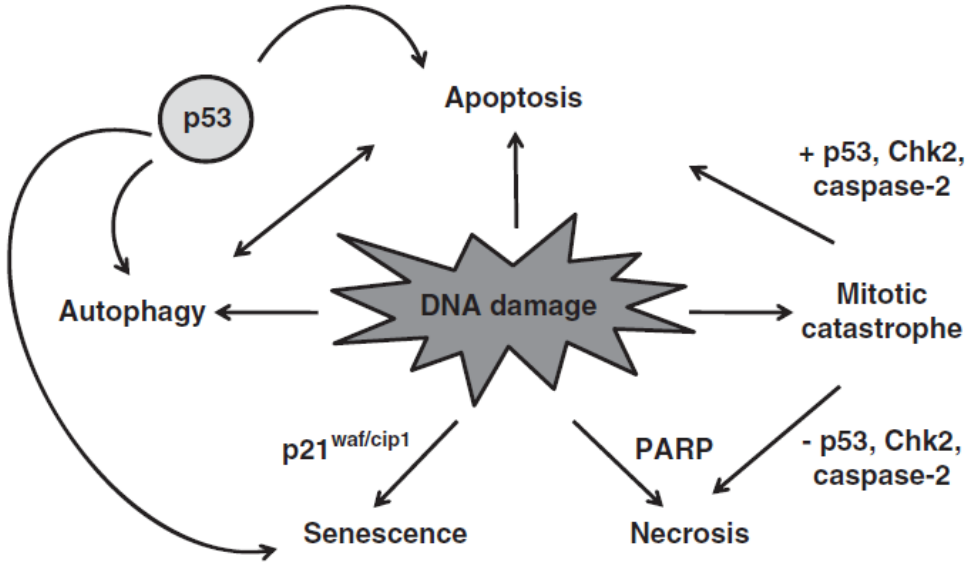

Figure 1.8. Overview of the four main modes of removing non-functioning cells induced by DNA damage. Severely damaged DNA can evoke necrosis, autophagy, apoptosis and senescence. The latter is not a form of cell death, but rather a state of stable cell arrest. p53 plays a central role in the signal transduction following DNA damage. It is a main actor in the apoptotic response and regulates the switch between senescence and apoptosis. p21 is also an important mediator of senescence. Necrosis is mostly mediated through ATP depletion and poly(ADP-ribose)polymerase (PARP) activation. Finally, autophagy depends on the presence/absence of functional p53.[171]

Cellular senescence is characterized by an irreversible growth arrest in the G_1 phase of the cell cycle. Due to this growth arrest, the proliferation of cells with severe DNA damage is limited. This irreversible growth arrest can be caused by several forms of cellular stress, such as activation of oncogenes, ROS and DNA damage. Senescence that is caused by one of these stresses is called premature cellular senescence.[172] Cellular senescence is considered an anti-proliferative response and a tumour suppressor mechanism.[173] p53/p21 and p16/Rb are the most important mediators of cellular senescence.[171] Activation of p53 following DNA damage leads to the activation of CKIs such as p16 and p21. Inhibition of CDK-cyclin complexes results in a cell cycle arrest, halting cellular proliferation. Hypo-phosphorylated Rb is the most crucial component responsible for senescence. Besides DNA damage, oxidative stress can also cause premature cellular senescence. Oxidative stress, through an increase in ROS, activates the p38 mitogen activated protein kinase (MAPK). Activated p38 MAPK leads to increased transcriptional activity of p53 and upregulation of p21. p21 activation results in inhibition of CDK-cyclin complexes leading to cell cycle arrest. A third major component of damage-induced senescence is the senescence-associated secretory phenotype (SASP). The SASP is mediated by nuclear facter κβ (NF-κβ) and includes pro-inflammatory cytokines (e.g. interleukin-6 (IL-6) and IL-8), chemokines, growth factors (e.g. transforming growth factor-β (TGFβ)) and proteases.[174, 175] These proteins can cause inflammation in the vicinity of senescent cells, but can also trigger senescence. TGFβ, for example, can trigger senescence in a paracrine manner. The mechanism by which TGFβ achieves this includes the generation of ROS and DNA damage, which ultimately leads to the activation of p21 (Figure 1.9).[176]

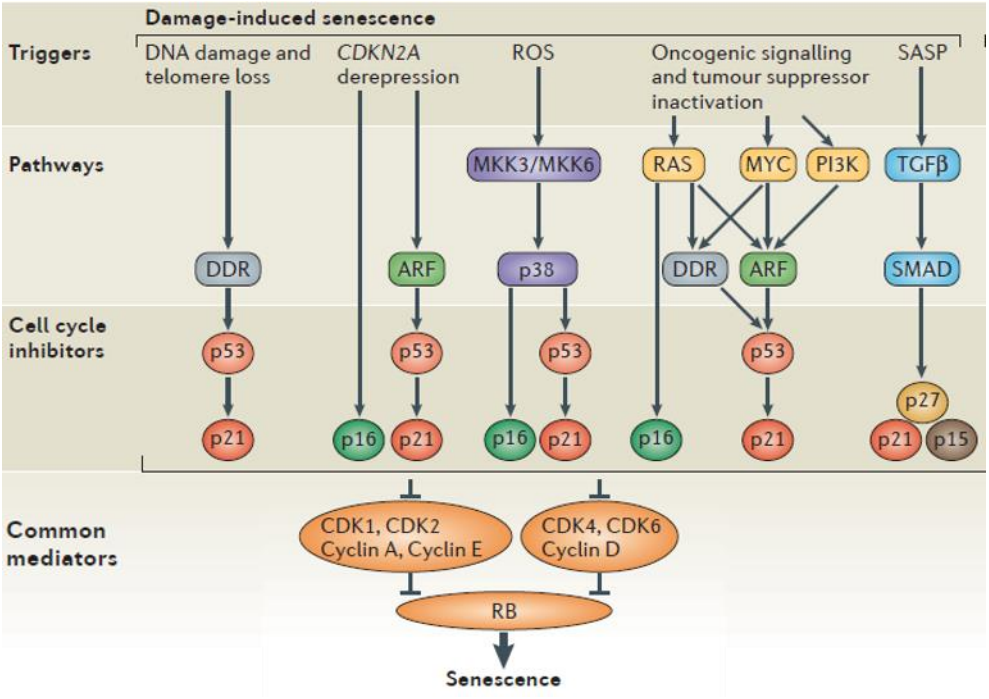

Figure 1.9. Overview of molecular pathways involved in damage-induced senescence. DNA damage, reactive oxygen species (ROS) and the senescence-associated secretory phenotype (SASP) all lead to activation of cell cycle inhibitors p21 and/or p16. These, in turn, will inhibit important cyclin-dependent kinases (CKD), whose inhibition leads to the inhibition of the retinoblastoma protein (Rb), which is the crucial component responsible for senescence induction. Figure adapted from Muñoz-Espin and Serrano (2014).[176] DDR = DNA damage response

Apoptosis is also known as 'programmed cell death'. Like premature cellular senescence, it is an response to cellular stress and occurs when DNA damage repair is slow or incomplete.[171] It is therefore an important mechanism for maintaining homeostasis and for removing cells during different developmental processes. It also limits the number of cells that have damaged DNA, which could lead to an accumulation of mutations that could lead to carcinogenesis. This way, apoptosis is a cellular mechanism that help to prevent tumour formation.[177, 178] When a cell goes into apoptosis, morphological changes occur. These changes include peripheral condensation of nuclear DNA without disassembly of the nuclear envelope, plasma membrane blebbing, and cleavage of the nucleus into membrane-enclosed structures, which are known as apoptotic bodies.[179] Based on these morphological changes, apoptosis can be distinguished from necrosis (see below). Unlike necrosis, apoptosis does not result in the release of intracellular components into the extracellular space.[171] Since apoptosis is 'programmed', it is no surprise that it is a complex process that can proceed through at least two major pathways: the extrinsic and intrinsic pathways (Figure

1.10).[180] Both pathways can be induced by severe or unrepairable DNA damage.[177] Activation of members of a family of cysteine aspartyl proteases (caspases) is a hallmark of apoptosis. They play a central role during the execution-phase of apoptosis, and they can amplify the apoptosis signal though caspase cascades. Caspases 8 and 9 are mostly regulators of apoptosis, whereas caspases 3, 6, and 7 are important effectors of apoptosis.[181] The extrinsic pathway relies on death ligands that bind to the death receptors on the cell surface. This leads the activation of caspase 3, which is an important effector which starts a caspase cascade that eventually leads to apoptosis. The intrinsic pathway, which is typically initiated by severe DNA damage, starts with the activation of p53. If Bax is activated by p53, it causes the release of cytochrome c from the mitochondria, which leads to the activation of caspase 3 by caspase 9, after which caspase 3 starts the caspase cascade that leads to apoptosis, similarly to the extrinsic pathway.[182]

Necrosis is an acute form of cell death, usually following rapid energy, i.e. ATP, loss. Necrosis is mostly an unregulated form of cell death, however evidence shows that it could be regulated by poly(ADP-ribosyl)ation. Other proteins potentially involved are among other p53, p21 and DNA-PKcs.[183] Besides rapid energy loss, necrosis also occurs following direct cellular trauma. Eventually necrosis results in loss of cell membrane integrity and release of intracellular components into the extracellular space, which could induce a local inflammatory reaction.[184]

Autophagy, which translates to 'self-eating', is a well-known catabolic mechanism for the degradation of proteins and other subcellular components by lysosomal proteolysis. It could be triggered in response to several stress stimuli, including DNA damage. Autophagic cell death is characterized by the presence of autophagic structures and, unlike in apoptosis, chromatin condensation in the later stages of the autophagic process. The process of autophagy may be regulated by p53.[171, 185]

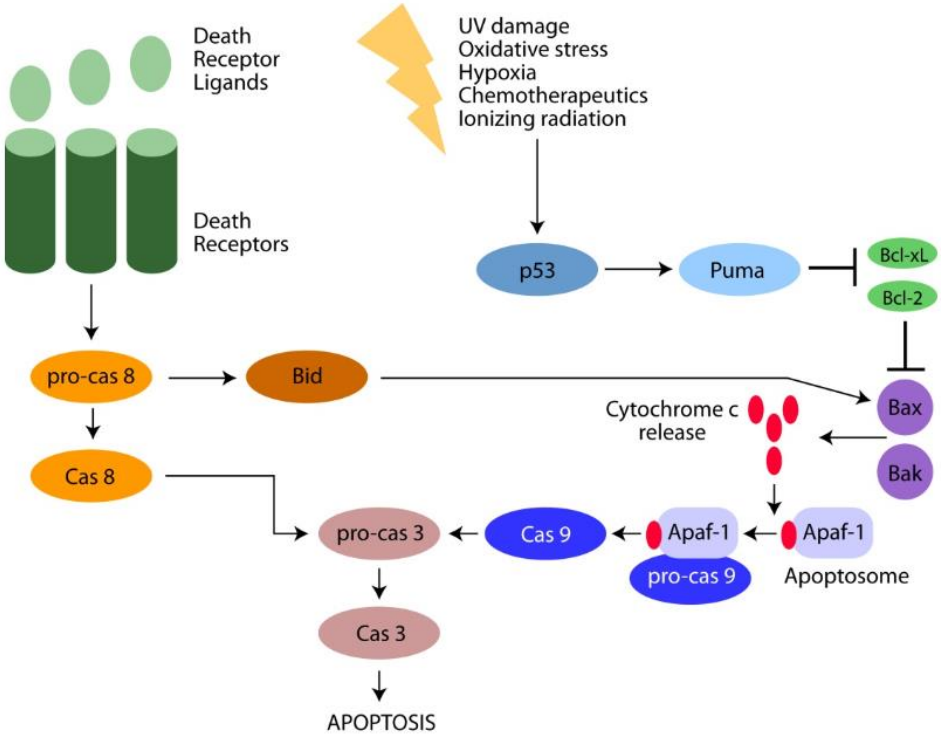

Figure 1.10. Extrinsic and intrinsic apoptotic pathways. The extrinsic pathway (left) relies on death ligands that bind to the death receptors on the cell surface. This leads to the conversion of inactive pro-caspase 8 into the active caspase 8. Caspase 8 then activates caspase 3, which starts a caspase cascade that eventually leads to apoptosis. The intrinsic pathway (right) is initiated by the activation of p53. p53 activates its apoptosis-related target genes, such as Bcl-2 associated X (Bax), Bcl-2 homologous antagonist killer (Bak), p53 up-regulated modulator of apoptosis (Puma), and apoptotic protease activating factor 1 (Apaf1). If Bax is activated by p53, it causes the release of cytochrome c from the mitochondria. Cytochrome c and Apaf1 then form the apoptosome. The apoptosome than activates pro-caspase 9 to form caspase 9. Finally, caspase 9 activates caspase 3 and caspase 3 then start the caspase cascade that leads to apoptosis. Note that the extrinsic and intrinsic pathway intersect at the level of caspase 3.[182]

1.3.5 DNA damage measurements

There are a lot of different assays available that can be used to assess IR-induced DNA damage, DNA damage repair, and the cellular outcome. One can look at DNA damage induction, cell survival, chromosomal aberrations, etc.. *In vivo*, mostly cytogenetic assays are performed, since they are well-established. Examples are the dicentric chromosome assay, chromosome aberrations, and micronucleus (MN) assay. Besides these cytogenetic assays, there are assays that

focus on DNA damage and repair (kinetics), such as the comet assay, pulsed-field gel electrophoresis and the γH2AX assay. Finally there are assays that focus on cellular endpoints, including cell cycle assays and senescence assays. Although the dicentric chromosome assay, MN assay, and comet assay have been used before to study cellular effects following medical diagnostic imaging (see Appendices 1, 2 and 3), the focus of this section will be on the γH2AX/53BP1 assay, cell cycle analysis and senescence assay, as these assays were performed during this PhD research.

1.3.5.1 Assessing DNA damage and repair through the γH2AX/53BP1 assay

As described in '1.3.4 Radiation-induced DNA damage and the DNA damage response', phosphorylation of H2AX at the site of DNA DSBs leads to the formation of γH2AX foci. The maximum number of foci is detectable 30 minutes to one hour after IR exposure. Depending on the cell type and the radiation dose, the number of foci usually decreases to baseline levels within a few days, mostly within 24 hours.[186, 187] Thus, counting γH2AX foci at different time points is an endpoint that can be used to assess the formation and repair kinetics of DNA DSBs following IR exposure. Similarly, 53BP1, after phosphorylation and activation, forms foci at the site of DNA DSBs.[79] Both γH2AX and 53BP1 foci show a quantitative relationship between the number of foci and the number of DSBs that are present.[140, 188, 189] Therefore, one γH2AX and/or 53BP1 focus represents one or several clustered DNA DSBs.[78, 190]

γH2AX and/or 53BP1 foci are most frequently scored via immunocyto- and/or immunohistochemistry followed by fluorescence microscopic analysis. Alternatively, flow cytometry can be used to detect fluorescence intensity.[191] Microscopically, foci can be counted by manual scoring through the eye piece or of digital images, or by automated scoring by using image scoring software.[187] Automated scoring has several advantages over manual scoring such as the potential for high throughput, exclusion of scorer subjectivity and elimination of the time-consuming counting process. Flow cytometrical analysis, on the other hand, has the advantage that is faster than microscopic analysis. However, it is less sensitive because it cannot discriminate foci from background staining spots.[144] This is important following low dose exposure, such as those used in diagnostic radiology, where sensitive scoring is required. γH2AX increases has been detected following radiography and CT examination, thus it can be detected following IR exposure of a few mSv and even less (see Appendices 1 & 2).

γH2AX is formed following phosphorylation of H2AX during the DDR. However, even in the absence of DSBs artefactual γH2AX foci can be formed. This could be due to non-specific immunostaining or formation of antibody aggregates during the staining process. It has been hypothesized that anti-γH2AX antibodies

could bind to parts of Golgi vesicles and/or the endoplasmatic reticulum.[186] γH2AX can also be observed in the S phase of the cell cycle.[78, 137] Furthermore, γH2AX foci can also be detected in early apoptotic DNA breakage.[137]

To reduce the impact of these artefactual γH2AX foci, a double immunostaining for both γH2AX and 53BP1 can be used. This enhances the sensitivity of the microscopic analysis of DNA DSBs. It was shown that γH2AX IRIF co-localize very reliably with 53BP1 IRIF.[79, 146, 192-194] An added benefit is that 53BP1 does not co-localize with γH2AX in early apoptotic cells. Therefore the quantification of co-localized γH2AX/53BP1 foci can rule out misclassification of early apoptotic DNA breakage, which would induce γH2AX foci, but not 53BP1 foci.[195, 196]

1.3.5.2 Cell cycle analysis

One of the main cellular outcomes following (severe) DNA damage, is the induction of cell cycle arrest (Figure 1.11). This arrest allows the cell time to repair the damage. Monitoring of the cell cycle can be performed through gene expression analysis of genes that are essential for the cell cycle. Similarly, proteomic techniques can be used to monitor levels of important cell cycle mediators (e.g. p53 and p21). Finally, flow cytometry is frequently used to analyse the specific cell cycle phases.[148] Flow cytometrical analysis of cell cycle progression is relatively simple and uses an intercalating DNA dye alongside a nucleotide analogue, which can be detected via antibodies (e.g. 5-bromo-2'-deoxyuridine (BrdU)). Whilst an intercalating DNA dye allows distinction between the G1/G_0, S, and G_2/M phases based on nucleic acid content, addition of the stain of a nucleotide analogue allows for a clearer distinction between the G1/G_0 and G_2/M phases on the one hand, and the S phase on the other hand. Since the nucleotide analogue is incorporated into newly synthetized DNA, only S phase cells will stain positive when using anti-nucleotide analogue antibodies, resulting in a clearer distinction than solely relying on a DNA dye. [148, 197]

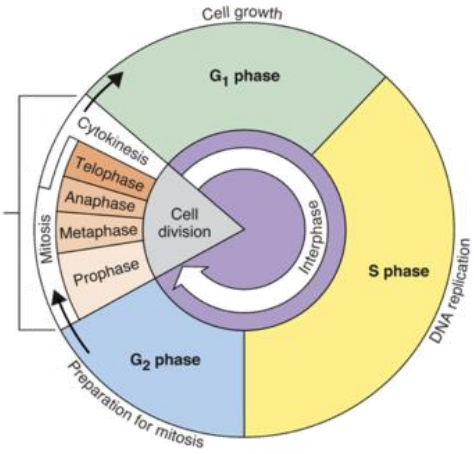

Figure 1.11. Overview of the cell cycle. The cell cycle is composed of four main phases: 1) the G_1 phase, or cell growth phase, 2) the S phase, or DNA replication phase, 3) the G_2 phase, or mitosis preparation phase, and 4) the mitosis phase. The mitosis phase itself consists of the prophase, metaphase, anaphase, and telophase. These phases make up the actual cell division.[198]

1.3.5.3 Premature cellular senescence

If a cell suffers severe DNA damage, it could become senescent. This is characterized by an irreversible cell cycle arrest.[199] Therefore, markers of cell cycle arrest can be used to assess if a cell became senescent prematurely. The hallmark of senescent cells is the increase in β-galactosidase activity. This has led to the development of the X-gal assay, which is based on the increased β-galactosidase activity. It is a microscopic assay, which allows for detection of senescent cells.[173, 200] Senescent cell can also be detected through analysis of the SASP. Cytokines such as IL-6, IL-8, insulin-like growth factor binding proteins 2 (IGFBP-2), and IGFBP-3 can be detected using proteomic approaches, as well as genomic techniques.[174, 201] IL-6 and IL-8 are pro-inflammatory cytokines, which are associated with DNA damage and which can cause (persistent) cell cycle arrest through paracrine and autocrine signalling.[202] IGFBP-2 and IGFBP-3 are proteins to which insulin-like growth factors (IGF) are bound. When bound to IGFBP-2 and IGFBP-3, they cannot interact with their receptor, leading to inhibition of cell growth which is generally induced by IGF.[203, 204] Because of their ability to sequester IGF and thereby inhibiting cell growth, IGFBP-2 and IGFBP-3 have been studied as markers for cellular senescence. Indeed, both increased levels of IGFBP-2 and -3 have been found to be associated with senescence.[202, 205, 206]

1.4 Radiation protection: guidelines and risk assessment

Exposure to IR can cause detrimental effects, certainly after exposure to high doses. These detrimental effects are either tissue reactions (formerly known as deterministic effects) or stochastic effects. Almost immediately after the discovery of X-rays in 1895 tissue reactions were observed.[207-209] They are associated with doses above 100 milligray (mGy) and occur within hours up to a few weeks, sometimes even up to several years. Examples are skin burns following radiotherapy and cataract. For tissue reactions, a threshold dose exists below which no tissue reactions are observed.[210] Stochastic effects (e.g. radiation-induced carcinogenesis) are mostly associated with low doses of IR, which are defined to be lower than 100 mGy, but are also observed following high IR doses. They occur over a longer period of time then tissue reactions (i.e. months up to several years). The ICRP aims to protect people from radiation-induced stochastic effects by advising on radiation protection guidelines and regulations.[10, 211]

One of the greatest challenges in radiation protection today is determining the detrimental effects of exposure to doses lower than 100 mGy, i.e. the stochastic effects. For doses higher than 100 mGy, epidemiological studies support a linear-no-threshold (LNT) model. These epidemiological studies that validate this LNT model include studies with atomic bomb survivors, medically and occupationally exposed populations and environmentally exposed groups (e.g. people living in Ukraine following the Chernobyl disaster).[212] Policy makers use models based on these data to estimate the stochastic effects (i.e. risks) associated with exposure to doses lower than 100 mGy. These models include the LNT model, the threshold model, the hormetic (or adaptive) model and the hypersensitivity model (Figure 1.12).

The LNT model is currently used by policy makers for cancer risk estimation following exposure to low doses of IR. It assumes that for every dose a person is exposed to, there is a proportional increase in detrimental effects, such as cancer risk. The LNT model also assumes that there is no threshold dose below which no detrimental effects occur. However, other models exist in this low dose range such as the threshold model that assumes that a certain threshold dose must be exceeded in order to initiate a biological response. Per definition, no detrimental effects are expected to occur below this threshold dose. Note that this model resembles the model for tissue reactions, in which also a threshold dose must be exceeded before tissue reactions occur. Thirdly, there is the hormetic model. This model suggests that exposure to low doses of IR could induce beneficial effects, leading to a radio-adaptive response, resulting in reduced risk.[213] Finally, the

hypersensitivity model suggests that our cells/tissues are hypersensitive to very low doses of IR, thus leading to greater biological risks in the low dose range.[214] Thus far, there is a lack of evidence to definitely prove or disprove these models. Epidemiological data supports the LNT model, but only above 100 mGy. For doses lower than 100 mGy there is no clear consensus due to a lack of statistical power of the epidemiological data.[215-220] This has led to criticism on the LNT model in recent years, since there is increasingly more evidence that disproves this model in the low dose range.[218, 219, 221]

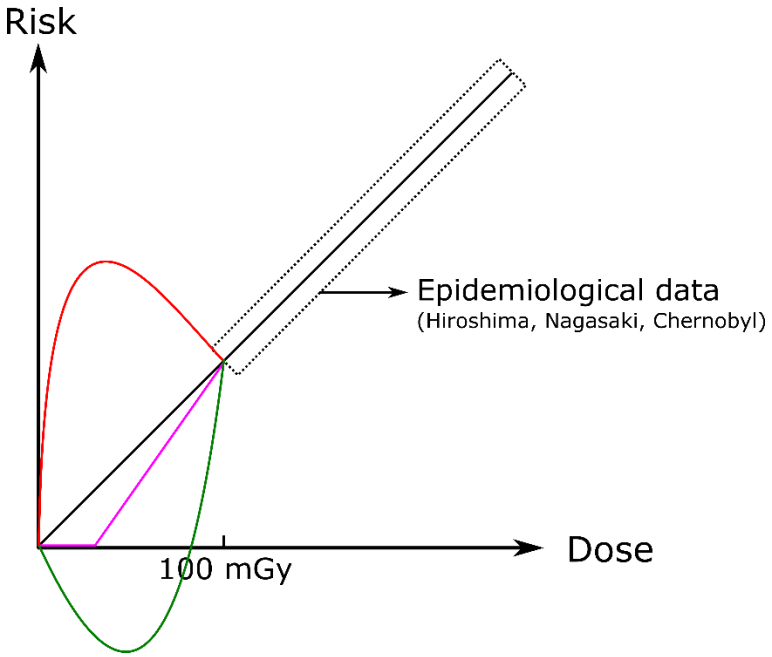

Figure 1.12. Graphical representation of the different models explaining the dose-response relationship in the low dose range. Four models are represented that show potential dose-response relationships for radiation exposure below 100 milliGray. The linear-no-threshold model (black line), the linear-threshold model (pink line), the hermetic model (green line) and the hypersensitivity model (red line). As depicted by the linear part of the curve, the effects associated with doses higher than 100 milliGray are well understood thanks to epidemiological data that is available from the Hiroshima and Nagasaki bombings, as well as the Chernobyl disaster.

1.5 The oral cavity

The oral cavity is a region in the human body that is comprised of the lips, hard palate, soft palate, the retromolar trigone, the front two-thirds of the tongue, the gingiva, teeth, buccal mucosa (BM), and the floor of the mouth under the tongue (Figure 1.13).[222] This relatively small region contains a lot of different tissues, for example muscle tissue, bone and cartilage tissue, and glandular tissue. [222] To study the effects of low dose IR exposure due to CBCT examinations in the dentomaxillofacial region, however, this thesis is limited to the study of dental stem cells, buccal mucosal cells (BMCs), and saliva samples.

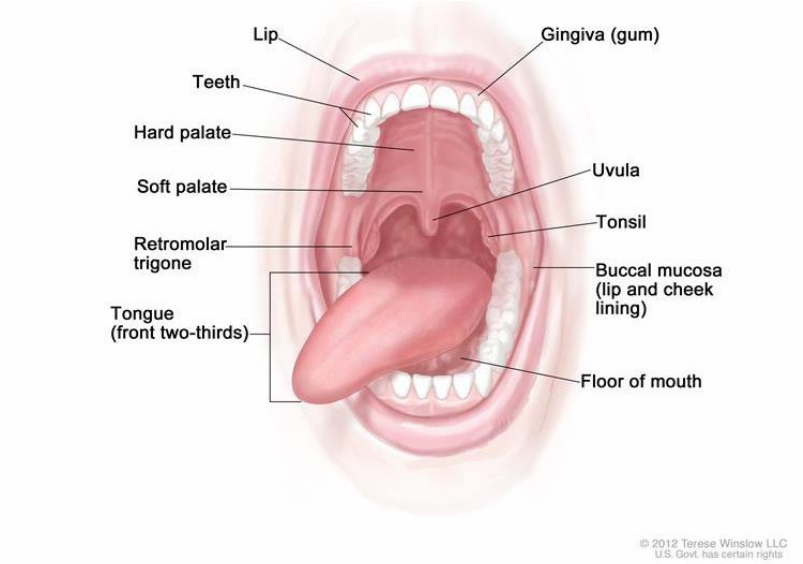

Figure 1.13. Overview of the anatomy of the oral cavity.

1.5.1 Dental stem cells

Recently, teeth have been described as the most natural, non-invasive source of mesenchymal stem cells (MSCs). Indeed, teeth harbor several types of MSCs. A major breakthrough was achieved in 2000, when Gronthos *et al.* identified and isolated progenitor cells form the dental pulp from adults. These cells were aptly dubbed dental pulp stem cells (DPSCs).[223] Later on, dental pulp stem cells were also extracted from deciduous teeth (SHEDs).[224] Since then, stem cells were also isolated from the apical papilla (SCAPs), the dental follicle (DFSCs), and the periodontal ligament (PDLSCs) (Figure 1.14).[225-227]

DPSCs and SHEDs, which are both MSCs originating from the dental pulp, have the capability to differentiate into odontoblasts. This is important *in vivo*, since mature odontoblasts cannot repair damaged dentin. Thus when dentin is damaged, DPSCs migrate from the dental pulp to the dentin surface, where they differentiate into odontoblasts. These newly formed odontoblasts will then produce reparative dentin, which is of poorer quality than the primary dentin, but still provide protection to the dental pulp.[228, 229] Therefore, DPSCs are thoroughly investigated as a natural way of repairing teeth by using DPSCs to produce dental tissues.[230, 231]

SCAPs are related to developing tooth roots. It has been shown that the presence of SCAPs is required for the continuation of root maturation.[226] Furthermore, it was reported that SCAPs are superior to DPSCs when it comes to plasticity, and versatility.[232] As a tool in tissue engineering, SCAPs are being studied for their odontogenic, osteogenic, angiogenic, and neurogenic capabilities. Finally, because of their angiogenic and neurogenic capabilities, they are also of interest for wound healing and treatment of neurodegenerative diseases.[233]

Finally, DFSCs are found in the connective tissue that surrounds the developing teeth. Like DPSCs/SHEDs and SCAPs, they are associated with tooth development. They have the ability to differentiate into osteoblasts, chondrocytes, and adipocytes *in vitro*. Furthermore, they can form calcified nodules, indicating that they can differentiate into cementum. Finally, they can also generate periodontal ligament. Their differentiation capabilities are similar to those of SCAPs.[234] DFSCs are currently investigated for tooth root regeneration.[235]

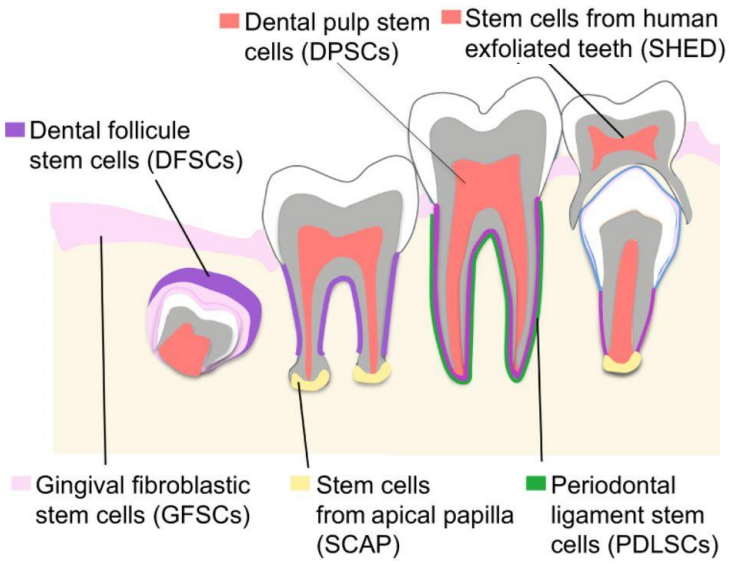

Figure 1.14. Overview of the different types of dental stem cells and their *in vivo* location. Figure adapted from Sharpe (2016).[236]

1.5.2 Buccal mucosal cells

The BM is a mucous membrane that lines the inside of the cheeks. It is a specialized, non-keratinized stratified squamous epithelium. This entails that the BM consists of several layers of cells that rest on connective tissue. The outer layers lose their nuclei, and slough off due to sheer stress in the mouth. The basal cells, on the other hand, serve as progenitor cells for the upper layers.[237]

BMCs have several major functions in the oral cavity. The most prevalent one is that of primary protection of the BM against external aggressors such as microorganisms and toxic substances. Furthermore, they can also secrete several classes of inflammatory mediators.[238] Because of this barrier function, BMCs are useful for studying the effects of exposure to environmental agents.[239, 240]

BMCs are easy to use as a biological sample, since they are easily accessible and they can be collected in a minimally invasive way.[237] They are being increasingly used for research and diagnosis. They have been used, for example, to diagnose diseases such as Prader-Willi syndrome, for verifying the increasing risk for gonadoblastoma in Turner syndrome patients, and to estimate cancer risk through detection of the *HNF1B* gene mutation.[241-243] Finally, they are also used to study the effects of exposure to genotoxins, such as IR.[239, 244-246]

1.5.3 Saliva

Saliva is the whole fluid present in the oral cavity. It originates mainly from three major salivary glands: the parotid, submandibular, and sublingual glands. Small portions originate from minor salivary glands, gingival crevicular fluid containing bacteria, BMCs, erythrocytes, leukocytes, and food debris.[247]

In vivo, its main functions are providing protection to and maintain the integrity of the BM. It does this through lubrication, buffering action, and antibacterial and antiviral activity. Finally, saliva is also important in food digestion as it contains digestive enzymes.[247] Over 1000 salivary proteins have been described so far. Most of these can also be found in plasma. Besides proteins, saliva also contains electrolytes, immunoglobulins, metabolites, hormones, and vitamins.[248-250] Because of this, saliva is often referred to as 'the mirror of the body'.[251]

Like BMCs, saliva samples are easy to collect. It can be collected non-invasively and painlessly.[249] Since the early 1990s, it is increasingly studied as a diagnostic fluid.[251, 252] Since then, it has been found that it is a suitable biofluid for –omics and disease studies.[122, 247] Genomic DNA has been isolated from saliva and has been used in several genomic studies, such as genome-wide microarrays.[253] It has also been used for clinical genetic testing, pharmacogenomics testing, diagnostic DNA testing, and population studies.[247] Furthermore, salivary proteomics has been used to detect several diseases, such

as cardiovascular disease, type II diabetes mellitus, and squamous cell carcinoma.[254-257] Additionally, salivary metabolomics has gained attention as a disease diagnostic, stratification, and early detection tool. The salivary metabolome provides a 'snapshot' of gene function, enzyme kinetic activity, and changes in metabolic reactions. For example, mass spectrometry studies have identified metabolites as biomarkers for oral squamous cell carcinoma.[258] Most of these –omics studies were reviewed by Nunes *et al*. (2015).[247] Finally, saliva has been used to study biomarkers of both high and low IR dose exposure.[134-136, 259]

1.6 References

1. Hall EJ, Giaccia AJ. Radiobiology for the radiologist. Lippincott Williams & Wilkins; 2012.
2. WHO. What is Ionizing Radiation? 2014/11/15. Available from: http://www.who.int/ionizing_radiation/about/what_is_ir/en/.
3. Martin A, Harbison S, Beach K, Cole P. An Introduction to Radiation Protection. CRC Press; 2012.
4. Dendy PP, Heaton B. Physics for diagnostic radiology. 3rd ed. Boca Raton: CRC Press; 2012. xv, 695 p. p.
5. Kudriashov IB, Kudriashov YB. Radiation Biophysics (Ionizing radiations). Nova Publishers; 2008.
6. Maalouf M, Durante M, Foray N. Biological effects of space radiation on human cells: history, advances and outcomes. J Radiat Res. 2011;52(2):126-46.
7. Gonzalez. Biological effects of low doses of ionizing radiation: A fuller picture. International Atomic Energy Agency IAEA; 1994 1994.
8. Pelliccioni M. Overview of fluence-to-effective dose and fluence-to ambient dose equivalent conversion coefficients for high energy radiation calculated using the FLUKA code. Radiation protection dosimetry. 2000;88(4):279-97.
9. Huda W, Ogden KM, Khorasani MR. Converting dose-length product to effective dose at CT. Radiology. 2008;248(3):995-1003.
10. ICRP. The 2007 Recommendations of the International Commission on Radiological Protection. ICRP Publication 103. Ann ICRP. 2007;37(2-4).
11. Giussani A. Issues related to the concept of organ dose. Luxembourg: European Union; 2018.
12. UNSCEAR. Sources and effects of ionizing radiation - UNSCEAR 2008 Report to the General Assembly with Scientific Annexes 2010;Volume 1.
13. Venkatesh E, Elluru SV. Cone beam computed tomography: basics and applications in dentistry. J Istanb Univ Fac Dent. 2017;51(3 Suppl 1):S102-S21.
14. Tang FR, Loganovsky K. Low dose or low dose rate ionizing radiation-induced health effect in the human. J Environ Radioact. 2018;192:32-47.
15. EuropeanCommission. Radiation Protection N°180 - Medical Radiation Exposure of the European Population. Luxembourgs: European Union; 2014.
16. Brenner DJ, Hall EJ. Computed tomography--an increasing source of radiation exposure. N Engl J Med. 2007;357(22):2277-84.
17. Wambani JS, Korir GK, Tries MA, Korir IK, Sakwa JM. Patient radiation exposure during general fluoroscopy examinations. J Appl Clin Med Phys. 2014;15(2):4555.
18. Etard C, Bigand E, Salvat C, Vidal V, Beregi JP, Hornbeck A, et al. Patient dose in interventional radiology: a multicentre study of the most frequent procedures in France. European radiology. 2017;27(10):4281-90.
19. RadiologyInfo.org. Radiation Dose in X-ray and CT exams. Accessed on 2018-12-06. Available from: https://www.radiologyinfo.org/en/pdf/safety-xray.pdf.
20. OECD. Health care utilisation [Internet]. Accessed on 2018-12-06.; Available from: https://www.oecd-ilibrary.org/content/data/data-00542-en.
21. OECD. Computed Tomography (CT) exams (indicator) [Internet]. Accessed on 2018-12-06.; Available from: https://data.oecd.org/healthcare/computed-tomography-ct-exams.htm.
22. Mozzo P, Procacci C, Tacconi A, Martini PT, Andreis IA. A new volumetric CT machine for dental imaging based on the cone-beam technique: preliminary results. European radiology. 1998;8(9):1558-64.
23. Arai Y, Tammisalo E, Iwai K, Hashimoto K, Shinoda K. Development of a compact computed tomographic apparatus for dental use. Dentomaxillofac Radiol. 1999;28(4):245-8.
24. Scarfe WC, Farman AG. What is cone-beam CT and how does it work? Dent Clin North Am. 2008;52(4):707-30, v.

25. Dawood A, Patel S, Brown J. Cone beam CT in dental practice. British dental journal. 2009;207(1):23-8.
26. Scarfe WC, Farman AG, Sukovic P. Clinical applications of cone-beam computed tomography in dental practice. J Can Dent Assoc. 2006;72(1):75-80.
27. De Vos W, Casselman J, Swennen GR. Cone-beam computerized tomography (CBCT) imaging of the oral and maxillofacial region: a systematic review of the literature. Int J Oral Maxillofac Surg. 2009;38(6):609-25.
28. Snel R, Van De Maele E, Politis C, Jacobs R. Digital dental radiology in Belgium: a nationwide survey. Dentomaxillofac Radiol. 2018;47(8):20180045.
29. Pauwels R. Cone beam CT for dental and maxillofacial imaging: dose matters. Radiation protection dosimetry. 2015;165(1-4):156-61.
30. Pauwels R, Beinsberger J, Collaert B, Theodorakou C, Rogers J, Walker A, et al. Effective dose range for dental cone beam computed tomography scanners. European journal of radiology. 2012;81(2):267-71.
31. Theodorakou C, Walker A, Horner K, Pauwels R, Bogaerts R, Jacobs R, et al. Estimation of paediatric organ and effective doses from dental cone beam CT using anthropomorphic phantoms. Br J Radiol. 2012;85(1010):153-60.
32. Marcu M, Hedesiu M, Salmon B, Pauwels R, Stratis A, Oenning ACC, et al. Estimation of the radiation dose for pediatric CBCT indications: a prospective study on ProMax3D. Int J Paediatr Dent. 2018.
33. Signorelli L, Patcas R, Peltomaki T, Schatzle M. Radiation dose of cone-beam computed tomography compared to conventional radiographs in orthodontics. Journal of orofacial orthopedics = Fortschritte der Kieferorthopadie : Organ/official journal Deutsche Gesellschaft fur Kieferorthopadie. 2016;77(1):9-15.
34. Li G. Patient radiation dose and protection from cone-beam computed tomography. Imaging Sci Dent. 2013;43(2):63-9.
35. Loubele M, Bogaerts R, Van Dijck E, Pauwels R, Vanheusden S, Suetens P, et al. Comparison between effective radiation dose of CBCT and MSCT scanners for dentomaxillofacial applications. European journal of radiology. 2009;71(3):461-8.
36. Oenning AC, Jacobs R, Pauwels R, Stratis A, Hedesiu M, Salmon B, et al. Cone-beam CT in paediatric dentistry: DIMITRA project position statement. Pediatr Radiol. 2017.
37. Mupparapu M, Nadeau C. Oral and Maxillofacial Imaging. Dent Clin North Am. 2016;60(1):1-37.
38. Dreizin D, Nam AJ, Tirada N, Levin MD, Stein DM, Bodanapally UK, et al. Multidetector CT of Mandibular Fractures, Reductions, and Complications: A Clinically Relevant Primer for the Radiologist. Radiographics : a review publication of the Radiological Society of North America, Inc. 2016;36(5):1539-64.
39. UNSCEAR. UNSCEAR 2013 Report: Sources, effects and risks of ionizing radiation - Volume II Annex B - Effects of radiation exposure of children. 2013.
40. Holmberg O, Czarwinski R, Mettler F. The importance and unique aspects of radiation protection in medicine. European journal of radiology. 2010;76(1):6-10.
41. Ron E. Ionizing radiation and cancer risk: evidence from epidemiology. Radiat Res. 1998;150(5 Suppl):S30-41.
42. ICRP. Recommendations of the International Commission on Radiological Protection. ICRP Publication 60. Ann. ICRP 21. 1990.
43. Brenner DJ. Estimating cancer risks from pediatric CT: going from the qualitative to the quantitative. Pediatr Radiol. 2002;32(4):228-1; discussion 42-4.
44. Hall EJ. Lessons we have learned from our children: cancer risks from diagnostic radiology. Pediatr Radiol. 2002;32(10):700-6.
45. Schroeder AR, Redberg RF. The harm in looking. JAMA Pediatr. 2013;167(8):693-5.
46. Gee A. Radiation Concerns Rise With Patients' Exposure. New York Times. 2012 June 13 2012.
47. Bogdanich W. CMJ. Radiation Worries for Children in Dentists' Chairs. New York Times. 2010.
48. Mulvihill DJ, Jhawar S, Kostis JB, Goyal S. Diagnostic Medical Imaging in Pediatric Patients and Subsequent Cancer Risk. Acad Radiol. 2017;24(11):1456-62.

49. Miglioretti DL, Johnson E, Williams A, Greenlee RT, Weinmann S, Solberg LI, et al. The use of computed tomography in pediatrics and the associated radiation exposure and estimated cancer risk. JAMA Pediatr. 2013;167(8):700-7.
50. Pearce MS, Salotti JA, Little MP, McHugh K, Lee C, Kim KP, et al. Radiation exposure from CT scans in childhood and subsequent risk of leukaemia and brain tumours: a retrospective cohort study. Lancet. 2012;380(9840):499-505.
51. Mathews JD, Forsythe AV, Brady Z, Butler MW, Goergen SK, Byrnes GB, et al. Cancer risk in 680,000 people exposed to computed tomography scans in childhood or adolescence: data linkage study of 11 million Australians. BMJ. 2013;346:f2360.
52. Krille L, Dreger S, Schindel R, Albrecht T, Asmussen M, Barkhausen J, et al. Risk of cancer incidence before the age of 15 years after exposure to ionising radiation from computed tomography: results from a German cohort study. Radiat Environ Biophys. 2015;54(1):1-12.
53. Huang WY, Muo CH, Lin CY, Jen YM, Yang MH, Lin JC, et al. Paediatric head CT scan and subsequent risk of malignancy and benign brain tumour: a nation-wide population-based cohort study. Br J Cancer. 2014;110(9):2354-60.
54. Hall EJ, Brenner DJ. Cancer risks from diagnostic radiology: the impact of new epidemiological data. Br J Radiol. 2012;85(1020):e1316-7.
55. Brenner DJ, Hall EJ. Cancer risks from CT scans: now we have data, what next? Radiology. 2012;265(2):330-1.
56. Stewart A, Webb J, Hewitt D. A survey of childhood malignancies. Br Med J. 1958;1(5086):1495-508.
57. Winn DM, Li FP, Robison LL, Mulvihill JJ, Daigle AE, Fraumeni JF, Jr. A case-control study of the etiology of Ewing's sarcoma. Cancer Epidemiol Biomarkers Prev. 1992;1(7):525-32.
58. Shu XO, Jin F, Linet MS, Zheng W, Clemens J, Mills J, et al. Diagnostic-X-Ray and Ultrasound Exposure and Risk of Childhood-Cancer. Brit J Cancer. 1994;70(3):531-6.
59. Polhemus DW, Koch R. Leukemia and medical radiation. Pediatrics. 1959;23(3):453-61.
60. Graham S, Levin ML, Lilienfeld AM, Schuman LM, Gibson R, Dowd JE, et al. Preconception, intrauterine, and postnatal irradiation as related to leukemia. Natl Cancer Inst Monogr. 1966;19:347-71.
61. Shu XO, Potter JD, Linet MS, Severson RK, Han D, Kersey JH, et al. Diagnostic X-rays and ultrasound exposure and risk of childhood acute lymphoblastic leukemia by immunophenotype. Cancer Epidemiol Biomarkers Prev. 2002;11(2):177-85.
62. Infante-Rivard C, Mathonnet G, Sinnett D. Risk of childhood leukemia associated with diagnostic irradiation and polymorphisms in DNA repair genes. Environ Health Perspect. 2000;108(6):495-8.
63. Bartley K, Metayer C, Selvin S, Ducore J, Buffler P. Diagnostic X-rays and risk of childhood leukaemia. Int J Epidemiol. 2010;39(6):1628-37.
64. Howe GR, Burch JD, Chiarelli AM, Risch HA, Choi BC. An exploratory case-control study of brain tumors in children. Cancer Res. 1989;49(15):4349-52.
65. Hoffman DA, Lonstein JE, Morin MM, Visscher W, Harris BS, 3rd, Boice JD, Jr. Breast cancer in women with scoliosis exposed to multiple diagnostic x rays. J Natl Cancer Inst. 1989;81(17):1307-12.
66. Doody MM, Lonstein JE, Stovall M, Hacker DG, Luckyanov N, Land CE. Breast cancer mortality after diagnostic radiography: findings from the U.S. Scoliosis Cohort Study. Spine (Phila Pa 1976). 2000;25(16):2052-63.
67. Ronckers CM, Doody MM, Lonstein JE, Stovall M, Land CE. Multiple diagnostic X-rays for spine deformities and risk of breast cancer. Cancer Epidemiol Biomarkers Prev. 2008;17(3):605-13.
68. Yeh JK, Chen CH. Estimated radiation risk of cancer from dental cone-beam computed tomography imaging in orthodontics patients. BMC Oral Health. 2018;18(1):131.
69. Pauwels R, Cockmartin L, Ivanauskaite D, Urboniene A, Gavala S, Donta C, et al. Estimating cancer risk from dental cone-beam CT exposures based on skin dosimetry. Phys Med Biol. 2014;59(14):3877-91.

70. Carlin V, Artioli AJ, Matsumoto MA, Filho HN, Borgo E, Oshima CT, et al. Biomonitoring of DNA damage and cytotoxicity in individuals exposed to cone beam computed tomography. Dentomaxillofac Radiol. 2010;39(5):295-9.
71. Lorenzoni DC, Fracalossi AC, Carlin V, Ribeiro DA, Sant'anna EF. Mutagenicity and cytotoxicity in patients submitted to ionizing radiation. Angle Orthod. 2013;83(1):104-9.
72. Yang P, Hao S, Gong X, Li G. Cytogenetic biomonitoring in individuals exposed to cone beam CT: comparison among exfoliated buccal mucosa cells, cells of tongue and epithelial gingival cells. Dentomaxillofac Radiol. 2017;46(5):20160413.
73. da Fonte JBM, de Andrade TM, Albuquerque RLC, de Melo MDB, Takeshita WM. Evidence of genotoxicity and cytotoxicity of X-rays in the oral mucosa epithelium of adults subjected to cone beam CT. Dentomaxillofac Rad. 2018;47(2).
74. Li G, Yang P, Hao S, Hu W, Liang C, Zou BS, et al. Buccal mucosa cell damage in individuals following dental X-ray examinations. Sci Rep. 2018;8(1):2509.
75. Lomax ME, Folkes LK, O'Neill P. Biological consequences of radiation-induced DNA damage: relevance to radiotherapy. Clinical oncology. 2013;25(10):578-85.
76. OpenStax.Chemistry. Biological effects of radiation 2019-01-25. Available from: https://cnx.org/contents/ImShFeDW@8/Biological-Effects-of-Radiation.
77. D. K. Maurya TPAD. Role of Radioprotectors in the Inhibition of DNA Damage and Modulation of DNA Repair After Exposure to Gamma-Radiation. In: Chen CC, editor. Selected Topics in DNA Repair: InTech.; 2011.
78. Lobrich M, Shibata A, Beucher A, Fisher A, Ensminger M, Goodarzi AA, et al. gammaH2AX foci analysis for monitoring DNA double-strand break repair: strengths, limitations and optimization. Cell cycle (Georgetown, Tex). 2010;9(4):662-9.
79. Panier S, Boulton SJ. Double-strand break repair: 53BP1 comes into focus. Nature reviews Molecular cell biology. 2014;15(1):7-18.
80. Khanna KK, Jackson SP. DNA double-strand breaks: signaling, repair and the cancer connection. Nat Genet. 2001;27(3):247-54.
81. Jackson SP. Sensing and repairing DNA double-strand breaks. Carcinogenesis. 2002;23(5):687-96.
82. Le Caer S. Water Radiolysis: Influence of Oxide Surfaces on H-2 Production under Ionizing Radiation. Water-Sui. 2011;3(1):235-53.
83. Islam MT. Radiation interactions with biological systems. Int J Radiat Biol. 2017;93(5):487-93.
84. Azzam EI, Jay-Gerin JP, Pain D. Ionizing radiation-induced metabolic oxidative stress and prolonged cell injury. Cancer letters. 2012;327(1-2):48-60.
85. Halliwell B, Clement MV, Long LH. Hydrogen peroxide in the human body. FEBS Lett. 2000;486(1):10-3.
86. He L, He T, Farrar S, Ji L, Liu T, Ma X. Antioxidants Maintain Cellular Redox Homeostasis by Elimination of Reactive Oxygen Species. Cell Physiol Biochem. 2017;44(2):532-53.
87. D'Autreaux B, Toledano MB. ROS as signalling molecules: mechanisms that generate specificity in ROS homeostasis. Nature reviews Molecular cell biology. 2007;8(10):813-24.
88. Holmstrom KM, Finkel T. Cellular mechanisms and physiological consequences of redox-dependent signalling. Nature reviews Molecular cell biology. 2014;15(6):411-21.
89. Brieger K, Schiavone S, Miller FJ, Jr., Krause KH. Reactive oxygen species: from health to disease. Swiss Med Wkly. 2012;142:w13659.
90. Ratnam DV, Ankola DD, Bhardwaj V, Sahana DK, Kumar MN. Role of antioxidants in prophylaxis and therapy: A pharmaceutical perspective. J Control Release. 2006;113(3):189-207.
91. Christofidou-Solomidou M, Muzykantov VR. Antioxidant strategies in respiratory medicine. Treat Respir Med. 2006;5(1):47-78.
92. Fukai T, Ushio-Fukai M. Superoxide dismutases: role in redox signaling, vascular function, and diseases. Antioxid Redox Signal. 2011;15(6):1583-606.
93. Lubos E, Loscalzo J, Handy DE. Glutathione peroxidase-1 in health and disease: from molecular mechanisms to therapeutic opportunities. Antioxid Redox Signal. 2011;15(7):1957-97.
94. Jee JP, Lim SJ, Park JS, Kim CK. Stabilization of all-trans retinol by loading lipophilic antioxidants in solid lipid nanoparticles. Eur J Pharm Biopharm. 2006;63(2):134-9.

95. Barros AI, Nunes FM, Goncalves B, Bennett RN, Silva AP. Effect of cooking on total vitamin C contents and antioxidant activity of sweet chestnuts (Castanea sativa Mill.). Food Chem. 2011;128(1):165-72.
96. Tabassum A, Bristow RG, Venkateswaran V. Ingestion of selenium and other antioxidants during prostate cancer radiotherapy: a good thing? Cancer Treat Rev. 2010;36(3):230-4.
97. Prasad AS, Bao B, Beck FW, Kucuk O, Sarkar FH. Antioxidant effect of zinc in humans. Free Radic Biol Med. 2004;37(8):1182-90.
98. Waring WS, Webb DJ, Maxwell SR. Systemic uric acid administration increases serum antioxidant capacity in healthy volunteers. J Cardiovasc Pharmacol. 2001;38(3):365-71.
99. Halliwell B, Gutteridge JMC. Measurement of reactive species. Free Radicals in Biology and Medicine: Oxford University Press; 2015.
100. Han JY, Hong JT, Oh KW. In vivo Electron Spin Resonance: An Effective New Tool for Reactive Oxygen Species/Reactive Nitrogen Species Measurement. Arch Pharm Res. 2010;33(9):1293-9.
101. Halliwell B. Establishing the significance and optimal intake of dietary antioxidants: the biomarker concept. Nutr Rev. 1999;57(4):104-13.
102. Dalle-Donne I, Rossi R, Colombo R, Giustarini D, Milzani A. Biomarkers of oxidative damage in human disease. Clin Chem. 2006;52(4):601-23.
103. Frijhoff J, Winyard PG, Zarkovic N, Davies SS, Stocker R, Cheng D, et al. Clinical Relevance of Biomarkers of Oxidative Stress. Antioxid Redox Signal. 2015;23(14):1144-70.
104. Dean RT, Fu S, Stocker R, Davies MJ. Biochemistry and pathology of radical-mediated protein oxidation. Biochem J. 1997;324 (Pt 1):1-18.
105. Pantke U, Volk T, Schmutzler M, Kox WJ, Sitte N, Grune T. Oxidized proteins as a marker of oxidative stress during coronary heart surgery. Free Radic Biol Med. 1999;27(9-10):1080-6.
106. Trpkovic A, Resanovic I, Stanimirovic J, Radak D, Mousa SA, Cenic-Milosevic D, et al. Oxidized low-density lipoprotein as a biomarker of cardiovascular diseases. Crit Rev Clin Lab Sci. 2015;52(2):70-85.
107. Holvoet P, Donck J, Landeloos M, Brouwers E, Luijtens K, Arnout J, et al. Correlation between oxidized low density lipoproteins and von Willebrand factor in chronic renal failure. Thromb Haemost. 1996;76(5):663-9.
108. Negre-Salvayre A, Auge N, Ayala V, Basaga H, Boada J, Brenke R, et al. Pathological aspects of lipid peroxidation. Free Radic Res. 2010;44(10):1125-71.
109. Spickett CM, Wiswedel I, Siems W, Zarkovic K, Zarkovic N. Advances in methods for the determination of biologically relevant lipid peroxidation products. Free Radic Res. 2010;44(10):1172-202.
110. Loft S, Poulsen HE. Cancer risk and oxidative DNA damage in man. J Mol Med (Berl). 1996;74(6):297-312.
111. Poulsen HE, Prieme H, Loft S. Role of oxidative DNA damage in cancer initiation and promotion. Eur J Cancer Prev. 1998;7(1):9-16.
112. Kasai H, Nishimura S. Hydroxylation of deoxyguanosine at the C-8 position by ascorbic acid and other reducing agents. Nucleic Acids Res. 1984;12(4):2137-45.
113. Kasai H, Nishimura S. Hydroxylation of deoxy guanosine at the C-8 position by polyphenols and aminophenols in the presence of hydrogen peroxide and ferric ion. Gan. 1984;75(7):565-6.
114. Nishimura S. 8-Hydroxyguanine: a base for discovery. DNA Repair (Amst). 2011;10(11):1078-83.
115. Shakeri Manesh S, Sangsuwan T, Pour Khavari A, Fotouhi A, Emami SN, Haghdoost S. MTH1, an 8-oxo-2'-deoxyguanosine triphosphatase, and MYH, a DNA glycosylase, cooperate to inhibit mutations induced by chronic exposure to oxidative stress of ionising radiation. Mutagenesis. 2017;32(3):389-96.
116. Haghdoost S, Czene S, Naslund I, Skog S, Harms-Ringdahl M. Extracellular 8-oxo-dG as a sensitive parameter for oxidative stress in vivo and in vitro. Free Radic Res. 2005;39(2):153-62.
117. Cooke MS, Singh R, Hall GK, Mistry V, Duarte TL, Farmer PB, et al. Evaluation of enzyme-linked immunosorbent assay and liquid chromatography-tandem mass

spectrometry methodology for the analysis of 8-oxo-7,8-dihydro-2'-deoxyguanosine in saliva and urine. Free Radic Biol Med. 2006;41(12):1829-36.
118. Evans MD, Saparbaev M, Cooke MS. DNA repair and the origins of urinary oxidized 2'-deoxyribonucleosides. Mutagenesis. 2010;25(5):433-42.
119. Rossner P, Jr., Mistry V, Singh R, Sram RJ, Cooke MS. Urinary 8-oxo-7,8-dihydro-2'-deoxyguanosine values determined by a modified ELISA improves agreement with HPLC-MS/MS. Biochem Biophys Res Commun. 2013;440(4):725-30.
120. Cooke MS, Evans MD, Dizdaroglu M, Lunec J. Oxidative DNA damage: mechanisms, mutation, and disease. FASEB J. 2003;17(10):1195-214.
121. Breton J, Sichel F, Pottier D, Prevost V. Measurement of 8-oxo-7,8-dihydro-2'-deoxyguanosine in peripheral blood mononuclear cells: optimisation and application to samples from a case-control study on cancers of the oesophagus and cardia. Free Radic Res. 2005;39(1):21-30.
122. Tothova L, Kamodyova N, Cervenka T, Celec P. Salivary markers of oxidative stress in oral diseases. Front Cell Infect Microbiol. 2015;5:73.
123. Arunachalam R. Salivary 8-Hydroxydeoxyguanosine – a valuable indicator for oxidative DNA damage in periodontal disease. The Saudi Journal for Dental Research. 2014;6:15-20.
124. de Sousa MC, Vieira RB, Dos Santos DS, Carvalho CA, Camargo SE, Mancini MN, et al. Antioxidants and biomarkers of oxidative damage in the saliva of patients with Down's syndrome. Arch Oral Biol. 2015;60(4):600-5.
125. Bahar G, Feinmesser R, Shpitzer T, Popovtzer A, Nagler RM. Salivary analysis in oral cancer patients: DNA and protein oxidation, reactive nitrogen species, and antioxidant profile. Cancer. 2007;109(1):54-9.
126. Golenia A, Leskiewicz M, Regulska M, Budziszewska B, Szczesny E, Jagiella J, et al. Catalase activity in blood fractions of patients with sporadic ALS. Pharmacol Rep. 2014;66(4):704-7.
127. Ahmadi-Motamayel F, Vaziri-Amjad S, Goodarzi MT, Poorolajal J. Evaluation of Salivary Vitamin C and Catalase in HIV Positive and Healthy HIV Negative Control Group. Infect Disord Drug Targets. 2017;17(2):101-5.
128. Ahmadi-Motamayel F, Falsafi P, Goodarzi MT, Poorolajal J. Evaluation of salivary catalase, vitamin C, and alpha-amylase in smokers and non-smokers: a retrospective cohort study. J Oral Pathol Med. 2017;46(5):377-80.
129. Almerich-Silla JM, Montiel-Company JM, Pastor S, Serrano F, Puig-Silla M, Dasi F. Oxidative Stress Parameters in Saliva and Its Association with Periodontal Disease and Types of Bacteria. Dis Markers. 2015;2015:653537.
130. Nalkiran I, Turan S, Arikan S, Kahraman OT, Acar L, Yaylim I, et al. Determination of gene expression and serum levels of MnSOD and GPX1 in colorectal cancer. Anticancer Res. 2015;35(1):255-9.
131. Puthran SS, Sudha K, Rao GM, Shetty BV. Oxidative stress and low dose ionizing radiation. Indian J Physiol Pharmacol. 2009;53(2):181-4.
132. Pernot E, Hall J, Baatout S, Benotmane MA, Blanchardon E, Bouffler S, et al. Ionizing radiation biomarkers for potential use in epidemiological studies. Mutat Res. 2012;751(2):258-86.
133. Tharmalingam S, Sreetharan S, Kulesza AV, Boreham DR, Tai TC. Low-Dose Ionizing Radiation Exposure, Oxidative Stress and Epigenetic Programing of Health and Disease. Radiat Res. 2017;188(4.2):525-38.
134. Pernot E, Cardis E, Badie C. Usefulness of saliva samples for biomarker studies in radiation research. Cancer Epidemiol Biomarkers Prev. 2014;23(12):2673-80.
135. Hall J, Jeggo PA, West C, Gomolka M, Quintens R, Badie C, et al. Ionizing radiation biomarkers in epidemiological studies - An update. Mutat Res. 2017;771:59-84.
136. Moore HD, Ivey RG, Voytovich UJ, Lin C, Stirewalt DL, Pogosova-Agadjanyan EL, et al. The human salivary proteome is radiation responsive. Radiat Res. 2014;181(5):521-30.
137. Ciccia A, Elledge SJ. The DNA damage response: making it safe to play with knives. Mol Cell. 2010;40(2):179-204.
138. Sulli G, Di Micco R, d'Adda di Fagagna F. Crosstalk between chromatin state and DNA damage response in cellular senescence and cancer. Nat Rev Cancer. 2012;12(10):709-20.

139. De la Torre C, Pincheira J, Lopez-Saez JF. Human syndromes with genomic instability and multiprotein machines that repair DNA double-strand breaks. Histol Histopathol. 2003;18(1):225-43.
140. Goodarzi AA, Jeggo PA. Irradiation induced foci (IRIF) as a biomarker for radiosensitivity. Mutat Res. 2012;736(1-2):39-47.
141. Bonner WM, Redon CE, Dickey JS, Nakamura AJ, Sedelnikova OA, Solier S, et al. GammaH2AX and cancer. Nat Rev Cancer. 2008;8(12):957-67.
142. Kinner A, Wu W, Staudt C, Iliakis G. Gamma-H2AX in recognition and signaling of DNA double-strand breaks in the context of chromatin. Nucleic Acids Res. 2008;36(17):5678-94.
143. Riches LC, Lynch AM, Gooderham NJ. Early events in the mammalian response to DNA double-strand breaks. Mutagenesis. 2008;23(5):331-9.
144. Redon CE, Weyemi U, Parekh PR, Huang D, Burrell AS, Bonner WM. gamma-H2AX and other histone post-translational modifications in the clinic. Biochim Biophys Acta. 2012;1819(7):743-56.
145. Kleiner RE, Verma P, Molloy KR, Chait BT, Kapoor TM. Chemical proteomics reveals a gammaH2AX-53BP1 interaction in the DNA damage response. Nat Chem Biol. 2015;11(10):807-14.
146. Markova E, Schultz N, Belyaev IY. Kinetics and dose-response of residual 53BP1/gamma-H2AX foci: co-localization, relationship with DSB repair and clonogenic survival. Int J Radiat Biol. 2007;83(5):319-29.
147. Markova E, Vasilyev S, Belyaev I. 53BP1 foci as a marker of tumor cell radiosensitivity. Neoplasma. 2015;62(5):770-6.
148. Baselet B, Belmans N, Coninx E, Lowe D, Janssen A, Michaux A, et al. Functional Gene Analysis Reveals Cell Cycle Changes and Inflammation in Endothelial Cells Irradiated with a Single X-ray Dose. Front Pharmacol. 2017;8:213.
149. Lou Z, Minter-Dykhouse K, Franco S, Gostissa M, Rivera MA, Celeste A, et al. MDC1 maintains genomic stability by participating in the amplification of ATM-dependent DNA damage signals. Mol Cell. 2006;21(2):187-200.
150. Stucki M, Clapperton JA, Mohammad D, Yaffe MB, Smerdon SJ, Jackson SP. MDC1 directly binds phosphorylated histone H2AX to regulate cellular responses to DNA double-strand breaks. Cell. 2005;123(7):1213-26.
151. Ivashkevich A, Redon CE, Nakamura AJ, Martin RF, Martin OA. Use of the gamma-H2AX assay to monitor DNA damage and repair in translational cancer research. Cancer letters. 2012;327(1-2):123-33.
152. Kobayashi J, Iwabuchi K, Miyagawa K, Sonoda E, Suzuki K, Takata M, et al. Current topics in DNA double-strand break repair. J Radiat Res. 2008;49(2):93-103.
153. Caspari T, Carr AM. Checkpoints: How to flag up double-strand breaks. Current Biology. 2002;12(3):R105-R7.
154. Barnum KJ, O'Connell MJ. Cell cycle regulation by checkpoints. Methods Mol Biol. 2014;1170:29-40.
155. Besson A, Dowdy SF, Roberts JM. CDK inhibitors: cell cycle regulators and beyond. Dev Cell. 2008;14(2):159-69.
156. Santivasi WL, Xia F. Ionizing Radiation-Induced DNA Damage, Response, and Repair. Antioxid Redox Sign. 2014;21(2):251-9.
157. Shimada M, Nakanishi M. DNA damage checkpoints and cancer. J Mol Histol. 2006;37(5-7):253-60.
158. Bartek J, Lukas J. Pathways governing G1/S transition and their response to DNA damage. FEBS Lett. 2001;490(3):117-22.
159. Bohgaki T, Bohgaki M, Hakem R. DNA double-strand break signaling and human disorders. Genome Integr. 2010;1(1):15.
160. Yaneva M, Kowalewski T, Lieber MR. Interaction of DNA-dependent protein kinase with DNA and with Ku: biochemical and atomic-force microscopy studies. EMBO J. 1997;16(16):5098-112.
161. Giacinti C, Giordano A. RB and cell cycle progression. Oncogene. 2006;25(38):5220-7.
162. Falck J, Petrini JH, Williams BR, Lukas J, Bartek J. The DNA damage-dependent intra-S phase checkpoint is regulated by parallel pathways. Nat Genet. 2002;30(3):290-4.

163. Pawlik TM, Keyomarsi K. Role of cell cycle in mediating sensitivity to radiotherapy. Int J Radiat Oncol Biol Phys. 2004;59(4):928-42.
164. Jeggo P, Lavin MF. Cellular radiosensitivity: how much better do we understand it? Int J Radiat Biol. 2009;85(12):1061-81.
165. Chowdhury D, Choi YE, Brault ME. Charity begins at home: non-coding RNA functions in DNA repair. Nature reviews Molecular cell biology. 2013;14(3):181-9.
166. Lieber MR, Ma Y, Pannicke U, Schwarz K. Mechanism and regulation of human non-homologous DNA end-joining. Nature reviews Molecular cell biology. 2003;4(9):712-20.
167. Peng G, Lin SY. Exploiting the homologous recombination DNA repair network for targeted cancer therapy. World J Clin Oncol. 2011;2(2):73-9.
168. Iliakis G, Murmann T, Soni A. Alternative end-joining repair pathways are the ultimate backup for abrogated classical non-homologous end-joining and homologous recombination repair: Implications for the formation of chromosome translocations. Mutat Res Genet Toxicol Environ Mutagen. 2015;793:166-75.
169. Price BD, D'Andrea AD. Chromatin remodeling at DNA double-strand breaks. Cell. 2013;152(6):1344-54.
170. Bunting SF, Callen E, Wong N, Chen HT, Polato F, Gunn A, et al. 53BP1 inhibits homologous recombination in Brca1-deficient cells by blocking resection of DNA breaks. Cell. 2010;141(2):243-54.
171. Surova O, Zhivotovsky B. Various modes of cell death induced by DNA damage. Oncogene. 2013;32(33):3789-97.
172. Nagano T, Nakano M, Nakashima A, Onishi K, Yamao S, Enari M, et al. Identification of cellular senescence-specific genes by comparative transcriptomics. Sci Rep. 2016;6:31758.
173. Itahana K, Campisi J, Dimri GP. Methods to detect biomarkers of cellular senescence: the senescence-associated beta-galactosidase assay. Methods Mol Biol. 2007;371:21-31.
174. Ortiz-Montero P, Londono-Vallejo A, Vernot JP. Senescence-associated IL-6 and IL-8 cytokines induce a self- and cross-reinforced senescence/inflammatory milieu strengthening tumorigenic capabilities in the MCF-7 breast cancer cell line. Cell Commun Signal. 2017;15(1):17.
175. Byun HO, Lee YK, Kim JM, Yoon G. From cell senescence to age-related diseases: differential mechanisms of action of senescence-associated secretory phenotypes. BMB Rep. 2015;48(10):549-58.
176. Munoz-Espin D, Serrano M. Cellular senescence: from physiology to pathology. Nature reviews Molecular cell biology. 2014;15(7):482-96.
177. Eriksson D, Stigbrand T. Radiation-induced cell death mechanisms. Tumour Biol. 2010;31(4):363-72.
178. Norbury CJ, Hickson ID. Cellular responses to DNA damage. Annu Rev Pharmacol Toxicol. 2001;41:367-401.
179. Glucksmann A. Cell deaths in normal vertebrate ontogeny. Biol Rev Camb Philos Soc. 1951;26(1):59-86.
180. Elmore S. Apoptosis: a review of programmed cell death. Toxicol Pathol. 2007;35(4):495-516.
181. Roos WP, Kaina B. DNA damage-induced cell death: from specific DNA lesions to the DNA damage response and apoptosis. Cancer letters. 2013;332(2):237-48.
182. Panayi ND ME, Breshears ES, Burd R. Aberrant Death Pathways in Melanoma, Recent Advances in the Biology, Therapy and Management of Melanoma. In: LM D, editor.2013.
183. Berger NA. Poly(ADP-ribose) in the cellular response to DNA damage. Radiat Res. 1985;101(1):4-15.
184. Golstein P, Kroemer G. Cell death by necrosis: towards a molecular definition. Trends Biochem Sci. 2007;32(1):37-43.
185. Czarny P, Pawlowska E, Bialkowska-Warzecha J, Kaarniranta K, Blasiak J. Autophagy in DNA damage response. International journal of molecular sciences. 2015;16(2):2641-62.
186. Barnard S, Bouffler S, Rothkamm K. The shape of the radiation dose response for DNA double-strand break induction and repair. Genome Integr. 2013;4(1):1.
187. Rothkamm K, Barnard S, Moquet J, Ellender M, Rana Z, Burdak-Rothkamm S. DNA damage foci: Meaning and significance. Environ Mol Mutagen. 2015;56(6):491-504.

188. Asaithamby A, Chen DJ. Cellular responses to DNA double-strand breaks after low-dose gamma-irradiation. Nucleic Acids Res. 2009;37(12):3912-23.
189. Sedelnikova OA, Rogakou EP, Panyutin IG, Bonner WM. Quantitative detection of (125)IdU-induced DNA double-strand breaks with gamma-H2AX antibody. Radiat Res. 2002;158(4):486-92.
190. Rothkamm K, Horn S. gamma-H2AX as protein biomarker for radiation exposure. Ann Ist Super Sanita. 2009;45(3):265-71.
191. Ghardi M, Moreels M, Chatelain B, Chatelain C, Baatout S. Radiation-induced double strand breaks and subsequent apoptotic DNA fragmentation in human peripheral blood mononuclear cells. Int J Mol Med. 2012;29(5):769-80.
192. Horn S, Barnard S, Brady D, Prise KM, Rothkamm K. Combined analysis of gamma-H2AX/53BP1 foci and caspase activation in lymphocyte subsets detects recent and more remote radiation exposures. Radiat Res. 2013;180(6):603-9.
193. de Feraudy S, Revet I, Bezrookove V, Feeney L, Cleaver JE. A minority of foci or pan-nuclear apoptotic staining of gammaH2AX in the S phase after UV damage contain DNA double-strand breaks. Proc Natl Acad Sci U S A. 2010;107(15):6870-5.
194. Schultz LB, Chehab NH, Malikzay A, Halazonetis TD. p53 binding protein 1 (53BP1) is an early participant in the cellular response to DNA double-strand breaks. J Cell Biol. 2000;151(7):1381-90.
195. Solier S, Sordet O, Kohn KW, Pommier Y. Death receptor-induced activation of the Chk2- and histone H2AX-associated DNA damage response pathways. Mol Cell Biol. 2009;29(1):68-82.
196. Solier S, Pommier Y. The apoptotic ring: a novel entity with phosphorylated histones H2AX and H2B and activated DNA damage response kinases. Cell cycle (Georgetown, Tex). 2009;8(12):1853-9.
197. Welschinger R, Bendall LJ. Temporal Tracking of Cell Cycle Progression Using Flow Cytometry without the Need for Synchronization. J Vis Exp. 2015(102):e52840.
198. Socratic. Cell cycle overview 2019/03/22. Available from: https://socratic.org/biology/the-eukaryotic-cell/cell-cycle-overview.
199. Muthna D, Soukup T, Vavrova J, Mokry J, Cmielova J, Visek B, et al. Irradiation of Adult Human Dental Pulp Stem Cells Provokes Activation of p53, Cell Cycle Arrest, and Senescence but Not Apoptosis. Stem Cells and Development. 2010;19(12):1855-62.
200. Dimri GP, Lee X, Basile G, Acosta M, Scott G, Roskelley C, et al. A biomarker that identifies senescent human cells in culture and in aging skin in vivo. Proc Natl Acad Sci U S A. 1995;92(20):9363-7.
201. Virag P, Hedesiu M, Soritau O, Perde-Schrepler M, Brie I, Pall E, et al. Low-dose radiations derived from cone-beam CT induce transient DNA damage and persistent inflammatory reactions in stem cells from deciduous teeth. Dentomaxillofac Radiol. 2018:20170462.
202. Coppe JP, Desprez PY, Krtolica A, Campisi J. The senescence-associated secretory phenotype: the dark side of tumor suppression. Annu Rev Pathol. 2010;5:99-118.
203. Yau SW, Azar WJ, Sabin MA, Werther GA, Russo VC. IGFBP-2 - taking the lead in growth, metabolism and cancer. J Cell Commun Signal. 2015;9(2):125-42.
204. Wang S, Moerman EJ, Jones RA, Thweatt R, Goldstein S. Characterization of IGFBP-3, PAI-1 and SPARC mRNA expression in senescent fibroblasts. Mech Ageing Dev. 1996;92(2-3):121-32.
205. Pickard A, McCance DJ. IGF-Binding Protein 2 - Oncogene or Tumor Suppressor? Front Endocrinol (Lausanne). 2015;6:25.
206. Baege AC, Disbrow GL, Schlegel R. IGFBP-3, a marker of cellular senescence, is overexpressed in human papillomavirus-immortalized cervical cells and enhances IGF-1-induced mitogenesis. J Virol. 2004;78(11):5720-7.
207. Stevens L. Injurious effects on the skin. Br Med J. 1896;1:998.
208. Gilchrist T. A case of dermatitis due to the x rays. Bull Johns Hopkins Hosp. 1897;8:17-22.
209. Frieben A. Demonstration eines Cancroids des rechten Handrückens, das sich nach langdauernder Einwirking von Röntgen-strahlen bei einem 33 jährigen Mann entwickelt hatte. Fortschr Rontgenstr. 1902;6:106.

210. Little MP, Wakeford R, Tawn EJ, Bouffler SD, Berrington de Gonzalez A. Risks associated with low doses and low dose rates of ionizing radiation: why linearity may be (almost) the best we can do. Radiology. 2009;251(1):6-12.
211. Walker JS. Permissible dose : a history of radiation protection in the twentieth century. Berkeley: University of California Press; 2000. xii, 168 p. p.
212. UNSCEAR. UNSCEAR 2006 Report to the General Assembly with Scientific Annexes. Effects of Ionizing Radiation. Volume I Report and Annexes A and B. 2008.
213. Feinendegen LE. Evidence for beneficial low level radiation effects and radiation hormesis. Br J Radiol. 2005;78(925):3-7.
214. Robertson A, Allen J, Laney R, Curnow A. The cellular and molecular carcinogenic effects of radon exposure: a review. International journal of molecular sciences. 2013;14(7):14024-63.
215. Boice JD, Jr. The linear nonthreshold (LNT) model as used in radiation protection: an NCRP update. Int J Radiat Biol. 2017;93(10):1079-92.
216. Siegel JA, Greenspan BS, Maurer AH, Taylor AT, Phillips WT, Van Nostrand D, et al. The BEIR VII Estimates of Low-Dose Radiation Health Risks Are Based on Faulty Assumptions and Data Analyses: A Call for Reassessment. J Nucl Med. 2018;59(7):1017-9.
217. Vaiserman A, Koliada A, Zabuga O, Socol Y. Health Impacts of Low-Dose Ionizing Radiation: Current Scientific Debates and Regulatory Issues. Dose Response. 2018;16(3):1559325818796331.
218. Tubiana M, Feinendegen LE, Yang C, Kaminski JM. The linear no-threshold relationship is inconsistent with radiation biologic and experimental data. Radiology. 2009;251(1):13-22.
219. Feinendegen LE, Pollycove M, Neumann RD. Whole-body responses to low-level radiation exposure: New concepts in mammalian radiobiology. Exp Hematol. 2007;35(4):37-46.
220. Land CE. Low-dose extrapolation of radiation health risks: some implications of uncertainty for radiation protection at low doses. Health Phys. 2009;97(5):407-15.
221. Feinendegen LE. Evidence for beneficial low level radiation effects and radiation hormesis. Brit J Radiol. 2005;78(925):3-7.
222. Laine FJ, Smoker WR. Oral cavity: anatomy and pathology. Semin Ultrasound CT MR. 1995;16(6):527-45.
223. Gronthos S, Mankani M, Brahim J, Robey PG, Shi S. Postnatal human dental pulp stem cells (DPSCs) in vitro and in vivo. Proc Natl Acad Sci U S A. 2000;97(25):13625-30.
224. Miura M, Gronthos S, Zhao M, Lu B, Fisher LW, Robey PG, et al. SHED: stem cells from human exfoliated deciduous teeth. Proc Natl Acad Sci U S A. 2003;100(10):5807-12.
225. Morsczeck C, Gotz W, Schierholz J, Zeilhofer F, Kuhn U, Mohl C, et al. Isolation of precursor cells (PCs) from human dental follicle of wisdom teeth. Matrix Biol. 2005;24(2):155-65.
226. Sonoyama W, Liu Y, Yamaza T, Tuan RS, Wang S, Shi S, et al. Characterization of the apical papilla and its residing stem cells from human immature permanent teeth: a pilot study. J Endod. 2008;34(2):166-71.
227. Seo BM, Miura M, Gronthos S, Bartold PM, Batouli S, Brahim J, et al. Investigation of multipotent postnatal stem cells from human periodontal ligament. Lancet. 2004;364(9429):149-55.
228. Liu H, Gronthos S, Shi S. Dental pulp stem cells. Methods Enzymol. 2006;419:99-113.
229. Tatullo M, Marrelli M, Shakesheff KM, White LJ. Dental pulp stem cells: function, isolation and applications in regenerative medicine. J Tissue Eng Regen Med. 2015;9(11):1205-16.
230. Hilkens P, Meschi N, Lambrechts P, Bronckaers A, Lambrichts I. Dental Stem Cells in Pulp Regeneration: Near Future or Long Road Ahead? Stem Cells Dev. 2015;24(14):1610-22.
231. Lambrichts I, Driesen RB, Dillen Y, Gervois P, Ratajczak J, Vangansewinkel T, et al. Dental Pulp Stem Cells: Their Potential in Reinnervation and Angiogenesis by Using Scaffolds. J Endod. 2017;43(9S):S12-S6.
232. Yuan C, Wang P, Zhu L, Dissanayaka WL, Green DW, Tong EH, et al. Coculture of stem cells from apical papilla and human umbilical vein endothelial cell under hypoxia

increases the formation of three-dimensional vessel-like structures in vitro. Tissue Eng Part A. 2015;21(5-6):1163-72.
233. Nada OA, El Backly RM. Stem Cells From the Apical Papilla (SCAP) as a Tool for Endogenous Tissue Regeneration. Front Bioeng Biotechnol. 2018;6:103.
234. Lee S-M, Zhang Q. Dental stem cells: Sources and Potential applications. Current Oral Health Reports. 2014;1(1):34-42.
235. Guo W, Gong K, Shi H, Zhu G, He Y, Ding B, et al. Dental follicle cells and treated dentin matrix scaffold for tissue engineering the tooth root. Biomaterials. 2012;33(5):1291-302.
236. Sharpe PT. Dental mesenchymal stem cells. Development. 2016;143(13):2273-80.
237. Thomas P, Holland N, Bolognesi C, Kirsch-Volders M, Bonassi S, Zeiger E, et al. Buccal micronucleus cytome assay. Nat Protoc. 2009;4(6):825-37.
238. Russo FB, Pignatari GC, Fernandes IR, Dias JL, Beltrao-Braga PC. Epithelial cells from oral mucosa: How to cultivate them? Cytotechnology. 2016;68(5):2105-14.
239. Torres-Bugarin O, Zavala-Cerna MG, Nava A, Flores-Garcia A, Ramos-Ibarra ML. Potential uses, limitations, and basic procedures of micronuclei and nuclear abnormalities in buccal cells. Dis Markers. 2014;2014:956835.
240. Spivack SD, Hurteau GJ, Jain R, Kumar SV, Aldous KM, Gierthy JF, et al. Gene-environment interaction signatures by quantitative mRNA profiling in exfoliated buccal mucosal cells. Cancer Res. 2004;64(18):6805-13.
241. Munce T, Simpson R, Bowling F. Molecular characterization of Prader-Willi syndrome by real-time PCR. Genet Test. 2008;12(2):319-24.
242. Bianco B, Lipay MV, Melaragno MI, Guedes AD, Verreschi IT. Detection of hidden Y mosaicism in Turner's syndrome: importance in the prevention of gonadoblastoma. J Pediatr Endocrinol Metab. 2006;19(9):1113-7.
243. Laffargue F, Bourthoumieu S, Bellanne-Chantelot C, Guigonis V, Yardin C. Could FISH on buccal smears become a new method of screening in children suspect of HNF1B anomaly? Eur J Med Genet. 2013;56(2):93-7.
244. Siddiqui MS, Francois M, Fenech MF, Leifert WR. gammaH2AX responses in human buccal cells exposed to ionizing radiation. Cytometry A. 2015;87(4):296-308.
245. Sarto F, Tomanin R, Giacomelli L, Iannini G, Cupiraggi AR. The micronucleus assay in human exfoliated cells of the nose and mouth: application to occupational exposures to chromic acid and ethylene oxide. Mutat Res. 1990;244(4):345-51.
246. Gonzalez JE, Roch-Lefevre SH, Mandina T, Garcia O, Roy L. Induction of gamma-H2AX foci in human exfoliated buccal cells after in vitro exposure to ionising radiation. Int J Radiat Biol. 2010;86(9):752-9.
247. Nunes LA, Mussavira S, Bindhu OS. Clinical and diagnostic utility of saliva as a non-invasive diagnostic fluid: a systematic review. Biochem Med (Zagreb). 2015;25(2):177-92.
248. Malamud D. Saliva as a diagnostic fluid. Dent Clin North Am. 2011;55(1):159-78.
249. Lee JM, Garon E, Wong DT. Salivary diagnostics. Orthod Craniofac Res. 2009;12(3):206-11.
250. Aps JK, Martens LC. Review: The physiology of saliva and transfer of drugs into saliva. Forensic Sci Int. 2005;150(2-3):119-31.
251. Mandel ID. Salivary diagnosis: more than a lick and a promise. Journal of the American Dental Association (1939). 1993;124(1):85-7.
252. Miller SM. Saliva testing--a nontraditional diagnostic tool. Clin Lab Sci. 1994;7(1):39-44.
253. Li Y, Denny P, Ho CM, Montemagno C, Shi W, Qi F, et al. The Oral Fluid MEMS/NEMS Chip (OFMNC): diagnostic and translational applications. Adv Dent Res. 2005;18(1):3-5.
254. Christodoulides N, Mohanty S, Miller CS, Langub MC, Floriano PN, Dharshan P, et al. Application of microchip assay system for the measurement of C-reactive protein in human saliva. Lab Chip. 2005;5(3):261-9.
255. Rao PV, Reddy AP, Lu X, Dasari S, Krishnaprasad A, Biggs E, et al. Proteomic identification of salivary biomarkers of type-2 diabetes. J Proteome Res. 2009;8(1):239-45.
256. Hu S, Arellano M, Boontheung P, Wang J, Zhou H, Jiang J, et al. Salivary proteomics for oral cancer biomarker discovery. Clin Cancer Res. 2008;14(19):6246-52.

257. Franzmann EJ, Reategui EP, Carraway KL, Hamilton KL, Weed DT, Goodwin WJ. Salivary soluble CD44: a potential molecular marker for head and neck cancer. Cancer Epidemiol Biomarkers Prev. 2005;14(3):735-9.
258. Wang Q, Gao P, Wang X, Duan Y. Investigation and identification of potential biomarkers in human saliva for the early diagnosis of oral squamous cell carcinoma. Clin Chim Acta. 2014;427:79-85.
259. Soni S, Agrawal P, Kumar N, Mittal G, Nishad DK, Chaudhury NK, et al. Salivary biochemical markers as potential acute toxicity parameters for acute radiation injury: A study on small experimental animals. Hum Exp Toxicol. 2016;35(3):221-8.

Chapter 2:

Scope and aim of the research

Nowadays, one of the prime challenges in radiation protection is assessing the possible biological effects of exposure to low doses of IR. Unfortunately, data are only conclusive for exposure to doses above 100 mGy. Although the ICRP aims to protect people from radiation-induced stochastic effects by advising on radiation protection guidelines and regulations, conclusive data on low dose (i.e. below 100 mGy) health effects remain elusive.[1-8] Data on low dose effects, however, are of importance in medical imaging applications of IR, such as CT and, more recently, CBCT, which typically use doses far below 100 mGy [9-12].

CBCT is a relatively new and innovative diagnostic imaging technique introduced in oral health care at the turn of the century.[13, 14] Its growing use lies in the diagnostic potential related to the transition from two-dimensional to three-dimensional dentomaxillofacial diagnostic imaging.[15-18] CBCT technology has rapidly evolved in the past decade. Nowadays it has become a widely available diagnostic tool for clinicians and has therefore found applications in multiple dental specialties, including implant planning, endodontics, orthodontics and maxillofacial surgery.[13, 14, 16, 19-22] CBCT relies on X-rays for its image acquisition. As in CT, the absorbed IR dose in CBCT heavily depends on selectable exposure parameters that determine the image quality such as kVp, mAs, field of view (FOV), amount of 2D projections, reconstitution algorithm, etc..[10-12, 16, 23] Therefore, a wide range of CBCT doses is observed, typically ranging from about 0.010 to 1.100 mSv per examination.[10, 11, 23-27] CBCT doses are lower than CT doses (organ dose of about 15 mSv), however, they are higher than classical 2D dental radiography techniques (organ dose of 0.001 – 0.1 mSv).[12, 16, 28-31]

IR is capable of damaging biomolecules (e.g. DNA or proteins) directly or indirectly via the hydrolysis of water which generates free radicals, such as ROS.[32, 33] Since more than 60% of a cell consists of water, most of the damage is caused indirectly via ROS (e.g. the hydroxyl radical, superoxide radicals and hydrogen peroxide).[30, 34] An excess of ROS causes oxidative stress. In the context of oral pathology, oxidative stress is associated with periodontitis, dental caries and oral cancers.[35, 36] ROS can cause oxidative DNA damage through oxidative base lesions, of which over 20 different ones have been identified.[37] An example is 8-oxo-7,8-dihydro-2'-deoxyguanosine (8-oxo-dG), a mutagenic base modification.[38] Other types of DNA lesions include single strand breaks, double strand breaks (DSBs) and base alterations.[34, 39] DSBs are the most critical DNA lesions caused by IR. When not repaired correctly, DSBs can lead to chromosome rearrangements, mutations and loss of genetic information.[40-45] To protect themselves, eukaryotic cells have developed the DNA damage response (DDR), a set of signalling and DNA repair pathways.[46-48] The DDR consists of a signalling cascade that results in the recruitment of multiple DDR proteins to the vicinity of DSBs, including histone H2AX phosphorylated on serine 139 (γH2AX) and p53-binding protein 1 (53BP1). Both γH2AX and 53BP1 form DNA damage foci and show a quantitative relationship between the number of foci and the number of DSBs [49, 50].

Because of the potential adverse health effects of IR exposure clinical studies following patients after medical diagnostic imaging procedures have been performed. Multiple controversial studies indicate that exposure of children to diagnostic radiology may lead to radiation-induced malignancies later in life. Retrospective studies observed that the use of CT scans in children could triple the risk of leukaemia and brain cancers [51-53]. Furthermore, it was estimated that the probability to develop radiation-induced malignancies after CBCT exposure is 6 cases per 1,000,000 CBCT scans on average [54-56]. Despite these potential links between diagnostic radiology and radiation-induced malignancies, absolute evidence from prospective studies is scarce [4, 9]. Given that children are more radiosensitive than adults, this raised questions about potential radiation-induced health effects associated with diagnostic radiology in children [10, 11, 57-60]. IR doses associated with paediatric dental CBCT became a major concern for the general public when the New York Times published two articles about the topic (2010 and 2012).[61, 62] Most CBCT examinations are performed on children (< 18 years old), mostly during orthodontics, but also during pedodontic procedures.[10, 60]

Currently, epidemiological studies are lacking for CBCT exposure. As a consequence, researchers have to rely on radiobiological evidence as well as prospective studies that monitor current patients, rather than historical cohorts. Radiobiological research can help to gain more insights into the underlying mechanisms.[1, 63]

The overall aim of this thesis was to investigate the biological effects of low dose IR associated with dental CBCT in different age categories. Emphasis was placed on 1) the DNA damage response and repair kinetics following low dose IR exposure through immunofluorescent staining for γH2AX and 53BP1, and 2) the (anti)oxidative stress response following low dose radiation exposure. These parameters were monitored in dental stem cells, buccal mucosa cells (BMCs), and/or saliva samples collected from pediatric and adult patients prior and after CBCT examination.

Dental stem cells are mesenchymal stem cells that reside inside, or closely to, the teeth. Several types of stem cells have been identified since the early 2000s: dental pulp stem cells (DPSCs), dental pulp stem cells from deciduous teeth (SHEDs), stem cells from the apical papilla (SCAPs), dental follicle stem cells (DFSCs), and periodontal ligament stem cells (PDLSCs).[64-68] All of them have crucial functions in tooth development and repair.

The buccal mucosa (BM), which lines the oral cavity, is an easily accessible source for collecting BMCs in a minimally invasive, pain-free way.[69] BMCs have been used to study (amongst others) the impact of nutrition, lifestyle factors and exposure to genotoxins, including exposure to IR.[70, 71] IR-induced genotoxicity can be monitored in BMCs by measuring γH2AX levels and can be used to monitor radiation exposure and DNA damage in radiotherapy patients.[72, 73]

Saliva is a bodily fluid that is secreted into the oral cavity. It originates mainly from the parotid, submandibular and sublingual glands and is an aqueous solution (> 99% water) containing both organic and inorganic molecules.[74] Saliva, commonly referred to as 'mirror of the body', has several advantages over other biological samples, such as blood. It is readily available, collection can be done in a non-invasive way, and its use is very cost-effective.[75, 76] These advantages make saliva an ideal sample to collect from paediatric patients and for use in diagnostics.[76, 77] Currently, salivary diagnostics is becoming increasingly important in radiation biomarker research.[75, 78] Since X-rays induce most damage to biomolecules via ROS, measuring ROS and their effects in saliva samples are good indicators of radiation exposure.

Firstly, the protocols for the detection of DNA DSBs in BMCs, and 8-oxo-dG and total antioxidant capacity in saliva samples were optimized and validated before use in pediatric patients (**Chapter 3**). Next, DNA damage induction and repair were studied *ex vivo* in buccal mucosa cells obtained from adults and children following dental CBCT. Simultaneously, we monitored oxidative damage by measuring 8-oxo-dG levels in saliva samples from the same cohort of patients (**Chapter 4**). In **Chapter 5**, *in vitro* experiments with paediatric dental stem cells were performed in which the γH2AX/53BP1 assay for DNA damage induction and repair, cell cycle progression, and premature cellular senescence were analysed. Finally, time-dependent antioxidant responses were monitored in buccal mucosal cells and saliva samples from patients following CBCT examination (**Chapter 6**). Our experimental data provide insight into the cellular and subcellular changes that occur after low dose IR exposure, both in patients of different age categories exposed to dental CBCT, as well as *in vitro*. These data may eventually contribute to the improvement of radiation protection guidelines and regulations by introducing age-specific guidelines for medical diagnostic radiology.

References

1. Boice JD, Jr. The linear nonthreshold (LNT) model as used in radiation protection: an NCRP update. Int J Radiat Biol. 2017;93(10):1079-92.
2. Siegel JA, Greenspan BS, Maurer AH, Taylor AT, Phillips WT, Van Nostrand D, et al. The BEIR VII Estimates of Low-Dose Radiation Health Risks Are Based on Faulty Assumptions and Data Analyses: A Call for Reassessment. J Nucl Med. 2018;59(7):1017-9.
3. Vaiserman A, Koliada A, Zabuga O, Socol Y. Health Impacts of Low-Dose Ionizing Radiation: Current Scientific Debates and Regulatory Issues. Dose Response. 2018;16(3):1559325818796331.
4. Tubiana M, Feinendegen LE, Yang C, Kaminski JM. The linear no-threshold relationship is inconsistent with radiation biologic and experimental data. Radiology. 2009;251(1):13-22.
5. Feinendegen LE, Pollycove M, Neumann RD. Whole-body responses to low-level radiation exposure: New concepts in mammalian radiobiology. Exp Hematol. 2007;35(4):37-46.
6. Land CE. Low-dose extrapolation of radiation health risks: some implications of uncertainty for radiation protection at low doses. Health Phys. 2009;97(5):407-15.
7. ICRP. The 2007 Recommendations of the International Commission on Radiological Protection. ICRP Publication 103. Ann ICRP. 2007;37(2-4).
8. Walker JS. Permissible dose : a history of radiation protection in the twentieth century. Berkeley: University of California Press; 2000. xii, 168 p. p.
9. Lee CY, Koval TM, Suzuki JB. Low-Dose Radiation Risks of Computerized Tomography and Cone Beam Computerized Tomography: Reducing the Fear and Controversy. J Oral Implantol. 2015;41(5):e223-30.
10. Oenning AC, Jacobs R, Pauwels R, Stratis A, Hedesiu M, Salmon B, et al. Cone-beam CT in paediatric dentistry: DIMITRA project position statement. Pediatr Radiol. 2017.
11. Marcu M, Hedesiu M, Salmon B, Pauwels R, Stratis A, Oenning ACC, et al. Estimation of the radiation dose for pediatric CBCT indications: a prospective study on ProMax3D. Int J Paediatr Dent. 2018.
12. Pauwels R, Beinsberger J, Collaert B, Theodorakou C, Rogers J, Walker A, et al. Effective dose range for dental cone beam computed tomography scanners. European journal of radiology. 2012;81(2):267-71.
13. Arai Y, Tammisalo E, Iwai K, Hashimoto K, Shinoda K. Development of a compact computed tomographic apparatus for dental use. Dentomaxillofac Radiol. 1999;28(4):245-8.
14. Mozzo P, Procacci C, Tacconi A, Martini PT, Andreis IA. A new volumetric CT machine for dental imaging based on the cone-beam technique: preliminary results. European radiology. 1998;8(9):1558-64.
15. Scarfe WC, Farman AG. What is cone-beam CT and how does it work? Dent Clin North Am. 2008;52(4):707-30, v.
16. Pauwels R. Cone beam CT for dental and maxillofacial imaging: dose matters. Radiation protection dosimetry. 2015;165(1-4):156-61.
17. Dawood A, Patel S, Brown J. Cone beam CT in dental practice. British dental journal. 2009;207(1):23-8.
18. Kapila SD, Nervina JM. CBCT in orthodontics: assessment of treatment outcomes and indications for its use. Dentomaxillofac Radiol. 2015;44(1):20140282.
19. De Vos W, Casselman J, Swennen GR. Cone-beam computerized tomography (CBCT) imaging of the oral and maxillofacial region: a systematic review of the literature. Int J Oral Maxillofac Surg. 2009;38(6):609-25.
20. Suomalainen A, Pakbaznejad Esmaeili E, Robinson S. Dentomaxillofacial imaging with panoramic views and cone beam CT. Insights Imaging. 2015;6(1):1-16.
21. Shah N, Bansal N, Logani A. Recent advances in imaging technologies in dentistry. World journal of radiology. 2014;6(10):794-807.

22. Scarfe WC, Farman AG, Sukovic P. Clinical applications of cone-beam computed tomography in dental practice. J Can Dent Assoc. 2006;72(1):75-80.
23. Ludlow JB, Davies-Ludlow LE, White SC. Patient risk related to common dental radiographic examinations: the impact of 2007 International Commission on Radiological Protection recommendations regarding dose calculation. Journal of the American Dental Association (1939). 2008;139(9):1237-43.
24. Signorelli L, Patcas R, Peltomaki T, Schatzle M. Radiation dose of cone-beam computed tomography compared to conventional radiographs in orthodontics. Journal of orofacial orthopedics = Fortschritte der Kieferorthopadie : Organ/official journal Deutsche Gesellschaft fur Kieferorthopadie. 2016;77(1):9-15.
25. Li G. Patient radiation dose and protection from cone-beam computed tomography. Imaging Sci Dent. 2013;43(2):63-9.
26. Loubele M, Bogaerts R, Van Dijck E, Pauwels R, Vanheusden S, Suetens P, et al. Comparison between effective radiation dose of CBCT and MSCT scanners for dentomaxillofacial applications. European journal of radiology. 2009;71(3):461-8.
27. Centre for Radiation CaEH. Guidance on the safe use of dental cone bean CT (computed tomography) equipment. Oxfordshire: Health Protection Agency; 2010.
28. Theodorakou C, Walker A, Horner K, Pauwels R, Bogaerts R, Jacobs R. Estimation of paediatric organ and effective doses from dental cone beam CT using anthropomorphic phantoms. Br J Radiol. 2012;85(1010):153-60.
29. Department of Public Health EaSDoHP-F, Women and Children's Health Cluster (FWC). Communicating radiation risks in paediatric imaging - Information to support healthcare discussions about benefit and risk. Switserland: World Health Organization; 2016.
30. Brenner DJ, Hall EJ. Computed tomography--an increasing source of radiation exposure. N Engl J Med. 2007;357(22):2277-84.
31. RadiologyInfo.org. Radiation Dose in X-ray and CT exams. Accessed on 2018-12-06. Available from: https://www.radiologyinfo.org/en/pdf/safety-xray.pdf.
32. UNSCEAR. SOURCES AND EFFECTS OF IONIZING RADIATION. 2000;Volume II: Effects.
33. UNSCEAR. UNSCEAR 2013 Report: Sources, effects and risks of ionizing radiation - Volume II Annex B - Effects of radiation exposure of children. 2013.
34. D. K. Maurya TPAD. Role of Radioprotectors in the Inhibition of DNA Damage and Modulation of DNA Repair After Exposure to Gamma-Radiation. In: Chen CC, editor. Selected Topics in DNA Repair: InTech.; 2011.
35. Chapple IL, Matthews JB. The role of reactive oxygen and antioxidant species in periodontal tissue destruction. Periodontol 2000. 2007;43:160-232.
36. Tothova L, Kamodyova N, Cervenka T, Celec P. Salivary markers of oxidative stress in oral diseases. Front Cell Infect Microbiol. 2015;5:73.
37. Cooke MS, Evans MD, Dizdaroglu M, Lunec J. Oxidative DNA damage: mechanisms, mutation, and disease. FASEB J. 2003;17(10):1195-214.
38. Kasai H, Nishimura S. Hydroxylation of deoxy guanosine at the C-8 position by polyphenols and aminophenols in the presence of hydrogen peroxide and ferric ion. Gan. 1984;75(7):565-6.
39. Lobrich M, Shibata A, Beucher A, Fisher A, Ensminger M, Goodarzi AA, et al. gammaH2AX foci analysis for monitoring DNA double-strand break repair: strengths, limitations and optimization. Cell cycle (Georgetown, Tex). 2010;9(4):662-9.
40. Dugle DL, Gillespie CJ, Chapman JD. DNA strand breaks, repair, and survival in x-irradiated mammalian cells. Proc Natl Acad Sci U S A. 1976;73(3):809-12.
41. Olive PL. The role of DNA single- and double-strand breaks in cell killing by ionizing radiation. Radiat Res. 1998;150(5 Suppl):S42-51.
42. Jackson SP. Sensing and repairing DNA double-strand breaks. Carcinogenesis. 2002;23(5):687-96.
43. Richardson C, Jasin M. Frequent chromosomal translocations induced by DNA double-strand breaks. Nature. 2000;405(6787):697-700.
44. Vamvakas S, Vock EH, Lutz WK. On the role of DNA double-strand breaks in toxicity and carcinogenesis. Crit Rev Toxicol. 1997;27(2):155-74.

45. Khanna KK, Jackson SP. DNA double-strand breaks: signaling, repair and the cancer connection. Nat Genet. 2001;27(3):247-54.
46. Kinner A, Wu W, Staudt C, Iliakis G. Gamma-H2AX in recognition and signaling of DNA double-strand breaks in the context of chromatin. Nucleic Acids Res. 2008;36(17):5678-94.
47. Riches LC, Lynch AM, Gooderham NJ. Early events in the mammalian response to DNA double-strand breaks. Mutagenesis. 2008;23(5):331-9.
48. Ciccia A, Elledge SJ. The DNA damage response: making it safe to play with knives. Mol Cell. 2010;40(2):179-204.
49. Goodarzi AA, Jeggo PA. Irradiation induced foci (IRIF) as a biomarker for radiosensitivity. Mutat Res. 2012;736(1-2):39-47.
50. Asaithamby A, Chen DJ. Cellular responses to DNA double-strand breaks after low-dose gamma-irradiation. Nucleic Acids Res. 2009;37(12):3912-23.
51. Pearce MS, Salotti JA, Little MP, McHugh K, Lee C, Kim KP, et al. Radiation exposure from CT scans in childhood and subsequent risk of leukaemia and brain tumours: a retrospective cohort study. Lancet. 2012;380(9840):499-505.
52. Huang WY, Muo CH, Lin CY, Jen YM, Yang MH, Lin JC, et al. Paediatric head CT scan and subsequent risk of malignancy and benign brain tumour: a nation-wide population-based cohort study. Br J Cancer. 2014;110(9):2354-60.
53. Krille L, Dreger S, Schindel R, Albrecht T, Asmussen M, Barkhausen J, et al. Risk of cancer incidence before the age of 15 years after exposure to ionising radiation from computed tomography: results from a German cohort study. Radiat Environ Biophys. 2015;54(1):1-12.
54. Pauwels R, Cockmartin L, Ivanauskaite D, Urboniene A, Gavala S, Donta C, et al. Estimating cancer risk from dental cone-beam CT exposures based on skin dosimetry. Phys Med Biol. 2014;59(14):3877-91.
55. Aanenson JW, Till JE, Grogan HA. Understanding and communicating radiation dose and risk from cone beam computed tomography in dentistry. J Prosthet Dent. 2018.
56. Yeh JK, Chen CH. Estimated radiation risk of cancer from dental cone-beam computed tomography imaging in orthodontics patients. BMC Oral Health. 2018;18(1):131.
57. Brenner DJ. Estimating cancer risks from pediatric CT: going from the qualitative to the quantitative. Pediatr Radiol. 2002;32(4):228-1; discussion 42-4.
58. Hall EJ. Lessons we have learned from our children: cancer risks from diagnostic radiology. Pediatr Radiol. 2002;32(10):700-6.
59. Schroeder AR, Redberg RF. The harm in looking. JAMA Pediatr. 2013;167(8):693-5.
60. De Grauwe A, Ayaz I, Shujaat S, Dimitrov S, Gbadegbegnon L, Vande Vannet B, et al. CBCT in orthodontics: a systematic review on justification of CBCT in a paediatric population prior to orthodontic treatment. Eur J Orthod. 2018.
61. Bogdanich W. CMJ. Radiation Worries for Children in Dentists' Chairs. New York Times. 2010.
62. Gee A. Radiation Concerns Rise With Patients' Exposure. New York Times. 2012 June 13 2012.
63. Ruhm W, Eidemuller M, Kaiser JC. Biologically-based mechanistic models of radiation-related carcinogenesis applied to epidemiological data. Int J Radiat Biol. 2017;93(10):1093-117.
64. Gronthos S, Mankani M, Brahim J, Robey PG, Shi S. Postnatal human dental pulp stem cells (DPSCs) in vitro and in vivo. Proc Natl Acad Sci U S A. 2000;97(25):13625-30.
65. Miura M, Gronthos S, Zhao M, Lu B, Fisher LW, Robey PG, et al. SHED: stem cells from human exfoliated deciduous teeth. Proc Natl Acad Sci U S A. 2003;100(10):5807-12.
66. Morsczeck C, Gotz W, Schierholz J, Zeilhofer F, Kuhn U, Mohl C, et al. Isolation of precursor cells (PCs) from human dental follicle of wisdom teeth. Matrix Biol. 2005;24(2):155-65.
67. Sonoyama W, Liu Y, Yamaza T, Tuan RS, Wang S, Shi S, et al. Characterization of the apical papilla and its residing stem cells from human immature permanent teeth: a pilot study. J Endod. 2008;34(2):166-71.
68. Seo BM, Miura M, Gronthos S, Bartold PM, Batouli S, Brahim J, et al. Investigation of multipotent postnatal stem cells from human periodontal ligament. Lancet. 2004;364(9429):149-55.

69. Thomas P, Holland N, Bolognesi C, Kirsch-Volders M, Bonassi S, Zeiger E, et al. Buccal micronucleus cytome assay. Nat Protoc. 2009;4(6):825-37.
70. Ozkul Y, Donmez H, Erenmemisoglu A, Demirtas H, Imamoglu N. Induction of micronuclei by smokeless tobacco on buccal mucosa cells of habitual users. Mutagenesis. 1997;12(4):285-7.
71. Kashyap B, Reddy PS. Micronuclei assay of exfoliated oral buccal cells: means to assess the nuclear abnormalities in different diseases. J Cancer Res Ther. 2012;8(2):184-91.
72. Gonzalez JE, Roch-Lefevre SH, Mandina T, Garcia O, Roy L. Induction of gamma-H2AX foci in human exfoliated buccal cells after in vitro exposure to ionising radiation. Int J Radiat Biol. 2010;86(9):752-9.
73. Siddiqui MS, Francois M, Fenech MF, Leifert WR. gammaH2AX responses in human buccal cells exposed to ionizing radiation. Cytometry A. 2015;87(4):296-308.
74. Humphrey SP, Williamson RT. A review of saliva: normal composition, flow, and function. J Prosthet Dent. 2001;85(2):162-9.
75. Pernot E, Cardis E, Badie C. Usefulness of saliva samples for biomarker studies in radiation research. Cancer Epidemiol Biomarkers Prev. 2014;23(12):2673-80.
76. Hassaneen M, Maron JL. Salivary Diagnostics in Pediatrics: Applicability, Translatability, and Limitations. Front Public Health. 2017;5:83.
77. Farnaud SJ, Kosti O, Getting SJ, Renshaw D. Saliva: physiology and diagnostic potential in health and disease. ScientificWorldJournal. 2010;10:434-56.
78. Moore HD, Ivey RG, Voytovich UJ, Lin C, Stirewalt DL, Pogosova-Agadjanyan EL, et al. The human salivary proteome is radiation responsive. Radiat Res. 2014;181(5):521-30.

Chapter 3:

Method validation to assess *in vivo* cellular and subcellular changes in buccal mucosa cells and saliva following CBCT examinations

Belmans N, Gilles L, Virag P, Hedesiu M, Salmon B, Baatout S, Lucas S, Jacobs R, Lambrichts I, and Moreels M (2019) Method validation to assess in vivo cellular and subcellular changes in buccal mucosa cells and saliva following CBCT examinations. *Dentomaxillofacial Radiology – Published online April 5th, 2019 - doi:10.1259/dmfr.20180428*

3.1 Abstract

Objectives

Cone-beam computed tomography (CBCT) is a medical imaging technique used in dental medicine. However, there are no conclusive data available indicating that exposure to X-ray doses used by CBCT are harmless. We aim, for the first time, to characterize the potential age-dependent cellular and subcellular effects related to exposure to CBCT imaging. Current objective is to describe and validate the protocol for characterization of cellular and subcellular changes after diagnostic CBCT.

Methods

Development and validation of a dedicated two-part protocol: 1) assessing DNA double strand breaks (DSBs) in buccal mucosal (BM) cells and 2) oxidative stress measurements in saliva samples. BM cells and saliva samples are collected prior to and 0.5 hours after CBCT examination. BM cells are also collected 24 hours after CBCT examination. DNA DSBs are monitored in BM cells via immunocytochemical staining for γH2AX and 53BP1. 8-oxo-7,8-dihydro-2'-deoxyguanosine (8-oxo-dG) and total antioxidant capacity are measured in saliva to assess oxidative damage.

Results

Validation experiments show that sufficient BM cells are collected (97.1% ± 1.4%) and that γH2AX/53BP1 foci can be detected before and after CBCT examination. Collection and analysis of saliva samples, either sham exposed or exposed to IR, show that changes in 8-oxo-dG and total antioxidant capacity can be detected in saliva samples after CBCT examination.

Conclusion

The DIMITRA Research Group presents a two-part protocol to analyse potential age-related biological differences following CBCT examinations. This protocol was validated for collecting BM cells and saliva and for analysing these samples for DNA DSBs and oxidative stress markers, respectively.

Keywords:
Dental Cone-Beam Computed Tomography – DNA Double Strand Breaks – Oxidative stress – Buccal mucosal cells - Saliva

3.2 Introduction

Dental cone-beam computed tomography (CBCT) is a relatively new and innovative diagnostic imaging technique introduced in oral health care at the turn of the century.[1, 2] Its growing use lies in the diagnostic potential related to the transition from two-dimensional (2D) to three-dimensional (3D) dentomaxillofacial diagnostic imaging.[3-6] CBCT uses a cone-shaped X-ray beam and a 2D detector to generate 3D images. Briefly, the source-detector rotates around the patient once, while generating a series of 2D images. These images are then reconstructed into a 3D volume data set using a specialized algorithm.[3, 7-9] Specifically designed to produce cross-sectional images of the oral and maxillofacial region, combined with its low cost and easy accessibility, CBCT technology has rapidly evolved in the past decade. Nowadays it has become a widely available diagnostic tool for clinicians and has therefore found applications in multiple dental specialties, including implant planning, endodontics, orthodontics and maxillofacial surgery.[1, 2, 4, 8, 10-12]

Like other medical imaging techniques, such as computed tomography (CT), CBCT uses X-rays for its image acquisition. However, ionizing radiation (IR) is capable of damaging biomolecules (e.g. DNA or proteins) directly or indirectly via the hydrolysis of water which generates free radicals, such as reactive oxygen species (ROS).[13, 14] Although CBCT is defined as a low dose imaging technique by the European High-Level Expert Group on European Low Dose Risk Research (HLEG) (www.hleg.de), it is misleading to see it as a 'low-dose' imaging modality just because it only takes one rotation compared to multiple rotations in conventional CT. As in CT, the absorbed dose in CBCT heavily depends on selectable exposure parameters that determine the image quality such as kVp, mAs, field of view (FOV), amount of 2D projections, reconstitution algorithm, etc..[4, 15-18] Therefore, a wide range of CBCT doses is observed, typically ranging from about 0.010 to 1.100 mSv per examination.[15, 17-22] CBCT doses are lower than CT doses (organ dose of about 15 mSv), however, they are higher than classical 2D dental radiography techniques (organ dose of 0.001 – 0.1 mSv).[4, 16, 23-26]

More recently, the dose of ionizing radiation delivered to pediatric patients has become a major concern among clinicians worldwide.[20, 24] In 2010, the New York Times was the first major newspaper to bring this concern to the attention of the general public when they published the article entitled "Radiation Worries for Children in Dentists' Chairs".[27] In practice, especially in orthodontics, a large portion of CBCT examinations is performed on children (< 18 years old), who are known to be more radiosensitive than adults.[18, 28-30] These concerns about the dose, combined with an increasing amount of radiological examinations annually,

have led to questions about the biological uncertainties associated with radiation-induced health risks at low doses in dental radiology.[24, 31, 32]

Exposure to IR, such as X-rays, could result in damage to important biomolecules, either directly, but mostly indirectly via generation of free radicals, usually through hydrolysis of water. These radicals (e.g. reactive oxygen species (ROS)) can in turn damage biomolecules in nano- to microseconds.[14] Since more than 60% of a cell consists of water, most of the DNA damage is caused indirectly via ROS (e.g. the hydroxyl radical, superoxide radicals and hydrogen peroxide).[25, 33] An excess of ROS causes oxidative stress. In the context of oral pathology, oxidative stress is associated with periodontitis, dental caries and oral cancers.[34, 35] ROS can cause oxidative DNA damage through oxidative base lesions, of which over 20 different lesions have been identified.[36] An example hereof is 8-oxo-7,8-dihydro-2'-deoxyguanosine (8-oxo-dG), a mutagenic base modification.[37] Other types of DNA lesions include single strand breaks, double strand breaks (DSBs) and base alterations.[33, 38] DNA double strand breaks (DSBs) are the most critical DNA lesions caused by IR. When not repaired correctly, DSBs can lead to chromosome rearrangements, mutations and loss of genetic information.[39-44] To protect themselves, eukaryotic cells have developed the DNA damage response (DDR), a set of signalling and DNA repair pathways.[45-47]

Human buccal mucosa (BM) cells are useful for determining exposure to several environmental factors.[48, 49] Furthermore, BM cells are an easy accessible source of cells that can be sampled in a minimally invasive way.[50, 51] As such, they are being increasingly used to investigate the effects of exposure to genotoxins that can cause DNA damage and cell death.[48, 51, 52]

Another easy accessible biological sample is saliva, which, like BM cells, is easy to collect in an inexpensive, painless and non-invasive way.[53] Known as the 'mirror of the body', saliva is finding its way to research and the clinic as a diagnostic fluid.[35, 54, 55] To date, the salivary metabolome has been described and saliva has been used to link oxidative stress markers to several oral diseases, such as dental caries and periodontitis.[34, 35, 56]

Effective dose (ED), measured in mSv, is a dose quantity that takes following factors into account: 1) the absorbed dose to all organs of the body, 2) the relative harm of the type of radiation, and 3) the radiosensitivity of each organ. Although ED is an accepted term since its introduction in radiation protection, it is often criticized. For example the weighing factors used to calculate the ED are determined by scientific committees and may evolve over time.[57-59] Furthermore, the ED is independent of gender and age at exposure, whereas epidemiological data indicate that both gender and age at exposure are important parameters.[60]

A European project funded by the Open Project for European Radiation Research Area (OPERRA) denoted as DIMITRA (Dentomaxillofacial Paediatric Imaging: An Investigation Towards Low Dose Radiation Induced Risks) was

initiated in order to characterize any potential cellular and subcellular effects induced by dental CBCT imaging, with a focus on age- and gender specificity and with reference to simulated ED (www.dimitra.be). In vitro results from DIMITRA were published previously, showing transient increases in DNA DSBs and changes in inflammatory cytokines after CBCT exposure of dental stem cells *in vitro*.[61] The objective of the present report is to describe and validate a two-part protocol enabling the DIMITRA project to assess the potential age-related cellular and subcellular effects using DNA DSB detection in buccal mucosal cells and salivary oxidative stress measurement. To the best of our knowledge, a protocol and method validation for characterizing cellular and subcellular effects of CBCT exposure has not yet been described.

3.3 Materials and methods

3.3.1 Description of the DIMITRA protocol

Synthetic swabs (EpiCentre®, Madison, USA) are used to collect BM cells from eligible patients. Eligibility criteria are: having no systemic or acute diseases, taking no medication (antibiotics or anti-inflammatory drugs), having a good oral hygiene and giving informed consent prior to conclusion. When eligible, patients were asked to complete a questionnaire (supplementary data 1). At least one hour prior to BM cell collection, subjects are asked not to eat, brush their teeth or smoke. Just before BM cell collection, subjects rinse their mouth twice with water to remove excess debris. BM cells are collected from each patient just before, 0.5 hours after and 24 hours after CBCT examination (figure 3.1), using a protocol modified from Thomas et al. (2009).[50] The 24 hours samples are collected at the patients' homes. To this end patients receive detailed instruction sheets (supplementary data 2). After collection, samples are sent to SCK•CEN via a professional courier service.

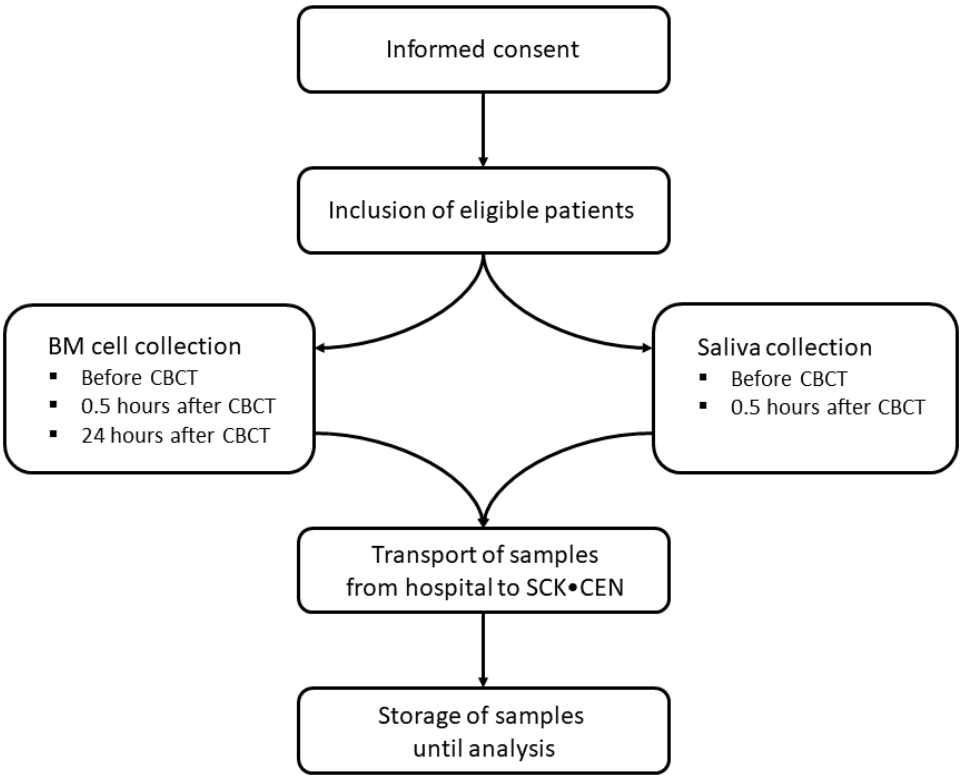

Figure 3.1. Flow chart for patient inclusion and patient sampling. *CBCT = Cone Beam Computed Tomography; BM = Buccal mucosa*

3.3.2 Buccal mucosal cell collection and fixation

Per patient six 15 ml conical tubes (Cellstar®, Greiner Bio-One, Vilvoorde, Belgium) (one for each time point and cheek side) containing 10 ml of Saccomanno's fixative (SF) (50% ethanol, 2% polyethylene glycol, 48% MilliQ water) are prepared. The swab is taken out of the package by the plastic handle. It is important not to touch the swab itself. Then the swab is placed against the middle of the patient's cheek. For reproducibility, the same cheek was used every time. Next, it is pressed firmly against the cheek and moved in an upward-downward motion while turning the swab for at least 30 seconds. The swab is then placed into SF in the 15 ml conical tube and shaken in such a manner that the cells are dislodged and released into SF. The tubes are then stored at 4°C (for up to 7 days) before shipment to SCK•CEN by courier service.

Within 7 days after sample collection, the BM cells are harvested from SF. For this purpose, the 15 ml conical tubes are centrifuged at 580g for 10 minutes at room temperature (RT). The supernatant is aspirated until about 1 ml is left. 5 ml of autoclaved buccal buffer (BuBu) (0.01 M Tris-HCl, 0.1 M EDTA, 0.02 M NaCl, 1% FBS, pH = 7) is added to the tube, after which the cells are vortexed briefly. Then, the cells are centrifuged at 580g for 10 minutes at RT. The supernatant is removed completely and the cells are washed with 5 ml BuBu and centrifuged at 580g for 10 minutes at RT. This washing step is repeated twice to inactivate DNAses from the oral cavity and to remove excess debris and bacteria. After washing, the supernatant is removed and the cells are resuspended in 5 ml of BuBu and vortexed briefly. Next, the BM cells are passed through a 100 µm nylon filter (Falcon®, VWR Belgium, Leuven, Belgium) into a 50 ml conical tube (Cellstar®, Greiner Bio-One, Vilvoorde, Belgium) to remove large aggregates of unseparated cells. The 50 ml conical tube holding the filter is then centrifuged at 580g for 10 minutes at RT. Afterwards, the BM cells in the filtrate are transferred to a new 15 ml conical tube. Then the BM cells are centrifuged one last time at 580g for 5 minutes at RT. The supernatant is removed and the BM cells are resuspended in 1 ml of BuBu. The BM cells are then centrifuged at 580g for 5 minutes at RT and the supernatant is discarded afterwards. Then, the BM cells are fixed in 500 µl of 2% paraformaldehyde (PFA) (Sigma Aldrich, St-Louis, MO, USA) while vortexing the BM cells and adding the PFA dropwise. The BM cells are incubated for at least 15 minutes at RT. After incubation, the BM cells are centrifuged at 580g for 5 minutes. The supernatant is discarded and the BM cells are washed twice using 1x phosphate-buffered saline (PBS) (Gibco, Life Technologies, Ghent, Belgium). After the last washing step, the BM cells are resuspended in 1 ml 1x PBS. The BM cells can now be stored at 4°C for a longer period or used immediately for immunocytochemical staining.

3.3.3 Immunocytological staining for DNA double strand breaks: γH2AX and 53BP1 staining

Before immunocytochemical staining, the BM cells need to be transferred from the 15 ml conical tubes to coverslips by cytocentrifugation. The BM cells are washed using 200 µl of 1x PBS twice. During washing, poly-L-lysine coated coverslips, which assure good attachment of the BM cells, are placed on a microscope slide which is then inserted in a cytofunnel (ThermoFisher, Waltham, MA, USA). Next, 100 µl of cell suspension is pipetted into each sample cup of a Cytofunnel. The cytofunnels are centrifuged at 1200 rpm for 10 minutes in a cytocentrifuge (ThermoFisher, Waltham, MA, USA) at RT, causing the BM cells to adhere to the coverslip inside the cytofunnel. After centrifugation, the coverslips are removed and placed into a 4-well culture plate (Nunc, ThermoFisher Scientific,

Roskilde, Denmark) so the BM cells are facing up. The BM cells are allowed to air-dry for 2 minutes at RT.

Immunocytochemical staining was performed using a protocol as previously described by our group.[62-64] First the BM cells are washed twice using cold 1x PBS for 5 minutes on a rocking platform. After washing, the BM cells are permeabilized for 3 minutes using 0.25% Triton X-100 in 1x PBS at RT. Next, the BM cells are washed three times with 1x PBS. Then the BM cells are blocked with 1x pre-immunized goat serum (ThermoFisher Scientific, Waltham, MA USA) in a solution of 1x TBST, 0.005 g/v% TSA blocking powder (PerkinElmer, FP1012, Zaventem, Belgium) (TNB) for 1 hour at RT. After blocking the primary mouse monoclonal anti-γH2AX antibody (Millipore 05-636, Merck, Overijse, Belgium) (1:300 in TNB) and rabbit polyclonal anti-53BP1 antibody (Novus Biologicals NB100-304, Abingdon, UK) (1:1000 in TNB) are added. Next, the BM cells are incubated overnight at 4°C on a rocking platform. After incubation, the BM cells are washed three times with 1x PBS. Then the secondary goat anti-mouse Alexa Fluor® 488-labeled antibody (1:300 in TNB) and goat anti-rabbit Alexa Fluor® 568-labeld antibody (1:1000 in TNB) (ThermoFisher Scientific, A11001, Waltham, MA USA) were added. The BM cells are incubated for 1 hour on a rocking platform in the dark. Afterwards, the BM cells are washed twice using 1x PBS. Next, slides are mounted with ProLong Diamond antifade medium with 4',6-diamidino-2-phenylindole (DAPI) (ThermoFisher Scientific, Waltham, MA USA).

Finally, images are acquired with a Nikon Eclipse Ti fluorescence microscope using a 40× dry objective (Nikon, Tokyo, Japan). Images are analyzed using open source Fiji software.[65] The software allows to analyze each nucleus based on the DAPI signal. Within each nucleus, the intensity signals from the Alexa 488 and Alexa 568 fluorochromes are analyzed after which the number of co-localized γH2AX and 53BP1 foci per nucleus are determined in an automated manner using the Cellblocks toolbox (figure 3.2).[66]

3.3.4 Saliva collection and analysis

Saliva samples are collected right before and 0.5 hours after CBCT examination (figure 3.1) using the passive drool method, which is considered to be the 'gold standard' for saliva sampling.[67] As with the BM cells (saliva is sampled at the same time), subjects are asked not to eat, brush their teeth or smoke one hour prior to saliva sampling. Just before saliva collection, subjects will rinse their mouth twice with water to remove excess debris. If blood is detected in the saliva, the sample is not included for this study. The saliva samples will be stored at -20°C immediately after collection before shipment to SCK•CEN by courier service. Once at SCK•CEN samples will be centrifuged at 10 000g at 4°C to remove most of the mucus and the supernatant will be stored at -80°C.

The stored samples will be used to determine 8-oxo-dG concentrations and the total antioxidant capacity (figure 3.2).

3.3.5 8-oxo-dG determination

8-oxo-dG concentrations will be determined by competitive enzyme-linked immunosorbent assay (ELISA) (Health Biomarkers Sweden AB, Stockholm, Sweden). To remove substances other than 8-oxo-dG which could cross-react with the monoclonal antibody used in the ELISA-kit, 800 µL sample will be purified prior to ELISA using a C18 solid phase extraction column (Varian, Lake Forest, CA, USA) after which the samples are freeze-dried. This purification is performed twice.[68]

The 8-oxo-dG concentration of saliva will be measured based on a modified ELISA protocol provided by Health Biomarkers Sweden AB (Stockholm, Sweden). The protocol will be performed as previously described by Haghdoost *et al*..[69] Briefly, 270 µl of purified sample/standard will be mixed with 165 µl of primary antibody (80 ng/ml) mix in Eppendorf tubes. Next the samples will be incubated for 2 hours at 37°C. During incubation, the ELISA plate will be washed twice using 1x PBS. After incubation 140 µl of sample/standard will be loaded onto the plate in triplicate. The plate will be incubated overnight at 4°C on a horizontal shaker. Next the plate will be washed three times using 1x washing solution. After washing 140 µl of secondary antibody mix is added to each well. The plate is incubated for 2 hours at RT on a horizontal shaker. Next the plate is washed three times with 1x washing solution and once more with 1x PBS. Finally, the reaction is visualized by the addition of 140 µl chromogenic substrate 3,3',5,5'-Tetramethylbenzidine (One-Step substrate system; Dako, Glostrup Municipality, Denmark), and further incubation in the dark for 15 minutes. The reaction is stopped by adding 70 µl of 2M H_2SO_4. The absorbance is measured at 450 nm (signal) and 570 nm (background) using a microplate reader (ClarioStar, BMG Labtech, Ortenberg, Germany) (figure 3.2).

3.3.6 Total antioxidant capacity

To determine the antioxidant capacity of saliva samples, the ferric reducing antioxidant power (FRAP) assay is used (Cell Biolabs, CA, USA). The FRAP assay will be performed according to the manufacturer's instructions. Briefly, per well of a 96-well plate 100 µl of sample/standard and 100 µl of reaction reagent are added. Next the samples/standards are incubated for 10 minutes at RT on a horizontal shaker. Finally, the absorbance will be measured at 560 nm using a

microplate reader (ClarioStar, BMG Labtech, Ortenberg, Germany). The results will be expressed as Iron(II) concentration (µM) or FRAP value (figure 3.2).

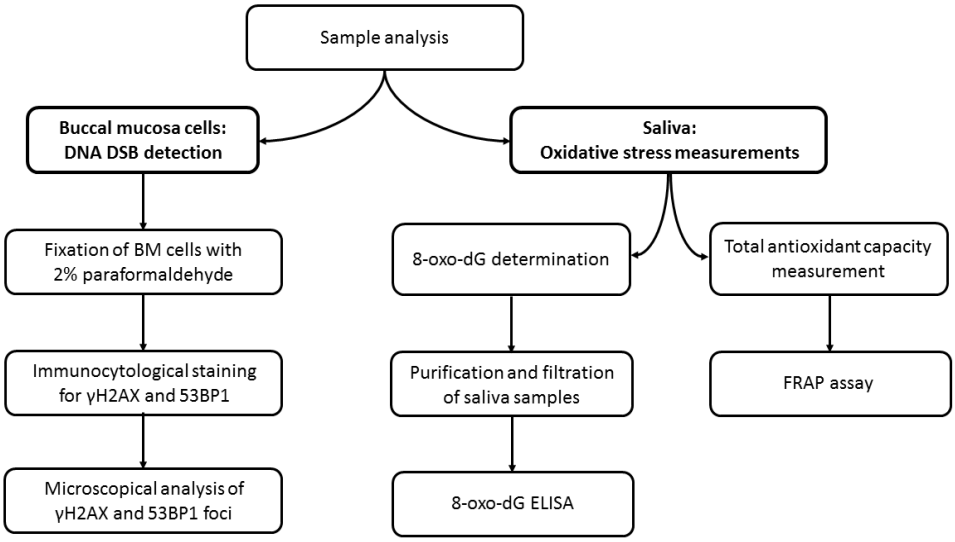

Figure 3.2. Flow chart for sample analysis. Schematic view of DNA double strand break detection in buccal mucosal cells and oxidative stress measurements in saliva samples. *DSB = Double-strand break; BM = Buccal mucosa; γH2AX = phosphorylated histone 2AX on Ser139; 53BP1 = p53-binding protein 1; 8-oxo-dG = 8-oxo-7,8-dihydro-2'-deoxyguanosine; FRAP = Ferric Reducing Antioxidant Power; ELISA = Enzyme-linked Immunosorbent assay*

3.4 Protocol validation

3.4.1 Pilot study population

Healthy adults (N = 6) are included in this pilot study to validate the DIMITRA study protocol. These patients are referred for a CBCT examination. All patients were asked to sign informed consent forms prior to being included in the study. The validation study was approved by the ethical committees of the participating hospitals, since this is part of the scope of the DIMITRA study.

3.4.2 Flow cytometrical identification of buccal mucosal cells

Cells collected using the method described earlier are identified with the epithelial cell marker cytokeratin 4 (CK4) and lymphoid cell marker CD45 to identify the amount of BM cells collected with the swab. A431 and PC3 (courtesy of Katrien Konings) cell lines are used as a positive control for CK4 expression. Jurkat cells are used as a positive control for CD45 expression.

All cells are washed with 1xPBS and fixed in ice-cold (-20°C) 70% ethanol at a concentration of 1x106 cells/ml or 2x106 cells/ml (Jurkat). Next, cells are washed once with a solution of 1x PBS, 5% FBS (GIBCO, Life Technologies, Ghent, Belgium) and 0.25% Triton X-100 (Sigma-Aldrich chemistry, St-Louis, MO USA) (PFT) and are then blocked for 1h at RT in PFT. After blocking, cells are incubated with a rabbit anti-CK4 antibody (diluted 1:100 in PFT) overnight at 4°C on a horizontal shaker. Next, cells are washed twice with PFT. Subsequently, Alexa 488-conjugated donkey anti-rabbit secondary antibody (diluted 1:200 in PFT) and primary mouse anti-human CD45 antibody labelled with allophycocyanin (diluted 1:50 in PFT) are added and the cells were incubated for 2h at RT in the dark. After incubation, the cells are washed twice with PFT and treated with 10 µg/ml of the DNA dye 7-AminoActinomycin D (7-AAD) for 15 min at RT. 7-AAD is used to distinguish cellular material from debris. Furthermore, it gives information about the current cell cycle phase of the samples. Finally, the samples are filtered on a BD conical tube (Falcon ®, Corning, NY, USA) and analyzed on the BD AccuriTM C6 Flow Cytometer (BD Biosciences, San Jose, CA USA). At least 10.000 events are measured. Single-colour stained cells are included for colour compensation. Gating is based on using A431, PC3 and Jurkat cells as positive/negative control for CK4 or CD45. Cells in G1/G0 phase and CK4+ are identified as BM cells.

3.4.3 Histological staining for epithelial cell identification

Cells are collected using the method described earlier and were stained using Giemsa to allow for histological examination of the cells collected in the swab. After the cells are fixed in 2% PFA, they are spotted on poly-L-lysine coated coverslips (see above). Next, the cells are stained with Giemsa (1:50 in 0.2M acetate buffer, pH = 3.36) (VWR International, Radnor, PA, USA) for 1 hour at RT. After incubation, the cells are washed twice with milliQ water. Next, the slides are mounted with DPX (VWR International, Radnor, PA, USA). Finally, images are acquired with a Nikon Eclipse Ti microscope using a 20× dry objective for brightfield image acquisition (Nikon, Tokyo, Japan).

3.4.4 Statistics

Statistical analyses is performed using GraphPad Prism 7.02 (GraphPad Inc., CA, USA). Induction of DNA DSBs in BM cells is analysed using repeated measures ANOVA. Both 8-oxo-dG concentrations and FRAP values before and after CBCT are compared using a paired t-test. To perform the above listed parametric tests, values should be normally distributed and the variances should be equal. Should these conditions not be met, non-parametric alternatives are used. P values lower than 0.05 are considered as statistically significant. Age-related effects are not considered during the validation experiment.

3.5 Results

Validation of the described protocol was performed on samples collected from adults (Table 3.1). BM cells were collected from adult volunteers (n = 6) using buccal swabs. Characterization of the cells collected by the swabs was performed using flow cytometrical and light microscopical analysis. $CK4^+$ cells (that were in G1/G0 phase) were identified as BM cells. Flow cytometrical analysis showed that 97.1% ± 1.4% of the cells were CK4+ BM cells, whereas less than 1% of cells were $CD45^+$. These $CD45^+$ cells are most likely leukocytes (figure 3.3). Further histological analysis confirmed that the collected cells are indeed BM cells, in various stages of exfoliation: some are nucleated, while others are not (figure 3.4A, arrowheads).

Table 3.1. Overview of scan parameters per patient included in this validation study.

Patient	Age	Sex	Device	Field of view	mAs	kV	Acquisition time (seconds)
1	57	Female	Newtom VGi evo	10x5	11	110	5
2	41	Female	Newtom VGi evo	10x5	6	110	5
3	30	Female	Newtom VGi evo	10x10	8	110	5
4	30	Male	Newtom VGi evo	10x10	10	110	5
5	71	Male	Newtom VGi evo	10x10	8	110	5
6	27	Female	Newtom VGi evo	10x10	8	110	5

mAs = milliamperage; kV = kilovoltage

The presence of DNA DSBs in BM cells was detected using an immunocytochemical staining for γH2AX and 53BP1 (figure 3.4B-E). Analysis of colocalized γH2AX and 53BP1 foci shows that 0.015 ± 0.012 foci/nuclei were counted before CBCT and 0.028 ± 0.028 foci/nuclei were counted after (p = 0.99).

Saliva samples were collected from adults that were subjected to CBCT examination twice: once without IR exposure (sham control = group 1) and once with IR exposure (= group 2). These samples (n = 5) were used to validate the protocols for the 8-oxo-dG and FRAP determination.

The change in 8-oxo-dG levels before and after CBCT exposure between group 1 and group 2 was compared. Group 1 showed no difference (-0.09 ± 0.44 ng/ml; p = 0.88) in 8-oxo-dG levels whereas an increasing trend was found in group 2 (2.5 ± 3.0 ng/ml; p = 0.19). Comparison of the changes in both groups was not significant (p = 0.15), but it shows that after IR exposure (due to CBCT examination) changes in 8-oxo-dG levels can be detected.

In combination with the 8-oxo-dG ELISA, a FRAP assay was performed. When comparing FRAP values before and after CBCT examination, results show that the FRAP value does not change in group 1 (-3.6 ± 69; p > 0.99), but there is a decreasing trend in group 2 (-18 ± 49; p = 0.31). The change between both groups does not differ significantly (*p* = 0.89), but these data show that after IR exposure (due to CBCT examination) changes in FRAP values can be detected.

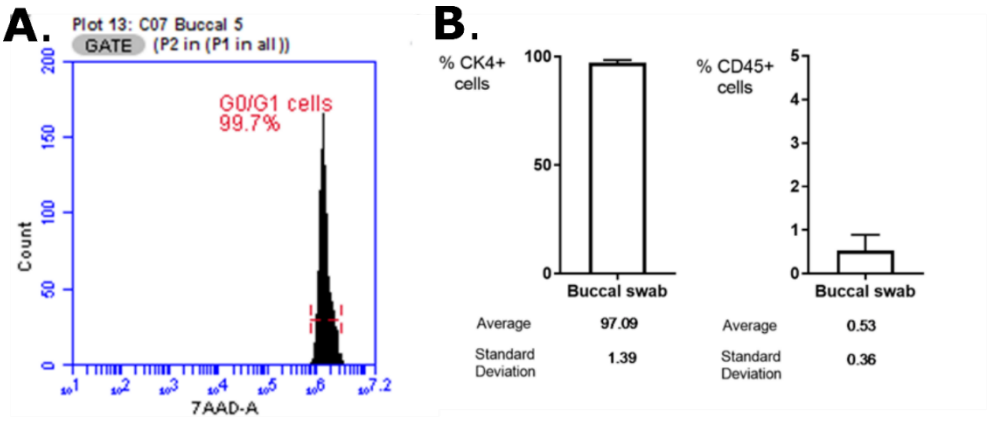

Figure 3.3. Flow cytometrical identification of cells collected by buccal swab. **A.** Overview of the cells that were in G_1/G_0 phase. Note that no S or G_2/M phase were observed, indicating that the cells are fully differentiated cells. **B.** Over 97% of the cells collected by buccal swab are $CK4^+$ epithelial cells (= buccal cells), whereas less than 1% are $CD45^+$, indicating that cells of hematological lineage are present (N = 6).

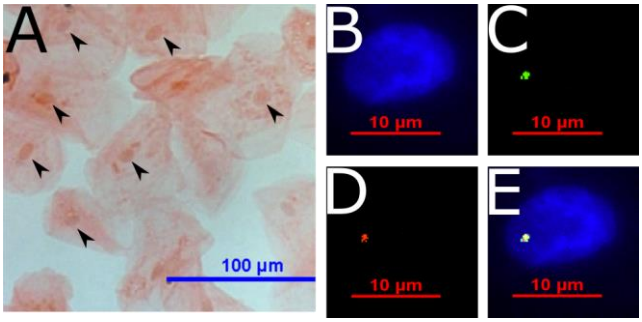

Figure 3.4. Microscopical identification of cells collected by buccal swab. **A.** Giemsa stain clearly shows nucleated epithelial cells (arrowheads), as well as unnucleated cells. This indicates that cells from all mucosal layers are collected. Enough nucleated cells are collected to perform immunocytochemistry. **B-E.** Buccal cells with DNA double strand break identified by colocolization of γH2AX and 53BP1. **B.** Buccal cell nucleus, DAPI stain. **C.** γH2AX-positive focus. **D.** 53BP1-positive focus. **E.** Merged image of B, D and E.

3.6 Discussion

Currently, the main challenge in the field of radiation protection is identifying biomarkers that allow detection of cellular and subcellular changes due to exposure to low doses of IR (< 0.1 Gy). These biomarkers could then be used to predict low dose IR-associated risks. To this end, blood is the most commonly used sample to study cellular and subcellular changes in the low dose range, such as the doses used in medical diagnostic imaging. Blood contains numerous cells that can be used for a variety of assays used in low dose radiation research, such as the micronucleus assay, dicentric assay, comet assay, γH2AX assay, oxidative stress tests (e.g. 8-oxo-dG) and even gene expression assays.[70-76] The advantage of blood sampling is that a standardized protocol can be used, the procedure is easy and small volumes suffice for most tests performed. However, the major limitation of drawing blood is that the procedure is invasive, which can cause discomfort to the patient, especially to pediatric patients.[70]

The DIMITRA Research Group provides a two-part protocol to assess potential cellular and subcellular effects after exposure to low doses of IR, i.e. CBCT examinations. This protocol focusses on non-invasive samples, i.e. BM cells and saliva samples. Compared to blood samples, BM cells and saliva samples have several major advantages: collection is non-invasive, cheap, painless and therefore allows easy repeated sampling.[50, 51, 53] This opens new opportunities for use in (oral) healthcare with an increased suitability when pediatric patients are involved. The two-part protocol focusses on detection of DNA DSBs and oxidative stress markers. Oxidative stress can induce oxidative DNA damage which has mutagenic and tumorigenic potential.[77] DNA DSBs, which can (partly) be caused by oxidative stress, is associated with carcinogenesis, an important health risk related to IR exposure.[78, 79] Therefore, DNA DSB formation and repair are important markers to assess potential health risks in patients exposed to IR.

The current paper describes and validates this two-part protocol. The collection method for BM cells was validated by flow cytometry (presence of G_1/G_0 phase $CK4^+$ cells) and light microscopy (Giemsa staining). BM cells from different mucosal layers were collected, although the majority of the cells were nucleated. These results show that this collection method yields sufficient BM cells for microscopical analysis. The use of γH2AX foci in BM cells is described before as is the use of a γH2AX/53BP1 immunofluorescent staining for the detection of DNA DSBs.[51, 64, 80-82] However, to the best of our knowledge, this is the first time that a protocol is proposed to detect DNA DSBs after CBCT examination, although other genotoxicity markers have been published before.[83] Our validation data show that that ex vivo BM cells can be used to perform γH2AX/53BP1 analysis. Future studies will investigate whether age-dependent differences can be detected in the amount of DNA DSBs after CBCT examination. For saliva collection, a protocol was

described based on the passive drool method, after which the samples are immediately stored at -20°C. Comparison between sham exposure and IR exposure, i.e. CBCT examination, shows that changes in 8-oxo-dG and FRAP levels can be detected in saliva samples after CBCT examination. These findings confirm that the methods described in this paper are suited for evaluating potential effects of low dose IR exposure in BM cells and saliva samples. The changes detected here are small, but can be attributed to the age of the volunteers: adults are more radioresistant than children, therefore we hypothesize that the effects of low dose IR exposure might be greater in children.

Despite the aforementioned advantages and validation of the DIMITRA study protocol, some precautions should be taken into account when using BM cells and saliva. BM consists of several layers of cells, thus sampling should be done in an uniformed way to avoid differences in cell type distribution. For example, it is known that the amount of basal cells increases when the cheek is sampled repeatedly.[48, 50] Therefore, the authors suggest to collect some test samples prior to the actual study and to characterize the cells that are collected, as described earlier. Although cigarette/cigar smoke is a known cytotoxin and genotoxin to BM cells[84], one limitation of this validation protocol is that 'smoking' was not included in the exclusion criteria. Therefore, it is recommended to add 'smoking' as an exclusion criterion when conducting studies in which BM cells are collected for this type of study.

Saliva composition can be affected by several factors, such as the collection itself, time of day, intake of antioxidants, time since tooth-brushing, presence of blood, drug intake, etc.. Moreover, some (pediatric) patients might not be able to produce (enough) saliva spontaneously. However, the authors recommend to not induce salivation actively, since this will create a bias when compared with spontaneous salivation.[35] To keep this type of bias to a minimum, our protocol is based on the passive drooling method to collect saliva, which is regarded as the gold standard.[67] Additional information from the patients on drug intake, previous radiation exposure, etc. should be obtained as well through a questionnaire.

For the post-imaging assessment, 30 minutes and 24 hours were chosen for γH2AX/53BP1 staining based on previous results from SCK•CEN, in which the peak response is seen after 30 to 60 minutes and most DNA damage is resolved after 24 hours.[62-64] For the 8-oxo-dG analysis and FRAP assay, we chose time points based on Haghdoost *et al*., who tested 8-oxo-dG after 30 minutes.[69] This coincides with BM cell sampling, which is an advantage since this way DNA DSB and 8-oxo-dG levels can be correlated. The results show that changes, especially in oxidative stress markers, can be detected at this time. However, it is possible that the selected time points are not the most optimal ones. Finally, we are not certain that the described methods for detecting DNA damage will be sensitive enough to detect changes following CBCT examination in children, since to the

best of the authors' knowledge, this type of study has not been performed before. Current time points are selected based on literature, as mentioned above, but also out of practical consideration: i.e. not letting the patient wait too long after the CBCT examination. If necessary, and if patients are willing, it may be possible to include additional time points (e.g. 60 minutes after CBCT examination).

The DIMITRA study protocol presented here is designed to be cost effective, quick, painless and non-invasive. The use of this protocol, however, is not limited to this study and can be easily implemented in other (radio)biological studies. For example, this protocol can be used in a similar setting in which patients are exposed to a head and neck CT, or in cancer patients treated for head and neck cancer. Furthermore, the use of saliva can be used to monitor patients exposed to short- and long-lived radionuclides for diagnostics/therapy. These examples expand the use of this protocol from risk assessment in medical diagnostics, to follow-up/monitoring of radiotherapy patients, two distinctive field in medicine using ionizing radiation.

3.7 Conclusion

It is well-known that children are more radiosensitive than adults. Together with the increasing amount of radiological examinations annually, this has recently led to societal concerns about exposure to IR during medical procedures. The DIMITRA Research Group presents a dedicated, two-part protocol to analyse potential age-related biological differences in response to CBCT examinations in both pediatric and adult patients. This protocol was validated for collecting BM cells and saliva, as well as for analysing BM cells and saliva samples for DNA damage and oxidative stress markers, respectively. After validation in this paper, this dedicated protocol can be used in different age categories to detect potential cellular and subcellular effects following dental CBCT imaging.

3.8 References

1. Arai Y, Tammisalo E, Iwai K, Hashimoto K, Shinoda K. Development of a compact computed tomographic apparatus for dental use. Dentomaxillofac Radiol. 1999;28(4):245-8.
2. Mozzo P, Procacci C, Tacconi A, Martini PT, Andreis IA. A new volumetric CT machine for dental imaging based on the cone-beam technique: preliminary results. European radiology. 1998;8(9):1558-64.
3. Scarfe WC, Farman AG. What is cone-beam CT and how does it work? Dent Clin North Am. 2008;52(4):707-30, v.
4. Pauwels R. Cone beam CT for dental and maxillofacial imaging: dose matters. Radiation protection dosimetry. 2015;165(1-4):156-61.
5. Dawood A, Patel S, Brown J. Cone beam CT in dental practice. British dental journal. 2009;207(1):23-8.
6. Kapila SD, Nervina JM. CBCT in orthodontics: assessment of treatment outcomes and indications for its use. Dentomaxillofac Radiol. 2015;44(1):20140282.
7. Scarfe WC, Farman AG, Levin MD, Gane D, Scarfe WC, Farman AG, et al. Essentials of maxillofacial cone beam computed tomography - Clinical applications of cone-beam computed tomography in dental practice. Alpha Omegan. 2010;103(2):62-7.
8. De Vos W, Casselman J, Swennen GR. Cone-beam computerized tomography (CBCT) imaging of the oral and maxillofacial region: a systematic review of the literature. Int J Oral Maxillofac Surg. 2009;38(6):609-25.
9. Feldkamp LA, Davis LC, Kress JW. Practical Cone-Beam Algorithm. J Opt Soc Am A. 1984;1(6):612-9.
10. Suomalainen A, Pakbaznejad Esmaeili E, Robinson S. Dentomaxillofacial imaging with panoramic views and cone beam CT. Insights Imaging. 2015;6(1):1-16.
11. Shah N, Bansal N, Logani A. Recent advances in imaging technologies in dentistry. World journal of radiology. 2014;6(10):794-807.
12. Scarfe WC, Farman AG, Sukovic P. Clinical applications of cone-beam computed tomography in dental practice. J Can Dent Assoc. 2006;72(1):75-80.
13. UNSCEAR. SOURCES AND EFFECTS OF IONIZING RADIATION. 2000;Volume II: Effects.
14. UNSCEAR. UNSCEAR 2013 Report: Sources, effects and risks of ionizing radiation - Volume II Annex B - Effects of radiation exposure of children. 2013.
15. Ludlow JB, Davies-Ludlow LE, White SC. Patient risk related to common dental radiographic examinations: the impact of 2007 International Commission on Radiological Protection recommendations regarding dose calculation. Journal of the American Dental Association (1939). 2008;139(9):1237-43.
16. Pauwels R, Beinsberger J, Collaert B, Theodorakou C, Rogers J, Walker A, et al. Effective dose range for dental cone beam computed tomography scanners. European journal of radiology. 2012;81(2):267-71.
17. Oenning AC, Jacobs R, Pauwels R, Stratis A, Hedesiu M, Salmon B, et al. Cone-beam CT in paediatric dentistry: DIMITRA project position statement. Pediatr Radiol. 2017.
18. Marcu M, Hedesiu M, Salmon B, Pauwels R, Stratis A, Oenning ACC, et al. Estimation of the radiation dose for pediatric CBCT indications: a prospective study on ProMax3D. Int J Paediatr Dent. 2018.
19. Signorelli L, Patcas R, Peltomaki T, Schatzle M. Radiation dose of cone-beam computed tomography compared to conventional radiographs in orthodontics. Journal of orofacial orthopedics = Fortschritte der Kieferorthopadie : Organ/official journal Deutsche Gesellschaft fur Kieferorthopadie. 2016;77(1):9-15.
20. Li G. Patient radiation dose and protection from cone-beam computed tomography. Imaging Sci Dent. 2013;43(2):63-9.

21. Loubele M, Bogaerts R, Van Dijck E, Pauwels R, Vanheusden S, Suetens P, et al. Comparison between effective radiation dose of CBCT and MSCT scanners for dentomaxillofacial applications. European journal of radiology. 2009;71(3):461-8.
22. Centre for Radiation CaEH. Guidance on the safe use of dental cone bean CT (computed tomography) equipment. Oxfordshire: Health Protection Agency; 2010.
23. Theodorakou C, Walker A, Horner K, Pauwels R, Bogaerts R, Jacobs R. Estimation of paediatric organ and effective doses from dental cone beam CT using anthropomorphic phantoms. Br J Radiol. 2012;85(1010):153-60.
24. Department of Public Health EaSDoHP-F, Women and Children's Health Cluster (FWC). Communicating radiation risks in paediatric imaging - Information to support healthcare discussions about benefit and risk. Switserland: World Health Organization; 2016.
25. Brenner DJ, Hall EJ. Computed tomography--an increasing source of radiation exposure. N Engl J Med. 2007;357(22):2277-84.
26. RadiologyInfo.org. Radiation Dose in X-ray and CT exams. Accessed on 2018-12-06. Available from: https://www.radiologyinfo.org/en/pdf/safety-xray.pdf.
27. Bogdanich W. CMJ. Radiation Worries for Children in Dentists' Chairs. New York Times. 2010.
28. Brenner DJ. Estimating cancer risks from pediatric CT: going from the qualitative to the quantitative. Pediatr Radiol. 2002;32(4):228-1; discussion 42-4.
29. Hall EJ. Lessons we have learned from our children: cancer risks from diagnostic radiology. Pediatr Radiol. 2002;32(10):700-6.
30. Berrington de Gonzalez A, Darby S. Risk of cancer from diagnostic X-rays: estimates for the UK and 14 other countries. Lancet. 2004;363(9406):345-51.
31. UNSCEAR. SOURCES AND EFFECTS OF IONIZING RADIATION: UNSCEAR 2008 Report. New York: United Nations; 2010.
32. Holmberg O, Czarwinski R, Mettler F. The importance and unique aspects of radiation protection in medicine. European journal of radiology. 2010;76(1):6-10.
33. D. K. Maurya TPAD. Role of Radioprotectors in the Inhibition of DNA Damage and Modulation of DNA Repair After Exposure to Gamma-Radiation. In: Chen CC, editor. Selected Topics in DNA Repair: InTech.; 2011.
34. Chapple IL, Matthews JB. The role of reactive oxygen and antioxidant species in periodontal tissue destruction. Periodontol 2000. 2007;43:160-232.
35. Tothova L, Kamodyova N, Cervenka T, Celec P. Salivary markers of oxidative stress in oral diseases. Front Cell Infect Microbiol. 2015;5:73.
36. Cooke MS, Evans MD, Dizdaroglu M, Lunec J. Oxidative DNA damage: mechanisms, mutation, and disease. FASEB J. 2003;17(10):1195-214.
37. Kasai H, Nishimura S. Hydroxylation of deoxy guanosine at the C-8 position by polyphenols and aminophenols in the presence of hydrogen peroxide and ferric ion. Gan. 1984;75(7):565-6.
38. Lobrich M, Shibata A, Beucher A, Fisher A, Ensminger M, Goodarzi AA, et al. gammaH2AX foci analysis for monitoring DNA double-strand break repair: strengths, limitations and optimization. Cell cycle (Georgetown, Tex). 2010;9(4):662-9.
39. Dugle DL, Gillespie CJ, Chapman JD. DNA strand breaks, repair, and survival in x-irradiated mammalian cells. Proc Natl Acad Sci U S A. 1976;73(3):809-12.
40. Olive PL. The role of DNA single- and double-strand breaks in cell killing by ionizing radiation. Radiat Res. 1998;150(5 Suppl):S42-51.
41. Jackson SP. Sensing and repairing DNA double-strand breaks. Carcinogenesis. 2002;23(5):687-96.
42. Richardson C, Jasin M. Frequent chromosomal translocations induced by DNA double-strand breaks. Nature. 2000;405(6787):697-700.
43. Vamvakas S, Vock EH, Lutz WK. On the role of DNA double-strand breaks in toxicity and carcinogenesis. Crit Rev Toxicol. 1997;27(2):155-74.
44. Khanna KK, Jackson SP. DNA double-strand breaks: signaling, repair and the cancer connection. Nat Genet. 2001;27(3):247-54.

45. Kinner A, Wu W, Staudt C, Iliakis G. Gamma-H2AX in recognition and signaling of DNA double-strand breaks in the context of chromatin. Nucleic Acids Res. 2008;36(17):5678-94.
46. Riches LC, Lynch AM, Gooderham NJ. Early events in the mammalian response to DNA double-strand breaks. Mutagenesis. 2008;23(5):331-9.
47. Ciccia A, Elledge SJ. The DNA damage response: making it safe to play with knives. Mol Cell. 2010;40(2):179-204.
48. Torres-Bugarin O, Zavala-Cerna MG, Nava A, Flores-Garcia A, Ramos-Ibarra ML. Potential uses, limitations, and basic procedures of micronuclei and nuclear abnormalities in buccal cells. Dis Markers. 2014;2014:956835.
49. Spivack SD, Hurteau GJ, Jain R, Kumar SV, Aldous KM, Gierthy JF, et al. Gene-environment interaction signatures by quantitative mRNA profiling in exfoliated buccal mucosal cells. Cancer Res. 2004;64(18):6805-13.
50. Thomas P, Holland N, Bolognesi C, Kirsch-Volders M, Bonassi S, Zeiger E, et al. Buccal micronucleus cytome assay. Nat Protoc. 2009;4(6):825-37.
51. Siddiqui MS, Francois M, Fenech MF, Leifert WR. gammaH2AX responses in human buccal cells exposed to ionizing radiation. Cytometry A. 2015;87(4):296-308.
52. Sarto F, Tomanin R, Giacomelli L, Iannini G, Cupiraggi AR. The micronucleus assay in human exfoliated cells of the nose and mouth: application to occupational exposures to chromic acid and ethylene oxide. Mutat Res. 1990;244(4):345-51.
53. Lee JM, Garon E, Wong DT. Salivary diagnostics. Orthod Craniofac Res. 2009;12(3):206-11.
54. Mandel ID. Salivary diagnosis: more than a lick and a promise. Journal of the American Dental Association (1939). 1993;124(1):85-7.
55. Miller SM. Saliva testing--a nontraditional diagnostic tool. Clin Lab Sci. 1994;7(1):39-44.
56. Dame ZT, Aziat F, Mandal R, Krishnamurthy R, Bouatra S, Borzouie S, et al. The human saliva metabolome. Metabolomics. 2015;11(6):1864-83.
57. ICRP. Recommendations of the ICRP. ICRP Publication 26. 1977(Ann. ICRP 1 (3)).
58. ICRP. 1990 Recommendations of the International Commission on Radiological Protection. ICRP Publication 60. 1991(Ann. ICRP 21 (1-3).
59. ICRP. The 2007 Recommendations of the International Commission on Radiological Protection. ICRP Publication 103. 2007(Ann. ICRP 37 (2-4)).
60. Stratis A. Customized Monte Carlo Modelling for Paediatric Patient Dosimetry in Dental and Maxillofacial Cone Beam Computed Tomography Imaging [Doctoral Thesis]. Leuven University Press: KU Leuven; 2018.
61. Virag P, Hedesiu M, Soritau O, Perde-Schrepler M, Brie I, Pall E, et al. Low-dose radiations derived from cone-beam CT induce transient DNA damage and persistent inflammatory reactions in stem cells from deciduous teeth. Dentomaxillofac Radiol. 2018:20170462.
62. Suetens A, Konings K, Moreels M, Quintens R, Verslegers M, Soors E, et al. Higher Initial DNA Damage and Persistent Cell Cycle Arrest after Carbon Ion Irradiation Compared to X-irradiation in Prostate and Colon Cancer Cells. Front Oncol. 2016;6:87.
63. Ghardi M, Moreels M, Chatelain B, Chatelain C, Baatout S. Radiation-induced double strand breaks and subsequent apoptotic DNA fragmentation in human peripheral blood mononuclear cells. Int J Mol Med. 2012;29(5):769-80.
64. Baselet B, Belmans N, Coninx E, Lowe D, Janssen A, Michaux A, et al. Functional Gene Analysis Reveals Cell Cycle Changes and Inflammation in Endothelial Cells Irradiated with a Single X-ray Dose. Front Pharmacol. 2017;8:213.
65. Schindelin J, Arganda-Carreras I, Frise E, Kaynig V, Longair M, Pietzsch T, et al. Fiji: an open-source platform for biological-image analysis. Nat Methods. 2012;9(7):676-82.
66. De Vos WH, Van Neste L, Dieriks B, Joss GH, Van Oostveldt P. High content image cytometry in the context of subnuclear organization. Cytometry A. 2010;77(1):64-75.
67. Munro CL, Grap MJ, Jablonski R, Boyle A. Oral health measurement in nursing research: state of the science. Biol Res Nurs. 2006;8(1):35-42.
68. Shakeri Manesh S, Sangsuwan T, Pour Khavari A, Fotouhi A, Emami SN, Haghdoost S. MTH1, an 8-oxo-2'-deoxyguanosine triphosphatase, and MYH, a DNA glycosylase,

cooperate to inhibit mutations induced by chronic exposure to oxidative stress of ionising radiation. Mutagenesis. 2017;32(3):389-96.
69. Haghdoost S, Czene S, Naslund I, Skog S, Harms-Ringdahl M. Extracellular 8-oxo-dG as a sensitive parameter for oxidative stress in vivo and in vitro. Free Radic Res. 2005;39(2):153-62.
70. Vandevoorde C, Gomolka M, Roessler U, Samaga D, Lindholm C, Fernet M, et al. EPI-CT: in vitro assessment of the applicability of the gamma-H2AX-foci assay as cellular biomarker for exposure in a multicentre study of children in diagnostic radiology. Int J Radiat Biol. 2015;91(8):653-63.
71. El-Saghire H, Thierens H, Monsieurs P, Michaux A, Vandevoorde C, Baatout S. Gene set enrichment analysis highlights different gene expression profiles in whole blood samples X-irradiated with low and high doses. Int J Radiat Biol. 2013;89(8):628-38.
72. Sudprasert W, Navasumrit P, Ruchirawat M. Effects of low-dose gamma radiation on DNA damage, chromosomal aberration and expression of repair genes in human blood cells. Int J Hyg Environ Health. 2006;209(6):503-11.
73. Ponzinibbio MV, Crudeli C, Peral-Garcia P, Seoane A. Low-dose radiation employed in diagnostic imaging causes genetic effects in cultured cells. Acta Radiol. 2010;51(9):1028-33.
74. Das Roy L, Giri S, Singh S, Giri A. Effects of radiation and vitamin C treatment on metronidazole genotoxicity in mice. Mutat Res. 2013;753(2):65-71.
75. Ainsbury EA, Al-Hafidh J, Bajinskis A, Barnard S, Barquinero JF, Beinke C, et al. Inter- and intra-laboratory comparison of a multibiodosimetric approach to triage in a simulated, large scale radiation emergency. Int J Radiat Biol. 2014;90(2):193-202.
76. Sangsuwan T, Haghdoost S. The nucleotide pool, a target for low-dose gamma-ray-induced oxidative stress. Radiat Res. 2008;170(6):776-83.
77. Tsuzuki T, Nakatsu Y, Nakabeppu Y. Significance of error-avoiding mechanisms for oxidative DNA damage in carcinogenesis. Cancer Sci. 2007;98(4):465-70.
78. Magnander K, Elmroth K. Biological consequences of formation and repair of complex DNA damage. Cancer letters. 2012;327(1-2):90-6.
79. Kryston TB, Georgiev AB, Pissis P, Georgakilas AG. Role of oxidative stress and DNA damage in human carcinogenesis. Mutat Res. 2011;711(1-2):193-201.
80. Gonzalez JE, Roch-Lefevre SH, Mandina T, Garcia O, Roy L. Induction of gamma-H2AX foci in human exfoliated buccal cells after in vitro exposure to ionising radiation. Int J Radiat Biol. 2010;86(9):752-9.
81. Vandevoorde C, Vral A, Vandekerckhove B, Philippe J, Thierens H. Radiation Sensitivity of Human CD34(+) Cells Versus Peripheral Blood T Lymphocytes of Newborns and Adults: DNA Repair and Mutagenic Effects. Radiat Res. 2016;185(6):580-90.
82. Deminice R, Sicchieri T, Payao PO, Jordao AA. Blood and salivary oxidative stress biomarkers following an acute session of resistance exercise in humans. Int J Sports Med. 2010;31(9):599-603.
83. da Fonte JBM, de Andrade TM, Albuquerque RLC, de Melo MDB, Takeshita WM. Evidence of genotoxicity and cytotoxicity of X-rays in the oral mucosa epithelium of adults subjected to cone beam CT. Dentomaxillofac Rad. 2018;47(2).
84. de Geus JL, Wambier LM, Bortoluzzi MC, Loguercio AD, Kossatz S, Reis A. Does smoking habit increase the micronuclei frequency in the oral mucosa of adults compared to non-smokers? A systematic review and meta-analysis. Clin Oral Investig. 2018;22(1):81-91.

Chapter 4:

Dental cone beam CT examination induces oxidative damage and antioxidant response in children's saliva

Belmans N, Gilles L, Vermeesen R, Virag P, Hedesiu M, Salmon B, Baatout S, Lucas S, Jacobs R, Lambrichts I, and Moreels M (2019) Dental cone beam CT examination induces oxidative damage and antioxidant response in children's saliva. *In review for Nature Scientific Reports*

4.1 Abstract

Assessing the possible biological effects of exposure to low doses of ionizing radiation (IR) is one of the prime challenges in radiation protection, especially in medical imaging. Today, radiobiological data on cone beam CT (CBCT) related biological effects are scarce.

In children and adults, the induction of DNA double strand breaks (DSBs) in buccal mucosa cells and 8-oxo-7,8-dihydro-2'-deoxyguanosine (8-oxo-dG) and antioxidant capacity in saliva samples after CBCT examination were examined.

No DNA DSBs induction was observed in children nor adults. In children only, an increase in 8-oxo-dG levels were observed 30 minutes after CBCT. At the same time an increase in antioxidant capacity was observed in children, whereas a decrease was observed in adults.

Our data indicate that children and adults react differently to IR doses associated with CBCT. Fully understanding these differences could lead to an optimal use of CBCT in different age categories as well as improved radiation protection guidelines.

4.2 Uncertainties concerning low dose ionizing radiation exposure and medical imaging

Nowadays, one of the prime challenges in radiation protection is assessing the possible biological effects of exposure to low doses of ionizing radiation (IR). Currently, the linear non-threshold (LNT) model is used to estimate risks involved in the low dose range. It assumes that there is no threshold dose below which no biological effects will occur and that the risk increases linearly with the absorbed dose.[1] Recently the LNT model has been heavily debated.[2] Although the LNT model is supported by epidemiological evidence in the high dose range (> 100 milliGray (mGy)), increasing evidence disproves it in the low dose range.[3-5] In addition, a lot of uncertainties still exist about low doses (< 100 mGy), due to a lack of statistical power of the epidemiological data. This is of importance in medical imaging applications of IR, such as computed tomography (CT) and, more recently, cone beam computed tomography (CBCT), which typically use doses far below 100 mGy, (typically between 0.01 – 0.10 mGy).[6-9]

Multiple controversial studies indicate that exposure of children to diagnostic radiology may lead to radiation-induced malignancies later in life. Retrospective studies observed that the use of CT scans in children could triple the risk of leukaemia and brain cancers.[10-12] A 24% increase in cancer incidence was seen in an Australian linker study, which indicated that the cancer incidence was greater after exposure at younger ages.[13] The EPI-CT study was set up to gain more insight into the potential adverse effects associated with CT examinations in children.[14] Finally, it was estimated that the probability to develop radiation-induced malignancies after CBCT exposure is 6 cases per 1,000,000 CBCT scans on average, with age at exposure and gender mostly influencing the risk.[15, 16] Despite these potential links between diagnostic radiology and radiation-induced malignancies, absolute evidence from prospective studies is scarce.[3, 6] Yeh *et al*. (2018) estimated the risks of dental CBCT and found that the risk of exposure-induced death (REID) values were highest in 10-year old subjects. These REID values were two times higher than in 30-year old subjects. The risk was higher in females than in males and the risk decreased with increasing age.[17] Radiobiological research can help explain the uncertainties of epidemiological studies as well as give more insights into the underlying mechanisms.[1, 18]

Since the introduction of CBCT in the late 1990s, its use has become widespread and is applied in several specialties in dental medicine including oral and maxillofacial surgery, orthodontics, periodontics and dental implants.[19-21]

Given that children are more radiosensitive than adults, this raised questions about potential radiation-induced health effects associated with diagnostic radiology in children.[7, 8, 22-25] IR doses associated with paediatric dental CBCT became a major concern for the general public when the New York Times published two articles about the topic (2010 and 2012).[26, 27] Especially in pedodontic and orthodontics, most CBCT examinations are performed on children (< 18 years old).[7, 25]

Exposure to IR, such as X-rays, could result in damage to important biomolecules either directly or indirectly. The former results in direct damage (e.g. ionization) to biomolecules. The latter leads to the generation of free radicals, usually through hydrolysis of water. These radicals (e.g. reactive oxygen species (ROS)) can in turn damage biomolecules in nano- to microseconds.[28]

IR can cause several types of DNA lesions, including single strand breaks, double strand breaks (DSBs) and base alterations.[29, 30] DNA DSBs are considered the most harmful because they are less likely to be repaired correctly.[31] Inaccurate repair of DSBs could result in mutations, chromosome rearrangements, chromosome aberrations and loss of genetic information.[32, 33] Therefore, eukaryotes have developed the DNA damage response (DDR).[34] The DDR consists of a signalling cascade that results in the recruitment of multiple DDR proteins to the vicinity of DSBs, including histone H2AX phosphorylated on serine 139 (γH2AX) and p53-binding protein 1 (53BP1). Both γH2AX and 53BP1 form DNA damage foci and show a quantitative relationship between the number of foci and the number of DSBs.[35, 36]

Since more than 60% of a cell consists of water, most of the DNA damage caused by X-rays is indirect via free radicals such as ROS (e.g. the hydroxyl radical, superoxide radicals and hydrogen peroxide).[29, 37] An excess of ROS causes oxidative stress in the cell which is countered by antioxidant defence mechanisms. In the context of oral pathology, oxidative stress is associated with periodontitis, dental caries and oral cancers.[38, 39] ROS can cause oxidative DNA damage through oxidative base lesions, of which over 20 have been identified.[40] An example of oxidative damage to DNA/nucleotides is 8-oxo-7,8-dihydro-2'-deoxyguanosine (8-oxo-dG), a mutagenic base modification.[41]

The buccal mucosa (BM), which lines the oral cavity, is an easily accessible source for collecting buccal mucosal cells (BMCs) in a minimally invasive, pain-free way.[42] BMCs have been used to study (amongst others) the impact of nutrition, lifestyle factors and exposure to genotoxins, including exposure to IR.[43, 44] IR-induced genotoxicity can be monitored in BMCs by measuring γH2AX levels and can be used to monitor radiation exposure and DNA damage in radiotherapy patients.[45, 46]

Saliva is a bodily fluid that is secreted into the oral cavity. It originates mainly from the parotid, submandibular and sublingual glands and is an aqueous solution (> 99% water) containing both organic and inorganic molecules.[47] Saliva, commonly referred to as 'mirror of the body', has several advantages over other biological samples, such as blood. It is readily available, collection can be done in a non-invasive way, and its use is very cost-effective.[48, 49] These advantages make saliva an ideal sample to collect from paediatric patients and for use in diagnostics.[49, 50] Currently, salivary diagnostics is becoming increasingly important in radiation biomarker research.[48, 51] Since X-rays induce most damage to biomolecules via ROS, measuring ROS and their effects in saliva samples could be a feasible indicator of radiation exposure.

The main aim of our study is to characterize the short-term radiation-induced effects associated with CBCT examinations, specifically in children. To this end, the sub-objectives were 1) to evaluate the induction of DNA DSBs in BMCs, and 2) to evaluate oxidative stress (by measuring 8-oxo-dG levels) as well as total antioxidant capacity in saliva samples.[52] These were monitored in children and adults, to identify potential age-related differences.

4.3 Materials & Methods

4.3.1 EU OPERRA - DIMITRA study

The DIMITRA study is an non-interventional, prospective study that focusses on radiation-induced effects related to diagnostic CBCT exposure in children. It is a multicentre study carried out in three European centres: the Oral and MaxilloFacial Surgery – Imaging & Pathology department (Katholieke Universiteit Leuven, Leuven, Belgium), the Dental Medicine Department of the Bretonneau Hospital (Paris, France) and the Iuliu Hatieganu University of Medicine and Pharmacy (Cluj-Napoca, Romania).[52] Ethical approval was obtained at the participating sites (B322201525196, Belgium; N°15-021, France; 208/21.04.2015, Romania).

4.3.2 Patient selection

Patients with various indications were referred to the clinic for CBCT examination. They were examined using CBCT device settings that match their individual needs. Thus the FOV, kV, mAs and resolution mode are adjusted to fit with each individual's indication and age, in agreement with the ALADAIP principle, as described in the DIMITRA position statement by Oenning *et al*..[7] Throughout the three participating centres, three CBCT devices were used: Accuitomo 170 (Mortia, Osaka, Japan), NewTom VGi evo (Cefla S.C., Imola, Italy) and Promax 3D (Planmeca OY, Helsinki, Finland).

Eligible patients were children/adolescents from 3 to 18 years old, as well as adults (> 18 years old), with good oral hygiene. Exclusion criteria were the presence of systemic diseases, the use of antibiotics or anti-inflammatory drugs, smoking and not giving informed consent prior to enrolment. In case of underage children, both parents needed to consent unless one parent has explicit permission from the other parent.[52]

4.3.3 Buccal mucosal cell collection and immunocytological staining

The collection and staining method were described in detail by Belmans *et al*. (2019).[52] Briefly, synthetic swabs were used to collect BMCs just before, 30 minutes and 24 hours after CBCT examination using a protocol modified from Thomas *et al*. (2009).[42] Before each swabbing the patient rinsed his/her mouth twice with water. The swabs were put in Saccomanno's fixative (50% ethanol and 2% polyethylene glycol in milliQ water) and stored at 4°C. Next, the BMCs were centrifuged at 580*g* for 10 minutes. Then they were washed three times in buccal

buffer (BuBu) (0.01 M Tris-HCl, 0.1 M EDTA, 0.02 M NaCl, 1% FBS, pH = 7). Next the BMCs were passed through a 100 µm nylon filter (Falcon®, VWR Belgium, Leuven, Belgium). Then the BMCs were washed one last time and pelleted. The pelleted BMCs were fixed in 500 µl of 2% paraformaldehyde (PFA) (Sigma Aldrich, St-Louis, MO, USA). Afterwards, the BMCs were washed twice with 1x phosphate-buffered saline (PBS) (Gibco, Life Technologies, Ghent, Belgium). Then they were spotted on coverslips by cytocentrifugation (ThermoFisher, Waltham, MA, USA). The coverslips were placed in 4-well culture plates (Nunc, ThermoFisher, Roskilde, Denmark) so that the BMCs were facing up.

The BMCs were washed with 1x PBS before permeabilization with 0.25% Triton X-100 in 1x PBS. After another washing step, the BMCs were blocked with 1x pre-immunized goat serum (ThermoFisher, Waltham, MA, USA) in 1x TBST and 0.005 g/v% TSA blocking powder (PerkinElmer, FP1012, Zaventem, Belgium) (TNB) for 1 hour at room temperature (RT). Afterwards, the BMCs were incubated with primary mouse monoclonal anti-γH2AX antibody (Millipore 05-636, Merck, Overijse, Belgium) (1:300 in TNB) and rabbit polyclonal anti-53BP1 antibody (Novus Biologicals NB100-304, Abdindon, UK) (1:1000 in TNB). Incubation was done overnight at 4°C on a rocking platform. After incubation, the BMCs were washed in 1x PBS. Then the BMCs were incubated for 1 hour at RT with goat anti-mouse Alexa Fluor® 488-labelled antibody (ThermoFisher, A11001, Waltham, MA, USA) (1:300 in TNB) and goat anti-rabbit Alexa Fluor® 568-labelled antibody (1:1000 in TNB) (ThermoFisher, A11011, Waltham, MA, USA). Afterwards the BMCs were washed with 1x PBS and finally the coverslips were mounted with Prolong Diamond antifade medium with 4',6-diamidino-2-phenylindole (DAPI) (ThermoFisher, Waltham, MA, USA).

Finally, images were acquired with a Nikon Eclipse Ti fluorescence microscope using a 40x dry objective (Nikon, Tokyo, Japan). Images were analysed with open source Fiji software[53], which analyses each nucleus based on the DAPI signal and within each nucleus the signals from Alexa Fluor® 488 and -568 represent the γH2AX and 53BP1 foci, respectively. The number of co-localized foci per nuclei were determined using the Cellblocks toolbox.[54]

4.3.4 Saliva collection

The collection of saliva samples was described in detail by Belmans *et al* (2019) [52]. In summary, saliva samples were collected right before and 30 minutes after CBCT examination using the passive drool method[55], and sampling coincided with the BMC collection. Immediately after collection, the whole saliva was stored at -20°C until shipment. After shipment to the lab, saliva samples were centrifuged at 10,000*g* at 4°C and the supernatant was stored at -80°C until further analysis.

4.3.5 8-oxo-dG enzyme-linked immunosorbent assay

8-oxo-dG was analysed using a 8-oxo-dG enzyme-linked immunosorbent assay (ELISA). Prior to this assay, 500 µl of saliva was purified twice on a C18 solid phase extraction column (Varian, Lake Forest, CA, USA) as described by Shakeri Manesh *et al*. (2017).[56] The 8-oxo-dG ELISA (Health Biomarkers Sweden AB, Stockholm, Sweden) was performed as described by Haghdoost *et al* (2005).[57] In short, 270 µl of sample/standard was added to 165 µl of primary antibody and incubated for 2 hours at 37°C on a shaker. The ELISA plate was washed with 1x PBS and 140 µl of sample/standard was loaded per well. The plate was incubated overnight at 4°C on a shaker. Next, the plate was washed with 1x washing solution and 140 µl of secondary antibody was added per well. After a 2 hour incubation at RT, the plate was washed with 1x washing solution. Afterwards, 140 µl of chromogenic substrate 3,3',5,5'-tetramethylbenzidine (One-step substrate system, Dako, Glostrup Municipality, Denmark) was added and the plate was incubated for 15 minutes at RT. The colour reaction was stopped by adding 2 M sulphuric acid. Finally, the absorbance was measured at 450 nm (signal) and 570 nm (background) using a microplate reader (ClarioStar, BMG Labtech, Ortenberg, Germany).

4.3.6 Total antioxidant capacity determination

The Ferric Reducing Antioxidant Power (FRAP) assay (Cell Biolabs, CA, USA) was performed on whole saliva according to the manufacturer's instructions. Briefly, 100 µl of sample/standard and 100 µl reaction reagent were added per well of a 96-well plate. Then the plate was incubated for 10 minutes at RT on a shaker. Finally, the absorbance was measured at 560 nm using a microplate reader (ClarioStar, BMG Labtech, Ortenberg, Germany).

4.3.7 Dose calculations – Monte Carlo simulation

A fully validated Monte Carlo (MC) framework, which was developed by the DIMITRA group, was used for dosimetric calculations.[58, 59] This MC simulation relies on a database of pediatric head voxel models.[60] By using this MC DIMITRA framework, absorbed organ doses were calculated for each individual patient. When simulating organ doses, the normalized absorbed organ dose values are provided in µGy/mAs. In the MC DIMITRA framework, normalized absorbed organ doses are related to the age of the patient via the following equation:

$$y = a \times \ln(x) + b$$

where y is the normalized absorbed organ dose (µGy/mAs), x is the age of the patient at the time of the scan, and the constants a and b are factors that depend

on the organ scanned, the clinical case, and the device used.[58] Simply multiplying the normalized absorbed organ dose by the mAs used for each specific scanning protocol results in an absorbed organ dose value. Thus the absolute organ dose can be calculated as follows:

$$y_{i,j} = [a \times \ln(x) + b] \times \mathrm{mAs}_j$$

where *i* represents a specific organ, and *j* stands for a specific examination. Note that this equation is not validated for adults, i.e. patients older than 18 years old. Therefore, no doses were simulated for adults using this equation.

4.3.8 Statistics

Statistical analysis was performed using GraphPad 7.02 (GraphPad Inc., CA, USA). The results of the DNA DSBs in BMCs were analysed using repeated measures one-way analysis of variance (ANOVA). 8-oxo-dG and FRAP assay results were analysed using two-tailed paired t-tests. To analyse differences between age groups and differences in radiation sensitivity, two-tailed unpaired t-tests were performed. While all tests listed above are parametric tests, non-parametric alternatives were used if conditions were not met. *P* values lower than .05 were considered as statistically significant. Results are shown as mean ± standard error of the mean (SEM).

4.4 Results

4.4.1 Patients and dose exposure

In total, 147 children that participated in this study were 11 ± 3 years old (age range: 3 – 18 years old). 73 boys and 74 girls were included. Besides, 23 adults (9 men and 14 women) that participated were 43 ± 17 years old (age range: 19 -77 years old). Three CBCT devices were used, namely Promax 3D (Planmeca, Finland), Accuitomo 170 (Morita, Osaka, Japan), NewTom VGi-evo (Cefla S.C., Imola, Italy), with average (simulated) absorbed doses to the salivary glands of 1613 ± 19 μGy, 2416 ± 324 μGy and 4283 ± 353 μGy, respectively.[61, 62] The study was approved by the ethical committees of the participating hospitals (see Material & Methods section). All patients (or their parents, in case of children) gave written informed consent (see supplementary data 1 and 5 and supplementary table 1).

4.4.2 DNA double strand break detection in exfoliated buccal mucosal cells before and after CBCT examination

The results from co-localized γH2AX and 53BP1 foci, which are a measure for DNA DSBs, show no changes in the amount of DSBs after CBCT examination, neither in children nor adults (figure 4.1).

In children (N = 38, degrees of freedom (DF) = 2, Friedman statistic = 2.7, p =.2538) a slight increase was seen in the amount of foci from 0.25 ± 0.054 foci/cell before CBCT to 0.47 ± 0.12 foci/cell 30 minutes after CBCT (p > .9999). 24 hours after CBCT the amount of foci returned to baseline levels (0.3 ± 0.09 foci/cell) (p > .9999). The decrease between 30 minutes after CBCT and 24 hours after, however, is not significant (p = .5614).

Similarly, no significant changes in the amount of co-localized γH2AX and 53BP1 foci were found in adult patients (N = 13, DF = 2, Friedman statistic = 1.0, p = .6065). Before CBCT, 0.0014 ± 0.0014 foci/cell were counted, which increased slightly to 0.0053 ± 0.0035 foci/cell 30 minutes after CBCT exposure (p > .9999). Contrary to the children, the number of foci per cell remained increased 24 hours after CBCT when compared to before CBCT (0.0061 ± 0.0051 foci/cell; p > .9999). Between 30 minutes after CBCT and 24 hours after CBCT no significant difference was observed (p > .9999).

Interestingly, the amount of foci per cell was significantly higher in children than in adults at every time point. Before CBCT 0.25 ± 0.054 foci/cell were observed in children and 0.0014 ± 0.0014 foci/cell were observed in adults (Mann-Whitney U value = 121, p = .0020). 30 minutes after CBCT, the amount of foci in children (0.47 ± 0.12 foci/cell) was significantly higher than the amount seen in

adults (0.0053 ± 0.0035 foci/cell) (Mann-Whitney U value = 145, p = .0146). Finally, 24 hours after CBCT exposure the amount of foci in children (0.3 ± 0.09 foci/cell) was higher than the amount of foci in adults (0.0061 ± 0.0051 foci/cell) (Mann-Whitney U value = 170, p = .0487).

Since both children and adults showed an increase 30 minutes after CBCT, these increases were compared (# foci/cell$_{30\ minutes\ after\ CBCT}$ - # foci/cell$_{before\ CBCT}$). The mean increase in children (0.17 ± 0.097 foci/cell) did not differ from the increase in adults (0.0078 ± 0.01 foci/cell) (Mann-Whitney U value = 412, p = .8089). Regarding the difference between 30 minutes after CBCT and 24 hours after, no significant difference was observed between children (-0.17 ± 0.11 foci/cell) and adults (0.00087 ± 0.0066 foci/cell) (Mann-Whitney U value = 196, p = .2105).

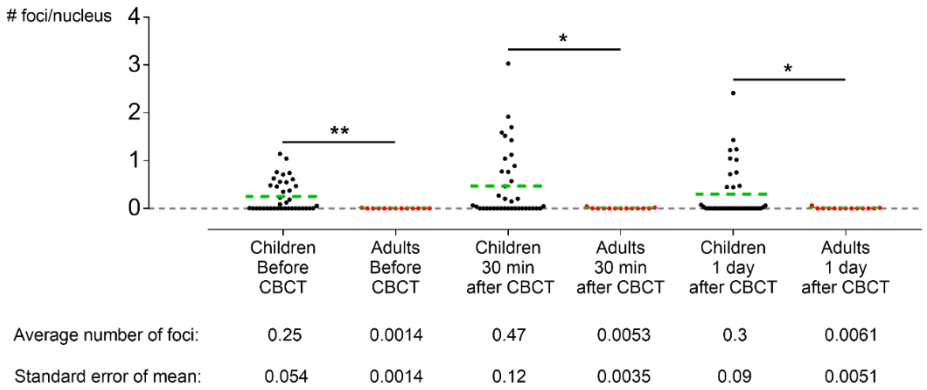

Figure 4.1. No DNA double strand breaks (DSBs) are induced in buccal mucosal cells (BMCs) after cone beam computed tomography (CBCT) examination, neither in children nor in adults. No significant increases in the amount of γH2AX/53BP1 co-localized foci were observed 30 minutes and 24 hours after CBCT examination in children (Black dots; N = 38, degrees of freedom = 2, Friedman statistic = 2.7, p = .2538) and in adults (Red dots; N = 13, degrees of freedom = 2, Friedman statistic = 1.0, p = .6065). Before (Mann-Whitney U value = 121, p = .0020), 30 minutes after (Mann-Whitney U value = 145, p = .0146) and 24 hours after CBCT (Mann-Whitney U value = 170, p = .0487) the amount of DSBs was significantly higher in children then in adults. Only the data from patients of which results were obtained for all time points were included. Green dotted line = average number of foci; * = p ≤ .05; ** = p ≤ .0021.

4.4.3 8-oxo-dG levels in saliva samples

8-oxo-dG levels were measured in saliva samples collected before and after CBCT examination. They were increased in children but not in adults 30 minutes after CBCT (figure 4.2).

In children, a significant increase in 8-oxo-dG levels was observed between samples taken before CBCT examination (1.86 ± 0.26 ng/ml) and 30 minutes after CBCT (4.11 ± 0.62 ng/ml) (N = 68, DF = 67, t value = 4, $p < .0001$), an average increase of 121 % (figure 4.2; supplementary data 3). In adults , an increase from 1.52 ± 0.34 ng/ml 8-oxo-dG before CBCT to 2.42 ± 0.55 ng/ml 30 minutes after CBCT was observed (N = 19, DF = 18, t value = 1.58, $p = .1317$), resulting in an average increase of 59% (figure 4.2). No differences were observed between the values of children and adults before CBCT (Mann-Whitney U value = 643.5, $p = .98$) and 30 minutes after CBCT (Mann-Whitney U value = 622.5, $p = .81$).

In the group of children, data were split based on gender (Table 4.1). Both in boys and girls the amount of 8-oxo-dG increased significantly after CBCT examination (N = 35, $p = .024$ and N = 33, t-value = 2.91, DF = 32, $p = .0065$, respectively). Furthermore, no differences between boys and girls was observed (Table 4.1). This was confirmed when the proportional change between values before and after CBCT were compared between boys and girls ($p = .6907$) (see supplementary data 2).

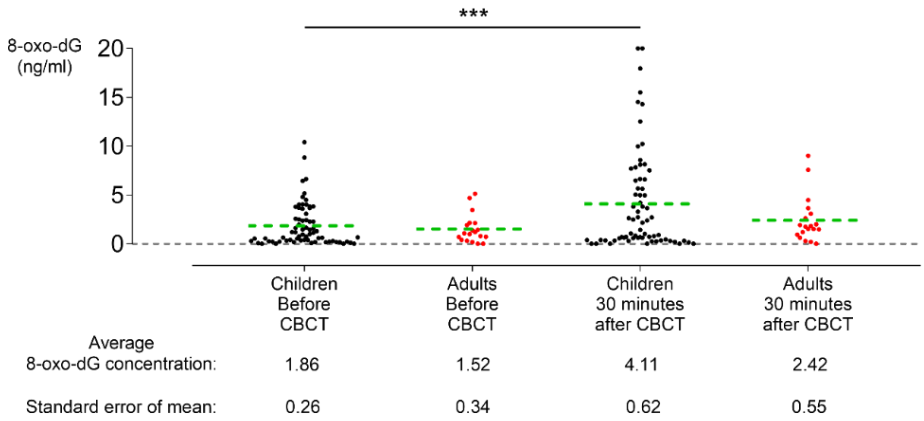

Figure 4.2. Excretion of 8-oxo-7,8-dihydro-2'-deoxyguanosine (8-oxo-dG) into saliva is increased after cone beam computed tomography (CBCT) examination in children but not in adults. Only data from patients of which results were obtained for both time points were included. In children there is a significant average increase of 121% in 8-oxo-dG excretion 30 minutes after CBCT examination (N = 68, DF = 67, t value = 4, $p < .0001$). In adults there is an average increase in 8-oxo-dG excretion of 59% (N = 19, DF = 18, t value = 1.58, $p = .1317$). Green dotted line = average; ****= $p < .0001$.

Table 4.1. Comparison between boys and girls for 8-oxo-dG excretion before and after cone beam computed tomography (CBCT) examination.

	Boys (N = 35)	**Girls (N = 33)**	***P* value**	**t-value**	**Degrees of freedom**
8-oxo-dG (ng/ml) Before CBCT	1.71 ± .27	2.01 ± .46	.63	Mann-Whitney U value = 537.5	N.A.
8-oxo-dG (ng/ml) 30 minutes after CBCT	4.21 ± .94	4.01 ± .83	.96	Mann-Whitney U value = 573.5	N.A.
***P* value**	.024	.0065			
t-value	(Wilcoxon test)	2.9			
Degrees of freedom	(Wilcoxon test)	32			

Plotting the proportional change in 8-oxo-dG levels of children against the absorbed dose received by the patients showed no visible trend or dose response (figure 4.3).

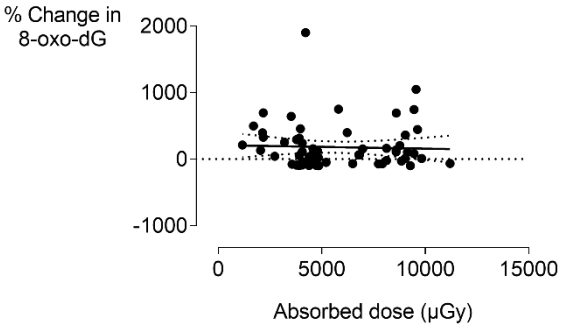

Figure 4.3. No dose response in 8-oxo-dG excretion in saliva 30 minutes after cone beam computed tomography in children. No visible dose response (linear or otherwise) was observed in 8-oxo-dG excretion in children. Radiation doses were the absorbed doses at the salivary glands as calculated by MC simulations.[60, 61]

4.4.4 Total antioxidant capacity in saliva samples

Ferric Reducing Antioxidant Power (FRAP) values were measured in saliva samples before and 30 minutes after CBCT examination. They were significantly increased in children and decreased significantly in adults 30 minutes after CBCT examination (figure 4.4).

Children showed a slight, but significant increase in FRAP value after CBCT examination. Thirty minutes after CBCT examination, FRAP values increased from 260.80 ± 11.87 to 277.90 ± 13.22, an increase of about 7% (N = 117, t-value = 1.98, DF = 116, p = .0498) (supplementary data 4). Contrary to the results in children, a decrease of about 9% in FRAP values was found in adults. FRAP values decreased from 202.90 ± 21.28 at baseline to 185.50 ± 20.74 30 minutes after CBCT examination (N = 17, t-value = 2.22, DF = 16, p= .0412). No significant differences were observed between children and adults before CBCT examination (t-value = 1.80, DF = 132, p = .0747). However, the FRAP values 30 minutes after CBCT examination were significantly higher in children than in adults (Welch-corrected t-value = 3.76, DF = 30.93, p= .0007). The response in children and adults differed significantly when comparing the average increase in children with the average decrease in adults (Welch-corrected t-value = 2.96, DF = 65, p = .0043).

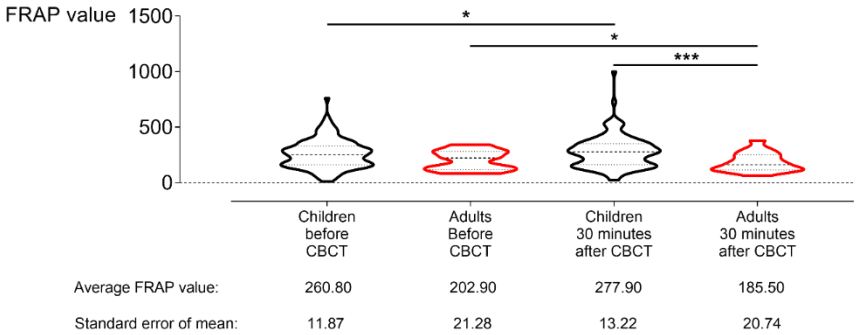

Figure 4.4. Ferric reducing antioxidant power (FRAP) values increase in saliva samples from children after cone beam computed tomography (CBCT) examination, while decreasing in saliva samples from adults. In children (black violin plots) a significant increase in FRAP values was observed 30 minutes after CBCT examination (N = 117, t-value = 1.98, degrees of freedom (DF) = 116, p = .0498). In adults (red violin plots) a significant decrease was observed 30 minutes after CBCT examination (N = 17, t-value = 2.22, DF = 16, p= .0412). The FRAP values 30 minutes after CBCT are significantly higher in children than in adults (Welch-corrected t-value = 3.76, DF = 30.93, p= .0007). The response in children and adults differs significantly, with an average increase of 17.10 ± 8.62 in children and an average decrease of 17.40 ± 7.84 in adults (Welch-corrected t-value = 2.96, DF = 65, p = .0043). * = $p \leq .05$; *** = $p \leq .0002$.

Table 4.2. Comparison between boys and girls FRAP values before and after cone beam computed tomography (CBCT) examination.

	Boys (N = 62)	Girls (N = 55)	*P* value	t-value	Degrees of freedom
FRAP value Before CBCT	265.90 ± 19.39	263.00 ± 16.85	.9318	0.086	132
FRAP value 30 minutes after CBCT	277.00 ± 22.84	295.40 ± 18.35	.4963	0.68	132
***P* value**	.4194	.0268			
t-value	0.81	2.28			
Degrees of Freedom	61	54			

Results were also analysed based on gender (table 4.2). In children, both boys and girls showed an increase in FRAP values, but the increase was only significant in girls (N = 62, t-value = 0.81, DF = 61, p = .4194 and N = 55, t-value = 2.28, DF = 54, p = .0268, respectively). Additionally, in both adult men and women a decrease was observed, but this was also only significant for women (N = 4, Wilcoxon test, p > .9999 and N = 13, t-value = 2.27, DF = 12, p = .0428, respectively). Furthermore, in children it was observed that the baseline levels were lower in the morning (225.10 ± 12.48) than baseline levels in the afternoon (282.30 ± 21.04) (Welch-corrected t-value = 2.34, DF = 82.42, p = .0217). The same was observed in adults (baseline morning: 174 ± 21; baseline afternoon: 269 ± 42), although this difference was not statistically significant (Mann-Whitney U value = 12, p = .0897). Therefore, the data from children were split into a morning and afternoon group. The salivary FRAP values did not significantly differ after CBCT examination if data were corrected for time of sample collection. In the morning groups, there was no significant change in both boys and girls (N = 24, Wilcoxon test, p = .97 and N = 10, t-value = 0.81, DF = 9, p = .7394, respectively). In the afternoon group, FRAP levels in boys did not change (N = 17, Wilcoxon test, p = .89). However, in girls from the afternoon group FRAP levels increased significantly (N = 24, t-value = 2.14, DF = 23, p = .0431).

4.5 Discussion

Determining the biological effects of exposure to low doses of IR, such as those used in medical imaging, of paramount concern in radiation protection today. This study aimed to characterize the short-term radiation-induced effects associated with CBCT examinations, specifically in children. To this end, the number of DNA DSBs was monitored in BMCs and 8-oxo-dG levels as well as total antioxidant capacity were monitored in saliva samples using previously optimized protocols.[52] We report that no induction of DNA DSBs was detected in BMCs, neither in children nor in adults. Furthermore, a significant increase in 8-oxo-dG and total antioxidant capacity was observed in saliva samples from children 30 minutes after CBCT examination. In contrast, no significant changes were observed in 8-oxo-dG levels in adults. Furthermore, a significant decrease in total antioxidant capacity was observed in saliva samples from adults 30 minutes after CBCT examination. Since no dose response was observed, the outcome of this study could help to clarify the controversy surrounding the LNT model as well as the uncertainty about potential adverse health effects after exposure to low doses of IR (< 100 mGy), such as those used in CBCT. Finally, the data from DNA DSBs after 24 hours also indicate that no delayed increase in the number of DSBs occurs after CBCT examination.

Exposure to IR can result in DSBs, which are considered very harmful, since inaccurate repair could result in mutations, chromosome rearrangements, chromosome aberrations and loss of genetic information.[29, 30, 32, 33] Our results indicate that exposure to radiation doses used in CBCT examinations (0.184 mGy –9.008 mGy in this study) does not induce DNA DSBs in BMCs from children and adults, as observed using a microscopic γH2AX/53BP1 co-localization assay. This assay was performed on samples collected before, 30 minutes and 24 hours after CBCT examination. Previously, both the γH2AX assay and the γH2AX/53BP1 assay were used to detect DNA DSBs after exposure to radiation doses used in diagnostic and interventional radiology, such as CT scans.[63-65] These studies report a significant increase in γH2AX foci in lymphocytes 1 hour after CT examination, which uses higher radiation doses than CBCT. Furthermore, our group recently showed that low doses associated with CBCT examinations are capable of inducing DNA DSBs *in vitro* in dental stem cells.[66] BMCs have also been used successfully as a biomarker for genotoxic effects, including using the γH2AX assay to detect radiation-induced DNA DSBs.[45, 67, 68] These studies report increase of genotoxic effects in BMCs after low dose IR exposure. Gonzalez *et al*. (2010) showed that *in vitro* exposure of BMCs to IR induces γH2AX foci.[45] Our findings indicate that CBCT examinations do not cause DNA DSBs in BMCs, which is in line with previous publications focusing on genotoxicity induced by radiological examinations. In

these studies, no genotoxic effects, i.e. micronucleated cells, were observed after low doses of IR, such as panoramic dental radiology and CBCT. These studies, however, all reported increases in other nuclear alterations (e.g. pyknosis, karyorrhexis and karyolysis) that are associated with increased cytotoxicity.[68-71] Recently, Preethi *et al*. (2016) reported significant increases in the number of micronucleated cells in BMCs after dental radiography in paediatric patients.[67] Furthermore, Yoon *et al*. (2009) reported a significant increase in γH2AX foci in BMCs of adults after dental radiography.[72]

Our data show 0.0014 ± 0.0014 co-localized γH2AX/53BP1 foci per cell in BMCs from adults at baseline. This number is remarkably lower than the 0.08 ± 0.02 γH2AX foci per cell in non-irradiated BMCs reported previously by Gonzalez *et al*. (2010) [45]. These different observations can be explained by the higher sensitivity of the γH2AX/53BP1 co-staining, which eliminates the detection of γH2AX foci observed during S-phase replication fork stalling [73]. In addition, Gonzalez *et al*. (2010) treated the BMCs differently, e.g. after collection they incubated the BMCs in cell growth medium at 37° Celsius, which can also affect the number of foci counted.[45]

Interestingly, we found before CBCT examination, but also 30 minutes and 24 hours after CBCT examination, the average number of γH2AX/53BP1 foci per cell was higher in children than in adults. This observation contradicts what has been published before, namely that aging is associated with accumulation of DNA damage.[74, 75] One would expect the level of DNA damage, at least before CBCT examination, to be higher in adults than in children. However, BMCs are the first barrier in the inhalation and ingestion routes. Therefore, they are exposed to several genotoxins. These can be found in environmental and lifestyle factors such as diet, mouthwash, smoke, air pollution, etc..[76-78] These factors can, at least partially, explain our observation, since children are more sensitive to these type of genotoxins compared to adults due to age-related differences in absorption, metabolism, development and body functions.[77]

Finally, we observed that the response after CBCT examination in children did not differ significantly from that of adults. This indicates that BMCs from children after CBCT examination do not show an increased radiosensitivity compared to BMCs from adults.[22-24] These findings are in line with results from Ribeiro *et al*. (2008). They compared the genotoxic and cytotoxic effects of dental radiography between children and adults and found no significant differences in micronucleus frequency or cytotoxicity.[79] However, the radiation doses used in radiography are lower than those used in CBCT, thus this should be interpreted with caution.

The mutagenic base modification 8-oxo-dG is a marker for oxidative damage to DNA/nucleotides and a useful biomarker of exposure to high doses of IR.[41, 57] This study shows that 8-oxo-dG levels excreted in saliva increased in children but not in adults 30 minutes after CBCT. Oxidative stress has been linked

to oral diseases such as periodontitis, dental caries and oral cancers.[38, 39] Because of its mutagenic potential, excretion of 8-oxo-dG depends on cellular DNA repair mechanisms, such as nucleotide excision repair, nucleotide incision repair and Nudix hydrolase activity.[80] Therefore, a reduced DNA repair capacity may result in accumulation of 8-oxo-dG in the cells, thus resulting in a decrease in 8-oxo-dG excretion. Since DNA repair capacity was shown to decrease with age, this could explain why the concentration of 8-oxo-dG in saliva samples of adults was not increased significantly after CBCT examination, as it was in children.[81, 82] Despite the significant increase in children and the limited increase in adults, no statistical differences were observed between both groups. This is most likely due to the limited group size of the adult group.

Previously, an association between the excretion of 8-oxo-dG and high radiation doses was described.[57] This association was not linear and showed saturation between 0.5 and 1 Gy. However, such dependency was not observed in this study, for example children that were exposed to 0.8 mGy showed a similar increase in 8-oxo-dG excretion as children exposed to 0.2 mGy. These data indicate that there is a high variability in individual radiosensitivity in our study population. Alternatively, it could be that the very low IR doses associated with CBCT elicit a small biological response which is unrelated to the IR dose, like an all-or-nothing mechanism. This is similar to the use of a 'priming dose' in adaptive response studies. Here a very low dose of a stressor (e.g. a chemical or IR) results in a small response which in turn prepares cells to an exposure of the same stressor at a higher dose.[83] Our results mimic the effects seen when applying such a 'priming dose'.

Although 8-oxo-dG was proposed as a marker for radiosensitivity, evidence is lacking or comes from radiotherapy patients, who receive doses that are a lot higher than the doses in our study population.[84]

We describe for the first time that salivary 8-oxo-dG levels are significantly increased in both boys and girls after CBCT examination. No significant gender differences in salivary 8-oxo-dG levels were observed. Previous measurements in urine and other cells showed similar results.[85-87] To the best of our knowledge, similar findings of 8-oxo-dG secretion in saliva in children were not reported before. Previous studies analysed oxidative stress markers in adults. These studies reported higher ROS production and oxidative stress biomarkers in men when compared to premenopausal women (reviewed by Kander *et al*. (2017)[88]). It is noteworthy that these studies are all related to cardiovascular diseases and not radiation exposure. However, there are studies that report higher oxidative status in females which contradicts the aforementioned studies.[89].

FRAP values give information about the total antioxidant capacity of biological samples. Our data shows on opposite response between children and adults 30 minutes after CBCT examination: salivary FRAP values increase significantly in children, whilst they decrease significantly in adults. Furthermore,

the response in children is significantly different from that in adults, indicating that children react differently to CBCT-associated radiation exposure. Interpretation of the data needs to be done cautiously, since the data show that the time of sampling (in the morning or in the afternoon) significantly affected the baseline salivary FRAP values in children. The highest values were measured in the afternoon. Similar circadian changes in FRAP values were observed before.[90] After correcting for time of sampling, no significant changes in salivary FRAP levels were observed, except for girls that were sampled in the afternoon. However, since pair-wise tests were used, this circadian influence is expected to be limited in this study.

Total antioxidant capacity has been used previously as a salivary biomarker related to periodontal disease and dental caries. Decreases in total antioxidant capacity have been linked to periodontal disease.[91]

The use of total antioxidant capacity as a biomarker has several limitations. Firstly, the total antioxidant capacity that is measured is the result of a complex mixture of antioxidants that is present in saliva. The major antioxidant in saliva has been reported to be uric acid, which accounts for more than 85% of the salivary antioxidant capacity. In addition, a wide array of other potent antioxidants are found in saliva, such as superoxide dismutase, catalase, glutathione peroxidase, ascorbic acid, several vitamins and albumin.[92, 93] In this regard, future analysis into the enzymatic activity of specific antioxidant enzymes, e.g. superoxide dismutase might be interesting. Secondly, a lot of biological variability of salivary total antioxidant capacity exists. We report an average salivary FRAP value of 202.90 ± 21.28 in adults at baseline, whereas an average of 610.83 ± 4.52 was reported before in healthy adults.[94] It is noteworthy that this patient population was Asian, where ours is European, which may suggest ethnical differences in salivary FRAP values. Finally, several confounding factors have been described that affect the saliva composition and can thus affect the total antioxidant capacity. Confounding factors may include circadian rhythm, gender, age and diet.[90, 92] This study also found an effect of circadian rhythm (see above), age and gender. Girls show a significant increase in salivary FRAP values, whereas women show a significant decrease. Both boys and men showed a change (an increase and decrease, respectively), but this was not significant. These findings indicate that females are more susceptible to changes in total antioxidant capacity following IR exposure and that the net effects depends on the age of the individual. However, it is important to note that our patient group is relatively small (N = 72 for girls and N = 13 for women). Increasing the sample size could therefore yield different results. These limitations could interfere with interpretation of the results. Therefore, it is important to take these confounding factors into account during the design of a study. As with 8-oxo-dG, no dose response relationship was observed for FRAP values.

In conclusion, our data provide evidence that CBCT examinations cause oxidative damage in children, as well as an increase in the antioxidant response. In adults, a slight increase in oxidative damage and a significant decrease in the antioxidant response were observed. These results indicate that children and adults react differently to low doses of IR associated with CBCT examinations. Despite this increase in oxidative damage, no induction of DNA DSBs in BMCs was observed in children nor in adults. Furthermore, we observed some gender-related differences. Girls/women showed a significant increase/decrease in FRAP values after CBCT examination, whereas boys/men do not. Our data demonstrate that saliva can be used for biomonitoring after IR exposure even if the radiation doses are very low (< 1 mGy). However, no dose response relationship was found, neither for 8-oxo-dG levels nor for FRAP values.

Nonetheless, these results should raise awareness about radiation protection and the 'As-Low-as- Diagnostically Acceptable being indication-oriented and patient-specific' (ALADAIP) principle among clinicians and radiologists.[7] However, this should be investigated into more depth to gather more information about the potential link between possible biological effects and the CBCT settings that were used. Furthermore, the effects observed and described in this study are short-term effects, i.e. within 30 minutes after CBCT examination. We can conclude that adverse effects, although very small, occur and that further research is warranted. These findings are an incentive for continuing research into the biological effects after CBCT examination, since fully understanding them could lead to an optimal use of CBCT in a paediatric population as well as improved radiation protection guidelines.

4.6 Competing interests

The authors declare that there are no competing interests.

4.7 Acknowledgements

The authors like to thank all patients (and their parents) for their willingness to contribute to this study. They also like to express their gratitude towards the hospital staff, especially Christelle Lefevre and the CRB facility (Dr. Sarah Tubiana, HUPNVS – APHP, France) for their indispensable help with the sample collection.

The DIMITRA project has received funding from the European Atomic Energy Community's Seventh Framework Programme FP7/2007–2011 under grant agreement no 604984 (OPERRA: Open Project for the European Radiation Research Area).

The DIMITRA Research Group that contributed to this paper consists of N. Belmans, M. Moreels, S. Baatout, B. Salmon, A.C. Oenning, C. Chaussain, C. Lefevre, M. Hedesiu, P. Virag, M. Baciut, M. Marcu, O. Almasan, R. Roman, A. Porumb, C. Dinu, H. RotaruC. Ratiu, O. Lucaciu, B. Crisan, S. Bran, G. Baciut, R. Jacobs, H. Bosmans, R. Bogaerts, C. Politis, A. Stratis, R. Pauwels, K. de F. Vasconcelos, L. Nicolielo, G. Zhang, E. Tijskens, M. Vranckx, A. Ockerman, E. Claerhout, E. Embrechts.

4.8 References

1. Boice JD, Jr. The linear nonthreshold (LNT) model as used in radiation protection: an NCRP update. Int J Radiat Biol. 2017;93(10):1079-92.
2. Calabrese EJ. From Muller to mechanism: How LNT became the default model for cancer risk assessment. Environ Pollut. 2018;241:289-302.
3. Tubiana M, Feinendegen LE, Yang C, Kaminski JM. The linear no-threshold relationship is inconsistent with radiation biologic and experimental data. Radiology. 2009;251(1):13-22.
4. Feinendegen LE, Pollycove M, Neumann RD. Whole-body responses to low-level radiation exposure: New concepts in mammalian radiobiology. Exp Hematol. 2007;35(4):37-46.
5. Feinendegen LE. Evidence for beneficial low level radiation effects and radiation hormesis. Brit J Radiol. 2005;78(925):3-7.
6. Lee CY, Koval TM, Suzuki JB. Low-Dose Radiation Risks of Computerized Tomography and Cone Beam Computerized Tomography: Reducing the Fear and Controversy. J Oral Implantol. 2015;41(5):e223-30.
7. Oenning AC, Jacobs R, Pauwels R, Stratis A, Hedesiu M, Salmon B, et al. Cone-beam CT in paediatric dentistry: DIMITRA project position statement. Pediatr Radiol. 2017.
8. Marcu M, Hedesiu M, Salmon B, Pauwels R, Stratis A, Oenning ACC, et al. Estimation of the radiation dose for pediatric CBCT indications: a prospective study on ProMax3D. Int J Paediatr Dent. 2018.
9. Pauwels R, Beinsberger J, Collaert B, Theodorakou C, Rogers J, Walker A, et al. Effective dose range for dental cone beam computed tomography scanners. European journal of radiology. 2012;81(2):267-71.
10. Pearce MS, Salotti JA, Little MP, McHugh K, Lee C, Kim KP, et al. Radiation exposure from CT scans in childhood and subsequent risk of leukaemia and brain tumours: a retrospective cohort study. Lancet. 2012;380(9840):499-505.
11. Huang WY, Muo CH, Lin CY, Jen YM, Yang MH, Lin JC, et al. Paediatric head CT scan and subsequent risk of malignancy and benign brain tumour: a nation-wide population-based cohort study. Br J Cancer. 2014;110(9):2354-60.
12. Krille L, Dreger S, Schindel R, Albrecht T, Asmussen M, Barkhausen J, et al. Risk of cancer incidence before the age of 15 years after exposure to ionising radiation from computed tomography: results from a German cohort study. Radiat Environ Biophys. 2015;54(1):1-12.
13. Mathews JD, Forsythe AV, Brady Z, Butler MW, Goergen SK, Byrnes GB, et al. Cancer risk in 680,000 people exposed to computed tomography scans in childhood or adolescence: data linkage study of 11 million Australians. BMJ. 2013;346:f2360.
14. Bosch de Basea M, Pearce MS, Kesminiene A, Bernier MO, Dabin J, Engels H, et al. EPI-CT: design, challenges and epidemiological methods of an international study on cancer risk after paediatric and young adult CT. J Radiol Prot. 2015;35(3):611-28.
15. Pauwels R, Cockmartin L, Ivanauskaite D, Urboniene A, Gavala S, Donta C, et al. Estimating cancer risk from dental cone-beam CT exposures based on skin dosimetry. Phys Med Biol. 2014;59(14):3877-91.
16. Aanenson JW, Till JE, Grogan HA. Understanding and communicating radiation dose and risk from cone beam computed tomography in dentistry. J Prosthet Dent. 2018.
17. Yeh JK, Chen CH. Estimated radiation risk of cancer from dental cone-beam computed tomography imaging in orthodontics patients. BMC Oral Health. 2018;18(1):131.
18. Ruhm W, Eidemuller M, Kaiser JC. Biologically-based mechanistic models of radiation-related carcinogenesis applied to epidemiological data. Int J Radiat Biol. 2017;93(10):1093-117.
19. Mozzo P, Procacci C, Tacconi A, Martini PT, Andreis IA. A new volumetric CT machine for dental imaging based on the cone-beam technique: preliminary results. European radiology. 1998;8(9):1558-64.

20. Arai Y, Tammisalo E, Iwai K, Hashimoto K, Shinoda K. Development of a compact computed tomographic apparatus for dental use. Dentomaxillofac Radiol. 1999;28(4):245-8.
21. Venkatesh E, Elluru SV. Cone beam computed tomography: basics and applications in dentistry. J Istanb Univ Fac Dent. 2017;51(3 Suppl 1):S102-S21.
22. Brenner DJ. Estimating cancer risks from pediatric CT: going from the qualitative to the quantitative. Pediatr Radiol. 2002;32(4):228-1; discussion 42-4.
23. Hall EJ. Lessons we have learned from our children: cancer risks from diagnostic radiology. Pediatr Radiol. 2002;32(10):700-6.
24. Schroeder AR, Redberg RF. The harm in looking. JAMA Pediatr. 2013;167(8):693-5.
25. De Grauwe A, Ayaz I, Shujaat S, Dimitrov S, Gbadegbegnon L, Vande Vannet B, et al. CBCT in orthodontics: a systematic review on justification of CBCT in a paediatric population prior to orthodontic treatment. Eur J Orthod. 2018.
26. Bogdanich W. CMJ. Radiation Worries for Children in Dentists' Chairs. New York Times. 2010.
27. Gee A. Radiation Concerns Rise With Patients' Exposure. New York Times. 2012 June 13 2012.
28. UNSCEAR. UNSCEAR 2013 Report: Sources, effects and risks of ionizing radiation - Volume II Annex B - Effects of radiation exposure of children. 2013.
29. D. K. Maurya TPAD. Role of Radioprotectors in the Inhibition of DNA Damage and Modulation of DNA Repair After Exposure to Gamma-Radiation. In: Chen CC, editor. Selected Topics in DNA Repair: InTech.; 2011.
30. Lobrich M, Shibata A, Beucher A, Fisher A, Ensminger M, Goodarzi AA, et al. gammaH2AX foci analysis for monitoring DNA double-strand break repair: strengths, limitations and optimization. Cell cycle (Georgetown, Tex). 2010;9(4):662-9.
31. Panier S, Boulton SJ. Double-strand break repair: 53BP1 comes into focus. Nature reviews Molecular cell biology. 2014;15(1):7-18.
32. Khanna KK, Jackson SP. DNA double-strand breaks: signaling, repair and the cancer connection. Nat Genet. 2001;27(3):247-54.
33. Jackson SP. Sensing and repairing DNA double-strand breaks. Carcinogenesis. 2002;23(5):687-96.
34. Ciccia A, Elledge SJ. The DNA damage response: making it safe to play with knives. Mol Cell. 2010;40(2):179-204.
35. Goodarzi AA, Jeggo PA. Irradiation induced foci (IRIF) as a biomarker for radiosensitivity. Mutat Res. 2012;736(1-2):39-47.
36. Asaithamby A, Chen DJ. Cellular responses to DNA double-strand breaks after low-dose gamma-irradiation. Nucleic Acids Res. 2009;37(12):3912-23.
37. Brenner DJ, Hall EJ. Computed tomography--an increasing source of radiation exposure. N Engl J Med. 2007;357(22):2277-84.
38. Chapple IL, Matthews JB. The role of reactive oxygen and antioxidant species in periodontal tissue destruction. Periodontol 2000. 2007;43:160-232.
39. Tothova L, Kamodyova N, Cervenka T, Celec P. Salivary markers of oxidative stress in oral diseases. Front Cell Infect Microbiol. 2015;5:73.
40. Cooke MS, Evans MD, Dizdaroglu M, Lunec J. Oxidative DNA damage: mechanisms, mutation, and disease. FASEB J. 2003;17(10):1195-214.
41. Kasai H, Nishimura S. Hydroxylation of deoxy guanosine at the C-8 position by polyphenols and aminophenols in the presence of hydrogen peroxide and ferric ion. Gan. 1984;75(7):565-6.
42. Thomas P, Holland N, Bolognesi C, Kirsch-Volders M, Bonassi S, Zeiger E, et al. Buccal micronucleus cytome assay. Nat Protoc. 2009;4(6):825-37.
43. Ozkul Y, Donmez H, Erenmemisoglu A, Demirtas H, Imamoglu N. Induction of micronuclei by smokeless tobacco on buccal mucosa cells of habitual users. Mutagenesis. 1997;12(4):285-7.
44. Kashyap B, Reddy PS. Micronuclei assay of exfoliated oral buccal cells: means to assess the nuclear abnormalities in different diseases. J Cancer Res Ther. 2012;8(2):184-91.

45. Gonzalez JE, Roch-Lefevre SH, Mandina T, Garcia O, Roy L. Induction of gamma-H2AX foci in human exfoliated buccal cells after in vitro exposure to ionising radiation. Int J Radiat Biol. 2010;86(9):752-9.
46. Siddiqui MS, Francois M, Fenech MF, Leifert WR. gammaH2AX responses in human buccal cells exposed to ionizing radiation. Cytometry A. 2015;87(4):296-308.
47. Humphrey SP, Williamson RT. A review of saliva: normal composition, flow, and function. J Prosthet Dent. 2001;85(2):162-9.
48. Pernot E, Cardis E, Badie C. Usefulness of saliva samples for biomarker studies in radiation research. Cancer Epidemiol Biomarkers Prev. 2014;23(12):2673-80.
49. Hassaneen M, Maron JL. Salivary Diagnostics in Pediatrics: Applicability, Translatability, and Limitations. Front Public Health. 2017;5:83.
50. Farnaud SJ, Kosti O, Getting SJ, Renshaw D. Saliva: physiology and diagnostic potential in health and disease. ScientificWorldJournal. 2010;10:434-56.
51. Moore HD, Ivey RG, Voytovich UJ, Lin C, Stirewalt DL, Pogosova-Agadjanyan EL, et al. The human salivary proteome is radiation responsive. Radiat Res. 2014;181(5):521-30.
52. Belmans N, Gilles L, Virag P, Hedesiu M, Salmon B, Baatout S, et al. Method validation to assess in vivo cellular and subcellular changes in buccal mucosa cells and saliva following CBCT examinations. Dentomaxillofac Radiol. 2019.
53. Schindelin J, Arganda-Carreras I, Frise E, Kaynig V, Longair M, Pietzsch T, et al. Fiji: an open-source platform for biological-image analysis. Nat Methods. 2012;9(7):676-82.
54. De Vos WH, Van Neste L, Dieriks B, Joss GH, Van Oostveldt P. High content image cytometry in the context of subnuclear organization. Cytometry A. 2010;77(1):64-75.
55. Munro CL, Grap MJ, Jablonski R, Boyle A. Oral health measurement in nursing research: state of the science. Biol Res Nurs. 2006;8(1):35-42.
56. Shakeri Manesh S, Sangsuwan T, Pour Khavari A, Fotouhi A, Emami SN, Haghdoost S. MTH1, an 8-oxo-2'-deoxyguanosine triphosphatase, and MYH, a DNA glycosylase, cooperate to inhibit mutations induced by chronic exposure to oxidative stress of ionising radiation. Mutagenesis. 2017;32(3):389-96.
57. Haghdoost S, Czene S, Naslund I, Skog S, Harms-Ringdahl M. Extracellular 8-oxo-dG as a sensitive parameter for oxidative stress in vivo and in vitro. Free Radic Res. 2005;39(2):153-62.
58. Stratis A. Customized Monte Carlo Modelling for Paediatric Patient Dosimetry in Dental and Maxillofacial Cone Beam Computed Tomography Imaging [Doctoral Thesis]. Leuven University Press: KU Leuven; 2018.
59. Stratis A, Zhang G, Lopez-Rendon X, Jacobs R, Bogaerts R, Bosmans H. Customisation of a Monte Carlo Dosimetry Tool for Dental Cone-Beam Ct Systems. Radiation protection dosimetry. 2016;169(1-4):378-85.
60. Stratis A, Touyz N, Zhang GZ, Jacobs R, Bogaerts R, Bosmans H, et al. Development of a paediatric head voxel model database for dosimetric applications. Brit J Radiol. 2017;90(1078).
61. Stratis A, Zhang G, Lopez-Rendon X, Politis C, Hermans R, Jacobs R, et al. Two examples of indication specific radiation dose calculations in dental CBCT and Multidetector CT scanners. Phys Med. 2017;41:71-7.
62. Stratis A, Touyz N, Zhang G, Jacobs R, Bogaerts R, Bosmans H, et al. Development of a paediatric head voxel model database for dosimetric applications. Br J Radiol. 2017;90(1078):20170051.
63. Kuefner MA, Brand M, Engert C, Schwab SA, Uder M. Radiation Induced DNA Double-Strand Breaks in Radiology. Rofo. 2015;187(10):872-8.
64. Halm BM, Franke AA, Lai JF, Turner HC, Brenner DJ, Zohrabian VM, et al. gamma-H2AX foci are increased in lymphocytes in vivo in young children 1 h after very low-dose X-irradiation: a pilot study. Pediatr Radiol. 2014;44(10):1310-7.
65. Shi L, Tashiro S. Estimation of the effects of medical diagnostic radiation exposure based on DNA damage. J Radiat Res. 2018;59(suppl_2):ii121-ii9.
66. Virag P, Hedesiu M, Soritau O, Perde-Schrepler M, Brie I, Pall E, et al. Low-dose radiations derived from cone-beam CT induce transient DNA damage and persistent inflammatory reactions in stem cells from deciduous teeth. Dentomaxillofac Radiol. 2018:20170462.

67. Preethi N, Chikkanarasaiah N, Bethur SS. Genotoxic effects of X-rays in buccal mucosal cells in children subjected to dental radiographs. BDJ Open. 2016;2:16001.
68. Agarwal P, Vinuth DP, Haranal S, Thippanna CK, Naresh N, Moger G. Genotoxic and cytotoxic effects of X-ray on buccal epithelial cells following panoramic radiography: A pediatric study. J Cytol. 2015;32(2):102-6.
69. Angelieri F, de Oliveira GR, Sannomiya EK, Ribeiro DA. DNA damage and cellular death in oral mucosa cells of children who have undergone panoramic dental radiography. Pediatr Radiol. 2007;37(6):561-5.
70. Ribeiro DA. Cytogenetic biomonitoring in oral mucosa cells following dental X-ray. Dentomaxillofac Radiol. 2012;41(3):181-4.
71. Carlin V, Artioli AJ, Matsumoto MA, Filho HN, Borgo E, Oshima CT, et al. Biomonitoring of DNA damage and cytotoxicity in individuals exposed to cone beam computed tomography. Dentomaxillofac Radiol. 2010;39(5):295-9.
72. Yoon AJ, Shen J, Wu HC, Angelopoulos C, Singer SR, Chen R, et al. Expression of activated checkpoint kinase 2 and histone 2AX in exfoliative oral cells after exposure to ionizing radiation. Radiat Res. 2009;171(6):771-5.
73. Horn S, Barnard S, Brady D, Prise KM, Rothkamm K. Combined analysis of gamma-H2AX/53BP1 foci and caspase activation in lymphocyte subsets detects recent and more remote radiation exposures. Radiat Res. 2013;180(6):603-9.
74. Gorbunova V, Seluanov A. DNA double strand break repair, aging and the chromatin connection. Mutat Res. 2016;788:2-6.
75. Ramsey MJ, Moore DH, 2nd, Briner JF, Lee DA, Olsen L, Senft JR, et al. The effects of age and lifestyle factors on the accumulation of cytogenetic damage as measured by chromosome painting. Mutat Res. 1995;338(1-6):95-106.
76. Khan S, Khan AU, Hasan S. Genotoxic assessment of chlorhexidine mouthwash on exfoliated buccal epithelial cells in chronic gingivitis patients. J Indian Soc Periodontol. 2016;20(6):584-91.
77. Cavalcante DN, Sposito JC, Crispim BD, Nascimento AV, Grisolia AB. Genotoxic and mutagenic effects of passive smoking and urban air pollutants in buccal mucosa cells of children enrolled in public school. Toxicol Mech Methods. 2017;27(5):346-51.
78. Shafi FA. Micronucleus frequency in buccal cells of males exposed to air pollution in Kufa City. Al-Mustansiriyah Journal of Science. 2017;28(02):43-7.
79. Ribeiro DA, de Oliveira G, de Castro G, Angelieri F. Cytogenetic biomonitoring in patients exposed to dental X-rays: comparison between adults and children. Dentomaxillofac Radiol. 2008;37(7):404-7.
80. Evans MD, Saparbaev M, Cooke MS. DNA repair and the origins of urinary oxidized 2'-deoxyribonucleosides. Mutagenesis. 2010;25(5):433-42.
81. Goukassian D, Gad F, Yaar M, Eller MS, Nehal US, Gilchrest BA. Mechanisms and implications of the age-associated decrease in DNA repair capacity. FASEB J. 2000;14(10):1325-34.
82. Gorbunova V, Seluanov A, Mao Z, Hine C. Changes in DNA repair during aging. Nucleic Acids Research. 2007;35(22):7466-74.
83. Dimova EG, Bryant PE, Chankova SG. "Adaptive response" - Some underlying mechanisms and open questions. Genet Mol Biol. 2008;31(2):396-408.
84. Haghdoost S, Svoboda P, Naslund I, Harms-Ringdahl M, Tilikides A, Skog S. Can 8-oxo-dG be used as a predictor for individual radiosensitivity? Int J Radiat Oncol Biol Phys. 2001;50(2):405-10.
85. Topic A, Francuski D, Markovic B, Stankovic M, Dobrivojevic S, Drca S, et al. Gender-related reference intervals of urinary 8-oxo-7,8-dihydro-2'-deoxyguanosine determined by liquid chromatography-tandem mass spectrometry in Serbian population. Clin Biochem. 2013;46(4-5):321-6.
86. Kaneko K, Kimata T, Tsuji S, Ohashi A, Imai Y, Sudo H, et al. Measurement of urinary 8-oxo-7,8-dihydro-2-deoxyguanosine in a novel point-of-care testing device to assess oxidative stress in children. Clin Chim Acta. 2012;413(23-24):1822-6.
87. Matosevic P, Klepac-Pulanic T, Kinda E, Augustin G, Brcic I, Jakic-Razumovic J. Immunohistochemical expression of 8-oxo-7,8-dihydro-2'-deoxyguanosine in cytoplasm of tumour and adjacent normal mucosa cells in patients with colorectal cancer. World J Surg Oncol. 2015;13:241.

88. Kander MC, Cui Y, Liu Z. Gender difference in oxidative stress: a new look at the mechanisms for cardiovascular diseases. J Cell Mol Med. 2017;21(5):1024-32.
89. Brunelli E, Domanico F, La Russa D, Pellegrino D. Sex differences in oxidative stress biomarkers. Curr Drug Targets. 2014;15(8):811-5.
90. Kamodyova N, Tothova L, Celec P. Salivary markers of oxidative stress and antioxidant status: influence of external factors. Dis Markers. 2013;34(5):313-21.
91. Zhang T, Andrukhov O, Haririan H, Muller-Kern M, Liu S, Liu Z, et al. Total Antioxidant Capacity and Total Oxidant Status in Saliva of Periodontitis Patients in Relation to Bacterial Load. Front Cell Infect Microbiol. 2015;5:97.
92. Battino M, Ferreiro MS, Gallardo I, Newman HN, Bullon P. The antioxidant capacity of saliva. J Clin Periodontol. 2002;29(3):189-94.
93. Moore S, Calder KA, Miller NJ, Rice-Evans CA. Antioxidant activity of saliva and periodontal disease. Free Radic Res. 1994;21(6):417-25.
94. Suma HR, Prabhu K, Shenoy RP, Annaswamy R, Rao S, Rao A. Estimation of salivary protein thiols and total antioxidant power of saliva in brain tumor patients. J Cancer Res Ther. 2010;6(3):278-81.

4.8 Supplementary Data

4.8.1 Supplementary Data 1

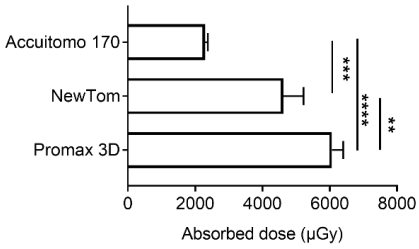

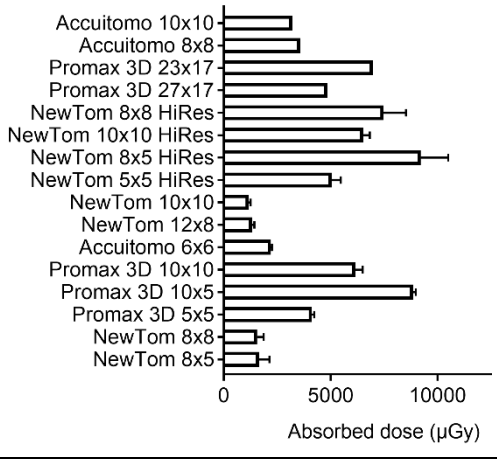

Absorbed radiation dose does not only depend on the device uses, but also on the field of view (FOV) and scanning protocol used during the examination. (left). Patients examined using a Promax 3D device receive on average a higher radiation dose than those examined with a Accuitomo 170 device or NewTom device. However, these data do not take into account the FOV or the scanning protocol. (right). Radiation dose increases with increasing FOV and resolution of the scan. This is seen for all devices (except for Accuitomo 170 for which only one scanning protocol was used). Furthermore, the radiation dose is higher when high resolution (HiRes) protocols were used. This explains the differences seen in the left panel, since for Planmeca ProMax and NewTom HiRes protocols were used, whereas only standard protocols were used in Accuitomo. No significances were shown in the right panel. ***: $p < .0002$; ****: $p < .0001$.

4.8.2 Supplementary Data 2

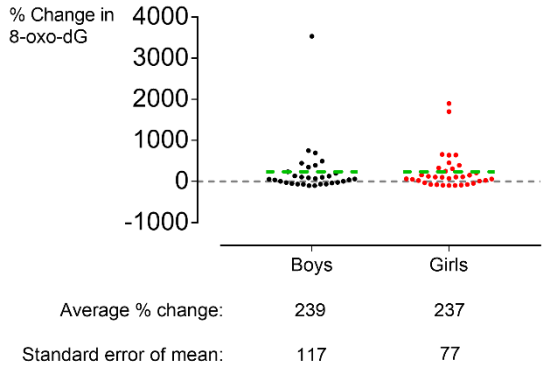

Comparison of % change in 8-oxo-dG excretion shows no difference between boys and girls. The proportional change in 8-oxo-dG levels does not differ between boys and girls (Mann-Whitney U value = 431, *p* = .203). Green dotted line = average.

4.8.3 Supplementary Data 3

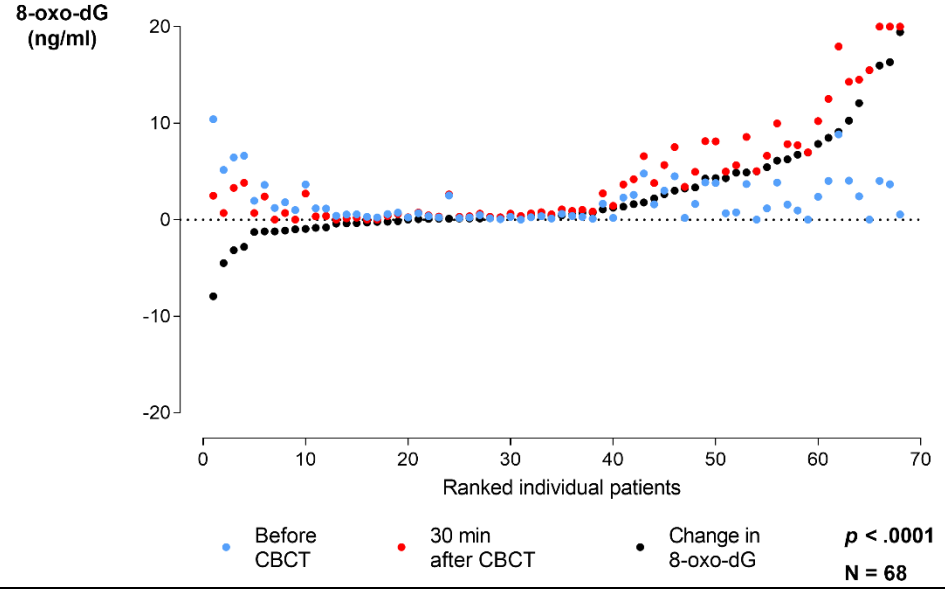

8-oxo-dG (ng/ml) concentration shown per individual pediatric patient. On the x-axis, individual patients are shown, ranked from smallest change in 8-oxo-dG concentration following cone beam computed tomography (CBCT) examination to largest change in 8-oxo-dG concentration following CBCT examination (black dots). The blue dots show the 8-oxo-dG concentration prior to CBCT. The red dots show the 8-oxo-dG concentration post CBCT.

4.8.4 Supplementary Data 4

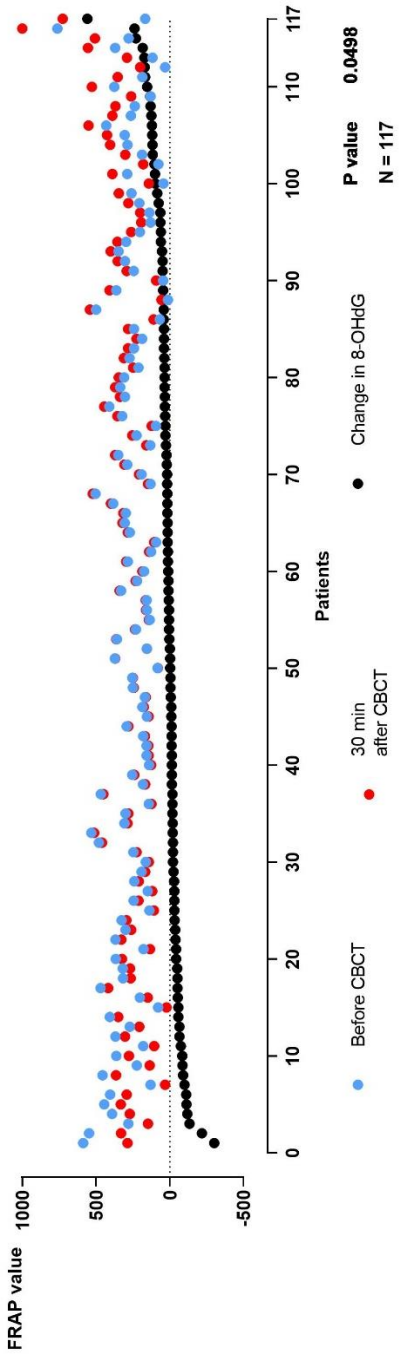

Ferric Reducing Antioxidant Power (FRAP) values shown per individual pediatric patient. On the x-axis, individual patients are shown, ranked from smallest change in FRAP value following cone beam computed tomography (CBCT) examination to largest change in FRAP value following CBCT examination (black dots). The blue dots show the FRAP values prior to CBCT. The red dots show the FRAP values post CBCT.

4.8.5 Supplementary Data 5

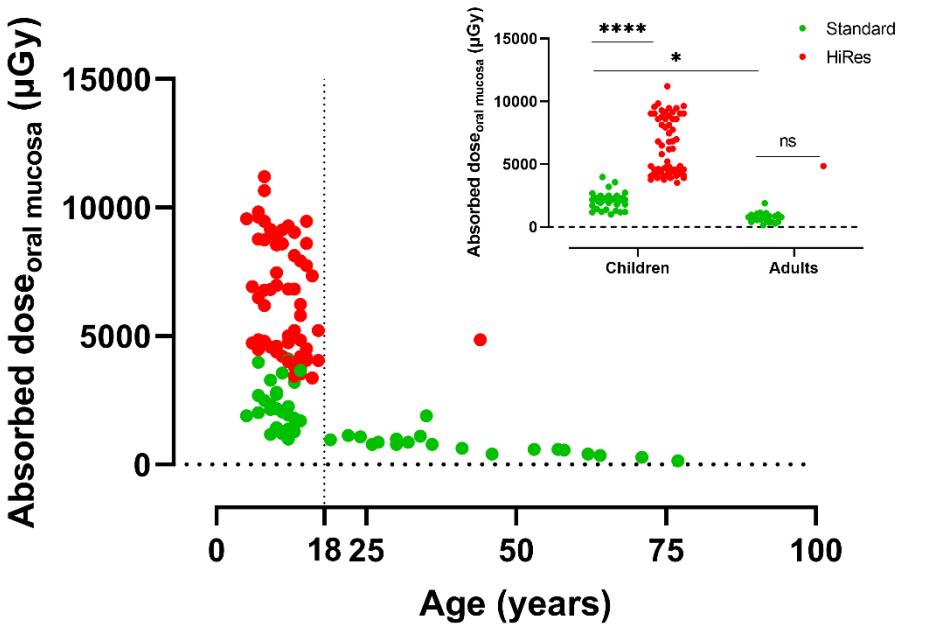

Absorbed radiation dose to the oral mucosa plotted against the age of the patient at the time of CBCT examination. (*large*) Monte Carlo simulated absorbed dose to the oral mucosa is plotted against the age of the patient at the time of the CBCT examination. This graph shows that most high resolution (i.e. high mAs) (red dots) protocols are performed in children. (*insert*) The absorbed dose is significantly higher in children compared to adults for standard scanning protocols (green dots). Furthermore, in children, the dose used in high resolution protocols (red dots) is significantly higher than that of standard imaging protocols. Note that the Monte Carlo framework used for dose calculations is not validated for adults and thus these data might deviate from actual values. *: $p < .05$; ****: $p < .0001$; HiRes = High resolution protocol.

4.8.6 Supplementary Table 1

Supplementary table 1. Individual patient study parameters of included patients.

Patient ID	Age (years)	Gender*	CBCT device**	Site of examination	Simulated absorbed dose[58]*** (µGy)
A1	58	M	NewTom	KU Leuven	
A2	62	F	NewTom	KU Leuven	
A3	32	F	NewTom	KU Leuven	
A4	36	F	NewTom	KU Leuven	
A5	62	F	NewTom	KU Leuven	
A6	26	M	NewTom	KU Leuven	
A7	44	M	NewTom	KU Leuven	
A8	22	M	NewTom	KU Leuven	
A9	19	F	NewTom	KU Leuven	
A10	64	F	NewTom	KU Leuven	
A11	46	F	NewTom	KU Leuven	
A12	35	F	Accuitomo	KU Leuven	
A13	53	F	NewTom	KU Leuven	
A14	57	F	NewTom	KU Leuven	
A15	41	F	NewTom	KU Leuven	
A16	30	F	NewTom	KU Leuven	
A17	30	M	NewTom	KU Leuven	
A18	71	M	NewTom	KU Leuven	
A19	27	F	NewTom	KU Leuven	
A20	24	F	NewTom	KU Leuven	
A21	34	M	NewTom	KU Leuven	
A22	Not known	M	NewTom	KU Leuven	
A23	77	M	NewTom	KU Leuven	
C1	8	M	NewTom	KU Leuven	6788
C2	7	M	NewTom	KU Leuven	4850
C3	Not known	F	NewTom	KU Leuven	3565
C4	8	M	NewTom	KU Leuven	6182
C5	10	M	NewTom	KU Leuven	4610
C6	16	M	NewTom	KU Leuven	/
C7	9	M	NewTom	KU Leuven	2141
C8	9	F	NewTom	KU Leuven	1168
C9	9	F	NewTom	KU Leuven	1168
C10	9	F	NewTom	KU Leuven	6811
C11	8	M	NewTom	KU Leuven	11206
C12	3	M	NewTom	KU Leuven	/
C13	9	F	NewTom	KU Leuven	2141
C14	14	F	NewTom	KU Leuven	3518
C15	14	M	NewTom	KU Leuven	6232
C16	7	M	NewTom	KU Leuven	9628
C17	12	M	NewTom	KU Leuven	1380
C18	11	F	NewTom	KU Leuven	9137
C19	9	M	NewTom	KU Leuven	2328

Patient ID	Age (years)	Gender*	CBCT device**	Site of examination	Simulated absorbed dose[58]*** (µGy)
C20	11	M	NewTom	KU Leuven	1208
C25	13	F	Accuitomo	KU Leuven	1803
C28	13	M	NewTom	KU Leuven	1288
C30	10	M	NewTom	KU Leuven	1433
C32	12	F	NewTom	KU Leuven	1918
C33	13	F	NewTom	KU Leuven	1803
C34	9	F	Accuitomo	KU Leuven	2328
C35	8	F	Accuitomo	KU Leuven	2496
C36	15	F	NewTom	KU Leuven	4503
C37	8	F	Accuitomo	KU Leuven	2496
C38	12	M	Accuitomo	KU Leuven	1918
C39	12	F	NewTom	KU Leuven	4110
C40	10	M	Accuitomo	KU Leuven	2178
C41	10	M	NewTom	KU Leuven	7460
C42	9	M	Accuitomo	KU Leuven	2328
C43	9	M	Accuitomo	KU Leuven	2328
C44	8	F	Accuitomo	KU Leuven	2496
C45	7	F	Accuitomo	KU Leuven	2687
C46	9	M	Accuitomo	KU Leuven	2328
C47	10	F	Accuitomo	KU Leuven	2178
C48	10	M	Accuitomo	KU Leuven	2178
C49	9	M	Accuitomo	KU Leuven	2328
C50	10	M	Accuitomo	KU Leuven	2178
C51	10	M	Accuitomo	KU Leuven	2178
C52	10	F	Accuitomo	KU Leuven	2178
C53	11	M	Accuitomo	KU Leuven	2042
C54	10	F	Accuitomo	KU Leuven	2178
C55	12	M	NewTom	KU Leuven	999
C56	13	F	Accuitomo	KU Leuven	2302
C57	14	M	Accuitomo	KU Leuven	1698
C58	7	M	NewTom	KU Leuven	8773
C59	12	F	NewTom	KU Leuven	6826
C60	13	M	NewTom	KU Leuven	5211
C61	11	M	Promax	Bretonneau	8590
C62	9	M	Promax	Bretonneau	4580
C63	14	F	Promax	Bretonneau	3777
C64	7	M	Promax	Bretonneau	2014
C65	11	F	Promax	Bretonneau	4215
C66	10	F	Promax	Bretonneau	6982
C67	7	F	Promax	Bretonneau	3973
C68	15	F	Promax	Bretonneau	9460
C69	9	M	Promax	Bretonneau	4580
C70	6	F	Promax	Bretonneau	4726
C71	12	M	Promax	Bretonneau	9279
C72	10	F	Promax	Bretonneau	4388
C73	13	M	Promax	Bretonneau	3912
C74	7	M	Promax	Bretonneau	4477

Patient ID	Age (years)	Gender*	CBCT device**	Site of examination	Simulated absorbed dose[58]*** (μGy)
C75	10	M	Promax	Bretonneau	2731
C76	12	M	Promax	Bretonneau	4057
C77	13	F	Promax	Bretonneau	3912
C78	15	F	Promax	Bretonneau	8600
C79	9	F	Promax	Bretonneau	4580
C80	7	M	Promax	Bretonneau	6492
C81	12	F	Promax	Bretonneau	4057
C82	13	M	Promax	Bretonneau	8132
C83	13	F	Promax	Bretonneau	3912
C84	14	M	Promax	Bretonneau	5805
C85	5	F	Promax	Bretonneau	9556
C86	8	F	Promax	Bretonneau	4794
C87	15	F	Promax	Bretonneau	4058
C88	7	M	Promax	Bretonneau	9828
C89	14	F	Promax	Bretonneau	4197
C90	14	M	Promax	Bretonneau	3777
C91	9	M	Promax	Bretonneau	4580
C92	15	F	Promax	Bretonneau	4058
C93	13	M	Promax	Bretonneau	8132
C94	10	M	Promax	Bretonneau	8851
C95	10	F	Promax	Bretonneau	4388
C96	13	F	Promax	Bretonneau	9036
C97	9	F	Promax	Bretonneau	4580
C98	9	F	Promax	Bretonneau	9140
C99	13	F	Promax	Bretonneau	9036
C100	14	F	Promax	Bretonneau	7929
C101	15	F	Promax	Bretonneau	7740
C102	10	M	Promax	Bretonneau	4388
C103	8	F	Promax	Bretonneau	9462
C104	11	F	Promax	Bretonneau	8590
C105	13	M	Promax	Bretonneau	9036
C106	14	M	Promax	Bretonneau	4838
C107	11	M	Promax	Bretonneau	8590
C108	12	M	Promax	Bretonneau	4057
C109	13	M	Promax	Bretonneau	9036
C110	10	M	Promax	Bretonneau	4388
C111	10	M	NewTom 3G	Iuliu Hatieganu	+
C112	8	F	NewTom 3G	Iuliu Hatieganu	+
C113	10	M	NewTom 3G	Iuliu Hatieganu	+
C114	10	M	NewTom 3G	Iuliu Hatieganu	+
C115	11	F	NewTom 3G	Iuliu Hatieganu	+
C116	9	F	NewTom 3G	Iuliu Hatieganu	+
C117	13	F	NewTom 3G	Iuliu Hatieganu	+
C118	15	F	NewTom 3G	Iuliu Hatieganu	+
C119	6	F	NewTom 3G	Iuliu Hatieganu	+
C120	8	F	NewTom 3G	Iuliu Hatieganu	+
C121	15	M	NewTom 3G	Iuliu Hatieganu	+

Patient ID	Age (years)	Gender*	CBCT device**	Site of examination	Simulated absorbed dose[58]*** (μGy)
C122	8	M	NewTom 3G	Iuliu Hatieganu	+
C123	18	F	NewTom 3G	Iuliu Hatieganu	+
C124	8	M	NewTom 3G	Iuliu Hatieganu	+
C125	9	F	NewTom 3G	Iuliu Hatieganu	+
C126	14	F	NewTom 3G	Iuliu Hatieganu	+
C128	12	F	Promax	Iuliu Hatieganu	10655
C129	12	F	Promax	Iuliu Hatieganu	5011
C130	12	F	Promax	Iuliu Hatieganu	4748
C131	16	M	Promax	Iuliu Hatieganu	7334
C132	13	F	NewTom 3G	Iuliu Hatieganu	+
C133	6	M	Promax	Iuliu Hatieganu	6920
C134	15	F	Promax	Iuliu Hatieganu	4154
C135	17	F	Promax	Iuliu Hatieganu	5218
C136	10	Not known	Not known	Iuliu Hatieganu	
C137	9	M	NewTom 3G	Iuliu Hatieganu	+
C138	8	F	Promax	Iuliu Hatieganu	8742
C139	10	M	Promax	Iuliu Hatieganu	6968
C140	10	M	Promax	Iuliu Hatieganu	8554
C141	12	M	Promax	Iuliu Hatieganu	4001
C142	13	F	Promax	Iuliu Hatieganu	6832
C143	13	F	Promax	Iuliu Hatieganu	3431
C144	13	F	Promax	Iuliu Hatieganu	3808
C145	5	M	Promax	Iuliu Hatieganu	1898
C146	12	F	Promax	Iuliu Hatieganu	5011
C148	10	M	NewTom 3G	Iuliu Hatieganu	+
C149	9	M	Promax	Iuliu Hatieganu	3290
C150	16	M	Promax	Iuliu Hatieganu	3363
C151	12	F	Promax	Iuliu Hatieganu	2251
C152	14	F	Promax	Iuliu Hatieganu	3661
C153	10	F	Promax	Iuliu Hatieganu	2814
C154	17	M	Promax	Iuliu Hatieganu	4050

*: F = female; M = male

**: NewTom = NewTom VGi-evo; Promax = Promax 3D; Accuitomo = Accuitomo 170

***: Absorbed dose calculated for the oral mucosa

+: No dose simulations were performed for NewTom 3G

Chapter 5:

In vitro assessment of the DNA damage response in dental stem cells following low dose X-ray exposure

Belmans N, Gilles L, Welkenhuysen J, Vermeesen R, Salmon B, Baatout S, Jacobs R., Lucas S, Lambrichts I, Moreels M *In vitro* assessment of the DNA damage response in dental stem cells following low dose X-ray exposure. *In final preparation – To be submitted September 2019*

5.1 Abstract

Mesenchymal stem cells (MSCs) are crucial for tissue homeostasis. Therefore assuring their genomic stability is essential. Exposure of stem cells to ionizing radiation (IR) is potentially detrimental for normal tissue homeostasis. Although it has been established that exposure to high doses of IR has severe adverse effects in MSCs, knowledge about the impact of low doses of IR is lacking. However, knowing the impact of low doses of IR is important for several MSC types, such as dental MSCs, due to the increasing use of (dental) imaging that relies on IR.

Here we investigated the effect of low doses of X-irradiation (< 0.1 Gray) on paediatric dental stem cells including dental pulp stem cells from deciduous teeth, dental follicle stem cells and stem cells from the apical papilla. DNA double strand break (DSB) formation and repair kinetics were monitored as well as cell cycle progression and cellular senescence.

Exposure to low doses of X-rays induces DNA DSBs as early as 30 minutes post-irradiation. The number of DSBs returned to baseline levels 24 hours after irradiation. Cell cycle analysis revealed marginal effects of IR on cell cycle progression, although a slight G_2/M phase block was seen in dental pulp stem cells from deciduous teeth 72 hours after irradiation. Despite this cell cycle block, no radiation-induced senescence was observed.

In conclusion, low IR doses were able to induce significant increases in the number of DNA DSBs, but cell cycle progression seems to be minimally affected. This highlights the need for more detailed and extensive studies on the effects of exposure to low IR doses on different mesenchymal stem cells.

5.2 Introduction

Mesenchymal stem cells (MSCs) are of paramount importance for tissue homeostasis which are potentially important targets of ionizing radiation (IR) exposure. They can accumulate genotoxic damage following IR exposure, which is either repaired efficiently, or they can accumulate irreversible damage. This irreversible damage can trigger apoptosis or senescence, or unrepaired DNA damage can persist and could lead to malignant transformation of the stem cells.[1] Changes in the functionality of MSCs could be considered a predictive indicator for future health hazards.[2, 3]

In 2000, Gronthos *et al.* identified and isolated odontogenic progenitor cells from the dental pulp from adult patients.[4] These cells were dubbed dental pulp stem cells (DPSCs). In the following years, several more types of dental stem cells were described, such as the dental follicle stem cells (DFSCs), stem cells from the apical papilla (SCAPs), pulp stem cells from human exfoliated deciduous teeth (SHEDs), and periodontal ligament stem cells (PDLSCs).[5-8] An overview of these cells and their potential use in dentistry is described by Bansal and Jain (2015).[9]

Today, one of the greatest challenges in radiation protection is unravelling the potential detrimental effects of exposure to low doses of IR (below 100 milliGray (mGy)). This is important because people are exposed to low dose IR on a daily basis, either from natural sources, or from man-made sources, such as medical diagnostics.[10] Although there are epidemiological data on exposure to doses higher than 100 mGy, i.e. high IR doses (e.g. from atomic bomb survivors, medically and occupationally exposed populations and environmentally exposed groups), no conclusive data exists on exposure to low doses of IR.[11] Currently, risk estimation for low dose exposure is based on linear extrapolation from these high dose data. This is the famous linear-no-threshold (LNT) model.[12-14] The LNT model assumes that there is a linear relationship between IR dose and the excessive cancer risk. When applying the LNT model, the following is assumed: 1) that there is a linear relationship between IR dose and the amount of radiation-induced DNA double strand breaks (DSB), 2) that each DNA DSB has the probability of inducing cellular transformations, and 3) that each transformation has the same probability of resulting in carcinogenesis.[15] However, in the low dose range (< 100 mGy), other phenomena than a linear response can occur. There is evidence that low doses of IR could have beneficial effects, such as hormesis and adaptive responses.[16, 17] Hormesis occurs when exposure to low IR doses produces a favourable effect, whereas high IR doses result in detrimental effects.[18] Adaptive responses occur when a very low dose, or priming dose, stimulates cells which results in increased resistance to a second, larger dose of the same trigger at a later time point. This could include the activation of genes

associated with DNA damage repair, stress scavenging, cell cycle control and apoptosis.[16, 17]

DNA DSBs are the most crucial DNA lesions that are associated with increased cancer risk and IR exposure. If not repaired correctly, DSBs can cause genomic instability, mutations, chromosome aberrations and translocations, and cell death.[19-22] To protect the DNA against these types of damage, eukaryotes have developed the DNA damage response (DDR).[21, 22] In short, cellular responses to IR-induced DNA DSBs are triggered by the activation of the ataxia telangiectasia mutated (ATM) kinase. The phosphorylation of histone H2AX on serine 139 (γH2AX) in the vicinity of the DNA DSB is one of the earliest ATM-dependent responses.[20, 23, 24] γH2AX forms so called DNA damage foci in the nucleus, or in the case of IR-induced DNA damage 'IR-induced foci' (IRIF). In general, IRIF are distinct sub-nuclear structures to which the DDR proteins re-localize. After phosphorylation, γH2AX initiates a signalling cascade leading to the recruitment of multiple DDR proteins, including tumour suppressor p53-binding protein 1 (53BP1).[19, 21, 25, 26]

53BP1 is a known DNA DSB sensor and a mediator and effector in the DDR to DSBs.[21, 27, 28] Similar to γH2AX, 53BP1 has several functions in the DDR, such as recruitment of DSB repair proteins, checkpoint signalling, determining the DSB repair pathway and synapsis of distal DNA ends during non-homologous end-joining (reviewed in Panier and Boulton).[27]

Evidence shows that both γH2AX and 53BP1 show a quantitative relationship between the number of foci and the number of DNA DSBs.[21, 26, 29, 30] Although γH2AX is a powerful tool to monitor DNA DSBs, artefacts do occur even in the absence of DSBs.[22] Both γH2AX and 53BP1 foci can be visualized using immunofluorescence microscopy and are detectable within minutes following exposure to IR.[26, 31] Therefore, using an immunostaining protocol for simultaneous detection of γH2AX and 53BP1 allows for better estimation of the amount of DSBs present and reduces the impact of artefacts, since it is known that γH2AX and 53BP1 co-localize in IRIF.[21, 32, 33]

DNA DSB could be efficiently repaired by the DDR, however, DNA DSBs could persist. This could lead to cell cycle arrest, premature cellular senescence, or apoptosis. As part of the DDR, cells halt their passage through the cell cycle, allowing DDR proteins to repair DNA damage. If this damage persists, the cell cycle could be irreversibly blocked. This cell cycle arrest can occur in all phases of the cell cycle, but it was found that most cells are most sensitive to IR-induced DNA damage in the G_2/M phase.[34-36] Cellular senescence is a state of irreversible growth arrest. This growth arrest occurs in the G_1 phase of the cell cycle, therefore cellular senescence is linked with changes in cell cycle progression. A hallmark of senescent cells is the increased β-galactosidase activity in comparison to normal cells. This can be detected by the so-called X-gal assay, which is considered as the gold standard for senescence testing.[37, 38] Senescent cells also display a senescence-associated secretory phenotype (SASP), which consists of several

chemokines, cytokines, and regulatory factors. Some of these SASP factors are linked with IR exposure, such as IL-6, IL-8, IGFBP-2 and IGFBP-3.[39, 40] IL-6 and IL-8 interact with their surface receptors, which initiates several intracellular pathways. Besides that, they can both induce or reinforce senescence in damaged cells in a paracrine/autocrine manner.[39, 40] IGFBP-2 and IGFBP-3 interact with insulin-like growth factor (IGF). They sequester IGF so it cannot bind to its receptor, which eventually leads to inhibition of cell proliferation.[41] It is known that premature cellular senescence can be caused by several stresses, such as (persisting) DNA damage or reactive oxygen species.[42] It has been reported before that exposure to (high) IR doses can cause premature cellular senescence. This was observed both in mesenchymal stem cells and normal tissue cells.[43-48] For low doses of IR, data is more scarce.[3, 49] Besides senescence, quiescence is also an important process in stem cells. Quiescence is characterized by a cell cycle arrest in the G_0 phase. This phase is similar to the G_1 phase, however cells do not progress into the S phase. Unlike senescence, quiescence is a state of reversible growth arrest. Quiescence occurs in cells that require a strict proliferation regime, such as stem cells. It allows stem cells to assure genomic integrity until they are needed for tissue repair, which is when they are stimulated to reprise the normal cell cycle.[50] Evidence on the effects of IR on quiescence in mesenchymal stem cells are scarce.[51, 52] Finally, cells can undergo apoptosis or programmed cell death. Like premature cellular senescence, it is a response to extensive cellular stress and mostly occurs when DNA damage repair is slow and/or incomplete.[53]

The aim of this study is to investigate the effects of low dose X-ray exposure (< 100 mGy) on SHED, DFSCs, and SCAPs extracted from pediatric patients. DNA DSB formation and repair, cell cycle progression, cellular quiescence, and cellular senescence were monitored at several time points after exposure. Our data present evidence that, although low doses of IR induce significant amounts of DNA DSBs, DNA damage is effectively repaired and does not affect cell cycle progression, nor induces premature cellular senescence in dental stem cells.

5.3 Material and methods

5.3.1 Culturing dental stem cells

Three types of dental stem cells were used in this experiment: dental pulp stem cells from deciduous teeth (SHED), dental follicle stem cells (DFSC) and stem cells from the apical papilla (SCAP). These cells were extracted from teeth as previously described.[4, 7, 8, 54] First, teeth were decontaminated using a povidone-iodine solution. Second, they were sectioned and exposed pulp tissues were collected. Third, these tissues were enzymatically digested using a type I collagenase and dispase solution. Finally, the cells were ready to be cultured. After extraction, the cells were seeded at a density of 10^4 cells per cm². They were grown in Dulbecco's Modified Eagle Medium (DMEM) containing 1 g/l D-glucose, GlutaMAX™ and 10% foetal bovine serum (FBS) at 37° C with 5% CO_2 in a humidified incubator. The medium was refreshed every 2 – 3 days. At 70% - 80% confluence the cells were passaged and seeded again at 10^4 cells per cm², or frozen in liquid nitrogen for later use. To be sure that the stem cells keep their phenotype, all stem cells were used between passages 1 and 5. Once enough cells were obtained they were seeded either into 8-chamber Labtek® II slides at 2 x 10^4 cells per well or in 24-well plates at 4 x 10^4 cells per well (Greiner Bio-One, Frickenhausen, Germany) 24 hours before irradiation. Six wells in each Labtek® were used, resulting in six technical replicates. Each Labtek® represented one time point per dose. In the 24-well plates cells were seeded in triplicates. For each cell type, cells from three donor children were used (Table 5.1).

Table 5.1: Overview of dental stem cell donors

	Age	Gender
Donor 1	12	Male
Donor 2	11	Female
Donor 3	8	Female

5.3.2 X-irradiation conditions

The irradiation of samples was performed at the Laboratory for Nuclear Calibrations (LNK) of the Belgian Nuclear Research Centre (SCK•CEN). In this experimental design, it is of importance to mimic commercially available CBCT devices as closely as possible. To this end X-rays with RQR9 beam quality, as defined in the ISO 4037 standard, were used since RQR9 beam quality can be used to simulate entrance beams used in diagnostic radiology. This beam quality is created on the XStrahl 320 kV tube of LNK. The X-ray tube used a tube voltage of 120 kiloVolt and a current of 1.8 milliAmpere. The distance between the focal

point and the sample center was 100 cm. The X-ray beam was oriented vertically. The inherent filtration was achieved by 3 mm of Be. Additional filtration was done with 2.9 mm of Al and a dose area product monitor ionization chamber. The beam diameter defined as Full Width at Half Maximum was 31 cm. The secondary standard air kerma measurements are traceable to international standards, in accordance with the ISO 17025 accreditation of LNK. The samples are always smaller than the beam diameter. Using these parameters low doses and low dose rates can be achieved which allows the simulation of diagnostic examinations. Using a dose rate of 900 mGy per hour the samples were irradiated with doses of 100 ± 1.9 mGy, 50 ± 0.9 mGy, 20 ± 0.38 mGy, 10 ± 0.19 mGy and 5 ± 0.10 mGy. Control (0 mGy) samples were transported to the irradiation facility, but they were not exposed to the radiation field (sham-irradiation).

5.3.4 Immunocytochemical staining for γH2AX and 53BP1

At specific time points after irradiation exposure (0.5, 1, 4 and 24 hours) the culture medium was removed from the Labteks™ (Nunc™, ThermoFisher Scientific, Waltham, MA, USA). Then the cells were washed twice using 1x phosphate buffered saline (PBS). After washing, they were fixed in 2% paraformaldehyde (PFA) in 1x PBS for at least 15 minutes at room temperature (RT). Next the PFA was removed and the cells were washed twice with 1x PBS.

Fixed stem cells were double stained for γH2AX and 53BP1, both markers for DNA DSBs. The 1x PBS was removed and then the cells were permeabilized by incubating them in 0.25% Triton X-100 in 1x PBS for 3 minutes at RT. Then the cells were washed three times in 1x PBS on a rocking platform. Next the cells were blocked in pre-immunized goat serum (PIG). The PIG was diluted (1:5) in Tris-HCl – NaCl blocking buffer (50 mM Tris-HCl, 150 mM NaCl, 0.1% Tween 20, 0.5% blocking reagent (FP1012, Perkin Elmer)) (TNB). The cells were blocked for one hour at RT on a rocking platform, during which the primary antibody solution was prepared. Primary antibodies were diluted in TNB, the mouse anti-human γH2AX monoclonal antibody (05-636, Millipore, Massachusetts, USA) was diluted 1:300 and the rabbit anti-human 53BP1 polyclonal antibody (NB100-304, Novus Biological, Abingdon, UK) was diluted 1:1000. After blocking, the cells were incubated with the primary antibody solution for 1 hour at 37° C on a rocking platform. After incubation, the cells were washed three times using 1x PBS. Next the secondary antibody solution was prepared. An Alexa fluor 488-labelled goat anti-mouse antibody (A11001, Life Technologies, Oregon, USA) and an Alexa fluor 568-labelled goat anti-rabbit antibody (A11011, Life Technologies, Oregon, USA) were diluted 1:300 and 1:1000 in TNB, respectively. The cells were incubated with the secondary antibody solution for another hour at 37° C on a rocking platform. After this final incubation step, the cells were washed twice using 1x PBS. Next the chambers were removed from the Labteks®. Then the samples were mounted using Prolong® Diamond Antifade Mountant with 4',6-diamidino-2-phenylindole

(DAPI) (P36962, Molecular Probes™ by Life Technologies, Oregon, USA) as nuclear counter stain. After mounting, the samples were stored at -20° C until imaging.

Images were acquired with a Nikon Eclipse Ti fluorescence microscope using a 40x dry objective (Nikon, Tokyo, Japan). Per technical replicate (n = 6 = number of chamber of a Labtek™ used) at least 250 cells were counted. Afterwards, the images were analysed using Fiji open source software.[55] Fiji allows for analysis of each separate nucleus based on the DAPI signal. Within each nucleus, the intensity signal for the Alexa fluorophores were analysed, after which the number of co-localized γH2AX and 53BP1 foci per nucleus were determined in a fully automated manner by using the Cellblocks tool.[56]

5.3.7 Cell cycle analysis

Cell cycle analysis was performed 1 h, 4 h, 24 h, and 72 h after X-irradiation as described before.[43] In short, dental stem cells were treated with 10 μM of BrdU for 1 hour. Afterwards, the cells were fixed with ice-cold 70% ethanol and stored for a minimum of 24 hours. Next, the cells were permeabilized and stained with rat anti-BrdU antibody, diluted 1 in 600 (AB6326, Abcam, Cambridge, UK). They were also stained with 10 μg/ml of a 7-amino-actinomycin D (7-AAD) solution (Sigma-Aldrich). Samples were analysed on a BD Accuri C6 flow cytometer, with a maximum flow speed of 300 events per second. At least 20,000 cells were counted per sample.

5.3.8 Quiescence assay

G_0 phase cells were identified 1 h, 4 h, 24 h, and 72 h after X-irradiation using a quiescence assay. Dental stem cells were fixed with ice-cold 70% ethanol following X-irradiation. Next, the cells were washed twice with 5% FBS (Gibco, Massachusetts, USA) and 0.25% Triton X-100 (Sigma-Aldrich, Missouri, USA) in 1x PBS (PFT). Next, the cells were stained in PFT with 10 μg/ml 7-AAD (A9400-1MG, Sigma-Aldrich, Missouri, USA) and 0.4 μg/ml pyronin Y (83200-5G, Sigma-Aldrich, Missouri, USA) for 20 minutes at RT. Samples were analysed on a BD Accuri C6 flow cytometer, with a maximum flow speed of 300 events per second. At least 20,000 cells were counted per sample.

5.3.9 B-galactosidase assay

Senescence was assessed 1, 3, 7, and 14 days after X-irradiation using the senescence-associated β-galactosidase assay (ab65351, Abcam, Cambridge, UK).[38] Cells were fixed for 15 minutes at RT using the fixative solution provided with the kit. Next the cells were washed twice with 1x PBS. Then, the cells were stained with 1 mg/ml X-gal solution at 37° C for 18 hours. Afterwards, the staining

was stopped by adding 1 M Na_2CO_3. Next, the cells were incubated for 1 hour at RT with a Giemsa dye, diluted 1:50 in 0.2 M acetate buffer (pH = 3.36). Finally, the cells were washed twice with Milli-Q water and allowed to air dry. At least 300 cells per sample were analysed using a Nikon Eclipse Ti bright field microscope using a 5x dry objective (Nikon, Tokyo, Japan).

5.3.10 Enzyme-linked immunosorbent assay (ELISA): IL-6, IL-8, IGFBP-2, and IGFBP-3

For senescence assays on cytokine secretion, supernatant was collected 1, 3, 7 and 14 days following irradiation. Dental stem cells were grown in 12-well plates. 1 ml of medium was collected at each time point. These samples were used for the ELISA for the detection of IL-6, IL-8, IGFBP-2 and IGFBP-3. ELISA was performed following manufacturer's instructions (DY206, DY208, DY674, and DY675, R&D Systems). Briefly, 96-well plates were coated overnight with a capture antibody. Next, the wells were washed with washing buffer. Blocking buffer was added and the plate was incubated for 1 hour at RT. After blocking, the plate was washed once with washing buffer. Next, the supernatant was added and incubated for 2 hours at RT. The plate was washed again, after which the detection antibodies were added and the plate was incubated for 2 hours at RT. Next, the plate was washed with washing buffer and a streptavidin-horse radish peroxidase-labelled antibody was added and the plate was incubated for 20 minutes in the dark at RT. Then, the plate was washed with washing buffer. Next, the substrate solution was added and the plate was incubated for 20 minutes in the dark at RT. Afterwards, 2 M H_2SO_4 was added to stop the substrate reaction. The optical density was measured at 450 nm and 570 nm using a spectrophotometer (CLARIOstar, BMG Labtech, Offenburg, Germany).

5.3.11 Statistical analysis

Statistical analyses were performed using GraphPad Prism 8.0.0 (GraphPad Software Inc., San Diego, USA). Graphs show mean ± standard error of the mean. Two-way analysis of variance followed by post-hoc tests was performed to analyse both time- and dose-dependent effects. $P < .05$ was considered statistically significant.

5.4 Results

5.4.1 Exposure to low doses of X-rays induces DSBs and activates the DNA damage response in dental stem cells

DNA DSB formation and repair kinetics were monitored in dental stem cells (SHED, DFSC, and SCAP), that were isolated from children, by microscopic analysis of co-localized γH2AX and 53BP1 foci (N = 3). The number of co-localized foci was determined 30 minutes, one hour, four hours and 24 hours after X-irradiation with 0, 5, 10, 20, 50, and 100 mGy (Figure 5.1). The number of co-localized foci increased with increasing radiation dose. Typically, the peak response was seen between 30 to 60 minutes post-irradiation. After this period, the number of foci decreased until baseline levels were reached 24 hours after exposure. More specifically, in SHED, exposure to 100 mGy induced significantly more co-localized foci 30 minutes and 1 h after irradiation compared to control cells (0 mGy) ($P < .0001$). A dose of 50 mGy also resulted in more co-localized foci 1 h after irradiation compared to 0 mGy ($P = .0303$). In the SCAPs, the number of co-localized foci, observed after exposure to 100 mGy, was significantly increased compared to 0 mGy 30 min, 1 h and 4 h after irradiation ($P < .0001$, $P < .0001$, $P = .0267$, respectively). Furthermore, compared to control samples, 50 mGy irradiated samples showed more foci 30 min and 1 h p.i ($P = .0018$, $P = .0004$, respectively) and 20 mGy irradiated samples showed more foci 1 h after irradiation ($P = .0416$). In DFSC, more γH2AX and 53BP1 co-localized foci were observed 30 min, 1 h and 4 h after exposure to 100 mGy ($P < .0001$, $P < .0001$, $P = .0374$, respectively). 30 min and 1 h after exposure to 50 mGy and 30 minutes after exposure to 20 mGy the amount of co-localized foci was increased as well in DFSC ($P < .0001$, $P = .0015$, $P = .0030$, respectively). Furthermore, linear regression plots show a linear dose response 30 min, 1 h and 4 h after irradiation. Moreover, the slope decreased over time returning to a constant basal response 24 h after irradiation. Our linear regression analysis also resulted in a slope of about 0.020 DNA DSBs per mGy (Table 5.2). No difference in radiation sensitivity was observed between the different stem cell types.

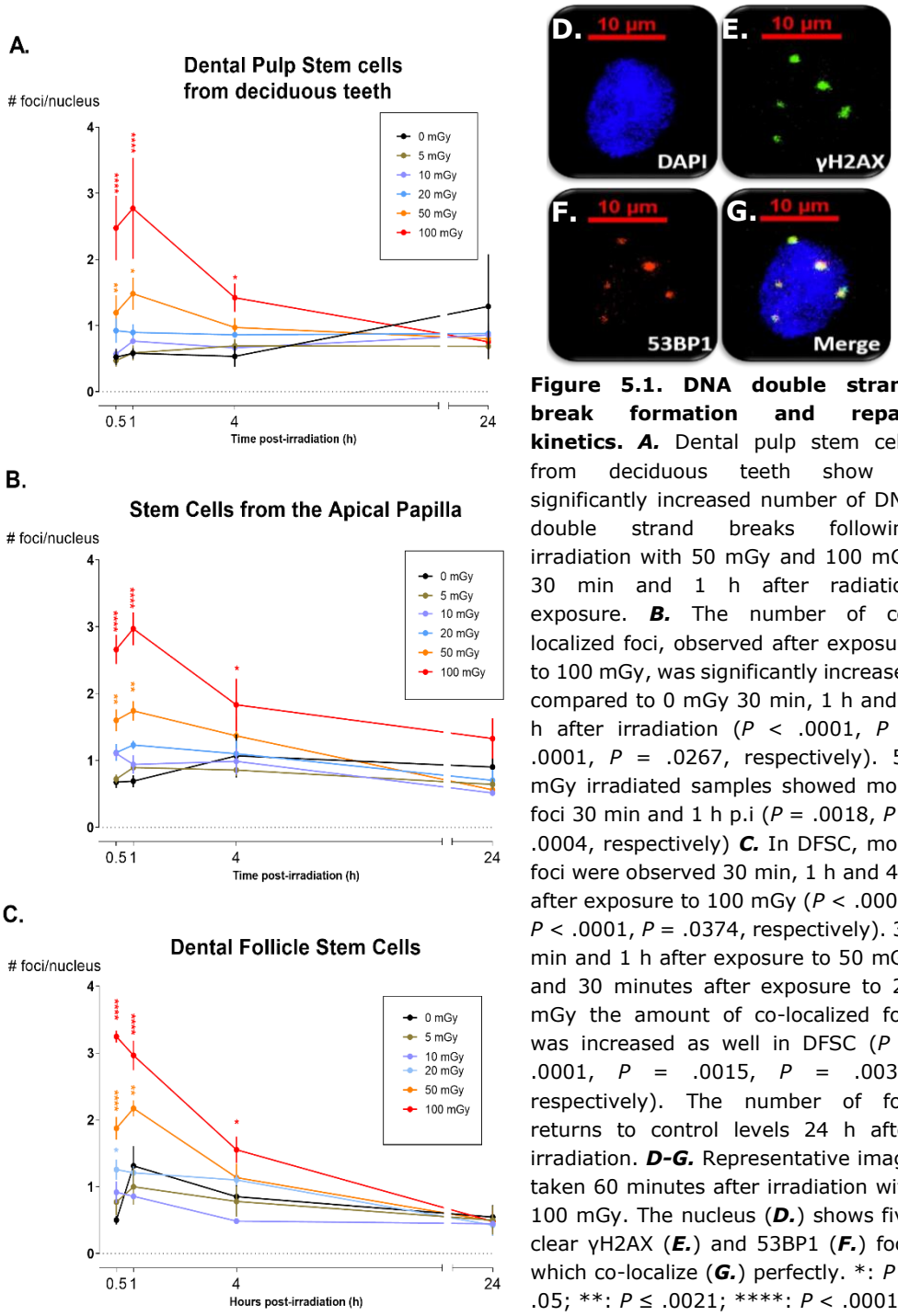

Figure 5.1. DNA double strand break formation and repair kinetics. ***A.*** Dental pulp stem cells from deciduous teeth show a significantly increased number of DNA double strand breaks following irradiation with 50 mGy and 100 mGy 30 min and 1 h after radiation exposure. ***B.*** The number of co-localized foci, observed after exposure to 100 mGy, was significantly increased compared to 0 mGy 30 min, 1 h and 4 h after irradiation ($P < .0001$, $P < .0001$, $P = .0267$, respectively). 50 mGy irradiated samples showed more foci 30 min and 1 h p.i ($P = .0018$, $P = .0004$, respectively) ***C.*** In DFSC, more foci were observed 30 min, 1 h and 4 h after exposure to 100 mGy ($P < .0001$, $P < .0001$, $P = .0374$, respectively). 30 min and 1 h after exposure to 50 mGy and 30 minutes after exposure to 20 mGy the amount of co-localized foci was increased as well in DFSC ($P < .0001$, $P = .0015$, $P = .0030$, respectively). The number of foci returns to control levels 24 h after irradiation. ***D-G.*** Representative image taken 60 minutes after irradiation with 100 mGy. The nucleus (***D.***) shows five clear γH2AX (***E.***) and 53BP1 (***F.***) foci, which co-localize (***G.***) perfectly. *: $P \leq .05$; **: $P \leq .0021$; ****: $P < .0001$

Table 5.2: Linear dose response relationship of co-localized γH2AX and 53BP1 foci in dental stem cells

Cell type	Time after irradiation	Slope (foci/mGy)	R^2 value	*P* value
Dental pulp stem cells from deciduous teeth (SHEDs)	30 minutes	0.020	0.97	0.0003
	1 hour	0.022	0.99	< 0.0001
	4 hours	0.008	0.96	0.0005
	24 hours	-0.002	0.18	0.40
Dental follicle stem cells (DFSCs)	30 minutes	0.026	0.99	< 0.0001
	1 hour	0.020	0.91	0.003
	4 hours	0.008	0.75	0.025
	24 hours	-0.0001	0.013	0.83
Stem cells from the apical papilla (SCAPs)	30 minutes	0.019	0.98	0.0002
	1 hour	0.022	0.99	< 0.0001
	4 hours	0.009	0.94	0.0012
	24 hours	0.005	0.47	0.13

5.4.2 Cell cycle progression is not influenced by low doses of X-rays in dental stem cells

Analysis of the percentage of cells that reside in a specific phase of the cell cycle has revealed that exposure to low doses of X-rays does not induce major cell cycle changes in dental stem cells (SHEDs and SCAPs) (N = 3 for each cell type). Except for a slightly reduced number of G_1/G_0 phase cells 72 h after irradiation in SHED (P = .019) and a slight increase in G_2/M phase cells 72 h after irradiation in SHED (P = .040) following a dose of 100 mGy, no changes were observed (Figure 5.2). We did observe that the amount of G_1/G_0 phase cells increases over time, whereas the amount of S- and G_2/M phase cells decreases over time, with almost no more cells in the S-phase after 72 h.

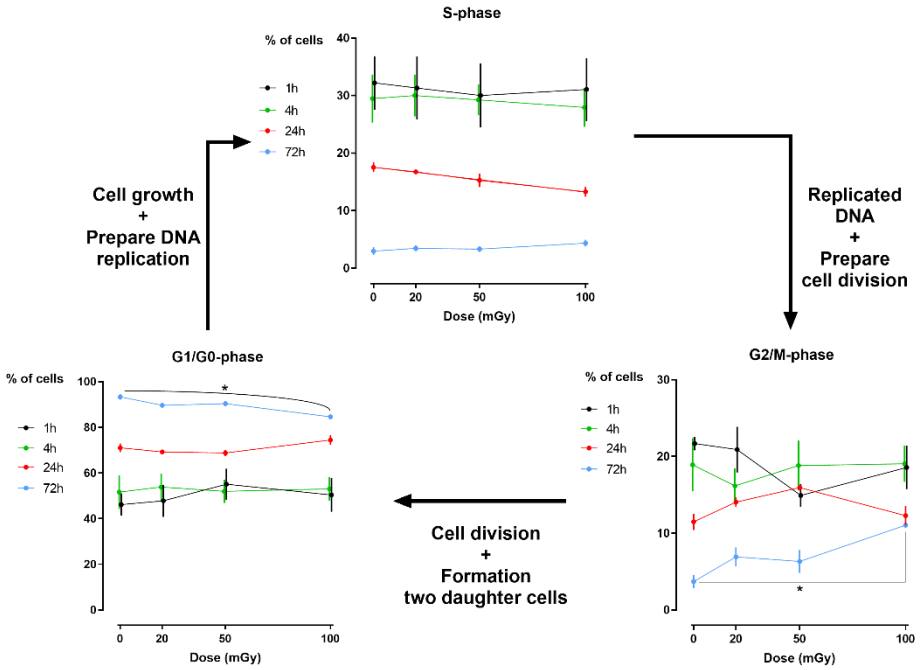

Figure 5.2. Cell cycle analysis of dental pulp stem cells from deciduous teeth. Dental pulp stem cells from deciduous teeth (SHEDs) show a significantly decreased number of G_1/G_0 phase cells 72 hours following X-irradiation with 100 mGy. Coincidently, a significant increase in the number of G_2/M phase cells was observed. *: $P \leq .05$

5.4.3 Low dose X-irradiation rapidly decreases the amount of quiescent cells

The effect of exposure to low doses of X-rays on cellular quiescence, determined by measuring the percentage of G_0 phase cells, was most pronounced 1 h after irradiation with 100 mGy. This was observed in SHEDs and SCAPs (N = 3). However, SHEDs showed still significant dose-dependent decreases in the percentage of quiescent cells 4 h and 72 h after irradiation (Figure 5.3 and Table 5.3). In SCAPs, only a decrease was seen 1 h after irradiation with 100 mGy (P = .030). It was also observed that the number of G_0 decreased significantly over time (Figure 5.3 and Table 5.3).

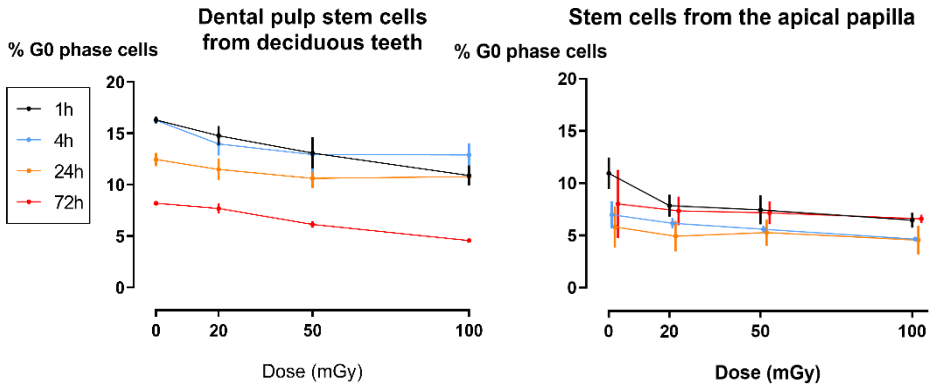

Figure 5.3. Dose response of the percentage of G0 phase dental pulp stem cells from deciduous teeth and stem cells from the apical papilla following low dose X-irradiation. The percentage of G_0 phase cells is plotted against the time after X-irradiation. Significances are summarized in the table 5.3.

Table 5.3: Significant differences in the percentage of quiescent cells in dental stem cells

Comparison	Dental pulp stem cells from deciduous teeth *P* value	Stem cells from the apical papilla *P* value
1 h:CTRL vs. 50 mGy	0.0107	N.A.
1 h:CTRL vs. 100 mGy	<0.0001	0.0296
1 h:20 mGy vs. 100 mGy	0.0011	N.A.
4 h:CTRL vs. 50 mGy	0.0072	N.A.
4 h:CTRL vs. 100 mGy	0.0064	N.A.
72 h: CTRL vs. 100 mGy	0.0025	N.A.
72 h:20 mGy vs. 100 mGy	0.0145	N.A.

5.4.4 Low dose radiation does not induce premature senescence in dental stem cells

ELISA for SASP markers IL-6, IL-8, IGFBP-2, and IGFBP-3 showed no signs of radiation-induced premature cellular senescence in SHEDs, DFSCs, and SCAPs up to 14 days after exposure (N = 3 for each cell type). Although the values for IL-6 and IL-8 in SHEDs increased significantly 14 days after irradiation exposure, this was mostly due to the time in culture, rather than a radiation-induced effect (P_{time} = .006 and P_{time} = .004, respectively). Levels of IGFBP-2 in SHEDs showed changes over time, but overall there was a decreasing trend, which was not influenced by radiation dose (P_{time} = .022). Finally, in SHEDs, IGFBP-3 showed a time dependent increase (P_{time} = .005) (Figure 5.4).

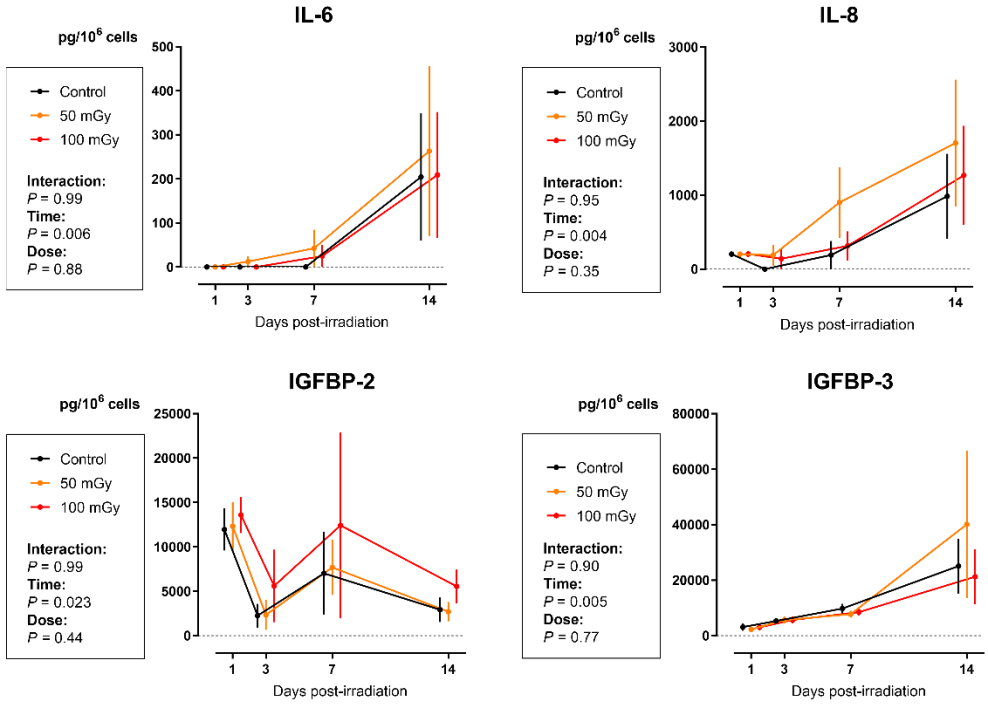

Figure 5.4. Senescence-associated secretory phenotype (SASP) protein secretion in dental pulp stem cells from deciduous teeth (SHEDs) following low dose ionizing radiation exposure The amount of interleukins (IL)-6 and IL-8, as well as the levels of insulin-like growth factor binding proteins (IGFBP)-2 and IGFBP-3 indicate that there no effect of low doses of ionizing radiation on the SASP. Two-way analysis of variance shows that time after exposure is the major contributor to the observed effects (e.g. for IGFBP-2: P_{time} = .023).

The data from SASP markers were confirmed by the β-galactosidase assay.[38] Data from dental stem cells show that there is an increase in the percentage of senescent cells, but this increase is time-dependent. Low dose radiation exposure does not induce cellular senescence in SHEDs, DFSCs, and SCAPs (N = 3 for each cell type)(Figure 5.5).

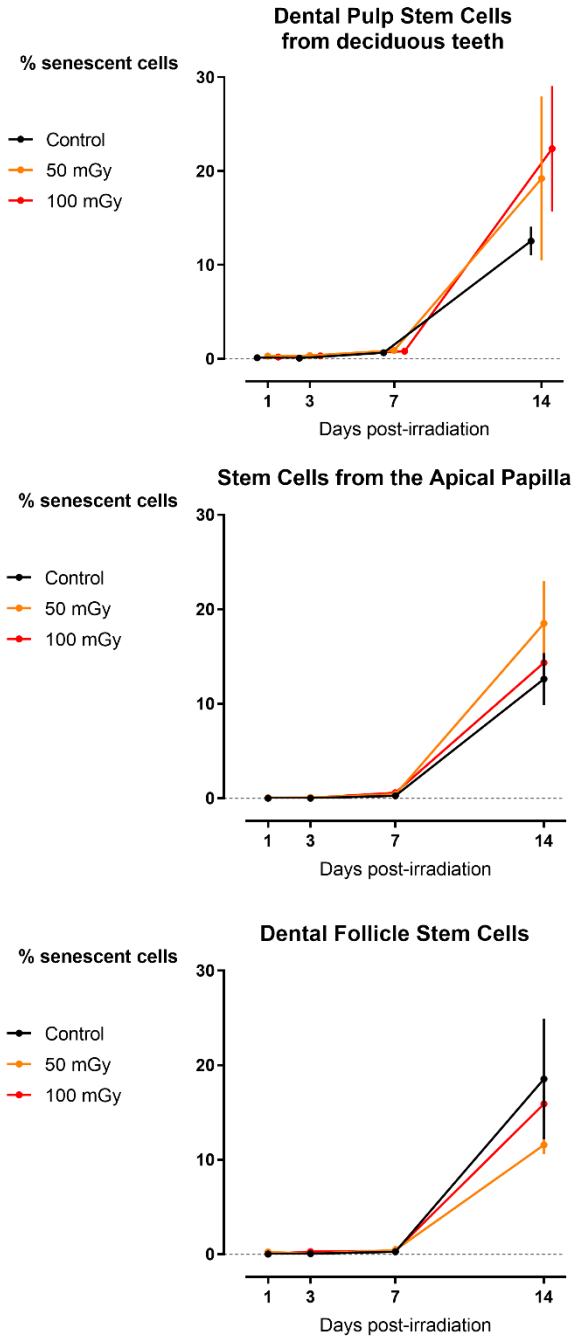

Figure 5.5. β-galactosidase assay in dental stem cells. The percentage of senescent cells indicates that low doses of ionizing radiation do not induce premature cellular senescence. Two-way analysis of variance shows that time after exposure is the major contributor to the observed effects (P_{time} < .0001 for all cell types).

5.5 Discussion

Determining the biological effects of low dose IR exposure currently is the greatest challenge in radiation protection. We aimed to investigate the DDR and its consequences in human dental stem cells (i.e. SHEDs, DFSCs and SCAPs) after exposure to X-ray doses below 100 mGy. SHEDs, DFSCs, and SCAPs are MSCs, which are adult stem cells which can be isolated from human teeth. MSCs support the maintenance of other cells, and the capacity of MSCs to differentiate into several cell types makes these cells unique and full of possibilities.[57] Therefore, maintaining the genetic stability of MSCs is of paramount importance. MSCs can accumulate genotoxic damage following IR exposure, which is either repaired efficiently, or they can accumulate irreversible damage. This persisting damage could lead to malignant transformation of the stem cells.[1]

The formation and repair kinetics of DNA DSBs was monitored via γH2AX/53BP1 immunostaining. Additionally, the impact of low dose radiation on cell cycle progression, cellular quiescence and premature cellular senescence were investigated. We report a significant increase in the amount of DNA DSBs 30 minutes and 1 hour after IR exposure. Repair kinetics clearly showed that the number of DSBs in dental stem cells returned to baseline levels 24 hours after IR exposure. Furthermore, a slight G_2/M phase arrest was seen 72 hours after irradiation in SHEDs, but not in SCAPs. Next, IR exposure resulted in reduced levels of G_0 cells in SHEDs and SCAP. However, in SCAP the decrease was only statistically significant 1 h after irradiation and only for irradiation with 100 mGy. For SHEDs, on the other hand, also 4 h and 72 h after irradiation a statistically significant decrease was observed. Finally, low dose X-ray exposure did not result in radiation-induced premature senescence in SHEDs, DFSCs, and SCAPs.

It is well-known that exposure to X-rays can induce DNA DSBs, which are considered very harmful because unrepaired DSBs could result in mutations, chromosome rearrangements/aberrations, and loss of genetic information.[25, 58-60] Our results show that exposure to low dose IR, with a relatively high dose rate of 0.9 Gy/h, induces significant increases in the number of DNA DSBs in dental stem cells 30 - 60 minutes after irradiation.[61] Similar results have been reported in human mesenchymal stem cells before.[3, 44, 62-66] However, some studies report a persistent increase of γH2AX foci up to 48 hours after irradiation, which was not observed in our study.[3, 62, 63] Linear regression analysis showed that the number of DNA DSBs increases linearly with the IR dose. The slopes in SHEDs, DFSCs and SCAPs ranged from 0.019 – 0.026 DNA DSBs per mGy. This is equivalent to 19 – 26 DNA DSBs per Gy, which is consistent with data published previously.[21, 67-70]

The formed DNA DSBs did not affect cell cycle progression in SCAPs, but we did observe a slight G_2/M phase block in SHEDs 72 hours following 100 mGy

exposure. Although this increase was minimal, it was statistically significant. This is in line with previous publications indicating that cells exhibit G_2/M phase arrest following exposure to high IR doses.[34-36, 44] However, there are data indicating that exposure to high doses of IR results in G_1 arrest in mesenchymal stem cells.[64] Furthermore, the lack of cell cycle changes in SCAPs is in line with data from Kurpinski *et al*. (2009), who also observed no changes in cell cycle distribution in bone marrow mesenchymal stem cells following X-irradiation with 100 mGy.[71] Our data, taken together with data from literature, indicate that the effect of X-irradiation on cell cycle progression is cell type-dependent.

Our cell cycle data reveal minimal changes in the G_1/G_0 phase of the cell cycle. However, our data show for the first time a significant decrease in the amount of quiescent or G_0 phase cells in SHEDs 72 h after X-irradiation with 100 mGy. This would indicate that if the amount of G_1/G_0 phase remains constant, but the amount of G_0 phase cells decreases, that the amount of G_1 phase cells increase proportionally to the decrease of G_0 phase cells. This indicates that low doses of IR stimulate SHEDs to re-enter the cell cycle. It has been described that certain extrinsic stresses such as IR-induced reactive oxygen species, which are generated by radiolysis of water following IR exposure, can stimulate stem cell to re-enter the cell cycle.[72] This could, at least partly, explain our observations.

Finally, we did not observe radiation-induced cellular senescence following exposure to low doses of IR, except for SHEDs where a slight increase in G_2/M arrest was observed 72 hours after irradiation after irradiation with 100 mGy. However, our data clearly showed time-dependent induction of senescence. This was seen both in results from the X-gal assay, which is considered the gold standard, as in analysis of the SASP. It has been reported before that high doses of IR can induce cellular senescence in mesenchymal stem cells.[44-46, 48, 73] However, evidence of low dose IR-induced senescence is scarce.[3, 74] These studies contradict our data. On the other hand, there are studies that support our findings.[63, 75] Due to these contradicting data and the fact that low dose radiation-induced senescence is poorly investigated, it is impossible to conclude at this time whether low doses of IR do cause cellular senescence in these cell or not. More detailed studies on this matter are warranted.[10]

In conclusion, we found that exposure of dental stem cells to low doses of X-rays results in the induction of DNA DSBs and that the number of DNA DSBs increases linearly with the radiation dose. After 24 hours, these DNA DSBs are efficiently repaired and returned to baseline levels. These observations are in line with the LNT model which is currently applied in radiation protection. We report for the first time, to the best of our knowledge, that exposure to low IR doses results in an acute dose-dependent decrease in the number of quiescent SHEDs and SCAPs, which is still observed 72 hours after X-irradiation in SHEDs. However, we did not find adverse effects on cell cycle progression. No persistent cell cycle changes, nor induction of premature cellular senescence were observed. Although

this is in line with previous studies, there are also studies indicating that low doses of IR can cause cell cycle arrest and senescence. We cannot conclude that there is no threshold for the biological effects of IR exposure. Our data highlight the need for more detailed and extensive studies on the effects of exposure to low doses of IR.

5.6 References

1. Rando TA. Stem cells, ageing and the quest for immortality. Nature. 2006;441(7097):1080-6.
2. Prise KM, Saran A. Concise review: stem cell effects in radiation risk. Stem Cells. 2011;29(9):1315-21.
3. Alessio N, Del Gaudio S, Capasso S, Di Bernardo G, Cappabianca S, Cipollaro M, et al. Low dose radiation induced senescence of human mesenchymal stromal cells and impaired the autophagy process. Oncotarget. 2015;6(10):8155-66.
4. Gronthos S, Mankani M, Brahim J, Robey PG, Shi S. Postnatal human dental pulp stem cells (DPSCs) in vitro and in vivo. Proc Natl Acad Sci U S A. 2000;97(25):13625-30.
5. Miura M, Gronthos S, Zhao M, Lu B, Fisher LW, Robey PG, et al. SHED: stem cells from human exfoliated deciduous teeth. Proc Natl Acad Sci U S A. 2003;100(10):5807-12.
6. Seo BM, Miura M, Gronthos S, Bartold PM, Batouli S, Brahim J, et al. Investigation of multipotent postnatal stem cells from human periodontal ligament. Lancet. 2004;364(9429):149-55.
7. Morsczeck C, Gotz W, Schierholz J, Zeilhofer F, Kuhn U, Mohl C, et al. Isolation of precursor cells (PCs) from human dental follicle of wisdom teeth. Matrix Biol. 2005;24(2):155-65.
8. Sonoyama W, Liu Y, Yamaza T, Tuan RS, Wang S, Shi S, et al. Characterization of the apical papilla and its residing stem cells from human immature permanent teeth: a pilot study. J Endod. 2008;34(2):166-71.
9. Bansal R, Jain A. Current overview on dental stem cells applications in regenerative dentistry. J Nat Sci Biol Med. 2015;6(1):29-34.
10. Squillaro T, Galano G, De Rosa R, Peluso G, Galderisi U. Concise Review: The Effect of Low-Dose Ionizing Radiation on Stem Cell Biology: A Contribution to Radiation Risk. Stem Cells. 2018;36(8):1146-53.
11. UNSCEAR. UNSCEAR 2006 Report to the General Assembly with Scientific Annexes. Effects of Ionizing Radiation. Volume I Report and Annexes A and B. 2008.
12. Martin LM, Marples B, Lynch TH, Hollywood D, Marignol L. Exposure to low dose ionising radiation: molecular and clinical consequences. Cancer letters. 2013;338(2):209-18.
13. Ruhm W, Eidemuller M, Kaiser JC. Biologically-based mechanistic models of radiation-related carcinogenesis applied to epidemiological data. Int J Radiat Biol. 2017;93(10):1093-117.
14. Ruhm W, Woloschak GE, Shore RE, Azizova TV, Grosche B, Niwa O, et al. Dose and dose-rate effects of ionizing radiation: a discussion in the light of radiological protection. Radiat Environ Biophys. 2015;54(4):379-401.
15. Tubiana M, Feinendegen LE, Yang C, Kaminski JM. The linear no-threshold relationship is inconsistent with radiation biologic and experimental data. Radiology. 2009;251(1):13-22.
16. Tang FR, Loke WK. Molecular mechanisms of low dose ionizing radiation-induced hormesis, adaptive responses, radioresistance, bystander effects, and genomic instability. Int J Radiat Biol. 2015;91(1):13-27.
17. Tang FR, Loganovsky K. Low dose or low dose rate ionizing radiation-induced health effect in the human. J Environ Radioact. 2018;192:32-47.
18. Mattson MP. Hormesis defined. Ageing Res Rev. 2008;7(1):1-7.
19. Kinner A, Wu W, Staudt C, Iliakis G. Gamma-H2AX in recognition and signaling of DNA double-strand breaks in the context of chromatin. Nucleic Acids Res. 2008;36(17):5678-94.
20. Rothkamm K, Horn S. gamma-H2AX as protein biomarker for radiation exposure. Ann Ist Super Sanita. 2009;45(3):265-71.
21. Asaithamby A, Chen DJ. Cellular responses to DNA double-strand breaks after low-dose gamma-irradiation. Nucleic Acids Res. 2009;37(12):3912-23.

22. Ciccia A, Elledge SJ. The DNA damage response: making it safe to play with knives. Mol Cell. 2010;40(2):179-204.
23. Rybak P, Hoang A, Bujnowicz L, Bernas T, Berniak K, Zarebski M, et al. Low level phosphorylation of histone H2AX on serine 139 (gammaH2AX) is not associated with DNA double-strand breaks. Oncotarget. 2016;7(31):49574-87.
24. Fernandez-Capetillo O, Chen HT, Celeste A, Ward I, Romanienko PJ, Morales JC, et al. DNA damage-induced G2-M checkpoint activation by histone H2AX and 53BP1. Nat Cell Biol. 2002;4(12):993-7.
25. D. K. Maurya TPAD. Role of Radioprotectors in the Inhibition of DNA Damage and Modulation of DNA Repair After Exposure to Gamma-Radiation. In: Chen CC, editor. Selected Topics in DNA Repair: InTech.; 2011.
26. Goodarzi AA, Jeggo PA. Irradiation induced foci (IRIF) as a biomarker for radiosensitivity. Mutat Res. 2012;736(1-2):39-47.
27. Panier S, Boulton SJ. Double-strand break repair: 53BP1 comes into focus. Nature reviews Molecular cell biology. 2014;15(1):7-18.
28. Huyen Y, Zgheib O, Ditullio RA, Jr., Gorgoulis VG, Zacharatos P, Petty TJ, et al. Methylated lysine 79 of histone H3 targets 53BP1 to DNA double-strand breaks. Nature. 2004;432(7015):406-11.
29. Sedelnikova OA, Rogakou EP, Panyutin IG, Bonner WM. Quantitative detection of (125)IdU-induced DNA double-strand breaks with gamma-H2AX antibody. Radiat Res. 2002;158(4):486-92.
30. Panier S, Durocher D. Regulatory ubiquitylation in response to DNA double-strand breaks. DNA Repair (Amst). 2009;8(4):436-43.
31. Rothkamm K, Barnard S, Moquet J, Ellender M, Rana Z, Burdak-Rothkamm S. DNA damage foci: Meaning and significance. Environ Mol Mutagen. 2015;56(6):491-504.
32. Horn S, Barnard S, Brady D, Prise KM, Rothkamm K. Combined analysis of gamma-H2AX/53BP1 foci and caspase activation in lymphocyte subsets detects recent and more remote radiation exposures. Radiat Res. 2013;180(6):603-9.
33. de Feraudy S, Revet I, Bezrookove V, Feeney L, Cleaver JE. A minority of foci or pan-nuclear apoptotic staining of gammaH2AX in the S phase after UV damage contain DNA double-strand breaks. Proc Natl Acad Sci U S A. 2010;107(15):6870-5.
34. Pawlik TM, Keyomarsi K. Role of cell cycle in mediating sensitivity to radiotherapy. Int J Radiat Oncol Biol Phys. 2004;59(4):928-42.
35. Santivasi WL, Xia F. Ionizing Radiation-Induced DNA Damage, Response, and Repair. Antioxid Redox Sign. 2014;21(2):251-9.
36. Suetens A, Konings K, Moreels M, Quintens R, Verslegers M, Soors E, et al. Higher Initial DNA Damage and Persistent Cell Cycle Arrest after Carbon Ion Irradiation Compared to X-irradiation in Prostate and Colon Cancer Cells. Front Oncol. 2016;6:87.
37. Itahana K, Campisi J, Dimri GP. Methods to detect biomarkers of cellular senescence: the senescence-associated beta-galactosidase assay. Methods Mol Biol. 2007;371:21-31.
38. Dimri GP, Lee X, Basile G, Acosta M, Scott G, Roskelley C, et al. A biomarker that identifies senescent human cells in culture and in aging skin in vivo. Proc Natl Acad Sci U S A. 1995;92(20):9363-7.
39. Borodkina AV, Deryabin PI, Giukova AA, Nikolsky NN. "Social Life" of Senescent Cells: What Is SASP and Why Study It? Acta Naturae. 2018;10(1):4-14.
40. Coppe JP, Desprez PY, Krtolica A, Campisi J. The senescence-associated secretory phenotype: the dark side of tumor suppression. Annu Rev Pathol. 2010;5:99-118.
41. Bowers LW, Rossi EL, O'Flanagan CH, deGraffenried LA, Hursting SD. The Role of the Insulin/IGF System in Cancer: Lessons Learned from Clinical Trials and the Energy Balance-Cancer Link. Front Endocrinol (Lausanne). 2015;6:77.
42. Nagano T, Nakano M, Nakashima A, Onishi K, Yamao S, Enari M, et al. Identification of cellular senescence-specific genes by comparative transcriptomics. Sci Rep. 2016;6:31758.
43. Baselet B, Belmans N, Coninx E, Lowe D, Janssen A, Michaux A, et al. Functional Gene Analysis Reveals Cell Cycle Changes and Inflammation in Endothelial Cells Irradiated with a Single X-ray Dose. Front Pharmacol. 2017;8:213.
44. Cmielova J, Havelek R, Kohlerova R, Soukup T, Bruckova L, Suchanek J, et al. The effect of ATM kinase inhibition on the initial response of human dental pulp and periodontal

ligament mesenchymal stem cells to ionizing radiation. International Journal of Radiation Biology. 2013;89(7):501-11.
45. Muthna D, Soukup T, Vavrova J, Mokry J, Cmielova J, Visek B, et al. Irradiation of Adult Human Dental Pulp Stem Cells Provokes Activation of p53, Cell Cycle Arrest, and Senescence but Not Apoptosis. Stem Cells and Development. 2010;19(12):1855-62.
46. Havelek R, Soukup T, Cmielova J, Seifrtova M, Suchanek J, Vavrova J, et al. Ionizing radiation induces senescence and differentiation of human dental pulp stem cells. Folia Biol (Praha). 2013;59(5):188-97.
47. Cmielova J, Havelek R, Soukup T, Jiroutova A, Visek B, Suchanek J, et al. Gamma radiation induces senescence in human adult mesenchymal stem cells from bone marrow and periodontal ligaments. Int J Radiat Biol. 2012;88(5):393-404.
48. Manda K, Kavanagh JN, Buttler D, Prise KM, Hildebrandt G. Low dose effects of ionizing radiation on normal tissue stem cells. Mutat Res Rev Mutat Res. 2014.
49. Ozcan S, Alessio N, Acar MB, Mert E, Omerli F, Peluso G, et al. Unbiased analysis of senescence associated secretory phenotype (SASP) to identify common components following different genotoxic stresses. Aging (Albany NY). 2016;8(7):1316-29.
50. Terzi MY, Izmirli M, Gogebakan B. The cell fate: senescence or quiescence. Mol Biol Rep. 2016;43(11):1213-20.
51. Ueno M, Aoto T, Mohri Y, Yokozeki H, Nishimura EK. Coupling of the radiosensitivity of melanocyte stem cells to their dormancy during the hair cycle. Pigment Cell Melanoma Res. 2014;27(4):540-51.
52. Chang J, Feng W, Wang Y, Luo Y, Allen AR, Koturbash I, et al. Whole-body proton irradiation causes long-term damage to hematopoietic stem cells in mice. Radiat Res. 2015;183(2):240-8.
53. Surova O, Zhivotovsky B. Various modes of cell death induced by DNA damage. Oncogene. 2013;32(33):3789-97.
54. Gorin C, Rochefort GY, Bascetin R, Ying H, Lesieur J, Sadoine J, et al. Priming Dental Pulp Stem Cells With Fibroblast Growth Factor-2 Increases Angiogenesis of Implanted Tissue-Engineered Constructs Through Hepatocyte Growth Factor and Vascular Endothelial Growth Factor Secretion. Stem Cells Transl Med. 2016;5(3):392-404.
55. Schindelin J, Arganda-Carreras I, Frise E, Kaynig V, Longair M, Pietzsch T, et al. Fiji: an open-source platform for biological-image analysis. Nat Methods. 2012;9(7):676-82.
56. De Vos WH, Van Neste L, Dieriks B, Joss GH, Van Oostveldt P. High content image cytometry in the context of subnuclear organization. Cytometry A. 2010;77(1):64-75.
57. Tanabe S. Role of mesenchymal stem cells in cell life and their signaling. World J Stem Cells. 2014;6(1):24-32.
58. Lobrich M, Shibata A, Beucher A, Fisher A, Ensminger M, Goodarzi AA, et al. gammaH2AX foci analysis for monitoring DNA double-strand break repair: strengths, limitations and optimization. Cell cycle (Georgetown, Tex). 2010;9(4):662-9.
59. Khanna KK, Jackson SP. DNA double-strand breaks: signaling, repair and the cancer connection. Nat Genet. 2001;27(3):247-54.
60. Jackson SP. Sensing and repairing DNA double-strand breaks. Carcinogenesis. 2002;23(5):687-96.
61. Wakeford R, Tawn EJ. The meaning of low dose and low dose-rate. J Radiol Prot. 2010;30(1):1-3.
62. Osipov AN, Pustovalova M, Grekhova A, Eremin P, Vorobyova N, Pulin A, et al. Low doses of X-rays induce prolonged and ATM-independent persistence of gammaH2AX foci in human gingival mesenchymal stem cells. Oncotarget. 2015;6(29):27275-87.
63. Pustovalova M, Astrelina capital Te C, Grekhova A, Vorobyeva N, Tsvetkova A, Blokhina T, et al. Residual gammaH2AX foci induced by low dose x-ray radiation in bone marrow mesenchymal stem cells do not cause accelerated senescence in the progeny of irradiated cells. Aging (Albany NY). 2017;9(11):2397-410.
64. Prendergast AM, Cruet-Hennequart S, Shaw G, Barry FP, Carty MP. Activation of DNA damage response pathways in human mesenchymal stem cells exposed to cisplatin or gamma-irradiation. Cell cycle (Georgetown, Tex). 2011;10(21):3768-77.
65. Oliver L, Hue E, Sery Q, Lafargue A, Pecqueur C, Paris F, et al. Differentiation-related response to DNA breaks in human mesenchymal stem cells. Stem Cells. 2013;31(4):800-7.

66. Tsvetkova A, Ozerov IV, Pustovalova M, Grekhova A, Eremin P, Vorobyeva N, et al. gammaH2AX, 53BP1 and Rad51 protein foci changes in mesenchymal stem cells during prolonged X-ray irradiation. Oncotarget. 2017;8(38):64317-29.
67. Markova E, Schultz N, Belyaev IY. Kinetics and dose-response of residual 53BP1/gamma-H2AX foci: co-localization, relationship with DSB repair and clonogenic survival. Int J Radiat Biol. 2007;83(5):319-29.
68. Rothkamm K, Lobrich M. Evidence for a lack of DNA double-strand break repair in human cells exposed to very low x-ray doses. Proc Natl Acad Sci U S A. 2003;100(9):5057-62.
69. Asaithamby A, Uematsu N, Chatterjee A, Story MD, Burma S, Chen DJ. Repair of HZE-particle-induced DNA double-strand breaks in normal human fibroblasts. Radiat Res. 2008;169(4):437-46.
70. Schultz LB, Chehab NH, Malikzay A, Halazonetis TD. p53 binding protein 1 (53BP1) is an early participant in the cellular response to DNA double-strand breaks. J Cell Biol. 2000;151(7):1381-90.
71. Kurpinski K, Jang DJ, Bhattacharya S, Rydberg B, Chu J, So J, et al. Differential effects of x-rays and high-energy 56Fe ions on human mesenchymal stem cells. Int J Radiat Oncol Biol Phys. 2009;73(3):869-77.
72. Nakamura-Ishizu A, Takizawa H, Suda T. The analysis, roles and regulation of quiescence in hematopoietic stem cells. Development. 2014;141(24):4656-66.
73. Ruhle A, Xia O, Perez RL, Trinh T, Richter W, Sarnowska A, et al. The Radiation Resistance of Human Multipotent Mesenchymal Stromal Cells Is Independent of Their Tissue of Origin. Int J Radiat Oncol Biol Phys. 2018;100(5):1259-69.
74. Musilli S, Nicolas N, El Ali Z, Orellana-Moreno P, Grand C, Tack K, et al. DNA damage induced by Strontium-90 exposure at low concentrations in mesenchymal stromal cells: the functional consequences. Sci Rep. 2017;7:41580.
75. Cho W, Kim ES, Kang CM, Ji YH, Kim JI, Park SJ, et al. Low-Dose Ionizing gamma-Radiation Promotes Proliferation of Human Mesenchymal Stem Cells and Maintains Their Stem Cell Characteristics. Tissue Eng Regen Med. 2017;14(4):421-32.

Chapter 6:

Antioxidant response in buccal mucosa cells and saliva samples following CBCT examination

Belmans N, Smeets K, Vermeesen R, Salmon B, Baatout S, Jacobs R., Lucas S, Lambrichts I, Moreels M Antioxidant response in buccal mucosa cells and saliva samples following CBCT examination. *In preparation*

6.1 Introduction

Reactive oxygen species (ROS), such as hydrogen peroxide (H_2O_2), the hydroxyl radical ($OH^{\bullet}$), and the superoxide anion ($O_2^{\bullet-}$), are formed by the partial reduction of molecular oxygen (O_2). Intracellular ROS are either generated endogenously during the process of mitochondrial phosphorylation, or they form following exposure to exogenous stimuli such as bacterial infections or ionizing radiation (IR). When the amount of ROS exceeds the balancing capacity of the intracellular antioxidants, which help regulate the cellular redox balance, an imbalance between oxidants and antioxidants occurs, which is called 'oxidative stress'.[1, 2] Oxidative stress could result in ROS-mediated damage to nucleic acids, lipids, and proteins. It has been linked to cardiovascular diseases, neurodegeneration, carcinogenesis, diabetes, and aging.[3-7] However, besides its involvement in pathogenesis of the aforementioned conditions, it has become clear during the past 25 years that ROS also serve as important signalling molecules that help regulate important biological and physiological processes, such as cellular differentiation, tissue regeneration, and prevention of aging.[2, 8, 9] In short, redox biology largely depends on H_2O_2, whereas $OH^{\bullet}$ and $O_2^{\bullet-}$ mostly cause oxidative stress, in normal physiological conditions.[2] In non-physiological conditions, however, ROS (especially $OH^{\bullet}$ and $O_2^{\bullet-}$) cause oxidative stress which can lead to severe DNA damage, including DNA breaks, base damage, destruction of sugars, cross links and telomere dysfunction.[10] This is the case with exposure to IR, which results in the radiolysis of intra- and extracellular water molecules, that in turn generates ROS.[11] IR-induced oxidative stress could, when the damage is not repaired efficiently, lead to cell death or mutations that could result in carcinogenesis. Of these IR-induced ROS, $OH^{\bullet}$ and $O_2^{\bullet-}$ are the most reactive ones. [12, 13]

Oxidative DNA damage is widely accepted to contribute to cancer development.[14, 15] However, oxidative DNA damage occurs continuously *in vivo* at the guanine DNA base and is usually caused by $OH^{\bullet}$. Measuring these oxidative DNA modifications could be potential biomarkers that predict cancer development later in life.[16] 7,8-dihydro-8-oxo-2'-deoxyguanosine (8-oxo-dG) is the most frequently measured oxidatively modified DNA base.[17, 18] It is so frequently measured because there are sensitive detection techniques available, it is formed by several important ROS including $O_2^{\bullet-}$ and $OH^{\bullet}$, and finally, it is a mutagenic lesion. The latter entails that cells have mechanisms to identify the presence of 8-oxo-dG and that they will remove 8-oxo-dG via nucleotide/base excision repair. 8-oxo-dG has been successfully measured in blood, urine and saliva samples.[19-25] It is known that 8-oxo-dG levels increase following high doses of IR.[26-30] We previously demonstrated that 8-oxo-dG levels increased significantly in saliva

samples of children 30 min following a cone-beam computed tomography (CBCT) examination (see Chapter 4).

The intracellular antioxidant system is an important mechanism to maintain intracellular redox homeostasis. It allows low concentrations of ROS to be present within the cell, while preventing accumulation of high levels of ROS in normal physiological conditions.[9] This delicate balance is essential for a normal cellular function.[31] The redox balance is maintained by endogenous antioxidants, including enzymatic antioxidants, hydrophilic antioxidants, and lipophilic radical antioxidants, which all counteract the surplus of free radicals and neutralize oxidants.[32] Superoxide dismutases (SOD), catalase (CAT), and glutathione peroxidases (GSH-Px) are examples of enzymatic antioxidants. They have the ability to decompose ROS.[33] SOD dismutates $O_2^{\bullet-}$ to H_2O_2 and O_2.[34] H_2O_2 is in turn neutralized by other enzymes such as CAT and GSH-Px.[35-39]

As discussed earlier, exposure to IR leads to oxidative stress through the formation of ROS from radiolysis of water. It was shown that high doses of IR significantly increase the gene expression and activities of SOD2, CAT, and GSH-Px. However, it has been shown that after irradiation with a low IR dose cells are primed for exposure to higher IR doses. Furthermore, these cells also show increased gene expression for genes encoding for antioxidants. Primed cells, in turn, show an increased antioxidant response in comparison to non-primed cells following high IR dose exposure, resulting in a higher radioresistance in these cells.[40, 41] Previously, we have demonstrated that the total antioxidant capacity increased in saliva from children following CBCT examinations. Interestingly, an opposite response was observed in adults, indicating potential age-dependent differences in anti-oxidant capacities. (Belmans *et al.*(2019), submitted; see chapter 4). Moreover, we showed that CBCT examinations increase the level of oxidative damage (i.e. 8-oxo-dG levels) in saliva samples from children. The changes in antioxidant capacity indicate that children and adults might respond differently to low doses of IR.[42] To gain more insight into the antioxidant response following CBCT examinations, we investigated the enzyme activity of the two major endogenous antioxidants, i.e. SOD, and CAT, in saliva samples from children following CBCT examination. Additionally the gene expression levels of *SOD1*, *CAT*, and *GPx1* were monitored in buccal mucosa cells (BMCs) from children and adults following CBCT examination.

6.2 Materials and methods

6.2.1 Patient selection

Patients with various indications were referred to the clinic for CBCT examination. They were examined using CBCT device settings that match their individual needs. Thus the field of view, tube voltage (kV), tube current (mAs) and resolution mode are adjusted to fit with each individual's indication and age, as described in the DIMITRA position statement by Oenning *et al*. (2017).[43]

The study was performed following current General Data Protection Regulation guidelines. Ethical approval was obtained at the Oral and MaxilloFacial Surgery – Imaging & Pathology department (Katholieke Universiteit Leuven, Leuven, Belgium) (B322201525196).

Eligible patients were children/adolescents from 3 to 18 years old, as well as adults (> 18 years old), with good oral hygiene. Exclusion criteria were the presence of systemic diseases, the use of antibiotics or anti-inflammatory drugs, smoking and not giving informed consent prior to enrolment. In case of underage children, both parents needed to consent unless one parent has explicit permission from the other parent.[44]

6.2.2 Saliva collection

Saliva samples were collected according to the DIMITRA study protocol.[44] In short, saliva samples were collected right before and 30 minutes after CBCT examination using the passive drool method. Immediately after collection, the whole saliva was stored at -20° C until shipment. After shipment to the lab, saliva samples were centrifuged at 10,000 g at 4° C and the supernatant was stored at -80° C until further analysis.

6.2.3 Buccal mucosa cell collection

The collection method was based on the protocol described in Belmans *et al*. (2019).[44] Briefly, synthetic swabs were used to collect BMCs just before, 30 minutes, 24 hours and 48 hours after CBCT examination. Before each swab the patient's mouth was rinsed twice with water. After sample collection, the swabs were transferred to tubes containing RNAprotect Cell Reagent (76526, Qiagen, Hilden, Germany).

6.2.4 Enzyme activity assay

The enzyme activity for both SOD and CAT were assessed using commercially available kits (706002 and 707002 respectively; Cayman Chemical, Michigan, USA). The assay kits were performed according to manufacturer's instructions. Briefly, standards/undiluted saliva samples were added to a 96-well plate. Next, radical detector (SOD) or assay buffer (CAT) was added to the wells. The enzymatic reactions were initiated by adding xanthine oxidase (SOD) or H_2O_2 (CAT). For the CAT assay, additional potassium hydroxide needs to be added. After incubation, the CAT reaction is stopped by adding potassium periodate and then the absorbance was read at 440 nm (SOD) or 540 nm (CAT) with a microplate reader (Clariostar, BMG Labtech, Ortenberg, Germany).

6.2.5 RNA isolation from RNAprotect Cell Reagent

For RNA isolation both TRIzol™ Reagent (15596026, Invitrogen™, Carlsbad, USA) and the Qiagen RNeasy Plus Micro kit (74034, Qiagen, Hilden, Germany) were used. Briefly, the samples were centrifuged for 1 hour at 2000 *g* at 4° C. Then the supernatant was removed and the pellet was lysed by adding 1 ml of TRIzol™ Reagent. The cells were incubated for 30 minutes at 37° C to allow for full cell lysis. Next, 200 µl of chloroform was added. Then, the samples were shaken vigorously and incubated for 3 minutes at room temperature (RT). Next, the samples were centrifuged at 12.000 *g* for 15 minutes at RT. Afterwards, the aqueous phase was transferred to a 1.5 ml microcentrifuge tube. Then, an equal amount of 70% ethanol (EtOH) was added to the sample after which the samples were put on the RNeasy spin column and centrifuged for 30 seconds at 14.000 *g*. Next, the RNeasy spin column was washed using RW1 buffer and the samples were centrifuged for 30 seconds at 14.000 *g*. Then the column was washed with RPE buffer and centrifuged for 30 seconds at 14.000 *g*. After this wash step, the column was washed with 80% EtOH and centrifuged for 2 minutes at 14.000 *g*. After washing, the column was put on a new 1.5 ml microcentrifuge tube and 20 µl of RNase-free water was added to the column. The column was then centrifuged for 1 minute at 14.000 *g*. The eluted RNA samples were stored on ice and RNA concentrations were determined using a NanoDrop™ 2000c (ThermoFisher Scientific, Waltham, MA, USA). After the RNA concentration was determined, the RNA samples were stored at -80° C.

6.2.6 cDNA synthesis

The Promega GoScript™ Transcriptase kit (A2801, Promega Benelux N.V., Leiden, The Netherlands) was used for cDNA synthesis. In short, RNA samples were thawed on ice. Then 300 ng of RNA was diluted to 14 µl using RNase-free water in sterile polymerase chain reaction (PCR) tubes. The samples were

centrifuged briefly. Then they were incubated for 5 minutes at 70° C. During incubation, the reverse transcription mix was prepared. After incubation, the samples were chilled on ice for at least 5 minutes. Next, 6 µl of reverse transcription mix was added to each sample. Then the samples were mixed gently and centrifuged briefly. The, the samples were incubated in a thermocycler (Proflex PCR system, ThermoFisher Scientific, Waltham, MA, USA). First for 5 minutes at 25° C, then at 42° C for 60 minutes, and finally 15 minutes at 70° C. Afterwards, the samples were diluted 1:3 in RNase-free water, resulting in a final concentration of 5 ng/µl cDNA. Finally, the samples were stored at -20° C.

6.2.7 Gene expression analysis using TaqMan™ probes and primers

Gene expression levels of *SOD1*, *CAT*, and *GPx1* are assessed using TaqMan™ gene expression assays (Hs00533490_m1, Hs00156308_m1, and Hs00829989_gH, respectively; ThermoFisher Scientific, Waltham, MA, USA). *PGK1* and *GAPDH* were used as reference genes (4333765F and Hs02786624_g1, respectively; ThermoFisher Scientific, Waltham, MA, USA). These reference genes were chosen based on previous data on patient samples following radiation exposure.[45] In short, cDNA samples and primer/probe sets were thawed on ice. A real-time polymerase chain reaction (qPCR) mastermix was prepared by diluting 20x primer/probe set and 2x TaqMan™ Universal Mastermix II with Uracil-N-glycosylase (Applied Biosystems, Foster City, CA, USA) in milliQ water. 15 µl of qPCR mastermix is added per well. Next, 5 µl of cDNA, which equals 25 ng, is added to each well. Then the samples are placed in the RotorGene Q series (Qiagen, Hilden, Germany). Samples were analysed using following set-up: 1) incubation at 50° C for 2 minutes followed by an incubation at 95° C for 10 minutes, 2) cycling between 15 seconds at 95° C and 60 seconds at 60 °C for 40 cycles. At the end of each incubation step at 60° C, a fluorescent signal was acquired. QPCR data was analysed using the Pfaffl method.[46]

6.2.8 Dose calculations – Monte Carlo simulation

A fully validated Monte Carlo framework, which was developed by the DIMITRA group, was used for dosimetric calculations.[47, 48] This Monte Carlo simulation relies on a database of pediatric head voxel models.[49] By using this Monte Carlo framework, absorbed organ doses were calculated for each individual patient. When simulating organ doses, the normalized absorbed organ dose values are provided in µGy/mAs. In this Monte Carlo framework, normalized absorbed organ doses are related to the age of the patient via the following equation:

$$y = a \times \ln(x) + b$$

where y is the normalized absorbed organ dose (μGy/mAs), x is the age of the patient at the time of the scan, and the constants a and b are factors that depend on the organ scanned, the clinical case, and the device used.[47] Simply multiplying the normalized absorbed organ dose by the mAs used for each specific scanning protocol results in an absorbed organ dose value. Thus the absolute organ dose can be calculated as follows:

$$y_{i,j} = [a \times \ln(x) + b] \times \mathrm{mAs}_j$$

where i represents a specific organ, and j stands for a specific examination. Note that this equation is not validated for adults, i.e. patients older than 18 years old. Therefore, no doses were simulated for adults using this equation.

6.2.9 Statistical analysis

Statistical analysis was performed using GraphPad 8.00 (GraphPad Inc., CA, USA). The results of the enzyme activity assays were analysed using two-tailed paired t-tests. To analyse differences between boys and girls, two-tailed unpaired t-tests were performed. For gene expression analysis, repeated measures one-way analysis of variance was performed. All tests listed above are parametric tests. If the conditions to test parametrically were not met, non-parametric alternatives were used. P values lower than .05 were considered as significant. Results are shown as mean ± standard error of the mean.

6.3 Results

6.3.1 Patients and dose exposure

For this study, the aim is to include 50 children referred for CBCT and about 10 children referred for head and neck CT. For adults, 15 patients will be included that were referred for CBCT as well as 10 that were referred for CT So far, 34 children and 20 adults are included in this study (Table 6.1). Note that not all patients samples have been analysed at this point. Therefore, no dose calculations are included.

Two CBCT devices were used, namely Accuitomo 170 (Morita, Osaka, Japan) and NewTom VGi-evo (Cefla S.C., Imola, Italy). The study was approved by the ethical committee of the participating hospital (see Material & Methods section). All patients (or their parents, in case of children) gave written informed consent.

Table 6.1: Overview of patients included in this study up to now

	# patients	**# CBCT examinations** (included/foreseen)	**# CT examinations** (included/foreseen)	**Age** (range)	**Gender** (m/f)
Children	34	34/50	-/10	7 - 17	16/18
Adults	20	12/15	8/10	18 - 84	10/10

6.3.1 CBCT examination leads to an increase in SOD activity which is dependent on gender

Analysis of the SOD activity in saliva samples from children shows a significant increase in SOD activity 30 minutes after CBCT examination. SOD activity (U/ml) increases from 3.74 ± 0.55 U/ml at baseline to 5.95 ± 0.78 U/ml 30 minutes after CBCT examination (N = 32, p = .0052) (Figure 6.1).

Analysis based on gender revealed that the SOD activity increases significantly in boys, but nog in girls (Figure 6.2). In boys, SOD activity increases from 3.10 ± 0.53 U/ml to 6.11 ± 1.25 U/ml after CBCT (N = 14, p = .0067). In girls, the SOD activity increases as well, from 4.24 ± 0.88 U/ml at baseline to 5.82 ± 1.03 U/ml 30 minutes after CBCT examination (N = 18; p = .13). Both at baseline (p = .64) and after CBCT examination (p = .99), there is no difference between boys and girls.

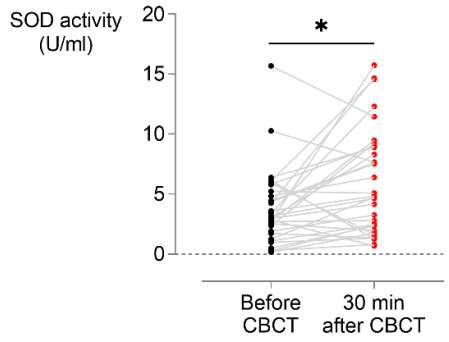

	Before CBCT	30 min after CBCT
Average SOD activity:	3.74	5.95
Standard error of mean:	0.55	0.78

Figure 6.1. Superoxide dismutase (SOD) activity 30 minutes after CBCT examination in saliva samples from children. The SOD activity increases significantly from 3.74 ± 0.55 U/ml before CBCT to 5.95 ± 0.78 U/ml after CBCT (N = 32, p = .0052). * = p < 0.01

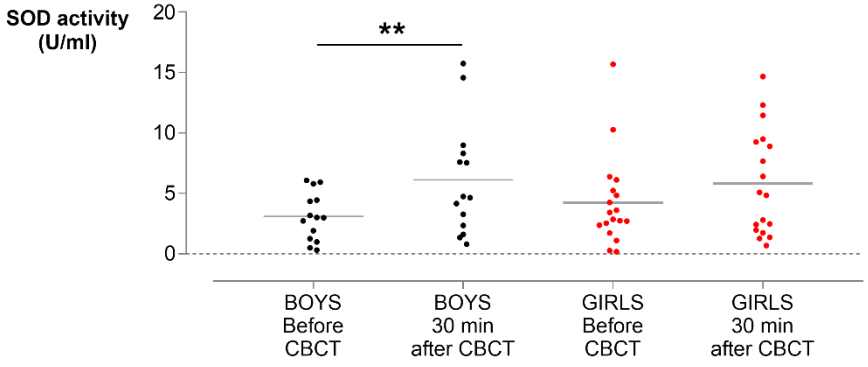

	BOYS Before CBCT	BOYS 30 min after CBCT	GIRLS Before CBCT	GIRLS 30 min after CBCT
Average SOD activity:	3.10	6.11	4.24	5.82
Standard error of mean:	0.53	1.25	0.88	1.03

Figure 6.2. Gender differences in superoxide dismutase (SOD) activity after CBCT examination in saliva samples from children. In boys, the SOD activity increases significantly from 3.10 ± 0.53 U/ml before CBCT to 6.11 ± 1.25 U/ml after CBCT (N = 14, p = .0067). In girls, the SOD activity varied from 4.24 ± 0.88 U/ml at baseline to 5.82 ± 1.03 U/ml after CBCT examination (N = 18, p = .13). At baseline (p = .64) and after CBCT examination (p : .99) there is no statistical difference between boys and girls. **: p = .0067; U = unit of enzyme catalytic activity (1 U = 1 µmol•min^{-1}).

6.3.2 CBCT examination leads to an increase in CAT activity

Analysis of the CAT activity in saliva samples from children shows an increase in CAT activity 30 minutes after CBCT examination. CAT activity (nmol/min/ml) increases from 7.68 ± 0.76 nmol/min/ml at baseline to 9.45 ±

0.71 nmol/min/ml 30 minutes after CBCT examination (N = 32, p = .0014) (Figure 6.3).

Analysis based on gender revealed that the CAT activity increases significantly in boys, but nog in girls (Figure 6.4). In boys, CAT activity increases from 7.11 ± 1.11 nmol/min/ml to 9.88 ± 1.10 nmol/min/ml after CBCT (N = 14, p = .017). In girls, the CAT activity increases as well, from 8.12 ± 1.06 nmol/min/ml at baseline to 9.11 ± 0.94 nmol/min/ml 30 minutes after CBCT examination (N = 18; p = .12). Both at baseline (p = .46) and after CBCT examination (p = .69), there is no difference between boys and girls.

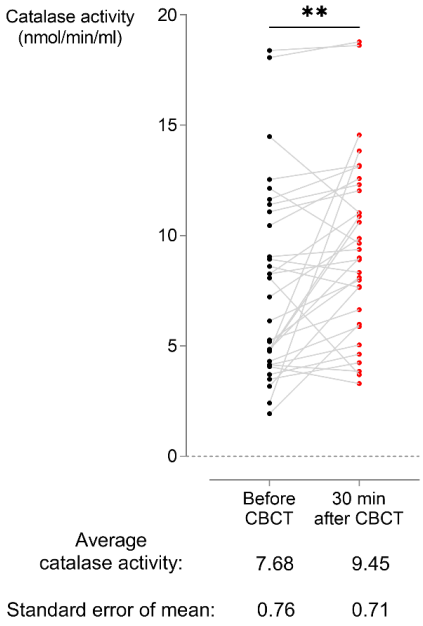

Figure 6.3. Catalase (CAT) activity 30 minutes after CBCT examination in saliva samples from children. The CAT activity increases significantly from 7.68 ± 0.76 nmol/min/ml before CBCT to 9.45 ± 0.71 nmol/min/ml after CBCT (N = 32, p = .0014). ** = p < 0.002

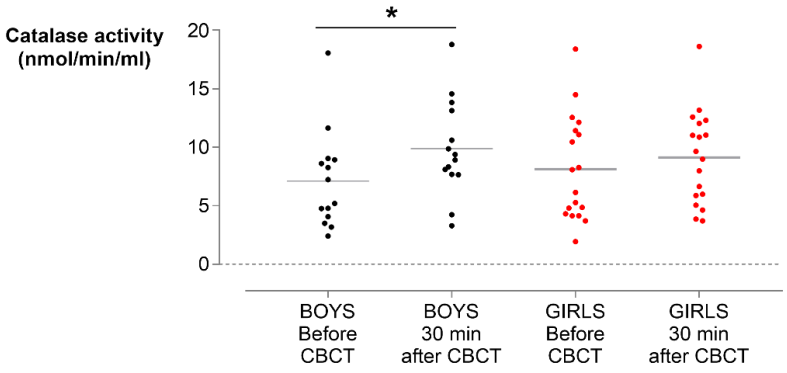

Figure 6.4. Catalase (CAT) activity 30 minutes after CBCT examination in saliva samples from boys and girls. In boys, the CAT activity increases significantly from 7.11 ± 1.11 nmol/min/ml at baseline to 9.88 ± 1.10 nmol/min/ml after CBCT (N = 14, p = .017). In girls, the CAT activity varied from 8.12 ± 1.06 nmol/min/ml at baseline to 9.11 ± 0.94 nmol/min/ml after CBCT (N = 18, p = .12). At baseline (p = .64) and after CBCT examination (p : .69) there is no statistical difference between boys and girls. *: p = .017

6.3.3 Changes in *SOD1, CAT,* and *GPx1* gene expression in children and adults

Relative *SOD1* gene expression changes statistically significantly after CBCT examination in children (p_{ANOVA} = .03). The relative gene expressions decreases from 0 ± 0.26 at baseline to -1.2 ± 0.41 30 minutes after CBCT examination (N = 28; p = .01). (Figure 6.5 A). 48 h after CBCT examination, *SOD1* gene expression was still decreased in children, i.e. -0.98 ± 0.19 compared to baseline (p = .0003). In adults, no significant changes were observed (N = 12; p_{ANOVA} = .53) (Figure 6.5 B).

Next, in children the relative *CAT* gene expression does not change following CBCT examination (N = 28)(Figure 6.5 C). Similarly, no relative gene expression changes were observed in adults (N = 12; p_{ANOVA} = .22) (Figure 6.5 D).

Finally, the relative *GPx1* gene expression changes statistically significantly in children after CBCT examination (N = 28; p_{ANOVA} = .0002). Post-hoc testing indicates that the relative gene expression decreases significantly from 0.00 ± 0.30 at baseline to -1.3 ± 0.35, 48 h after CBCT examination (N = 28; p = .007) (Figure 6.5 E). In adults, a statistically significant changes occur in relative *GPx1* gene expression (N = 12; p_{ANOVA} = .027) (Figure 6.5 F). Post-hoc testing indicates that the relative gene expression decreases significantly from 0.00 ± 0.37 at baseline to -1.4 ± 0.43, 48 h after CBCT examination (p = .007) (Figure 6.5 F).

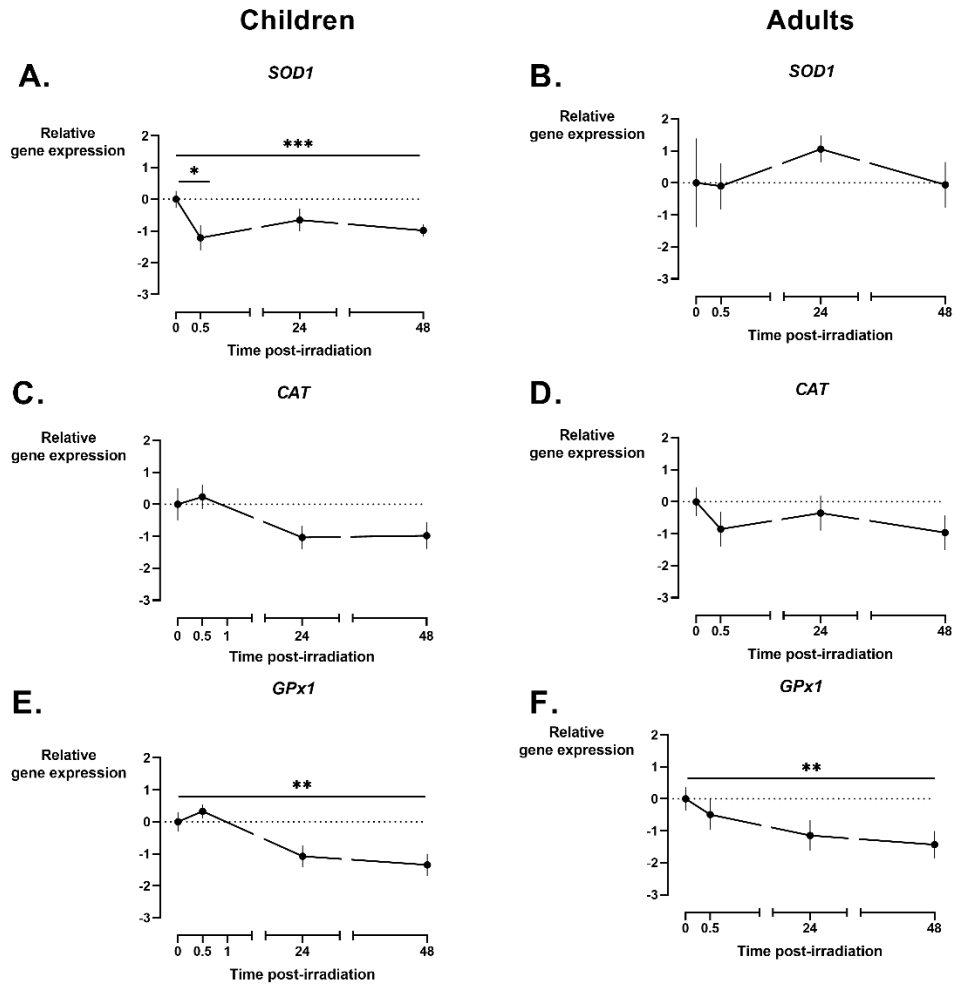

Figure 6.5. Relative gene expression changes in the SOD1, CAT, and GPx1 genes in children and adults. A. Relative *SOD1* gene expression changes statistically significantly 30 min after CBCT examination in children (p_{ANOVA} = .03). The relative gene expression decreases from -0.00 ± 0.26 at baseline to -1.2 ± 0.41 30 minutes after CBCT examination (N = 28; p = .01). 48 h after CBCT examination, *SOD1* gene expression was decreased in children, i.e. -0.98 ± 0.19 compared to baseline (p = .0003). **B.** In adults, no statistically significant changes were observed (N = 12; p_{ANOVA} = .53). **C.** The relative *CAT* gene expression does not change following CBCT examination in children (N = 28). **D.** No changes were observed in adults (N = 12; p_{ANOVA} = .22). **E.** The relative *GPx1* gene expression changes statistically significantly in children after CBCT examination (p_{ANOVA} = .0002). The relative gene expression decreases significantly from 0.00 ± 0.30 at baseline to -1.3 ± 0.35 48 h after CBCT examination (N = 28; p = .007). **F.** In adults, a statistically significant changes occurs in relative *GPx1* gene expression (N = 12; p_{ANOVA} = .027). The relative gene expression decreases statistically significantly from 0.00 ± 0.37 at baseline to -1.4 ± 0.43, 48 h after CBCT examination (p = .007) * = p < .05; **: p < .002*** = p < .0005

6.4 Discussion

Our preliminary data indicate that exposure to low doses of IR, such as those associated with CBCT examinations, leads to an increase in SOD and CAT activity in saliva samples from children 30 minutes after X-irradiation. These data imply that in response to CBCT induced oxidative damage, as measured by increased levels of 8-oxo dG (Belmans et al., submitted), the enzymatic activity of SOD and CAT increases in an attempt to scavenge the additional ROS that is formed due to low dose exposure. However, our gene expression data reveal that after CBCT examination the relative gene expression of *SOD1* and *GPx1* decreases in children. The relative gene expression for *SOD1* statistically significantly decreased 30 minutes after CBCT examination, and remained decreased 48 hours after the CBCT examination. Finally the relative gene expression of *GPx1* decreased only 48 h after CBCT examination in comparison to gene expression levels at baseline. In adults, no statistically significant changes in relative gene expression were observed, except for *GPx1*, where the relative gene expression decreased significantly 48 hours after CBCT examination, as it did in children. For *CAT* and *GPx1* expression, children and adults reacted similarly. However, our data indicate that they react differently when it comes to *SOD1* expression after CBCT examination. Children show a fast reduction in gene expression, whereas no changes occur in adults.

It is known that low doses of IR can induce ROS scavengers.[50] In occupational exposed staff, it has been shown that SOD activity is increased in comparison to controls, however, the CAT activity was found to be reduced.[51] Our data on enzyme activity are more in line with results from adaptive response studies. These studies show that exposure to low doses of IR increases the activity of antioxidant enzymes, which will protect the cells when they are exposed to a subsequent high IR dose.[41] Surprisingly, our gene expression data indicate that, although the enzyme activity increases, gene expression decreases, especially for *SOD1* (in children only) and *GPx1*. However, interpretation of these data should be done with caution, since these results are only preliminary.

For both SOD and CAT activity, we observed that the increase in enzyme activity was only statistically significantly increased in boys, not in girls. Gender-related differences were previously shown by Eken *et al*. (2012), who demonstrated that the SOD activity was significantly increased in exposed male radiation-exposed hospital staff, but not in female radiation-exposed hospital staff. They did not provide data on CAT activity and gender differences.[51] To the best of our knowledge this is the first time that this is observed in young boys and girls following CBCT examination.

It should be noted that these data are preliminary and show an acute increase in SOD and CAT activity, since it was only determined 30 minutes following CBCT examination. Data should also be collected at later time points to

see if the increase is persistent, and thus improves the individual's response to IR exposure, or that the increase is transient, and thus is a temporary defence mechanism countering ROS produced by the CBCT examination. Data on the relative gene expression hints at either acute (i.e. *SOD1*) or delayed (i.e. *GPx1*) decrease in gene expression levels after CBCT examination in children. In adults, only a delayed decrease in *GPx1* gene expression was observed. However, in this experiment, the sample size was rather small. Therefore, more subjects will be included. Additionally, as with the results presented in chapter 4, it would be interesting to also include adults (for enzyme activity assays). That way age-related differences could be studied as well. Furthermore, including adults for the enzyme activity assays could also give more insight in the gender differences that we have observed in young children. It would be interesting to see whether these differences persist in adulthood, or that the gender difference disappears, or even reverse, with increasing age.

To tackle the aforementioned issues, the Radiobiology Unit from the Belgian Nuclear Research Centre (Mol, Belgium) and the Department of Dentomaxillofacial Surgery and of Imaging and Pathology (KU Leuven, Leuven, Belgium) have applied for a research grant from the 'Fonds Wetenschappelijk Onderzoek Vlaanderen' (FWO). This FWO grant was awarded to the research groups and provides funds to continue this project from 2018 until 2021 under grant number G0A0918N.

6.5 References

1. Ray PD, Huang BW, Tsuji Y. Reactive oxygen species (ROS) homeostasis and redox regulation in cellular signaling. Cell Signal. 2012;24(5):981-90.
2. Schieber M, Chandel NS. ROS function in redox signaling and oxidative stress. Curr Biol. 2014;24(10):R453-62.
3. Trachootham D, Alexandre J, Huang P. Targeting cancer cells by ROS-mediated mechanisms: a radical therapeutic approach? Nat Rev Drug Discov. 2009;8(7):579-91.
4. Andersen JK. Oxidative stress in neurodegeneration: cause or consequence? Nat Med. 2004;10 Suppl:S18-25.
5. Shukla V, Mishra SK, Pant HC. Oxidative stress in neurodegeneration. Adv Pharmacol Sci. 2011;2011:572634.
6. Paravicini TM, Touyz RM. Redox signaling in hypertension. Cardiovasc Res. 2006;71(2):247-58.
7. Haigis MC, Yankner BA. The aging stress response. Mol Cell. 2010;40(2):333-44.
8. Finkel T. Signal transduction by reactive oxygen species. J Cell Biol. 2011;194(1):7-15.
9. D'Autreaux B, Toledano MB. ROS as signalling molecules: mechanisms that generate specificity in ROS homeostasis. Nature reviews Molecular cell biology. 2007;8(10):813-24.
10. Islam MT. Radiation interactions with biological systems. Int J Radiat Biol. 2017;93(5):487-93.
11. D. K. Maurya TPAD. Role of Radioprotectors in the Inhibition of DNA Damage and Modulation of DNA Repair After Exposure to Gamma-Radiation. In: Chen CC, editor. Selected Topics in DNA Repair: InTech.; 2011.
12. Halliwell B, Clement MV, Long LH. Hydrogen peroxide in the human body. FEBS Lett. 2000;486(1):10-3.
13. Azzam EI, Jay-Gerin JP, Pain D. Ionizing radiation-induced metabolic oxidative stress and prolonged cell injury. Cancer letters. 2012;327(1-2):48-60.
14. Loft S, Poulsen HE. Cancer risk and oxidative DNA damage in man. J Mol Med (Berl). 1996;74(6):297-312.
15. Poulsen HE, Prieme H, Loft S. Role of oxidative DNA damage in cancer initiation and promotion. Eur J Cancer Prev. 1998;7(1):9-16.
16. Halliwell B, Gutteridge JMC. Measurement of reactive species. Free Radicals in Biology and Medicine: Oxford University Press; 2015.
17. Kasai H, Nishimura S. Hydroxylation of deoxyguanosine at the C-8 position by ascorbic acid and other reducing agents. Nucleic Acids Res. 1984;12(4):2137-45.
18. Kasai H, Nishimura S. Hydroxylation of deoxy guanosine at the C-8 position by polyphenols and aminophenols in the presence of hydrogen peroxide and ferric ion. Gan. 1984;75(7):565-6.
19. Cooke MS, Singh R, Hall GK, Mistry V, Duarte TL, Farmer PB, et al. Evaluation of enzyme-linked immunosorbent assay and liquid chromatography-tandem mass spectrometry methodology for the analysis of 8-oxo-7,8-dihydro-2'-deoxyguanosine in saliva and urine. Free Radic Biol Med. 2006;41(12):1829-36.
20. Evans MD, Saparbaev M, Cooke MS. DNA repair and the origins of urinary oxidized 2'-deoxyribonucleosides. Mutagenesis. 2010;25(5):433-42.
21. Rossner P, Jr., Mistry V, Singh R, Sram RJ, Cooke MS. Urinary 8-oxo-7,8-dihydro-2'-deoxyguanosine values determined by a modified ELISA improves agreement with HPLC-MS/MS. Biochem Biophys Res Commun. 2013;440(4):725-30.
22. Cooke MS, Evans MD, Dizdaroglu M, Lunec J. Oxidative DNA damage: mechanisms, mutation, and disease. FASEB J. 2003;17(10):1195-214.
23. Breton J, Sichel F, Pottier D, Prevost V. Measurement of 8-oxo-7,8-dihydro-2'-deoxyguanosine in peripheral blood mononuclear cells: optimisation and application to samples from a case-control study on cancers of the oesophagus and cardia. Free Radic Res. 2005;39(1):21-30.

24. Tothova L, Kamodyova N, Cervenka T, Celec P. Salivary markers of oxidative stress in oral diseases. Front Cell Infect Microbiol. 2015;5:73.
25. Arunachalam R. Salivary 8-Hydroxydeoxyguanosine – a valuable indicator for oxidative DNA damage in periodontal disease. The Saudi Journal for Dental Research. 2014;6:15-20.
26. Haghdoost S, Sjolander L, Czene S, Harms-Ringdahl M. The nucleotide pool is a significant target for oxidative stress. Free Radic Biol Med. 2006;41(4):620-6.
27. Shakeri Manesh S, Sangsuwan T, Pour Khavari A, Fotouhi A, Emami SN, Haghdoost S. MTH1, an 8-oxo-2'-deoxyguanosine triphosphatase, and MYH, a DNA glycosylase, cooperate to inhibit mutations induced by chronic exposure to oxidative stress of ionising radiation. Mutagenesis. 2017;32(3):389-96.
28. Hall J, Jeggo PA, West C, Gomolka M, Quintens R, Badie C, et al. Ionizing radiation biomarkers in epidemiological studies - An update. Mutat Res. 2017;771:59-84.
29. Haghdoost S, Czene S, Naslund I, Skog S, Harms-Ringdahl M, Haghdoost S, et al. Extracellular 8-oxo-dG as a sensitive parameter for oxidative stress in vivo and in vitro
The nucleotide pool is a significant target for oxidative stress. Free Radic Res. 2005;39(2):153-62.
30. Haghdoost S, Svoboda P, Naslund I, Harms-Ringdahl M, Tilikides A, Skog S. Can 8-oxo-dG be used as a predictor for individual radiosensitivity? Int J Radiat Oncol Biol Phys. 2001;50(2):405-10.
31. Holmstrom KM, Finkel T. Cellular mechanisms and physiological consequences of redox-dependent signalling. Nature reviews Molecular cell biology. 2014;15(6):411-21.
32. Ratnam DV, Ankola DD, Bhardwaj V, Sahana DK, Kumar MN. Role of antioxidants in prophylaxis and therapy: A pharmaceutical perspective. J Control Release. 2006;113(3):189-207.
33. Christofidou-Solomidou M, Muzykantov VR. Antioxidant strategies in respiratory medicine. Treat Respir Med. 2006;5(1):47-78.
34. Fukai T, Ushio-Fukai M. Superoxide dismutases: role in redox signaling, vascular function, and diseases. Antioxid Redox Signal. 2011;15(6):1583-606.
35. Jee JP, Lim SJ, Park JS, Kim CK. Stabilization of all-trans retinol by loading lipophilic antioxidants in solid lipid nanoparticles. Eur J Pharm Biopharm. 2006;63(2):134-9.
36. Barros AI, Nunes FM, Goncalves B, Bennett RN, Silva AP. Effect of cooking on total vitamin C contents and antioxidant activity of sweet chestnuts (Castanea sativa Mill.). Food Chem. 2011;128(1):165-72.
37. Tabassum A, Bristow RG, Venkateswaran V. Ingestion of selenium and other antioxidants during prostate cancer radiotherapy: a good thing? Cancer Treat Rev. 2010;36(3):230-4.
38. Waring WS, Webb DJ, Maxwell SR. Systemic uric acid administration increases serum antioxidant capacity in healthy volunteers. J Cardiovasc Pharmacol. 2001;38(3):365-71.
39. He L, He T, Farrar S, Ji L, Liu T, Ma X. Antioxidants Maintain Cellular Redox Homeostasis by Elimination of Reactive Oxygen Species. Cell Physiol Biochem. 2017;44(2):532-53.
40. Paraswani N, Thoh M, Bhilwade HN, Ghosh A. Early antioxidant responses via the concerted activation of NF-kappaB and Nrf2 characterize the gamma-radiation-induced adaptive response in quiescent human peripheral blood mononuclear cells. Mutat Res. 2018;831:50-61.
41. Bravard A, Luccioni C, Moustacchi E, Rigaud O. Contribution of antioxidant enzymes to the adaptive response to ionizing radiation of human lymphoblasts. Int J Radiat Biol. 1999;75(5):639-45.
42. UNSCEAR. UNSCEAR 2013 Report: Sources, effects and risks of ionizing radiation - Volume II Annex B - Effects of radiation exposure of children. 2013.
43. Oenning AC, Jacobs R, Pauwels R, Stratis A, Hedesiu M, Salmon B, et al. Cone-beam CT in paediatric dentistry: DIMITRA project position statement. Pediatr Radiol. 2017.
44. Belmans N, Gilles L, Virag P, Hedesiu M, Salmon B, Baatout S, et al. Method validation to assess in vivo cellular and subcellular changes in buccal mucosa cells and saliva following CBCT examinations. Dentomaxillofac Radiol. 2019.

45. Macaeva E, Mysara M, De Vos WH, Baatout S, Quintens R. Gene expression-based biodosimetry for radiological incidents: assessment of dose and time after radiation exposure. Int J Radiat Biol. 2019;95(1):64-75.
46. Pfaffl MW. A new mathematical model for relative quantification in real-time RT-PCR. Nucleic Acids Res. 2001;29(9):e45.
47. Stratis A. Customized Monte Carlo Modelling for Paediatric Patient Dosimetry in Dental and Maxillofacial Cone Beam Computed Tomography Imaging [Doctoral Thesis]. Leuven University Press: KU Leuven; 2018.
48. Stratis A, Zhang G, Lopez-Rendon X, Jacobs R, Bogaerts R, Bosmans H. Customisation of a Monte Carlo Dosimetry Tool for Dental Cone-Beam Ct Systems. Radiation protection dosimetry. 2016;169(1-4):378-85.
49. Stratis A, Touyz N, Zhang GZ, Jacobs R, Bogaerts R, Bosmans H, et al. Development of a paediatric head voxel model database for dosimetric applications. Brit J Radiol. 2017;90(1078).
50. Mitchel RE. Low doses of radiation are protective in vitro and in vivo: evolutionary origins. Dose Response. 2006;4(2):75-90.
51. Eken A, Aydin A, Erdem O, Akay C, Sayal A, Somuncu I. Induced antioxidant activity in hospital staff occupationally exposed to ionizing radiation. Int J Radiat Biol. 2012;88(9):648-53.

Chapter 7:

General discussion and future perspectives

7.1 General discussion

Despite epidemiological evidence about biological risks associated with exposure to high doses of IR doses, there is no consensus on the risks associated with low dose IR exposure.[1] However, exposure to low IR doses is highly relevant to the general public, which is typically exposed to only a few mSv annually. While about half of this exposure originates from natural sources, the other half is due to medical diagnostic imaging.[2, 3] Since exposure to IR in medical diagnostics is the largest man-made source of IR exposure, it is important to know if there are any health risks associated with it.[2, 4] This is a particular concern in pediatric patients, since it is known that children are more sensitive to IR than adults.[5, 6] Although there are epidemiological data available on excessive cancer risk and childhood exposure to CT or radiography, these studies are performed retrospectively and have been criticized recently (see **Chapter 1**). The main aim of this thesis was to investigate if low doses of X-rays, as those associated with medical diagnostics, induce DNA damage and oxidative damage, and whether this is age-dependent. This was examined *in vitro* in dental stem cells from pediatric patients and *ex vivo* in buccal mucosa cells and saliva samples from pediatric and adult patients undergoing CBCT examinations.

In **Chapter 3** and **Chapter 4** we describe the *ex vivo* study that was conducted in pediatric and adult patients that were subjected to a CBCT examination. We aimed to investigate if children and adults show similar cellular and subcellular changes when exposed to very low IR doses.[5, 6] In this context, the formation of DNA DSBs in BMCs, and oxidative damage and antioxidant status of saliva samples was studies. In **Chapter 3** we describe the optimized study set-up, as well as the validation of the protocols used in this study. **Chapter 4** describes the results from this study.

This study is unique in that sense that saliva samples were used to investigate the effects of medical imaging (i.e. CBCT) for the first time. Therefore, prior to the start of patient inclusion, protocols for the *ex vivo* study were optimized and validated. In general, blood is the most commonly used sample to study cellular and subcellular changes after IR exposure. We opted to use BMCs and saliva since they can be collected in a non-invasive way. Furthermore, it is cheap and painless.[7-9], which makes this well-suited for pediatric patients. We validated our buccal swab cell collection method via flow cytometry and bright field microscopy, and confirmed that over 95% of the cells collected were BMCs. The use of the γH2AX/53BP1 assay in BMCs was described before.[8, 10-12] Our data showed that γH2AX/53BP1 can be detected in BMCs collected by buccal swabs. Furthermore, the saliva collection protocol, based on the passive drool method, described in chapter 3 allowed us to efficiently collect and store saliva samples

from patients. In these saliva samples, we validated the analysis of 8-oxo-dG/FRAP levels, for two main reasons: 1) to detect 8-oxo-dG/FRAP in saliva samples, and 2) to investigate if the psychological stress of being subjected to a medical scan potentially influences the 8-oxo-dG/FRAP levels in saliva. We found that after actual CBCT examination changes occurred in the 8-oxo-dG and FRAP levels. But no changes were detected following sham-irradiation. Since sham-irradiation and the actual CBCT examination occurred in the same patient, we were confident that the changes in 8-oxo-dG and FRAP levels were due to the IR.[13]

Despite the validation of our protocols, cautions need to be taken when using BMCs and saliva samples. BMCs should be collected in a uniform way to avoid differences in the distribution between cells from the different layers of the oral mucosa.[7, 14] Our validation experiment showed that our protocol allows for uniform sampling of BMCs. As with the BM cell distribution, saliva composition can also be affected by several factors, such as time of collection, the collection method, intake of dietary supplements, time since last time teeth were brushed, the presence of blood, etc.. Our collection protocol tries to make collection as uniform as possible by relying on the passive drool method, which is regarded as the gold standard.[15] By gathering additional information through questionnaires, other possible influences can be checked. The protocol that we described can be used in other settings within radiation protection research. For example, it could be used in patients subjected to CT examinations, nuclear medicine, or even interventional radiology. It would also be interesting to apply the protocol to occupationally exposed populations, such as interventional radiologists. They can be studied to monitor the response to repeated exposure to low doses of IR.

In chapter 4, we describe the results from these validated tests on BMC and saliva samples from children and adults. In doing so, we aimed to characterize the short term radiation-induced effects associated with CBCT examinations, hereby focussing on potential age-related differences. No DNA DSB induction was observed in BMCs, neither in children, nor in adults. The γH2AX/53BP1 assay has been used before to monitor DNA DSB formation after exposure to IR used in diagnostic and interventional radiology (e.g. CT scans).[16-18] Here it was reported that the number of DNA DSBs increased following CT examinations in which higher IR doses are used than in CBCT examinations. Furthermore, *in vitro* experiments presented in this thesis have demonstrated that when dental stem cells are irradiation using a CBCT device, DNA DSBs are induced.[19] γH2AX foci were detected in BMCs after IR exposure before and our validation experiments indicated that γH2AX/53BP1 foci could be detected after CBCT examination, we can assume that CBCT examinations do not statistically significantly increase the number of DNA DSBs in our patient population.[11, 13] This corresponds to earlier studies that studied genotoxicity markers following panoramic dental radiography and CBCT and did not find increased genotoxicity following IR exposure. However, all these studies reported increases in cytotoxicity markers (e.g. pyknosis and

karryorhexis), which was not evaluated in our study (see appendices 2 and 3). Despite these studies, there are some studies reporting increases in genotoxicity markers following dental radiography and CBCT examinations (see appendices 2 and 3). Finally, we found that the baseline number of DNA DSBs was statistically significantly higher in children than in adults. This observation, however, does not correspond to previous studies that show that aging is associated with an accumulation of DNA damage, partially due to a reduced DNA repair capacity.[20-23] Therefore, it was expected that the level of (baseline) DNA damage would be higher in adults. A possible explanation is that BMCs are the first barrier in inhalation and ingestion, thus they are exposed to several genotoxins. These genotoxins can be found in environmental and lifestyle factors such as diet, mouthwash, smoke, air pollution, etc..[24-26] Children are more sensitive to these type of genotoxins compared to adults due to age-related differences in absorption, metabolism, development and body functions.[25] Potentially, this is the underlying reason as to why the amount of DNA DSBs is statistically significantly higher in children than in adults.

Next, we observed a significant increase in 8-oxo-dG levels in saliva samples in children 30 minutes after CBCT examination. In adults, an increase was also observed, however this increase was not significant. As previously mentioned, this could be due to a reduced DNA repair capacity in adults. Because 8-oxo-dG has a mutagenic potential, it is removed by the cell when it is sensed by DNA repair mechanisms (e.g. NER/BER). If these mechanisms operate at reduced capacity, it could explain why less 8-oxo-dG was detected in saliva in adults compared to children. Despite this, no significant difference between the change in 8-oxo-dG excretion was observed between children and adults. Interestingly, no relation between 8-oxo-dG levels and absorbed dose to the salivary glands could be observed in our study. What we observe could be similar to phenomena observed in the 'adaptive radiation response'. In our case, the IR doses associated with CBCT result in a small biological response which seems unrelated to the IR dose, like an all-or-nothing mechanism, similar to the use of a 'priming dose' in adaptive response studies. An adaptive response occurs after a very low or 'priming' dose of a stressor (e.g. a chemical or IR) results in a small biological response. This small response allows the cell to adapt to the stressor by activating cellular defence mechanisms against that specific stressor. That way cells are prepared for an exposure of the same stressor at a higher or 'challenging' dose.[27] Our results mimic the effects seen when applying such a 'priming dose', i.e. an effect can be measured, but it is unrelated to the dose of the stressor that is used. This can be seen in the increase in antioxidant capacity and antioxidant enzyme activity that we observed in children. These increases were statistically significant, but were not related with the radiation dose. On the other hand, this lack of dose response can be due to a high inter-individual variability of radiation sensitivity. Finally, no gender differences were observed in 8-oxo-dG levels

following CBCT examination, neither in children, nor in adults. This resembles previous studies in urine and other samples of adults.[28-30]

In children we found a significant increase in the total antioxidant capacity 30 minutes after CBCT examination, whereas a significant decrease was found in adults. These data indicate that children and adults might respond differently to low doses of IR. Furthermore, besides age-related differences, gender also seems to play a role in the low dose response. We found that girls, but not boys, showed a statistically significant increase in FRAP values. Similarly, women, but not men, displayed a statistically significant decrease in FRAP values. These data indicate that antioxidant capacity is influenced the most in females, and that the age of the patient indicates if the antioxidant capacity will increase or decrease. Despite age- and gender-related differences, no dose-response relationship was seen in FRAP values, similar to 8-oxo-dG and DNA DSBs levels.

In conclusion, although CBCT induced biological changes, no relationship with the absorbed radiation dose was observed. This indicates that for low IR doses, the LNT model does not seem to apply in our patient population. Furthermore, age at time of exposure seems to correlate to the excretion of 8-oxo-dG and to the antioxidant response. Furthermore, gender also seems to affect the antioxidant response. Taken together, these data indicate that even very low IR doses can elicit biological responses. Therefore, these data should raise awareness about radiation protection when using CBCT devices. Thus, adherence to the ALADAIP principle is recommended.[31]

In **Chapter 5** we describe the DDR in pediatric dental stem cells *in vitro* following low doses of IR. We found that there was a transient induction of DNA DSBs in SHEDs, DFSCs, and SCAPs. As expected, the number of DSBs was highest after 30 to 60 minutes and returned to baseline levels 24 hours after radiation exposure. It is noteworthy that the number of DSBs increased linearly with the radiation dose in the range of 5 – 100 mGy. Linear regression analysis showed that 19 – 26 DSBs per Gy were formed, which is in line with observations in previous studies.[32-36] This analysis also reflected the efficient DNA repair, as the slope decreases over time until the slope becomes zero after 24 hours, which indicates that DNA DSBs are effectively repaired. Although these data support a LNT model, it should be noted that this is an *in vitro* model and that it does not give information concerning excessive cancer risk or malignant transformation of the dental stem cells, which should be considered when applying the LNT model for risk estimation.[37] No differences were observed in the amount of DSBs formed, nor in their repair kinetics between the three stem cell types studied here.

Despite the significant induction of DNA DSB that was observed, no major effects on cell cycle progression were observed. Only in SHEDs, a slight, but significant, G_2/M arrest was seen 72 hours after X-irradiation with 100 mGy. This was not observed in SCAPs. Although it is known that most cells are most sensitive to IR in the G_2/M phase, our data indicate that radiation sensitivity differs even

between similar cell types (SHED vs SCAP). Furthermore, during the G_2/M arrest, DSBs can be repaired both efficiently and error-free through HR.[38] However, DNA repair kinetics showed that the DSBs were already repaired 24 hours after irradiation, whereas the G_2/M phase arrest was only observed 72 hours after irradiation. The lack of persistent G_2/M arrest can be explained by the fact that persistent G_2/M arrest fails when the number of DSBs are low. It is estimated that 10 – 20 DSBs are required for efficient checkpoint activation.[39, 40] However, it might be interesting to study the G_2/M phase in more detail following low dose IR exposure, since it is known that there are two distinct types of G_2/M checkpoints that are activated following low IR doses. Both of these checkpoints show cell type-dependent threshold doses for activation.[41] This could in part explain the differences between SHEDs and SCAPs that is observed here. Our data indicate that X-ray doses below 100 mGy, although they cause DNA DSBs, do not cause a persistent activation of cell cycle checkpoints. This was observed before in mesenchymal stem cells for both low and high IR doses.[42, 43] However, it would be interesting to investigate the cell cycle checkpoints at later time point, in order to see if the G_2/M arrest in SHEDs is indeed transient, or that it persists for a longer period.

Linked to the cell cycle, we report for the first time, a dose-dependent decrease in the number of G_0 phase (quiescent) SHEDs and SCAPs after low dose X-irradiation. In SCAPs and SHEDs a significant decrease was seen as soon as 1 hour after irradiation. In the latter, this dose-dependent decrease was also observed 4 hours and 72 hours after irradiation. These data indicate that low X-ray doses can stimulate dental stem cells to re-enter the cell cycle, which could lead to a depletion of dental stem cells present. It has been described that an increase in ROS levels in stem cells could stimulate stem cell proliferation, given that the ROS concentration are not cytotoxic.[44, 45] We can assume that 100 mGy of X-rays produces low quantities of ROS, since it is estimated that 1 Gy of γ-rays (which are similar to X-rays) produces 0.28 $\mu mol \bullet kg^{-1}$ $OH^{\bullet}$ and 0.073 $\mu mol \bullet kg^{-1}$ H_2O_2.[46] These quantities could be sufficient to stimulate dental stem cells to re-enter the cell cycle, without being cytotoxic. It must be noted that we also observed a time-dependent decrease in the number of G_0 phase cells in SHEDs and SCAPs. This could be due to the build-up of ROS in the culture medium, since the medium was not changed between irradiation and cell collection. Therefore, the ROS accumulated this way could also have stimulated the dental stem cells to reprise the cell cycle, but our data indicates that it is reinforced by low doses of IR.

Additionally, no premature cellular senescence was observed following low dose IR exposure in dental stem cells. However, DNA DSBs have been identified as potent inducers of cellular senescence.[47] Investigation of SASP proteins IL-6, IL-8, IGFBP-2 and IGFBP-3 indicated a significant time-dependent induction of senescence but no dose-dependent changes were observed.[48, 49] IL-6 and IL-8 interact with the corresponding surface receptors and, trigger various intracellular

signalling cascades. Both are associated with DNA damage-induced premature senescence. Both can, in a paracrine manner, induce senescence in damaged cells and their neighbours.[48-50] IGFBP-2 and IGFBP-3 are regulatory factors that sequester IGF to prevent it binding to its receptor, thereby inhibiting cell proliferation.[51] Both IGFBP-2 and IGFBP-3 were found to be increased in senescent cells.[49] Our data indicates that SASP levels of IL-6, IL-8, IGFBP-2 and IGFBP-3 show similar profiles following X-irradiation. All of them indicate that there is no dose-dependent increase in the frequency of senescent dental stem cells following radiation exposure. These data were confirmed by the X-gal assay showing a time-dependent, but not dose-dependent increase in the frequency of X-gal positive cells.[52-54] A possible explanation is the lack of persistent DNA DSBs, which are a potent inducer of senescence.[55] As previously mentioned, no persistent DSBs were observed in our study. Additionally, it could be that our methods are not sensitive enough to detect early senescence. It might therefore be interesting to look at more sensitive assays, such as gene expression markers or DNA methylation changes.[56-59] Although previous studies showed IR-induced premature senescence in mesenchymal stem cells, these studies focused on high doses of IR.[60-63] Radiobiological evidence of low dose IR-induced senescence is rather scarce.[64, 65] Furthermore, studies that do describe a correlation between low doses of IR and premature senescence are contradicted by other studies, including our own.[66, 67]

From our data we can conclude that further research into the biological consequences of low dose IR exposure (e.g. senescence) on (dental) mesenchymal stem cells is warranted. Therefore, more in depth radiobiological studies that focus on more subtle changes should be conducted. Examples are high-throughput analysis techniques including next-generation sequencing or in-depth proteomics.

In **Chapter 6**, preliminary data about the antioxidant response following CBCT examinations in children and adults is described. The main focus is placed on anti-oxidant enzymes including SOD1, CAT, and GSH-Px1. These three important antioxidants were chosen because data from the DIMITRA project (see Chapter 4) showed that the total antioxidant response differed between children and adults.[13] Therefore, we assessed antioxidant enzyme activity in saliva samples. In addition gene expression levels of the three enzymes were studied in BMCs. Both saliva samples and BMCs were collected in children and adults.

These preliminary data show that, in saliva samples, the SOD and CAT enzyme activity increases significantly 30 minutes after CBCT examination in children. A possible explanation is that the enzymatic activity of SOD and CAT increase in an attempt to scavenge the additional ROS that is formed during the CBCT examination. Increased enzyme activity is also seen in male inhabitants (between 50 and 59 years old) of a high background radiation area (5.06 – 6.86 mSv per year) when compared to inhabitants of a control area (i.e. low

background radiation; 1.8 – 2.3 mSv per year). Here they found increased SOD, CAT and GSH-Px1 activities which were probably related to the high background radiation.[68] Interestingly, in our study the enzyme activity of both SOD and CAT increased significantly in boys, but not in girls. Similar results were described before for SOD activity in adult hospital staff. [69] Since the data from DIMITRA indicate that the total antioxidant response changes with increasing age, it is possible that this also occurs for the SOD and CAT enzyme activities.

Analysis of gene expression levels for *SOD1*, *CAT*, and *GPx1* shows that, overall, the relative gene expression levels decrease after CBCT examination, though not significantly for *CAT*. In children, *SOD1* gene expression levels decreased significantly 30 min after CBCT examination and remained decreased 48 hours later. The gene expression levels of *GPx1* decreased significantly from baseline to 48 hours after CBCT examination. These data are not in line with the enzyme activity assays, but rather seem to indicate a reduced transcription of the genes of interest. Similar results have been published before, but only after exposure to high IR doses.[70-72] Furthermore, increases in *SOD1*, *CAT*, and *GPx1* gene expression levels have been associated with increased radioresistance in cancer cells.[73-75]

The seemingly contradictory results from the enzyme activity assay and the gene expression assay indicate that exposure to low IR doses causes several subtle changes, which are the main reason why it is so difficult to find and validate good biomarkers for low IR dose exposure. If we compare the results from the SOD and CAT activity assays with the results from the FRAP assay (Chapter 4), these data however, support each other. The increase in FRAP values that were seen in children might be explained by the increased enzyme activity of the SOD and CAT enzymes that we observed here. However, on the gene level, contradictory results were obtained since the expression of the genes coding for these enzymes is reduced. Note that for *GPx1* the decrease in gene expression was only observed after 48 h. At this time point, the enzyme activity was not yet tested, thus no conclusion can be drawn about the link between gene expression levels and enzyme activity. Therefore, there is a need for more in-depth research on the effects (e.g. time-dependency) of low dose exposure on both the genomic and the proteomic levels.

Our *in vitro* data indicates that even at low IR doses, between 5 and 100 mGy, the number of DNA DSBs increases linearly with the IR doses. These data resemble data from high IR dose (i.e. doses over 100 mGy) exposure, and follow the LNT model (figure 1.12, Chapter 1).[1] However, our patient data indicate that levels of oxidative damage and the antioxidant response following exposure to low doses of IR is not correlated with the absorbed dose (10 mGy and below; figure 4.3, Chapter 4). Nevertheless, a measurable response is observed following exposure to IR during CBCT examinations, both in children and adults. These responses do not correlate with the different models explaining the dose-response

relationship in the low dose range (figure 1.12, Chapter 1). However, since our data concerns antioxidant responses following exposure to IR, the response we observed could be linked to a hormetic response. As discussed earlier, exposure to a low IR dose, could help prepare an organism to an exposure with a higher IR dose by increasing several defence mechanisms after exposure to the low IR dose, including antioxidant responses. This priming dose does not necessarily show a dose response, which could explain our observations.

In conclusion, low IR doses (< 100 mGy) induce significant numbers of DNA DSBs in dental stem cells *in vitro*. Despite the increased DNA damage, no effects on cell cycle progression were observed. However, the number of G_0 or quiescent cells decreases statistically significantly after low dose exposure. This indicates that the low levels of cellular stress that are caused by the IR stimulate the stem cells to re-enter the cell cycle. *Ex vivo*, we did not observe DNA DSBs following CBCT examination in children nor adults. However, we did find significant increases in 8-oxo-dG and FRAP levels in children 30 min after CBCT examination. In adults, a significant decrease in FRAP levels was observed at the same time point, but no changes in 8-oxo-dG levels were seen. These results indicate that there is no relation with the IR dose, indicating that the LNT model does not apply in this low dose range. On the other hand, our results indicate that there is an age-dependency in the response to IR exposure associated with CBCT examinations. Furthermore, these data on oxidative stress markers indicate that both age and gender play a role in the response to low doses of IR associated with CBCT examinations. Finally, preliminary data on SOD and CAT enzyme activity indicate that the activity of these important antioxidants increases significantly 30 minutes after CBCT examination in children. This increase was only significant in boys, not in girls. This observation supports the notion that gender plays a role in low dose IR response. However, the gene expression levels of the *SOD* and *GPx1* genes indicates that the expression of these genes decreases in BMCs in children after CBCT examination, and in adults, though only *GPx1* expression is decreased in adults. Therefore, more research is needed to further unravel the complex biological responses to low dose IR exposure.

7.2 Future perspectives

This study demonstrates that low doses of IR usually cause subtle (sub-) cellular changes. However, *in vitro* results often do not reflect or predict *ex vivo* data.[76-78] For example we showed a linear dose-response in the number of DNA DSBs following IR exposure *in vitro* (5 mGy – 100 mGy), but no changes in the number of DNA DSBs were observed in BMCs *ex vivo* of patients following CBCT examination. We admit that during CBCT examinations the IR doses are generally lower than 5 mGy, but still, one would expect a slight increase based on the *in vitro* data. To better understand (sub-)cellular changes following low dose IR exposure *in vitro* and *ex vivo* it might be interesting to include more complex *in vitro* models. Furthermore focussing on more specific molecular system and by using more sensitive detection methods *in vitro* and *ex vivo* could increase our current knowledge.

Organoids, a hot topic in science in recent years, are interesting *in vitro* models to study the effects of low dose IR exposure. They reflect the *in vivo* environment better than 2D cell cultures. Contrary to 2D cell cultures, 3D organoids, which are derived from tissue specific stem cells, are miniatures of selected tissues/organs, and they represent the architecture and even function of these specific tissues/organs.[79]

The main advantage of organoids is that the effects of low dose IR can be studied on different cell types of the same tissue, or on different tissues. Furthermore, this type of 3D *in vitro* model may help overcome the limitations of traditional 2D cell culture, such as an overestimation of the IR response.[80-83] For example, it has been shown that in 2D salivary gland stem cell cultures the amount of DNA damage is overestimated in comparison with salivary gland organoids, and that data from organoids better predict the *in vivo* response in mice.[81]

However, there are some limitations to the use of organoids. The most important limitation today is the reproducibility.[84] This can be attributed to the fact that these organoids do not have the native microenvironment that *in vivo* cells have. Therefore it is important to develop co-cultures with immune cells or other cells to improve the current use of organoids.[80]

To study the effects of CBCT examinations *in vitro* salivary gland organoids or oral mucosa organoids could be used.[81, 85-88] These models are highly similar to the *in vivo* salivary glands and oral mucosa, respectively. Therefore, investigating low dose radiation-induced effects in these *in vitro* models will result in data which are more indicative for the *in vivo* situation. This could help us to reveal potential targets or biomarkers for use in patients who undergo CBCT examinations.

We demonstrated in Chapter 4 that the total antioxidant capacity in saliva samples changes 30 min after CBCT examination. Furthermore, we found that these changes are age- and gender-dependent. Therefore, in order to further understand the low-dose radiation responses, we focused on changes in the antioxidant enzymes SOD, CAT and GSH-Px1. (see Chapter 6). However, it is important to look at other antioxidant systems which are present in the cell, such as the glutathione and thioredoxin systems.[72]

Important members of the glutathione system are: glutathione, glutathione synthase, glutathione reductase, GSH-Px, and glutathione S-transferase. It has been suggested that the glutathione system could play a role in counteracting radiation-induced cerebellar damage.[89] Data from a radiotherapy study has found that the glutathione levels in serum are depleted after high IR doses (≥ 4 Gy). It was proposed that serum glutathione can be used to predict chemoradioresponse in cervical cancers.[90, 91] Even after 0.5 Gy exposure in mouse splenocytes, the glutathione levels increased significantly.[92] Another study on radiotherapy for brain tumours reported that the levels of glutathione and the activity of gamma-glutamylcysteine synthetase, which synthesizes glutathione, are increased after high IR doses.[93] Moreover, one study also focused on the effect of low-dose irradiation on the glutathione system. In this study, different responses of the glutathione system to low (1 – 200 mSv) and high (200 – 1500 mSv) IR doses were measured in children living in the radionuclide-contaminated regions of Chernobyl.[94] Furthermore, it has been proposed that glutathione modulates the DNA repair activity, reducing radiosensitivity.[95]

The thioredoxin system consists of thioredoxin, thioredoxin reductase and nicotinamide adenine dinucleotide phosphate. The thioredoxin system can also include peroxiredoxin, which interacts thioredoxin to reduce hydroperoxides and H_2O_2.[72, 96] Similarly to the glutathione system, the thioredoxin system plays a central role in ROS detoxification.[72] In radiotherapy studies, the thioredoxin system was found to increase its activity after high dose IR exposure, increasing the radioresistance of tumours.[91] In breast cancer patients, peroxiredoxin levels were found to predict the clinical outcome following radiotherapy.[97] In radioresistant lung cancer cells, thioredoxin reductase was identified as contributing to the radioresistance of these cells.[98] This is also observed in other cancer cells.[99, 100] After lower IR doses (250 - 1000 mGy) the thioredoxin system is activated significantly in human blood cells.[101-103]

It is clear that the glutathione and thioredoxin systems are radioresponsive. Both of them seem to increase following IR exposure, protecting the cells from oxidative stress and trying to restore the redox balance. However, most studies were performed in the context of radiotherapy, and thus high IR doses. To the best of our knowledge, no studies exist that monitor these antioxidant systems following low dose IR exposure. Therefore, it could be interesting to monitor the glutathione and thioredoxin systems in patients subjected to medical imaging

procedures. This way, more insight can be gathered concerning the antioxidant response following medical imaging procedures and the maintenance of the redox balance following low dose IR exposure.

Although organoids and a more in-depth focus on antioxidant systems can greatly increase the knowledge on low dose IR-induced health effects, more information could also come from more sensitive techniques, such as liquid-chromatography tandem mass spectrometry or next-generation sequencing. These techniques allow for accurate detection of subtle changes on a proteomic an genetic level, respectively. Therefore, both techniques might be applicable to unravel inter-individual differences in responses to IR.

Liquid-chromatography tandem mass spectrometry (LC-MS) has a high specificity and sensitivity. Its multi-analytic potential make it an ideal alternative to immunoassays or conventional high-performance liquid chromatography.[104] LC-MS has been used to study exosomes following IR exposure. It was reported that exosomes from a head and neck cell carcinoma cell line showed changes after high-dose IR exposure. 236 proteins were detected specifically after irradiation and 69 proteins were down regulated after irradiation. Proteins overrepresented in exosomes from irradiated cells were involved in transcription, translation, protein turnover, cell division and cell signaling, which reflects radiation-induced changes in cellular processes like transient suppression of transcription and translation or stress-induced signaling.[105] LC-MS has been used to absolutely quantify H2AX phosphorylation. Since the formation of γH2AX is an important step in the DDR, this could be an alternative to immunostaining.[106, 107] LC-MS can also be used in saliva samples. It was reported that 1256 proteins were identified in saliva.[108] Since the results presented in Chapters 4 and 6 indicate that low doses of IR can induce changes in saliva, it is reasonable that with LC-MS more subtle changes can be detected. Furthermore, it has been described before that the salivary proteome is radioresponsive.[109] Therefore, it might be an interesting technique to implement in future low dose IR research in order to identify potential biomarkers of low dose IR exposure.

Next generation sequencing is a DNA sequencing technique that allows for the sequencing of the entire human genome in a single day. It also can capture almost the entire spectrum of mutations that can occur.[110] Next generation sequencing has revealed that in human fibroblast, there are certain chromosomal regions that are more prone to accumulating IR-induced alterations than others. This could point to a characteristic metasignature in the irradiated exome.[111] In thyroid cancer patients post-Chernobyl, next generation sequencing was used to detect the underlying genetic alterations underlying the thyroid cancer. Driver mutations were identified in 96.9% of thyroid cancers, including point mutations in 26.2% and gene fusions in 70.8% of cases. These data support a link between thyroid dose and generation of carcinogenic gene fusions associated with radiation exposure from the Chernobyl accident.[112] Furthermore, it has been shown that

the expression of various micro-RNA (miRNA) is altered in IR-exposed cells. Genome-wide expression changes of miRNA transcriptome by massively parallel sequencing of human cells exposed to IR, indicated that there are differences in the expression of many miRNA in a time-dependent fashion following IR exposure. Six statistically significant temporal expression profiles were identified.[113] This is important information since it is known that miRNA play an important role in post-transcriptional gene regulation in X-irradiated cells.[114]

Both LC-MS and next generation sequencing have proven to be powerful tools. Therefore, they are excellent techniques for research into biomarkers of IR exposure. In future research projects they can be implemented to look for biomarkers or to detect changes that are linked to inter-individual variability in radiosensitivity. To the best of our knowledge, this has not been done in patients exposed to medical imaging, such as CT or CBCT. Thus the potential findings can help improve radiation protection guidelines.

Salivary biomarkers have a huge potential when it comes to epidemiological cohort studies, mostly because it can be collected in a painless, non-invasive way.[9] Through the use of high-throughput technologies, as described before, the number of studies describing changes in saliva composition, i.e. salivary biomarkers, has increased over the last years. Multiple biomarkers for cancer and non-cancer diseases have been validated in saliva samples, however only a few salivary biomarkers of IR exposure have been described.[115-117] Thus far, only three immunomodulatory proteins were described to be linked with full body irradiations with high IR doses in humans.[109] Data presented in this thesis indicate that low doses of IR can also induce detectable changes in saliva samples, namely in 8-oxo-dG concentration. This opens new opportunities to use saliva in low dose radiation biomarker research.

Despite saliva being more and more used to identify biomarkers of disease, it is underused for identifying radiation biomarkers. However, due to recent technological advances, it shows a great potential and should be further investigated in order to gain more insight into salivary biomarkers of IR exposure.

Saliva samples could, in combination with next-generation sequencing, be used for genotyping experiments. This way, biomarkers related to genetic variants could be identified. These biomarkers have potential uses in identifying individual risks for IR exposure effects and IR susceptibility. Furthermore, saliva samples could be used to investigate IR-related epigenetic changes. This can be done by looking at miRNAs in saliva. Since miRNA expression profiles are tissue-specific, changes due to IR exposure in these profiles could be identified.[118]

As mentioned earlier, LC-MS can also be used in research into salivary biomarkers. It can provide insight on which proteins respond to both low and high doses of IR. Furthermore, it can help identify certain metabolites that could be linked to IR exposure. Unfortunately, the field of metabolomics is still in its infancy.[119]

Currently, radiation protection in medical imaging, both in adults and in children, is largely based on the 'as-low-as-reasonable-achievable' or ALARA principle. This principle stems from the belief that even if the true cancer risks of X-ray imaging are not known, minimizing IR exposure was sensible.[120] The ALARA principle is important for reducing the radiation risk in patients given the increased use of IR in medical imaging. The ALARA principle mostly focusses on justification of an examination relying on IR. In short, the benefits should be weighed against radiation risks, but imaging modalities not utilizing IR such as ultrasound and magnetic resonance imaging should be considered.[121]

In 2015, the ICRP has published guidelines concerning CBCT. One way to limit IR dose could be by using the 180°-240° rotation range, instead of a 360° full rotation. This feature allows keeping radiation-sensitive organs on the detector side, which results in protection of the more sensitive organs.[122] Other ICRP recommendations include monitoring of the radiation dose output of the CBCT device through comparison with reference levels, and using a feedback mechanisms to the CBCT device leading to automatic adjustment of the X-ray tube parameters. However, to date, radiation protection emphasises on IR dose management and avoidance of high dose exposure.[122] In CBCT, the FOV size is the most significant factor affecting patient dose. Therefore, CBCT devices that have the option to image small FOVs should be considered. Furthermore, devices with automatic exposure control are preferred. An example of such the device is the NewTom VGi EVO that has tube current modulation and which was used in this study. Other devices used in this study (i.e. Accuitomo and Planmeca) do not have this option. If manual selection of kV and mA is available, then multiple choices of kV-mA combinations are recommended to lower exposure settings for dose optimization.[123] Although these suggestions are well-known, current (intern)national recommendations for IR dose reduction are inconsistent and too general. Therefore, the DIMITRA research group aimed at providing indication-oriented and patient-specific recommendations concerning the use of CBCT in pediatric patients. This resulted in the newly dubbed ALADAIP principle.[31] This ALADAIP principle could provide a basis for personalized radiation protection guidelines, taking into account age, gender, etc., while maintaining adequate image quality. This personalized radiation protection could be combined with a radiation passport, allowing radiologists to personalize the radiation dose for each individual patient. Recently, the DIMITRA research group published results from a dosimetry study indicating that significant decreases in the effective dose can be achieved while maintaining the required image quality in pediatric CBCT.[124]

Although reducing the IR dose to which the patient is exposed is one way to decrease potential radiation induced risks, other measures can be taken to improve radiation protection. Our data indicates that intracellular antioxidants increase their activity to defend against the ROS produced by IR. Therefore one can speculate to use nutritional antioxidants as radioprotective agents. Several

studies reported the use of antioxidants as a protective measure against IR-induced ROS. The general consensus from these studies is that the combination of several nutritional antioxidants could help relieve the potential harmful effects of IR exposure through ROS scavenging.[125-128] Other potentially radioprotective compounds found in food (e.g. garlic, green tea, apples, citrus, and ginger) are flavonoids, which have antioxidant properties, phenolic acids, and phytohormones.[129] Today, the use of free radical scavengers is the most common countermeasure in radioprotection. However, the modulation of growth factors, cytokines and redox genes are emerging as effective alternative strategies. Furthermore, gene- and stem cell therapies are being developed as therapeutic radiation countermeasures and are expected to be applied in the near future to minimize the side effects of radiation exposure through tissue regeneration.[130] Although the latter is mostly for exposure to high IR doses, and less relevant for exposure to low doses such as those used in medical imaging. Finally, it is noteworthy that there is no conclusive evidence and that the supplementation of radioprotectors should always be combined with the ALARA and/or ALADAIP principle.

One important question today in medical imaging is "Dentomaxillofacial imaging in children, should we be concerned?" Based on our data, CBCT examinations do not induce DNA DSBs in BMCs in children nor in adults. It does, on the other hand, induce oxidative damage which was reflected by the significant increase in 8-oxo-dG levels in saliva samples from children 30 min after CBCT exposure. Interestingly, this significant increase was not observed in adults. Furthermore, in saliva samples from children, the total antioxidant capacity increases significantly 30 minutes after CBCT examination, whereas it decreases significantly in adults 30 minutes after CBCT examination. These data indicate that children and adults could respond differently to low doses of IR. Additionally, 30 minutes after CBCT examinations the salivary SOD and CAT activity increase in children. Gene expression levels of *SOD1*, and *GPx1*, however, decrease 30 minutes, and 48 hours after CBCT examination, respectively, in children. In adults on the other hand, only a decrease in *GPx1* gene expression is observed 48 hours after CBCT examination. These data indicate that in children, antioxidant responses are activated in order to defend against oxidative stress that is caused by the CBCT examination. However, at this stage, no conclusion can be made about the potential long-term effects based on these results. Therefore, it is recommended to strictly adhere to the ALADAIP principle and to prevent unnecessary exposure to any form of IR.

7.3 References

1. UNSCEAR. UNSCEAR 2006 Report to the General Assembly with Scientific Annexes. Effects of Ionizing Radiation. Volume I Report and Annexes A and B. 2008.
2. UNSCEAR. Sources and effects of ionizing radiation - UNSCEAR 2008 Report to the General Assembly with Scientific Annexes 2010;Volume 1.
3. EuropeanCommission. Radiation Protection N°180 - Medical Radiation Exposure of the European Population. Luxembourgs: European Union; 2014.
4. Tang FR, Loganovsky K. Low dose or low dose rate ionizing radiation-induced health effect in the human. J Environ Radioact. 2018;192:32-47.
5. ICRP. Recommendations of the International Commission on Radiological Protection. ICRP Publication 60. Ann. ICRP 21. 1990.
6. UNSCEAR. UNSCEAR 2013 Report: Sources, effects and risks of ionizing radiation - Volume II Annex B - Effects of radiation exposure of children. 2013.
7. Thomas P, Holland N, Bolognesi C, Kirsch-Volders M, Bonassi S, Zeiger E, et al. Buccal micronucleus cytome assay. Nat Protoc. 2009;4(6):825-37.
8. Siddiqui MS, Francois M, Fenech MF, Leifert WR. gammaH2AX responses in human buccal cells exposed to ionizing radiation. Cytometry A. 2015;87(4):296-308.
9. Lee JM, Garon E, Wong DT. Salivary diagnostics. Orthod Craniofac Res. 2009;12(3):206-11.
10. Baselet B, Belmans N, Coninx E, Lowe D, Janssen A, Michaux A, et al. Functional Gene Analysis Reveals Cell Cycle Changes and Inflammation in Endothelial Cells Irradiated with a Single X-ray Dose. Front Pharmacol. 2017;8:213.
11. Gonzalez JE, Roch-Lefevre SH, Mandina T, Garcia O, Roy L. Induction of gamma-H2AX foci in human exfoliated buccal cells after in vitro exposure to ionising radiation. Int J Radiat Biol. 2010;86(9):752-9.
12. Vandevoorde C, Vral A, Vandekerckhove B, Philippe J, Thierens H. Radiation Sensitivity of Human CD34(+) Cells Versus Peripheral Blood T Lymphocytes of Newborns and Adults: DNA Repair and Mutagenic Effects. Radiat Res. 2016;185(6):580-90.
13. Belmans N, Gilles L, Virag P, Hedesiu M, Salmon B, Baatout S, et al. Method validation to assess in vivo cellular and subcellular changes in buccal mucosa cells and saliva following CBCT examinations. Dentomaxillofac Radiol. 2019.
14. Torres-Bugarin O, Zavala-Cerna MG, Nava A, Flores-Garcia A, Ramos-Ibarra ML. Potential uses, limitations, and basic procedures of micronuclei and nuclear abnormalities in buccal cells. Dis Markers. 2014;2014:956835.
15. Munro CL, Grap MJ, Jablonski R, Boyle A. Oral health measurement in nursing research: state of the science. Biol Res Nurs. 2006;8(1):35-42.
16. Kuefner MA, Brand M, Engert C, Schwab SA, Uder M. Radiation Induced DNA Double-Strand Breaks in Radiology. Rofo. 2015;187(10):872-8.
17. Halm BM, Franke AA, Lai JF, Turner HC, Brenner DJ, Zohrabian VM, et al. gamma-H2AX foci are increased in lymphocytes in vivo in young children 1 h after very low-dose X-irradiation: a pilot study. Pediatr Radiol. 2014;44(10):1310-7.
18. Shi L, Tashiro S. Estimation of the effects of medical diagnostic radiation exposure based on DNA damage. J Radiat Res. 2018;59(suppl_2):ii121-ii9.
19. Virag P, Hedesiu M, Soritau O, Perde-Schrepler M, Brie I, Pall E, et al. Low-dose radiations derived from cone-beam CT induce transient DNA damage and persistent inflammatory reactions in stem cells from deciduous teeth. Dentomaxillofac Radiol. 2018:20170462.
20. Gorbunova V, Seluanov A. DNA double strand break repair, aging and the chromatin connection. Mutat Res. 2016;788:2-6.
21. Ramsey MJ, Moore DH, 2nd, Briner JF, Lee DA, Olsen L, Senft JR, et al. The effects of age and lifestyle factors on the accumulation of cytogenetic damage as measured by chromosome painting. Mutat Res. 1995;338(1-6):95-106.

22. Goukassian D, Gad F, Yaar M, Eller MS, Nehal US, Gilchrest BA. Mechanisms and implications of the age-associated decrease in DNA repair capacity. FASEB J. 2000;14(10):1325-34.
23. Gorbunova V, Seluanov A, Mao Z, Hine C. Changes in DNA repair during aging. Nucleic Acids Research. 2007;35(22):7466-74.
24. Khan S, Khan AU, Hasan S. Genotoxic assessment of chlorhexidine mouthwash on exfoliated buccal epithelial cells in chronic gingivitis patients. J Indian Soc Periodontol. 2016;20(6):584-91.
25. Cavalcante DN, Sposito JC, Crispim BD, Nascimento AV, Grisolia AB. Genotoxic and mutagenic effects of passive smoking and urban air pollutants in buccal mucosa cells of children enrolled in public school. Toxicol Mech Methods. 2017;27(5):346-51.
26. Shafi FA. Micronucleus frequency in buccal cells of males exposed to air pollution in Kufa City. Al-Mustansiriyah Journal of Science. 2017;28(02):43-7.
27. Dimova EG, Bryant PE, Chankova SG. "Adaptive response" - Some underlying mechanisms and open questions. Genet Mol Biol. 2008;31(2):396-408.
28. Topic A, Francuski D, Markovic B, Stankovic M, Dobrivojevic S, Drca S, et al. Gender-related reference intervals of urinary 8-oxo-7,8-dihydro-2'-deoxyguanosine determined by liquid chromatography-tandem mass spectrometry in Serbian population. Clin Biochem. 2013;46(4-5):321-6.
29. Kaneko K, Kimata T, Tsuji S, Ohashi A, Imai Y, Sudo H, et al. Measurement of urinary 8-oxo-7,8-dihydro-2-deoxyguanosine in a novel point-of-care testing device to assess oxidative stress in children. Clin Chim Acta. 2012;413(23-24):1822-6.
30. Matosevic P, Klepac-Pulanic T, Kinda E, Augustin G, Brcic I, Jakic-Razumovic J. Immunohistochemical expression of 8-oxo-7,8-dihydro-2'-deoxyguanosine in cytoplasm of tumour and adjacent normal mucosa cells in patients with colorectal cancer. World J Surg Oncol. 2015;13:241.
31. Oenning AC, Jacobs R, Pauwels R, Stratis A, Hedesiu M, Salmon B, et al. Cone-beam CT in paediatric dentistry: DIMITRA project position statement. Pediatr Radiol. 2017.
32. Asaithamby A, Chen DJ. Cellular responses to DNA double-strand breaks after low-dose gamma-irradiation. Nucleic Acids Res. 2009;37(12):3912-23.
33. Markova E, Schultz N, Belyaev IY. Kinetics and dose-response of residual 53BP1/gamma-H2AX foci: co-localization, relationship with DSB repair and clonogenic survival. Int J Radiat Biol. 2007;83(5):319-29.
34. Rothkamm K, Lobrich M. Evidence for a lack of DNA double-strand break repair in human cells exposed to very low x-ray doses. Proc Natl Acad Sci U S A. 2003;100(9):5057-62.
35. Asaithamby A, Uematsu N, Chatterjee A, Story MD, Burma S, Chen DJ. Repair of HZE-particle-induced DNA double-strand breaks in normal human fibroblasts. Radiat Res. 2008;169(4):437-46.
36. Schultz LB, Chehab NH, Malikzay A, Halazonetis TD. p53 binding protein 1 (53BP1) is an early participant in the cellular response to DNA double-strand breaks. J Cell Biol. 2000;151(7):1381-90.
37. Tubiana M, Feinendegen LE, Yang C, Kaminski JM. The linear no-threshold relationship is inconsistent with radiation biologic and experimental data. Radiology. 2009;251(1):13-22.
38. Santivasi WL, Xia F. Ionizing Radiation-Induced DNA Damage, Response, and Repair. Antioxid Redox Sign. 2014;21(2):251-9.
39. Goodarzi AA, Jeggo PA. The repair and signaling responses to DNA double-strand breaks. Adv Genet. 2013;82:1-45.
40. Deckbar D, Jeggo PA, Lobrich M. Understanding the limitations of radiation-induced cell cycle checkpoints. Crit Rev Biochem Mol Biol. 2011;46(4):271-83.
41. Fernet M, Megnin-Chanet F, Hall J, Favaudon V. Control of the G2/M checkpoints after exposure to low doses of ionising radiation: implications for hyper-radiosensitivity. DNA Repair (Amst). 2010;9(1):48-57.
42. Kurpinski K, Jang DJ, Bhattacharya S, Rydberg B, Chu J, So J, et al. Differential effects of x-rays and high-energy 56Fe ions on human mesenchymal stem cells. Int J Radiat Oncol Biol Phys. 2009;73(3):869-77.

43. Ruhle A, Xia O, Perez RL, Trinh T, Richter W, Sarnowska A, et al. The Radiation Resistance of Human Multipotent Mesenchymal Stromal Cells Is Independent of Their Tissue of Origin. Int J Radiat Oncol Biol Phys. 2018;100(5):1259-69.
44. Nakamura-Ishizu A, Takizawa H, Suda T. The analysis, roles and regulation of quiescence in hematopoietic stem cells. Development. 2014;141(24):4656-66.
45. Chaudhari P, Ye Z, Jang YY. Roles of reactive oxygen species in the fate of stem cells. Antioxid Redox Signal. 2014;20(12):1881-90.
46. Le Caer S. Water Radiolysis: Influence of Oxide Surfaces on H-2 Production under Ionizing Radiation. Water-Sui. 2011;3(1):235-53.
47. Di Leonardo A, Linke SP, Clarkin K, Wahl GM. DNA damage triggers a prolonged p53-dependent G1 arrest and long-term induction of Cip1 in normal human fibroblasts. Genes Dev. 1994;8(21):2540-51.
48. Borodkina AV, Deryabin PI, Giukova AA, Nikolsky NN. "Social Life" of Senescent Cells: What Is SASP and Why Study It? Acta Naturae. 2018;10(1):4-14.
49. Coppe JP, Desprez PY, Krtolica A, Campisi J. The senescence-associated secretory phenotype: the dark side of tumor suppression. Annu Rev Pathol. 2010;5:99-118.
50. Ortiz-Montero P, Londono-Vallejo A, Vernot JP. Senescence-associated IL-6 and IL-8 cytokines induce a self- and cross-reinforced senescence/inflammatory milieu strengthening tumorigenic capabilities in the MCF-7 breast cancer cell line. Cell Commun Signal. 2017;15(1):17.
51. Bowers LW, Rossi EL, O'Flanagan CH, deGraffenried LA, Hursting SD. The Role of the Insulin/IGF System in Cancer: Lessons Learned from Clinical Trials and the Energy Balance-Cancer Link. Front Endocrinol (Lausanne). 2015;6:77.
52. Dimri GP, Lee X, Basile G, Acosta M, Scott G, Roskelley C, et al. A biomarker that identifies senescent human cells in culture and in aging skin in vivo. Proc Natl Acad Sci U S A. 1995;92(20):9363-7.
53. Wagner W, Horn P, Castoldi M, Diehlmann A, Bork S, Saffrich R, et al. Replicative senescence of mesenchymal stem cells: a continuous and organized process. PLoS One. 2008;3(5):e2213.
54. Zhou S, Greenberger JS, Epperly MW, Goff JP, Adler C, Leboff MS, et al. Age-related intrinsic changes in human bone-marrow-derived mesenchymal stem cells and their differentiation to osteoblasts. Aging Cell. 2008;7(3):335-43.
55. Turinetto V, Vitale E, Giachino C. Senescence in Human Mesenchymal Stem Cells: Functional Changes and Implications in Stem Cell-Based Therapy. International journal of molecular sciences. 2016;17(7).
56. Wagner W, Bork S, Lepperdinger G, Joussen S, Ma N, Strunk D, et al. How to track cellular aging of mesenchymal stromal cells? Aging (Albany NY). 2010;2(4):224-30.
57. Bellayr IH, Catalano JG, Lababidi S, Yang AX, Lo Surdo JL, Bauer SR, et al. Gene markers of cellular aging in human multipotent stromal cells in culture. Stem Cell Res Ther. 2014;5(2):59.
58. Choi MR, In YH, Park J, Park T, Jung KH, Chai JC, et al. Genome-scale DNA methylation pattern profiling of human bone marrow mesenchymal stem cells in long-term culture. Exp Mol Med. 2012;44(8):503-12.
59. Koch CM, Joussen S, Schellenberg A, Lin Q, Zenke M, Wagner W. Monitoring of cellular senescence by DNA-methylation at specific CpG sites. Aging Cell. 2012;11(2):366-9.
60. Cmielova J, Havelek R, Kohlerova R, Soukup T, Bruckova L, Suchanek J, et al. The effect of ATM kinase inhibition on the initial response of human dental pulp and periodontal ligament mesenchymal stem cells to ionizing radiation. International Journal of Radiation Biology. 2013;89(7):501-11.
61. Havelek R, Soukup T, Cmielova J, Seifrtova M, Suchanek J, Vavrova J, et al. Ionizing radiation induces senescence and differentiation of human dental pulp stem cells. Folia Biol (Praha). 2013;59(5):188-97.
62. Muthna D, Soukup T, Vavrova J, Mokry J, Cmielova J, Visek B, et al. Irradiation of Adult Human Dental Pulp Stem Cells Provokes Activation of p53, Cell Cycle Arrest, and Senescence but Not Apoptosis. Stem Cells and Development. 2010;19(12):1855-62.
63. Manda K, Kavanagh JN, Buttler D, Prise KM, Hildebrandt G. Low dose effects of ionizing radiation on normal tissue stem cells. Mutat Res Rev Mutat Res. 2014.

64. Alessio N, Del Gaudio S, Capasso S, Di Bernardo G, Cappabianca S, Cipollaro M, et al. Low dose radiation induced senescence of human mesenchymal stromal cells and impaired the autophagy process. Oncotarget. 2015;6(10):8155-66.
65. Musilli S, Nicolas N, El Ali Z, Orellana-Moreno P, Grand C, Tack K, et al. DNA damage induced by Strontium-90 exposure at low concentrations in mesenchymal stromal cells: the functional consequences. Sci Rep. 2017;7:41580.
66. Pustovalova M, Astrelina capital Te C, Grekhova A, Vorobyeva N, Tsvetkova A, Blokhina T, et al. Residual gammaH2AX foci induced by low dose x-ray radiation in bone marrow mesenchymal stem cells do not cause accelerated senescence in the progeny of irradiated cells. Aging (Albany NY). 2017;9(11):2397-410.
67. Cho W, Kim ES, Kang CM, Ji YH, Kim JI, Park SJ, et al. Low-Dose Ionizing gamma-Radiation Promotes Proliferation of Human Mesenchymal Stem Cells and Maintains Their Stem Cell Characteristics. Tissue Eng Regen Med. 2017;14(4):421-32.
68. Su S, Zhou S, Wen C, Zou J, Zhang D, Geng J, et al. Evidence for Adaptive Response in a Molecular Epidemiological Study of the Inhabitants of a High Background-radiation Area of Yangjiang, China. Health Phys. 2018;115(2):227-34.
69. Eken A, Aydin A, Erdem O, Akay C, Sayal A, Somuncu I. Induced antioxidant activity in hospital staff occupationally exposed to ionizing radiation. Int J Radiat Biol. 2012;88(9):648-53.
70. Isoir M, Buard V, Gasser P, Voisin P, Lati E, Benderitter M. Human keratinocyte radiosensitivity is linked to redox modulation. J Dermatol Sci. 2006;41(1):55-65.
71. Vieira Dias J, Gloaguen C, Kereselidze D, Manens L, Tack K, Ebrahimian TG. Gamma Low-Dose-Rate Ionizing Radiation Stimulates Adaptive Functional and Molecular Response in Human Aortic Endothelial Cells in a Threshold-, Dose-, and Dose Rate-Dependent Manner. Dose Response. 2018;16(1):1559325818755238.
72. Jiang H, Wang H, De Ridder M. Targeting antioxidant enzymes as a radiosensitizing strategy. Cancer letters. 2018;438:154-64.
73. Lee HC, Kim DW, Jung KY, Park IC, Park MJ, Kim MS, et al. Increased expression of antioxidant enzymes in radioresistant variant from U251 human glioblastoma cell line. International Journal of Molecular Medicine. 2004;13(6):883-7.
74. Hardmeier R, Hoeger H, Fang-Kircher S, Khoschsorur A, Lubec G. Transcription and activity of antioxidant enzymes after ionizing irradiation in radiation-resistant and radiation-sensitive mice. Proc Natl Acad Sci U S A. 1997;94(14):7572-6.
75. Bravard A, Luccioni C, Moustacchi E, Rigaud O. Contribution of antioxidant enzymes to the adaptive response to ionizing radiation of human lymphoblasts. Int J Radiat Biol. 1999;75(5):639-45.
76. Bristow RG, Hill RP. Comparison between Invitro Radiosensitivity and Invivo Radioresponse in Murine Tumor-Cell Lines .2. Invivo Radioresponse Following Fractionated Treatment and Invitro Invivo Correlations. Int J Radiat Oncol. 1990;18(2):331-45.
77. McMahon SJ, Prise KM. Mechanistic Modelling of Radiation Responses. Cancers. 2019;11(2).
78. Stausbol-Gron B, Overgaard J. Relationship between tumour cell in vitro radiosensitivity and clinical outcome after curative radiotherapy for squamous cell carcinoma of the head and neck. Radiother Oncol. 1999;50(1):47-55.
79. Xu H, Lyu X, Yi M, Zhao W, Song Y, Wu K. Organoid technology and applications in cancer research. J Hematol Oncol. 2018;11(1):116.
80. Dutta D, Heo I, Clevers H. Disease Modeling in Stem Cell-Derived 3D Organoid Systems. Trends Mol Med. 2017;23(5):393-410.
81. Nagle PW, Hosper NA, Ploeg EM, van Goethem MJ, Brandenburg S, Langendijk JA, et al. The In Vitro Response of Tissue Stem Cells to Irradiation With Different Linear Energy Transfers. Int J Radiat Oncol Biol Phys. 2016;95(1):103-11.
82. Nagle PW, Plukker JTM, Muijs CT, van Luijk P, Coppes RP. Patient-derived tumor organoids for prediction of cancer treatment response. Semin Cancer Biol. 2018;53:258-64.
83. Bodgi L, Bahmad HF, Araji T, Al Choboq J, Bou-Gharios J, Cheaito K, et al. Assessing Radiosensitivity of Bladder Cancer in vitro: A 2D vs. 3D Approach. Frontiers in Oncology. 2019;9.
84. Huch M, Knoblich JA, Lutolf MP, Martinez-Arias A. The hope and the hype of organoid research. Development. 2017;144(6):938-41.

85. Tanaka J, Ogawa M, Hojo H, Kawashima Y, Mabuchi Y, Hata K, et al. Generation of orthotopically functional salivary gland from embryonic stem cells. Nat Commun. 2018;9(1):4216.
86. Hosseini ZF, Nelson DA, Moskwa N, Larsen M. Generating Embryonic Salivary Gland Organoids. Curr Protoc Cell Biol. 2018:e76.
87. Tschachojan V, Schroer H, Averbeck N, Mueller-Klieser W. Carbon ions and Xrays induce proinflammatory effects in 3D oral mucosa models with and without PBMCs. Oncol Rep. 2014;32(5):1820-8.
88. Nagle PW, Hosper NA, Barazzuol L, Jellema AL, Baanstra M, van Goethem MJ, et al. Lack of DNA Damage Response at Low Radiation Doses in Adult Stem Cells Contributes to Organ Dysfunction. Clin Cancer Res. 2018;24(24):6583-93.
89. Di Toro CG, Di Toro PA, Zieher LM, Guelman LR. Sensitivity of cerebellar glutathione system to neonatal ionizing radiation exposure. Neurotoxicology. 2007;28(3):555-61.
90. Vidyasagar MS, Kodali M, Prakash Saxena P, Upadhya D, Murali Krishna C, Vadhiraja BM, et al. Predictive and prognostic significance of glutathione levels and DNA damage in cervix cancer patients undergoing radiotherapy. Int J Radiat Oncol Biol Phys. 2010;78(2):343-9.
91. Patwardhan RS, Sharma D, Checker R, Thoh M, Sandur SK. Spatio-temporal changes in glutathione and thioredoxin redox couples during ionizing radiation-induced oxidative stress regulate tumor radio-resistance. Free Radic Res. 2015;49(10):1218-32.
92. Kojima S, Ishida H, Takahashi M, Yamaoka K. Elevation of glutathione induced by low-dose gamma rays and its involvement in increased natural killer activity. Radiat Res. 2002;157(3):275-80.
93. Shimizu T, Iwanaga M, Yasunaga A, Urata Y, Goto S, Shibata S, et al. Protective role of glutathione synthesis on radiation-induced DNA damage in rabbit brain. Cell Mol Neurobiol. 1998;18(3):299-310.
94. Ivanenko GF, Burlakova EB. [Response of the glutathione system to chronic irradiation of human population after the Chernobyl accident]. Izv Akad Nauk Ser Biol. 2005(1):9-17.
95. Chatterjee A. Reduced glutathione: a radioprotector or a modulator of DNA-repair activity? Nutrients. 2013;5(2):525-42.
96. Powis G, Montfort WR. Properties and biological activities of thioredoxins. Annu Rev Bioph Biom. 2001;30:421-55.
97. Woolston CM, Storr SJ, Ellis IO, Morgan DA, Martin SG. Expression of thioredoxin system and related peroxiredoxin proteins is associated with clinical outcome in radiotherapy treated early stage breast cancer. Radiother Oncol. 2011;100(2):308-13.
98. Selenius M, Hedman M, Brodin D, Gandin V, Rigobello MP, Flygare J, et al. Effects of redox modulation by inhibition of thioredoxin reductase on radiosensitivity and gene expression. J Cell Mol Med. 2012;16(7):1593-605.
99. Zhang Y, Martin SG. Redox proteins and radiotherapy. Clinical oncology. 2014;26(5):289-300.
100. Chen WC, McBride WH, Iwamoto KS, Barber CL, Wang CC, Oh YT, et al. Induction of radioprotective peroxiredoxin-I by ionizing irradiation. J Neurosci Res. 2002;70(6):794-8.
101. Hoshi Y, Tanooka H, Miyazaki K, Wakasugi H. Induction of thioredoxin in human lymphocytes with low-dose ionizing radiation. Biochim Biophys Acta. 1997;1359(1):65-70.
102. Baselet B, Sonveaux P, Baatout S, Aerts A. Pathological effects of ionizing radiation: endothelial activation and dysfunction. Cell Mol Life Sci. 2019;76(4):699-728.
103. Nishad S, Ghosh A. Dynamic changes in the proteome of human peripheral blood mononuclear cells with low dose ionizing radiation. Mutat Res Genet Toxicol Environ Mutagen. 2016;797:9-20.
104. Leung KS, Fong BM. LC-MS/MS in the routine clinical laboratory: has its time come? Anal Bioanal Chem. 2014;406(9-10):2289-301.
105. Jelonek K, Wojakowska A, Marczak L, Muer A, Tinhofer-Keilholz I, Lysek-Gladysinska M, et al. Ionizing radiation affects protein composition of exosomes secreted in vitro from head and neck squamous cell carcinoma. Acta Biochim Pol. 2015;62(2):265-72.
106. Matsuda S, Ikura T, Matsuda T. Absolute quantification of gammaH2AX using liquid chromatography-triple quadrupole tandem mass spectrometry. Anal Bioanal Chem. 2015;407(18):5521-7.

107. Matsuda S, Furuya K, Ikura M, Matsuda T, Ikura T. Absolute quantification of acetylation and phosphorylation of the histone variant H2AX upon ionizing radiation reveals distinct cellular responses in two cancer cell lines. Radiat Environ Biophys. 2015;54(4):403-11.
108. Sivadasan P, Gupta MK, Sathe GJ, Balakrishnan L, Palit P, Gowda H, et al. Human salivary proteome--a resource of potential biomarkers for oral cancer. J Proteomics. 2015;127(Pt A):89-95.
109. Moore HD, Ivey RG, Voytovich UJ, Lin C, Stirewalt DL, Pogosova-Agadjanyan EL, et al. The human salivary proteome is radiation responsive. Radiat Res. 2014;181(5):521-30.
110. Behjati S, Tarpey PS. What is next generation sequencing? Arch Dis Child Educ Pract Ed. 2013;98(6):236-8.
111. Nath N, Esche J, Muller J, Jensen LR, Port M, Stanke M, et al. Exome Sequencing Discloses Ionizing-radiation-induced DNA Variants in the Genome of Human Gingiva Fibroblasts. Health Phys. 2018;115(1):151-60.
112. Efanov AA, Brenner AV, Bogdanova TI, Kelly LM, Liu PY, Little MP, et al. Investigation of the Relationship Between Radiation Dose and Gene Mutations and Fusions in Post-Chernobyl Thyroid Cancer. Jnci-J Natl Cancer I. 2018;110(4):371-8.
113. Chaudhry MA, Omaruddin RA, Brumbaugh CD, Tariq MA, Pourmand N. Identification of radiation-induced microRNA transcriptome by next-generation massively parallel sequencing. J Radiat Res. 2013;54(5):808-22.
114. Chaudhry MA, Omaruddin RA, Kreger B, de Toledo SM, Azzam EI. Micro RNA responses to chronic or acute exposures to low dose ionizing radiation. Mol Biol Rep. 2012;39(7):7549-58.
115. Pernot E, Cardis E, Badie C. Usefulness of saliva samples for biomarker studies in radiation research. Cancer Epidemiol Biomarkers Prev. 2014;23(12):2673-80.
116. Nunes LA, Mussavira S, Bindhu OS. Clinical and diagnostic utility of saliva as a non-invasive diagnostic fluid: a systematic review. Biochem Med (Zagreb). 2015;25(2):177-92.
117. Malamud D. Saliva as a diagnostic fluid. Dent Clin North Am. 2011;55(1):159-78.
118. Hall J, Jeggo PA, West C, Gomolka M, Quintens R, Badie C, et al. Ionizing radiation biomarkers in epidemiological studies - An update. Mutat Res. 2017;771:59-84.
119. Bowen BP, Northen TR. Dealing with the unknown: metabolomics and metabolite atlases. J Am Soc Mass Spectrom. 2010;21(9):1471-6.
120. Cohen MD. ALARA, image gently and CT-induced cancer. Pediatr Radiol. 2015;45(4):465-70.
121. Leung RS. Radiation Protection of the Child from Diagnostic Imaging. Curr Pediatr Rev. 2015;11(4):235-42.
122. Rehani MM. Radiological protection in computed tomography and cone beam computed tomography. Ann ICRP. 2015;44(1 Suppl):229-35.
123. Tsapaki V. Radiation protection in dental radiology - Recent advances and future directions. Phys Med. 2017;44:222-6.
124. Oenning AC, Pauwels R, Stratis A, De Faria Vasconcelos K, Tijskens E, De Grauwe A, et al. Halve the dose while maintaining image quality in paediatric Cone Beam CT. Sci Rep. 2019;9(1):5521.
125. Giardi MT, Touloupakis E, Bertolotto D, Mascetti G. Preventive or potential therapeutic value of nutraceuticals against ionizing radiation-induced oxidative stress in exposed subjects and frequent fliers. International journal of molecular sciences. 2013;14(8):17168-92.
126. Greenberger J, Kagan V, Bayir H, Wipf P, Epperly M. Antioxidant Approaches to Management of Ionizing Irradiation Injury. Antioxidants (Basel). 2015;4(1):82-101.
127. Weiss JF, Landauer MR. Protection against ionizing radiation by antioxidant nutrients and phytochemicals. Toxicology. 2003;189(1-2):1-20.
128. Yahyapour R, Shabeeb D, Cheki M, Musa AE, Farhood B, Rezaeyan A, et al. Radiation Protection and Mitigation by Natural Antioxidants and Flavonoids: Implications to Radiotherapy and Radiation Disasters. Curr Mol Pharmacol. 2018;11(4):285-304.
129. Szejk M, Kolodziejczyk-Czepas J, Zbikowska HM. Radioprotectors in radiotherapy - advances in the potential application of phytochemicals. Postepy Hig Med Dosw (Online). 2016;70(0):722-34.

130. Mishra KN, Moftah BA, Alsbeih GA. Appraisal of mechanisms of radioprotection and therapeutic approaches of radiation countermeasures. Biomed Pharmacother. 2018;106:610-7.

Summary

One of the greatest challenges in radiation protection today is determining the detrimental effects of exposure to low doses of ionizing radiation (IR), i.e. doses lower than 100 mGy. Despite scientific but also public concerns related to IR doses used in medical imaging, which are well below 100 mGy, the number of radiological examinations continues to increase. This concern is even more important in pediatric patients, since it is known that they are more radiosensitive than adults. Currently some epidemiological data, although controversial, links computed tomography examination at a young age to increased cancer risk later in life. However, no such data exists for cone-beam computed tomography (CBCT).

The aim of this thesis was to investigate if exposure to low doses of X-rays, more specifically CBCT examinations, induces DNA damage and oxidative damage. Adults and children were studied to investigate age-related differences. DNA damage repair kinetics were studied *in vitro* in dental stem cells and *ex vivo* in buccal mucosal cells (BMCs). Oxidative damage was monitored in saliva samples. Both BMCs and saliva samples were collected from patients before and after CBCT examination.

After validating the *ex vivo* set-up (**Chapter 3**), we conducted a prospective clinical trial in children and adults who were referred for CBCT examination (**Chapter 4**). In both children and adults, no statistically significant induction of DNA double strand breaks (DSBs) was observed in BMCs gathered 30 minutes and 24 hours after CBCT examination. However, we did observe a significant increase in the amount of salivary 8-oxo-7,8-dihydro-2'-deoxyguanosine (8-oxo-dG) in children 30 minutes after CBCT examination, but not in adults. No statistical difference was observed between children and adults 30 minutes after CBCT examination. Additionally, a significant increase in salivary total antioxidant capacity was observed in children, whereas in adults a significant decrease was seen. This indicates that children and adults might react differently to CBCT examinations. Interestingly, the observed changes were not linked to the radiation dose received by the patient.

In vitro exposure to low IR doses of dental stem cells (**Chapter 5**) causes a significant increase in DNA DSBs 30 minutes after irradiation. These DSBs are repaired 24 hours after irradiation. The amount of DSBs increases linearly with increasing radiation dose in the dose range of 5–100 mGy. This significant induction of DSBs did not seem to affect the stem cells since no significant cell cycle changes were observed. However, a significant dose-dependent decrease in the number of quiescent cells was observed as soon as 1 hour after irradiation. Furthermore, no premature senescence was induced in dental stem cells following low dose irradiation.

Finally, preliminary *ex vivo* data (**Chapter 6**) indicate that the salivary activity of the antioxidants superoxide dismutase and catalase increases significantly 30 minutes after CBCT examination in children. This indicates that the oxidative damage is countered by endogenous antioxidants. However, when

looking at gene expression level in BMCs, a significant decrease was observed for *GPx1* gene expression 48 hours after CBCT examination in both children and adults. Furthermore, in children a significant decrease in *SOD1* gene expression was observed 30 minutes and 48 hours after CBCT examination.

In conclusion, our data indicates that tough low doses of IR induce DNA DSBs *in vitro*, this does not occur after CBCT examination in BMCs in children and adults. However, a significant increase in oxidative damage and antioxidant response was observed in children, but not in adults, suggesting that age does play a role in the response to low doses of IR. However, no conclusion could be drawn for long-term effects based on these results. Further research will have to show if adverse effects occur on the long term. Therefore, it is recommended to strictly adhere to radiation protection principles and to prevent unnecessary exposure to any form of IR.

Samenvatting

Eén van de grootste uitdagingen in stralingsbescherming vandaag de dag is het bepalen van negatieve effecten van blootstelling aan lage doses ioniserende straling, namelijk stralingsdoses lager van 100 mGy. Ondanks bedenkingen van wetenschappers, maar ook van het grote publiek, omtrent stralingsdoses die gebruikt worden bij medische beeldvorming, en die ver onder de 100 mGy liggen, blijft het aantal radiologische onderzoeken toenemen. Deze bezorgdheid is nog belangrijker als het om kinderen gaat, waarvan geweten is dat zij gevoeliger zijn dan volwassenen voor de effecten van straling. Momenteel zijn er (controversiële) epidemiologische data die een verband aantonen tussen *computed tomography* scans op jonge leeftijd en een verhoogd kankerrisico op latere leeftijd. Dergelijke data zijn echter niet voorhanden als het gaat om *cone-beam computed tomography* (CBCT).

Het doel van deze thesis was te onderzoeken of blootstelling aan lage stralingsdoses, zoals gebruikt bij CBCT-scans, DNA-schade en oxidatieve schade kan veroorzaken. Zowel kinderen als volwassenen werden bestudeerd om leeftijdsafhankelijke verschillen op te sporen. DNA-schade en de herstelsnelheid ervan werden *in vitro* bestudeerd in dentale stamcellen en *ex vivo* in wangepitheel cellen (BMCs). Oxidatieve schade werd specifiek onderzocht in speekselstalen. Zowel BMCs als speekselstalen werden verzameld van patiënten voor en na een CBCT-scan.

Nadat de *ex vivo* set-up geoptimaliseerd en gevalideerd werd (**Hoofdstuk 3**), werd een prospectieve studie uitgevoerd bij kinderen en volwassenen die een CBCT-scan ondergingen (**Hoofdstuk 4**). Noch bij kinderen, noch bij volwassenen werden DNA dubbelstrengsbreuken (DSBs) geobserveerd in BMCs 30 minuten en 24 uur na een CBCT-scan. Er werd echter een significante toename van 8-oxo-7,8-dihydro-2'-deoxyguanosine geobserveerd in de speekselstalen van kinderen 30 minuten na een CBCT-scan. Bij volwassenen werd dit echter niet waargenomen. Tussen kinderen en volwassenen werd voor deze merker geen verschil gevonden 30 minuten na de scan. Wel werd er bij kinderen een significante stijging waargenomen in de totale antioxidant capaciteit van speeksel, terwijl er bij volwassenen een significante daling werd vastgesteld. Deze observatie toont aan dat kinderen en volwassenen verschillend kunnen reageren op een CBCT-scan. De waargenomen veranderingen vertoonden echter geen relatie met de stralingsdosis waaraan de patiënt werd blootgesteld.

In vitro blootstelling van dentale stamcellen (**Hoofdstuk 5**) aan lage stralingsdoses resulteerde in een significante toename van het aantal DNA DSBs 30 minuten na stralingsblootstelling. De DSBs waren volledig hersteld 24 uur na stralingsblootstelling. De hoeveelheid DSBs nam lineair toe met de toegediende stralingsdosis in de range van 5 tot 100 mGy. Deze significante toename van DSBs lijkt de stamcellen verder niet te beïnvloeden aangezien er geen significante veranderingen in de celcyclus waargenomen werden. Er werd echter wel een significante dosisafhankelijke daling van het aantal quiëscente cellen

geobserveerd., dit al vanaf 1 uur na stralingsblootstelling. Verder werd er geen vervroegde senescentie waargenomen na blootstelling aan lage stralingsdoses.

Ten slotte tonen preliminaire *ex vivo* data (**Hoofdstuk 6**) aan dat de activiteit van de antioxidanten superoxide dismutase en catalase in speekselstalen toeneemt 30 minuten na een CBCT-scan bij kinderen. Dit wijst er op dat de oxidatieve schade tegengegaan wordt door endogene antioxidanten. Genexpressie analyse van deze antioxidanten in BMCs toont aan dat de genexpressie *GPx1* significant daalt 48 uur na een CBCT-scan zowel bij kinderen als volwassenen. Daarenboven werd bij kinderen ook een significante daling in *SOD1* genexpressie vastgesteld 30 minuten en 48 uur na een CBCT-scan.

We kunnen concluderen dat hoewel lage stralingsdoses DNA DSBs veroorzaken in dentale stamcellen *in vitro*, een CBCT-scan geen DSBs veroorzaakt in BMCs, noch in kinderen, noch in volwassenen. Er vond echter een significante stijging plaats van oxidatieve schade en van de antioxidant capaciteit in speekselstalen van kinderen 30 minuten na een CBCT-scan. In volwassenen werd dit niet waargenomen. Dit suggereert dat leeftijd op moment van blootstelling aan straling een invloed heeft op de reactie die deze straling veroorzaakt. Momenteel kan er echter geen conclusie getrokken worden over de lange termijn effecten van stralingsblootstelling ten gevolge van een CBCT-scan. Verder onderzoek zal moeten uitwijzen of er al dan niet nadelige effecten optreden op lange termijn. Daarom wordt er ten zeerste aangeraden om zich te houden aan de principes van stralingsbescherming, en ook om onnodige stralingsblootstelling zo veel mogelijk te vermijden.

Appendices

Appendix 1: Overview of the biological effects detected in patients following computed tomography

Assay	Gender	Age (years)	Gray: Absorbed dose Sievert: Effective dose	Time of sampling	Tissue examined	Tissue used	Biological effects	Reference
Dicentric/ring chromosomes	5 patients (gender not specified)	Adults (age not specified)	'Whole body dose'	NA	NA	NA	Dicentrics and rings significantly increased	Weber *et al.* (1995) [1]
	5 girls 5 boys	0.4 - 15	Range: 1.2 mGy – 31.3 mGy	Before and 20 min after CT	Thorax (8x) Abdomen (2x)	PBLs*	Dicentrics significantly increased; children younger than 9 are more sensitive than children between 10-15 years old	Stephan *et al*. (2007)[2]t
	7 females 3 males	62 - 81	Range: 619.1 mGy•cm – 5501.3 mGy•cm	Before CT and 2-28 days after CT	Chest (each patient) Cervix (3x) Abdomen (6x) Pelvis (6x)		Dicentrics significantly increased; no dose Response	Abe *et al.* (2015)[3]
	10 females 17 males	38.3 ± 16.7	Range: 1.18 mGy – 63.36 mGy	Before CT and 2-3h after CT	Abdomen (2x) Thorax (5x) Brain (20x)		Dicentrics significantly increased	Kanagaraj *et al.* (2015)[4]
	15 females 45 males	30 - 83	20.6 ± 9.6 mSv	Before CT and 15 min	Heart (39x) Liver (21x)		Dicentrics and rings significantly increased	Shi *et al.* (2018)[5]

				and >16h after CT				
Micronucleus Assay	10 females 17 males	38.3 ± 16.7	Range: 1.18 mGy – 63.36 mGy	Before CT and 2-3h after CT	Abdomen (2x) Thorax (5x) Brain (20x)		MN frequency significantly increased	Kanagaraj *et al.* (2015)[4]
	13 girls 14 boys	0 – 18 months	Range: 2.2 mGy – 126.1 mGy	2h before and 48h after CT	Abdomen/pelvis (5x) Brain/head (9x) Heart (3x) Chest (12x)	Reticulocytes	No change in MN frequency if there was no prior CT exposure. If there was prior CT exposure, there was a significant increase in MN frequency	Khattab *et al*. (2017)[6]
γH2AX assay	23 patients	Adults (age not specified)	Range: 157 - 1,514 mGy•cm	30 min up to 1 day after CT	Abdomen Head (numbers not specified)	PBLs	Increased number of γH2AX foci, which was linearly correlated with the dose-length product	Lobrich *et al*. (2005)[7]
	8 females 5 males	57 - 74	16.4 mGy (95% confidence interval: 15.1 - 17.7)	Before and 5 to 30 min after CT	Chest (1x) Whole body (12x)	PBMCs**	Increased number of γH2AX foci after scan.	Rothkamm *et al.* (2007)[8]
	5 females (3 with CM***) 22 males (10 with CM)	19 - 84	Range: 10.3 mGy – 13.8 mGy	Before, 0.5h, 1h, 2.5h and 5h after CT	Chest (26x) Chest+Abdomen (1x)	PBLs	Increase in the number of γH2AX foci immediately after CT. Patients examined using iopromide (300 mg of iodine per milliliter) (=CM) show	Grudzenski *et al*. (2009)[9]

							30% higher γH2AX foci compared to patients examined without CM.	
	12 females 22 males	26 - 82	Range: 2.0 mGy – 44.9 mGy	Before and 30 min after CT	Heart (all patients)		Increased number of γH2AX foci and correlation with dose length product.	Kuefner *et al*. (2010a)[10]
	8 females 28 males	26 - 78	Range: 2.1 mSv – 23.8 mSv	Before and 30 min after CT	Heart (all patients)		Increased number of γH2AX foci and correlation with dose length product.	Kuefner *et al*. (2010b)[11]
	10 females (4 with CM) 20 males (11 with CM)	25 - 87	Range: 85 mGy•cm – 900 mGy•cm	Before, 5 min and 1, 2 and 24 h after the CT	Abdomen (all patients)		Increased number of γH2AX foci. γH2AX foci levels were 58% higher in patients undergoing contrast-enhanced CT (iopromide 370 mg of iodine per milliliter) compared with those undergoing unenhanced CT. After 24h the number of foci returned to baseline levels.	Pathe *et al*. (2011)[12]
	30 females 39 males	18 - 85	Range: 2.2 mSv – 82.0 mSv	Before and 5 min after contrast-enhanced CT	Vascular (20x) Lungs (16x) Abdomen (21x)	T lymphocytes	Increased number of γH2AX foci. No effect of contrast material (not specified) was observed.	Beels *et al.* (2012)[13]
	19 females 47 males	26 - 82	Range: 1.0 mSv – 23.8 mSv	Before and 30 min after CT angiography	Heart (all patients)	PBLs	Increased number of γH2AX foci and a significant correlation with estimated effective dose was observed.	Brand *et al*. (2012)[14]ra

	13 females 15 males	60.4 ± 11.0	5.1 mSv ± 2.5 mSv	Before, 1h and 24 h after CT	Heart (all patients)		Increased number of γH2AX foci and excellent correlation between the biological effects and the estimated radiation doses. After 24h the number of foci returned to baseline levels.	Geisel *et al.* (2012)[15]
	11 females 22 males	29 - 81	Range: 311 – 1751 mGy•cm	Before and at various time points following 18F-Fluorodeoxyglucose application and up to 24 h after CT scan	Whole body (all patients)		Increased number of γH2AX foci and a significant correlation with dose length product was observed.	May *et al*. (2012)[16]
	3 females 4 males	44 - 74	Range: 13.3 mSv – 25.9 mSv	Before and 15 min after CT	Thorax and/or abdomen (number not specified)		Increased number of γH2AX foci	Kuefner *et al*. (2013)[17]
	3 boys	0.25 – 1.75	Range: 1.57 mSv – 2.86 mSv	Before and 1h after CT	Not specified		Increased number of γH2AX foci	Halm *et al.* (2014)[18]
	12 females 45 males	56 - 79	Range: 18.8 mSv – 48.8 mSv	Before, 5, 15, 30, 60, and 120 minutes; 6, 24, and 48 hours;	Heart (all patients)		Increased number of γH2AX foci.	Nguyen *et al.* (2015)[19]

				1 week; and 1 month after CT angiography				
	149 females (104 with CM) 96 males (75 with CM)	19 - 89	CM: 301 ± 120 mGy•cm No CM: 342 ± 116 mGy•cm	Before and immediately after CT	Chest (all patients)		Increased number of γH2AX foci and dose-enhancing effect of iodine containing contrast material was observed.	Piechowiak *et al.* (2015)[20]
	14 girls 37 boys	0.1 – 12.2	Range: 0.14 mGy – 2.84 mGy	Before and 5 min after CT	Chest (41x) Abdomen (10x)	T lymphocytes	Increased number of γH2AX foci, exposure to multiple CT scans causes more foci as compared to single scan	Vandevoorde *et al.* (2015)[21]
	5 females 40 males	30 - 76	138.2 ± 62.5 mGy (size-specific dose estimates)	Before, 15 min and a few days after CT	Heart (all patients)	PBLs	Increased number of γH2AX foci and a significant correlation with dose length product was observed.	Fukumoto *et al.* (2017)[22]
	27 females (15 with CM) 43 males (33 with CM)	29 - 80	CM: 294.3 ± 59.2 mGy•cm No CM: 275.8 ± 40.7 mGy•cm	Before, immediately after CT/CT urography and 8 min after the injection of CM	Urography (48x) Abdomen (22x)		Increased number of γH2AX foci. And dose-enhancing effect of contrast material (33.3 mg of iodine in 90 mL, Ultravist 370) was observed.	Wang *et al.* (2017)[23]

	20 females 40 males	17 - 75	Range of averages : 0 – 272.71 mSv	Within 1h after CT	Not specified		Increased number of γH2AX foci was found in cases versus control, the most significant DNA damage amongst cases was observed in cases with multiple CT scans.	Khan *et al.* (2018)[24]
*: Peripheral blood lymphocytes = PBLs; **: peripheral blood mononuclear cells = PBMCs; ***: contrast medium = CM								

1. Weber J, Scheid W, Traut H. Biological dosimetry after extensive diagnostic x-ray exposure. Health Phys. 1995;68(2):266-9.
2. Stephan G, Schneider K, Panzer W, Walsh L, Oestreicher U. Enhanced yield of chromosome aberrations after CT examinations in paediatric patients. Int J Radiat Biol. 2007;83(5):281-7.
3. Abe Y, Miura T, Yoshida MA, Ujiie R, Kurosu Y, Kato N, et al. Increase in dicentric chromosome formation after a single CT scan in adults. Sci Rep. 2015;5:13882.
4. Kanagaraj K, Abdul Syed Basheerudeen S, Tamizh Selvan G, Jose MT, Ozhimuthu A, Panneer Selvam S, et al. Assessment of dose and DNA damages in individuals exposed to low dose and low dose rate ionizing radiations during computed tomography imaging. Mutat Res Genet Toxicol Environ Mutagen. 2015;789-790:1-6.
5. Shi L, Fujioka K, Sakurai-Ozato N, Fukumoto W, Satoh K, Sun J, et al. Chromosomal Abnormalities in Human Lymphocytes after Computed Tomography Scan Procedure. Radiat Res. 2018;190(4):424-32.
6. Khattab M, Walker DM, Albertini RJ, Nicklas JA, Lundblad LKA, Vacek PM, et al. Frequencies of micronucleated reticulocytes, a dosimeter of DNA double strand breaks, in infants receiving computed tomography or cardiac catheterization. Mutat Res-Gen Tox En. 2017;820:8-18.
7. Lobrich M, Rief N, Kuhne M, Heckmann M, Fleckenstein J, Rube C, et al. In vivo formation and repair of DNA double-strand breaks after computed tomography examinations. Proc Natl Acad Sci U S A. 2005;102(25):8984-9.
8. Rothkamm K, Balroop S, Shekhdar J, Fernie P, Goh V. Leukocyte DNA damage after multi-detector row CT: a quantitative biomarker of low-level radiation exposure. Radiology. 2007;242(1):244-51.
9. Grudzenski S, Kuefner MA, Heckmann MB, Uder M, Lobrich M. Contrast medium-enhanced radiation damage caused by CT examinations. Radiology. 2009;253(3):706-14.
10. Kuefner MA, Hinkmann FM, Alibek S, Azoulay S, Anders K, Kalender WA, et al. Reduction of X-ray induced DNA double-strand breaks in blood lymphocytes during coronary CT angiography using high-pitch spiral data acquisition with prospective ECG-triggering. Invest Radiol. 2010;45(4):182-7.
11. Kuefner MA, Grudzenski S, Hamann J, Achenbach S, Lell M, Anders K, et al. Effect of CT scan protocols on x-ray-induced DNA double-strand breaks in blood lymphocytes of patients undergoing coronary CT angiography. European radiology. 2010;20(12):2917-24.
12. Pathe C, Eble K, Schmitz-Beuting D, Keil B, Kaestner B, Voelker M, et al. The presence of iodinated contrast agents amplifies DNA radiation damage in computed tomography. Contrast Media Mol Imaging. 2011;6(6):507-13.
13. Beels L, Bacher K, Smeets P, Verstraete K, Vral A, Thierens H. Dose-length product of scanners correlates with DNA damage in patients undergoing contrast CT. European journal of radiology. 2012;81(7):1495-9.

14. Brand M, Sommer M, Achenbach S, Anders K, Lell M, Lobrich M, et al. X-ray induced DNA double-strand breaks in coronary CT angiography: comparison of sequential, low-pitch helical and high-pitch helical data acquisition. European journal of radiology. 2012;81(3):e357-62.
15. Geisel D, Zimmermann E, Rief M, Greupner J, Laule M, Knebel F, et al. DNA double-strand breaks as potential indicators for the biological effects of ionising radiation exposure from cardiac CT and conventional coronary angiography: a randomised, controlled study. European radiology. 2012;22(8):1641-50.
16. May MS, Brand M, Wuest W, Anders K, Kuwert T, Prante O, et al. Induction and repair of DNA double-strand breaks in blood lymphocytes of patients undergoing (1)(8)F-FDG PET/CT examinations. Eur J Nucl Med Mol Imaging. 2012;39(11):1712-9.
17. Kuefner MA, Brand M, Engert C, Kappey H, Uder M, Distel LV. The effect of calyculin A on the dephosphorylation of the histone gamma-H2AX after formation of X-ray-induced DNA double-strand breaks in human blood lymphocytes. Int J Radiat Biol. 2013;89(6):424-32.
18. Halm BM, Franke AA, Lai JF, Turner HC, Brenner DJ, Zohrabian VM, et al. gamma-H2AX foci are increased in lymphocytes in vivo in young children 1 h after very low-dose X-irradiation: a pilot study. Pediatr Radiol. 2014;44(10):1310-7.
19. Nguyen PK, Lee WH, Li YF, Hong WX, Hu S, Chan C, et al. Assessment of the Radiation Effects of Cardiac CT Angiography Using Protein and Genetic Biomarkers. JACC Cardiovasc Imaging. 2015;8(8):873-84.
20. Piechowiak EI, Peter JF, Kleb B, Klose KJ, Heverhagen JT. Intravenous Iodinated Contrast Agents Amplify DNA Radiation Damage at CT. Radiology. 2015;275(3):692-7.
21. Vandevoorde C, Franck C, Bacher K, Breysem L, Smet MH, Ernst C, et al. gamma-H2AX foci as in vivo effect biomarker in children emphasize the importance to minimize x-ray doses in paediatric CT imaging. European radiology. 2015;25(3):800-11.
22. Fukumoto W, Ishida M, Sakai C, Tashiro S, Ishida T, Nakano Y, et al. DNA damage in lymphocytes induced by cardiac CT and comparison with physical exposure parameters. European radiology. 2017;27(4):1660-6.
23. Wang L, Li Q, Wang M, Hao GY, Jie-Bao, Hu S, et al. Enhanced radiation damage caused by iodinated contrast agents during CT examination. European journal of radiology. 2017;92:72-7.
24. Khan K, Tewari S, Awasthi NP, Mishra SP, Agarwal GR, Rastogi M, et al. Flow cytometric detection of gamma-H2AX to evaluate DNA damage by low dose diagnostic irradiation. Med Hypotheses. 2018;115:22-8.

Appendix 2: Overview of the biological effects detected in patients following X-ray radiography

Assay	Gender	Age (years)	Dose	Time of sampling	Tissue examined	Tissue used	Biological effects	References
Micronucleus assay	24 females 7 males	24 ± 1.023	21.4 µSv	Before and 10 days after examination	Oral cavity	Exfoliated oral mucosa cells	No induction of MN, and cytotoxicity (pyknosis, karyolysis). Significant induction of karyorrhexis.	Cerqueira *et al.* (2004)[1]
	9 girls 8 boys	7.70 ± 1.50	0.08 Roentgen* (Entrance dose)					Angelieri *et al.* (2007)[2]
	42 males	18 - 40	0.057 mSv (Average dose)			Cells of the lateral border of the tongue	No induction of MN, but increased cytotoxicity (pyknosis, karyolysis, karyorrhexis). The number of karyorrhexis and binucleated cells was greater after multiple X-rays	Da Silva *et al.* (2007)[3]
	20 females 12 males	24 - 73	Not mentioned	Before and 10 ± 2 days after examination		Exfoliated oral mucosa cells	No induction of MN, but increased cytotoxicity (pyknosis, karyolysis, karyorrhexis).	Popova *et al.* (2007)[4]
	31 females 9 males	26 ± 9.18	21.4 µSv	Before and 10 days after examination		Keratinized gingival cells	Significant induction of MN, and cytotoxicity (pyknosis, karyolysis, karyorrhexis)	Cerqueira *et al.* (2008)[5]

	28 females 11 males	39.6 ± 13	0.08 Roentgen (Entrance dose)			Exfoliated oral mucosa cells	No induction of MN, but increased cytotoxicity (pyknosis, karyolysis, karyorrhexis)	Ribeiro and Angelieri (2008)[6]
	6 females 11 males 9 girls 8 boys	39.6 ± 5.4 7.7 ± 1.5	0.08 Roentgen (Entrance dose)				Both in adults and children, no induction of MN, but increased cytotoxicity (pyknosis, karyolysis, karyorrhexis)	Ribeiro *et al.* (2008)[7]
	12 females 20 males	Mean: 38.65	0.08 Roentgen (Entrance dose)				No induction of MN, but increased cytotoxicity (pyknosis, karyolysis, karyorrhexis)	Angelieri *et al.* (2010a)[8]
	12 females 6 males	14.2 ± 1.4	Not mentioned					Angelieri *et al.* (2010b)[9]
	20 patients (gender not specified)	Children (Age not specified)	Not available	Not mentioned				El-Ashiry *et al.* (2010)[10]
	13 girls 7 boys	4 - 14	Range: 0.13 – 0.29 (entrance dose)	Before and 30 min after examination	Chest	Peripheral blood lymphocytes	Significant induction of MN	Gajski *et al.* (2011)[11]
	15 females 15 males	20 - 23	0.046 Roentgen (Entrance dose)	Before and 10 days after examination	Oral cavity	Exfoliated oral mucosa cells	No induction of MN, but increased cytotoxicity (pyknosis, karyolysis, karyorrhexis)	Ribeiro *et al.* (2011)[12]
	10 females 15 males	11.2 ± 1.4	Not available					Lorenzoni *et al.* (2012)[13]
	80 patients	Adults (age not specified)	Not available				No induction of MN in buccal cells.	Sheikh *et al.* (2012)[14]

							Significant induction of MN in gingival epithelial cells.	
	90 patients	Adults (age not specified)	Not available				No induction of MN, but increased cytotoxicity (pyknosis, karyolysis, karyorrhexis)	Thomas *et al.* (2012)[15]
	41 females 19 males	27.63 ± 10.93	0.325 mGy/sec (no exact dose mentioned)				Significant induction of MN	Waingade and Medikeri (2012)[16]
	32 females 21 males	25.21 ± 12.67	0.325 mGy/sec (no exact dose mentioned)			Exfoliated oral mucosa cells and keratinized gingiva cells	Significant induction of MN in oral mucosa cells and a significant correlation was observed between the age of the subjects and number of MN	Arora *et al.* (2014)[17]
	20 patients (gender not specified)	Children (age not specified)	21.4 mSv (average dose)			Exfoliated oral mucosa cells	No induction of MN, but increased cytotoxicity (pyknosis, karyolysis, karyorrhexis)	Agarwal *et al.* (2015)[18]
	20 girls 20 boys	7 - 12	Not mentioned	Before and 10 ± 2 days after examination			Significant induction of MN	Preethi *et al.* (2016)[19]
	70 females 28 males	23.63 ± 6.64	Range: 0.18 mGy – 3.54 mGy	Before and 10 days after examination			Significant induction of MN, and cytotoxicity (pyknosis, karyolysis, karyorrhexis) above 1 mGy. Below 1 mGy, only significant	Li *et al.* (2018)[20]

							induction of karyorrhexis.	
Comet assay	14 girls 6 boys	5 - 14	Range: 0 – 0.29	Before and 30 min after examination	Chest	Peripheral blood lymphocytes	Significant increase of DNA damage following radiography.	Milkovic *et al.* (2009)[21]
	20 patients (gender not specified)	Adults (age not specified)	Not mentioned	Before and 30 min or 24h after examination	Oral cavity	Exfoliated oral mucosa cells	Significant increase of DNA damage 30 min following radiography, but not after 24h	Yanuaryska *et al.* (2018)[22]
γH2AX assay	45 females 55 males	20 - 77	23.4 mGy (average dose)	Before and 20 min after examination	Oral cavity	Exfoliated oral mucosa cells	Increased number of γH2AX foci.	Yoon *et al.* (2009)[23]
	20 females	39 - 71	Range: 7.1 – 41.1	Before and 5 min after examination	Breasts	Systemic blood lymphocytes		Schwab *et al.* (2013)[24]

*: 1 Roentgen (R) = 2.58 x 10^{-4} C/kg

1. Cerqueira EM, Gomes-Filho IS, Trindade S, Lopes MA, Passos JS, Machado-Santelli GM. Genetic damage in exfoliated cells from oral mucosa of individuals exposed to X-rays during panoramic dental radiographies. Mutat Res. 2004;562(1-2):111-7.
2. Angelieri F, de Oliveira GR, Sannomiya EK, Ribeiro DA. DNA damage and cellular death in oral mucosa cells of children who have undergone panoramic dental radiography. Pediatr Radiol. 2007;37(6):561-5.
3. da Silva AE, Rados PV, da Silva Lauxen I, Gedoz L, Villarinho EA, Fontanella V. Nuclear changes in tongue epithelial cells following panoramic radiography. Mutat Res. 2007;632(1-2):121-5.
4. Popova L, Kishkilova D, Hadjidekova VB, Hristova RP, Atanasova P, Hadjidekova VV, et al. Micronucleus test in buccal epithelium cells from patients subjected to panoramic radiography. Dentomaxillofac Radiol. 2007;36(3):168-71.
5. Cerqueira EM, Meireles JR, Lopes MA, Junqueira VC, Gomes-Filho IS, Trindade S, et al. Genotoxic effects of X-rays on keratinized mucosa cells during panoramic dental radiography. Dentomaxillofac Radiol. 2008;37(7):398-403.
6. Ribeiro DA, Angelieri F. Cytogenetic biomonitoring of oral mucosa cells from adults exposed to dental X-rays. Radiat Med. 2008;26(6):325-30.
7. Ribeiro DA, de Oliveira G, de Castro G, Angelieri F. Cytogenetic biomonitoring in patients exposed to dental X-rays: comparison between adults and children. Dentomaxillofac Radiol. 2008;37(7):404-7.
8. Angelieri F, de Cassia Goncalves Moleirinho T, Carlin V, Oshima CT, Ribeiro DA. Biomonitoring of oral epithelial cells in smokers and non-smokers submitted to panoramic X-ray: comparison between buccal mucosa and lateral border of the tongue. Clin Oral Investig. 2010;14(6):669-74.

9. Angelieri F, Carlin V, Saez DM, Pozzi R, Ribeiro DA. Mutagenicity and cytotoxicity assessment in patients undergoing orthodontic radiographs. Dentomaxillofac Radiol. 2010;39(7):437-40.
10. El-Ashiry EA, Abo-Hager EA, Gawish AS. Genotoxic effects of dental panoramic radiograph in children. J Clin Pediatr Dent. 2010;35(1):69-74.
11. Gajski G, Milkovic D, Ranogajec-Komor M, Miljanic S, Garaj-Vrhovac V. Application of dosimetry systems and cytogenetic status of the child population exposed to diagnostic X-rays by use of the cytokinesis-block micronucleus cytome assay. J Appl Toxicol. 2011;31(7):608-17.
12. Ribeiro DA, Sannomiya EK, Pozzi R, Miranda SR, Angelieri F. Cellular death but not genetic damage in oral mucosa cells after exposure to digital lateral radiography. Clin Oral Investig. 2011;15(3):357-60.
13. Lorenzoni DC, Cuzzuol Fracalossi AC, Carlin V, Araki Ribeiro D, Sant' Anna EF. Cytogenetic biomonitoring in children submitting to a complete set of radiographs for orthodontic planning. Angle Orthod. 2012;82(4):585-90.
14. Sheikh S, Pallagatti S, Grewal H, Kalucha A, Kaur H. Genotoxicity of digital panoramic radiography on oral epithelial tissues. Quintessence Int. 2012;43(8):719-25.
15. Thomas P, Ramani P, Premkumar P, Natesan A, Sherlin HJ, Chandrasekar T. Micronuclei and other nuclear anomalies in buccal mucosa following exposure to X-ray radiation. Anal Quant Cytol Histol. 2012;34(3):161-9.
16. Waingade M, Medikeri RS. Analysis of micronuclei in buccal epithelial cells in patients subjected to panoramic radiography. Indian J Dent Res. 2012;23(5):574-8.
17. Arora P, Devi P, Wazir SS. Evaluation of genotoxicity in patients subjected to panoramic radiography by micronucleus assay on epithelial cells of the oral mucosa. J Dent (Tehran). 2014;11(1):47-55.
18. Agarwal P, Vinuth DP, Haranal S, Thippanna CK, Naresh N, Moger G. Genotoxic and cytotoxic effects of X-ray on buccal epithelial cells following panoramic radiography: A pediatric study. J Cytol. 2015;32(2):102-6.
19. Preethi N, Chikkanarasaiah N, Bethur SS. Genotoxic effects of X-rays in buccal mucosal cells in children subjected to dental radiographs. BDJ Open. 2016;2:16001.
20. Li G, Yang P, Hao S, Hu W, Liang C, Zou BS, et al. Buccal mucosa cell damage in individuals following dental X-ray examinations. Sci Rep. 2018;8(1):2509.
21. Milkovic D, Garaj-Vrhovac V, Ranogajec-Komor M, Miljanic S, Gajski G, Knezevic Z, et al. Primary DNA damage assessed with the comet assay and comparison to the absorbed dose of diagnostic X-rays in children. Int J Toxicol. 2009;28(5):405-16.
22. Yanuaryska RD. Comet Assay Assessment of DNA Damage in Buccal Mucosa Cells Exposed to X-Rays via Panoramic Radiography. J Dent Indones. 2018;25(1):53-7.
23. Yoon AJ, Shen J, Wu HC, Angelopoulos C, Singer SR, Chen R, et al. Expression of activated checkpoint kinase 2 and histone 2AX in exfoliative oral cells after exposure to ionizing radiation. Radiat Res. 2009;171(6):771-5.
24. Schwab SA, Brand M, Schlude IK, Wuest W, Meier-Meitinger M, Distel L, et al. X-ray induced formation of gamma-H2AX foci after full-field digital mammography and digital breast-tomosynthesis. PLoS One. 2013;8(7):e70660.

Appendix 3: Overview of the biological effects detected in patients following cone beam computed tomography

Assay	Gender	Age (years)	Dose	Time of sampling	Tissue examined	Tissue used	Biological effects	References
Micronucleus (MN) assay	9 females 10 males	26.8 ± 5.0	Not mentioned	Before and 10 days after cone beam computed tomography	Oral cavity	Exfoliated oral mucosa cells	No induction of MN, but induction cytotoxicity (pyknosis, karyolysis, karyorrhexis)	Carlin *et al.* (2010)[1]
	10 girls 14 boys	11 ± 1.2	Range: 287 µSv - 304 µSv					Lorenzoni *et al.* (2013)[2]
	39 females 7 males	23 - 42	Range: 448.15 - 730.79 mGy·cm^2					Yang *et al.* (2017)[3]
	17 females 12 males	45.8 ± 12.5	Not mentioned				Significant induction of MN, and cytotoxicity (pyknosis, karyolysis, karyorrhexis)	Da Fonte *et al.* (2018)[4]
	70 females 28 males	23.63 ± 6.64	Range: 0.18 mGy – 3.54 mGy				Significant induction of MN, and cytotoxicity (pyknosis, karyolysis, karyorrhexis) above 1 mGy. Below 1 mGy, only significant induction of karyorrhexis.	Li *et al.* (2018)[5]

1. Carlin V, Artioli AJ, Matsumoto MA, Filho HN, Borgo E, Oshima CT, et al. Biomonitoring of DNA damage and cytotoxicity in individuals exposed to cone beam computed tomography. Dentomaxillofac Radiol. 2010;39(5):295-9.
2. Lorenzoni DC, Fracalossi AC, Carlin V, Ribeiro DA, Sant'anna EF. Mutagenicity and cytotoxicity in patients submitted to ionizing radiation. Angle Orthod. 2013;83(1):104-9.
3. Yang P, Hao S, Gong X, Li G. Cytogenetic biomonitoring in individuals exposed to cone beam CT: comparison among exfoliated buccal mucosa cells, cells of tongue and epithelial gingival cells. Dentomaxillofac Radiol. 2017;46(5):20160413.
4. da Fonte JBM, de Andrade TM, Albuquerque RLC, de Melo MDB, Takeshita WM. Evidence of genotoxicity and cytotoxicity of X-rays in the oral mucosa epithelium of adults subjected to cone beam CT. Dentomaxillofac Rad. 2018;47(2).
5. Li G, Yang P, Hao S, Hu W, Liang C, Zou BS, et al. Buccal mucosa cell damage in individuals following dental X-ray examinations. Sci Rep. 2018;8(1):2509.

Curriculum Vitae

Personal information

Surname:	Belmans
First name:	Niels
Address:	Putstraat 1 0102, 2470 Retie, Belgium
Mobile phone:	+32 472 71 81 04
Email:	niels.belmans@gmail.com
Date of birth:	April 19th, 1992
Place of birth:	2400 Mol, Belgium
Nationality:	Belgian
Civil class:	Unmarried

Education

2015 – Present **PhD student, Biomedical Sciences**
University of Hasselt, Morphology Group, Biomedical Research Institute, Hasselt, Belgium;
Belgian Nuclear Research Centre (SCK•CEN), Mol, Belgium
Director: Prof. Ivo Lambrichts (UHasselt)
Co-director: Prof. Stéphane Lucas (UNamur) & Dr. Marjan Moreels (SCK•CEN)
Thesis title: Biological effects of ionizing radiation in medical imaging: a prospective study in children and adults following cone-beam computed tomography

2013 – 2015 **Master in Biomedical Sciences** (Great distinction)
University of Antwerp, Department of Biomedical Sciences, Antwerp, Belgium
Major: Clinical Scientific Research
Minor: Entrepreneurship and research
Thesis director: Prof. Sylvia Dewilde
Thesis title: Endothelial cell response after exposure to low dose X-ray radiation
Laboratory Animal course: **FELASA C** obtained

2010 – 2013 **Bachelor in Biomedical Sciences** (Great distinction)
University of Antwerp, Department of Biomedical Sciences, Antwerp, Belgium
Thesis director: Prof. Xaveer Van Ostade
Thesis title: Molecular mechanisms for Withaferine A.

2004 – 2010 **Latin-Sciences**
Rozenberg, S.O., Mol, Belgium

Travel grants and Awards

2018 **Research Award (oral presentation)**
Awarded at the European Congress of Dentomaxillofacial Radiology held in Luzern, Switzerland.

2017 **ERRS Young Investigator Award**
Travel support to attend the ERRS Annual Meeting in Essen, Germany.

2017 **EU CONCERT Travel Grant**
Grant to attend the 4th International Symposium on the System of Radiological Protection of ICRP and for the 2nd European Radiation Protection Research Week of the European Research Platforms in Paris, France.

Professional memberships

2018 – Present Netherlands Society for Radiobiology (NVRB)
2018 European Academy for Dentomaxillofacial Radiology (EADMFR)
2016 – Present European Radiation Research Society (ERRS)
2015 – Present Belgian Society for the Advancement in Cytometry (BSAC)

Courses attended

2018 **Grow yourself leadership course** – UHasselt, Belgium
2018 **FLAMES: GDPR** – UHasselt, Belgium
2017 **Career management in academia** – UHasselt, Belgium
2017 **Good clinical practices course** – UHasselt, Belgium
2017 **Good laboratory practices course** – UHasselt, Belgium
2017 **Basic biosafety training** – UHasselt, Belgium
2016 **FLAMES: Tools for time series** – KU Leuven, Belgium
2016 **Effective image editing** – UHasselt, Belgium
2016 **Effective graphical displays** – UHasselt, Belgium
2016 **PhD management: Successfully applying project & time management principles** – UHasselt, Belgium
2016 **Self-, peer-, and co-assessment course** – UHasselt, Belgium
2015 **Good Scientific Conduct course** – UHasselt, Belgium
2015 **Scientific Writing and Speaking** – SCK•CEN, Belgium
2015 **Upgrade your written English** – SCK•CEN, Belgium
2015 **FLAMES: Significance, p-values and t-tests** – UGhent, Belgium
2015 **Basic training in Radiation Protection** – SCK•CEN, Belgium

Supervision of students

10/2016 – 06/2017	**Liese Gilles (MSc)**, Biomedical Sciences, UHasselt, Hasselt, Belgium
09/2017 – 01/2018	**Kristof Smeets (BSc)**,Biotechnology, PXL, Hasselt, Belgium
02/2018 – 06/2018:	**Jonas Welkenhuysen (BSc)**, Biotechnology, PXL, Hasselt, Belgium
02/2019 – 06/2019:	**Jasper Gielen (BSc)**, Biotechnology, PXL, Hasselt, Belgium

List of publications

Publications in peer-reviewed journals

Published

1 Baselet B, **Belmans N**, Coninx E, Lowe D, Janssen A, Michaux A, Tabury K, Raj K, Quintens R, Benotmane MA, Baatout S, Sonveaux P and Aerts A (2017) Functional Gene Analysis Reveals Cell Cycle Changes and Inflammation in Endothelial Cells Irradiated with a Single X-ray Dose. Front. Pharmacol. 8:213. doi: 10.3389/fphar.2017.00213

2 Virag P, Hedesiu M, Soritau O, Perde-Schrepler M, Brie I, Pall E, Fischer-Fodor E, Bogdan L, Lucaciu O, **Belmans N**, Moreels M, Salmon B, Jacobs R Low-dose radiations derived from cone beam computed tomography induce transient DNA and inflammatory alterations in stem cells from deciduous teeth. DMFR (2018) 47. doi: 10.1259/dmfr.20170462

3 Oenning AC, Pauwels R, Stratis A, De Faria Vasconcelos K, Tijskens E, De Grauwe A, Jacobs R, Salmon B, Chaussain C, Bosmans H, Bogaerts R, Politis C, Nicolielo L, Zhang G, Vranckx M, Ockerman A, Baatout S, **Belmans N**, Moreels M, Hedesiu M, Virag P, Baciut M, Marcu M, Almasan O, Roman R, Barbur I, Dinu C, Rotaru H, Hurubeanu L, Istouan V, Lucaciu O, Leucuta D, Crisan B, Bogdan L, Candea C, Bran S, Baciut G; Halve the dose while maintaining image quality in paediatric cone beam CT – Sci Rep (2019) 9:5521 doi: 10.1038/s41598-019-41949-w

4 **Belmans N**, Gilles L, Virag P, Hedesiu M, Salmon B, Baatout S, Lucas S, Jacobs R, Lambrichts I, Moreels M; Method validation to assess in vivo cellular and subcellular changes in buccal mucosa cells and saliva following CBCT examinations – DMFR (2019) 48. doi: 10.1259/dmfr.20180428

5 Konings K, Vandevoorde C, **Belmans N**, Vermeesen R, Baselet B, Van Walleghem M, Janssen A, Isebaert S, Baatout S, Haustermans K, Moreels M; The combination of particle irradiation with the Hedgehog inhibitor GANT61 differently modulates migration of cancer cells compared to X-ray irradiation. Front. Oncol. (2019) 9:391 doi: 10.3389/fonc.2019.00391

Submitted

Belmans N, Gilles L, Vermeesen R, Virag P, Hedesiu M, Salmon B, Baatout S, Lucas S, Lambrichts I, Jacobs R, Moreels M; Dental cone-beam CT examination induces oxidative damage and antioxidant response in children's saliva – Nature Scientific Reports – *In review*

In preparation

1. **Belmans N**, Gilles L, Vermeesen R, Virag P, Hedesiu M, Salmon B, Baatout S, Lucas S, Lambrichts I, Jacobs R, Moreels M – Increased oxidative damage and antioxidant response in saliva samples from children following cone beam computed tomography examination - *in vivo* results paper
2. **Belmans N**, Gilles L, Salmon B, Baatout S, Lucas S, Lambrichts I, Moreels M – *In vitro* assessment of the DNA damage response in dental stem cells following low dose X-ray exposure – *in vitro* results paper
3. **Belmans N**, Baatout S, Moreels M – Health risks following medical X-ray diagnostics: Should we be concerned? – Literature review

Oral presentations

1. **Belmans N**, Baatout S, Moreels M; Tandheelkundige röntgenfoto's bij kinderen: Moeten we ons zorgen maken?; EHS Instituutsvergadering, February 19th, 2019, Mol, Belgium
2. **Belmans N**, Moreels M, Baatout S.; Biological effects of ionizing radiation in medical imaging: A prospective study in children and adults following dental cone-beam CT; Dutch Society for Radiobiology (NVRB), November 16th, 2018, Utrecht, The Netherlands
3. **Belmans N,** Moreels M, Baatout S, Lambrichts I; Increased oxidative stress and an adaptive antioxidant response in saliva after dental CBCT exposure in children; 44th European Radiation Research Congress, August 24th, 2018, Pecs, Hungary
4. **Belmans N.**, Baatout S., Moreels M.; Dental CBCT exposure in children: can we detect biological changes in saliva samples?; European Congress of Dentomaxillofacial Radiology, June 14th, 2018, Luzern, Switzerland
5. **Belmans N**; Dental CBCT exposure in children: can we detect biological changes in saliva samples?; Day of the PhDs, April 24th, 2018, Mol, Belgium
6. **Belmans N**, Gilles L, Vranckx M, Baatout S, Jacobs R, Lucas S, Lambrichts I, Moreels M; Age-related biological effects of dental cone-beam CT exposure; 2nd European Radiation Protection Research Week of the European Research Platforms, October 11th, 2017, Paris, France
7. **Belmans N**, Gilles L, Lucas S, Lambrichts I, Moreels M; Age-related biological effects of dental cone-beam CT exposure; 43rd European Radiation Research Congress, September 18th, 2017, Essen, Germany
8. **Belmans N**; DIMITRA Subtask 1: Characterizing the potential risks through radiation biology; Final OPERRA Meeting, May 24th, 2017, Budapest, Hungary
9. **Belmans N**; DIMITRA Task 1: *In vitro* DNA damage response and *ex vivo* DNA damage and oxidative stress analysis after dental CBCT examination

in children and adults; DIMITRA Team Meeting, January 13th, 2017, Cluj-Napoca, Romania

10. **Belmans N**; Dental pediatric imaging: an investigation towards low dose radiation induced risks; Day of the PhDs, October 27th, 2016, Mol, Belgium
11. **Belmans N**; Dental CBCT in children: *In vitro* and *ex vivo* DNA damage and oxidative stress analysis; Belgian Society for the Advancement of Cytometry Annual Meeting, October 21st, 2016, Brussels, Belgium
12. **Belmans N**, Moreels M, Baatout S; Impact of dental cone-beam CT in children: Low dose radiation effects on dental stem cells, buccal cells and saliva; OPERRA 2nd Periodic Meeting, June 9th, 2016, Kuopio, Finland
13. **Belmans N,** Baatout S, Lambrichts I, Moreels M; Dental pediatric imaging: an investigation into low dose radiation-induced risks, Seminar at BIOMED, February 29th, 2016, Hasselt, Belgium
14. **Belmans N,** Baatout S, Lambrichts I, Moreels M; Dental pediatric imaging: an investigation into low dose radiation-induced risks, EHS Meet & Greet, January 18th, 2016, Mol, Belgium
15. **Belmans N,** Baatout S, Lambrichts I, Moreels M; Dental pediatric imaging: an investigation into low dose radiation-induced risks – Protocols and necessities, DIMITRA Team Meeting, December 10th, 2015, Leuven, Belgium

Poster presentations

1. **Belmans N**, Vermeesen R, Baselet B, Moreels M; Saliva: Potential use as a health marker on Earth and in Space?; 25 years of Belgians in Space Event, October 6th, 2017, Mol, Belgium
2. **Belmans N**, Gilles L, Lambrichts I, Moreels M; Age-related biological effects of dental cone-beam CT exposure; Knowledge for Growth, May 18th, 2017, Ghent, Belgium
3. **Belmans N**; Dental CBCT in children: *In vitro* and *ex vivo* DNA damage and oxidative stress analysis; WAC Audit, October 26th, 2016, Mol, Belgium
4. **Belmans N**, Moreels M, Baatout S, Stratis A, Tijskens E, Bosmans H, Bogaerts R, Lambrichts I, Salmon B, Baciut M, Hedesiu M, Virag P, Jacobs R; DIMITRA Task 1: Assessing biological risks: Optimization of buccal swab and saliva collection protocols for pilot study in children; OPERRA 2nd Annual Meeting, June 7th-9th, 2016, Kuopio, Finland
5. Piroska Virag, Mihaela Hedesiu, Salmon Benjamin, **Niels Belmans**, Lucaciu Ondine, Mihaela Baciut, Reinhilde Jacobs. - Low dose radiation induced effects in dental pulp stem cells; OPERRA 2nd periodic meeting, June 7th-9th 2016, Kuopio, Finland
6. R. Jacobs, M. Hedesiu, M.Baciut, B. Salmon, A. Stratis, H. Bosmans, R. Bogaerts, C. Chaussain, S. Baatout, H. Derradji, **N. Belmans**, M. Moreels, A. Michaux, J. Buset, R Roman, M Marcu, V. Piroska, I. Barbur, H.Rotaru, C.Dinu, O.Almasan, D.Leucuta, B. Crisan, L. Bogdan, A. Coman, Gr. Baciut. - DIMITRA project Task 3: Epidemiology: cumulative radiation exposure and risk from dento-maxillofacial radiology during childhood.; OPERRA 2nd periodic meeting, June 7th-9th, 2016, Kuopio, Finland
7. R. Jacobs, H. Bosmans, R. Bogaerts, A. Stratis, C. Chaussain, B. Salmon, A. Oenning, M. Cohen, S. Baatout, H. Derradji, **N. Belmans**, M. Moreels, A. Michaux, J. Buset, M. Baciut, M. Hedesiu, V. Piroska. - DIMITRA Task 4 - Reducing risks through image quality optimization; OPERRA 2nd periodic meeting, June 7th-9th, 2016, Kuopio, Finland
8. R. Jacobs, H. Bosmans, R. Bogaerts, E. Van de Casteele, A. Stratis, C. Chaussain, B. Salmon, D. Le Denmat, S. Baatout, H. Derradji, **N. Belmans**, M. Moreels, A. Michaux, J. Buset, M. Baciut, M. Hedesiu, V. Piroska. - DIMITRA: Dentomaxillofacial paediatric imaging: an investigation towards low dose radiation induced risks. – MELODI 7th workshop; November 9th-11th, 2015, Munich, Germany

Acknowledgements

Equipped with his five senses, man explores the universe around him and calls the adventure 'science'.

Edwin Powell Hubble

My personal adventure started almost four years ago. And as with all adventures, a PhD project comes with ups and (unfortunately) downs. Luckily, I have met a lot of wonderful people along the way that helped me achieve the highs, but also (and maybe more importantly) guided me through the lows. In the end, all of them helped me to evolve as a human being and scientist. Since this PhD thesis would not have been possible without these individuals, I would like to devote this section to all who have contributed to my four-year-long adventure.

First of all, I would like to thank **Prof. Dr. Ivo Lambrichts**, my promotor. Thank you for accepting me as a PhD student. I really appreciate your critical and valuable comments and feedback on my work throughout the PhD project. I could not thank you enough for sharing your knowledge and expertise. **Prof. Dr. Stéphane Lucas**, my co-promotor, I would also like to express my gratitude for your support and feedback on my work. **Prof. Dr. Sarah Baatout**, thank you for welcoming me into the Radiobiology Unit at SCK•CEN. Your continuous support and passion for science, and radiobiology in particular, are inspiring. **Dr. Marjan Moreels**, my SCK•CEN mentor and co-promotor, I thank you for your amazing support and guidance over the last four years. Thank you for our nice discussions, your (many) critical revisions of my work, and helping me out whenever I had questions or doubts. You were always there when I needed advice or just a friendly chat. Thank you!

I also like to thank **Prof. Dr. Annelies Bronckaers** for being part of my internal doctoral committee. Thank you for the time you took for reviewing my work and for your valuable and thorough evaluation of my work. Furthermore, I would like to thank **Prof. Dr. Reinhilde Jacobs** and **Prof. Dr. Benjamin Salmon** for their willingness to be my external jury members, for reviewing my PhD thesis and for their constructive feedback. For chairing my doctoral jury, I would like to thank **Prof. Dr. Marcel Ameloot**.

I am also indebted to the members of **DIMITRA**. Once again my thanks goes out to **Prof. Dr. Reinhilde Jacobs**, fearless leader of the DIMITRA team. Your drive and enthusiasm are unmatched (of this I am sure!). Furthermore, I owe thanks to **Prof. Dr Benjamin Salmon** for helping (and providing me) with the dental

stem cells that were a crucial part of this project. Your advice and guidance concerning the cell cultures and data analyses are much appreciated. Next I would like to thank **dr. Piroska Virag** and **dr. Mihaela Hedesiu**. Thank you for reviewing my papers, but also for the nice team meetings and the unsurpassed hospitality you showed us when we visited Cluj-Napoca! For help with patient dosimetry, thanks is due to **dr. Andreas Stratis** and **dr. Ruben Pauwels**. Thanks to your Monte Carlo simulations we obtained valuable data for our analyses. Thank you **dr. Anne Carolina Costa Oenning**, **dr. Karla de Faria Vasconcelos**, **dr. Jeroen van Dessel**, **dr. Raluca Roman**, **Myrthel Vranckx**, **Anna Ockerman** and **Bennaree Awarun** for your support and friendship, and the wonderful time at ECDMFR2018!
Of course **Myrthel Vranckx** and **Anna Ockerman**, along with **Gabriela Casteels, Jeroen Martens** and **Birgit Coucke**, deserve additional thanks for helping me with collecting patient samples (kudos to all St.-Raphael staff that also contributed!), keeping patient records and navigating the biobank legislation. This thesis could not be completed without your help and support!

I would like to thank EHS scientists **dr. Pieter Monsieurs, dr. Mohamed Mysara** and **dr. Jürgen Claesen** for their help and support with my questions regarding statistics and experimental set-ups.

From the Laboratory for Nuclear Calibrations of SCK•CEN, I would like to thank **Bart Marlein**, **Raf Aarts**, and **dr. Cristian Mihailescu** for their help with setting up and performing the *in vitro* irradiations. Thank you Bart and Raf for the nice chats during the long waiting periods during the many irradiations.

Special thanks to **Betty Vandingelen** and **Veronique Pousset**, secretaries at SCK•CEN and UHasselt, respectively. Thank you for all your help with all the paper work and for all the nice chats.

I owe thanks to **Ann Janssen**, **Amelie Coolkens**, **Kevin Tabury**, and (most importantly, since he is probably the best lab technician EVER ☺) **Randy Vermeesen** for their help with cell cultures, microscopy, flow cytometry and protein assays. Especially **Kevin Tabury**, who taught me most of what he knows about microscopy at the beginning of my PhD, and **Randy Vermeesen**, who helped me with pretty much everything I asked him in the last part of my PhD, deserve my gratitude. Thank you **Randy** for being a great colleague and friend. It was my pleasure to help you with Luminex experiments in the morning, with freeze drying, …

I could not have coped without my office buddies. Thank you **Anu Yadav**, **Gleb Goussarov**, and especially **dr. Bo Byloos**. Anu we started our PhD together and shared all the hard times and struggles that come with doing a PhD. Gleb, you

started your PhD adventure two years ago and you still have a long road ahead, but you'll undoubtedly make it! And Bo, like you said before *'we hemme da toch mer wee schoun gedon!'*. I will always remember our (weird) talks and discussions (does *'slechte vlesekes'* ring a bell?), our mutual love for *cinema*, and of course, our 2016 road trip a.k.a. 'The Pimped Out Adventures of Bno and Neil', which was AMAZING! To me, as an office buddy you will always be second to none!

Dr Marlies Gijs, **dr. Annelies Suetens**, **dr. Tine Verreet**, **dr. Ellina Macaeva**, **dr. Kai Craenen**, and **dr. Katrien Konings**, the PhDs that came before, thank you for showing me that it can be done and for all the advice and fun moments in the lab. Special thanks to Katrien, who gave me the opportunity to participate in irradiation campaigns at GANIL. Thank you for the nice experience, fun and stress in the lab, but most importantly, thank you for showing me the importance of accurately planning experiments ahead of time ☺.

Dr. Bjorn Baselet, you deserve your own paragraph. You were an amazing mentor during my master thesis. You taught me much (if not all) of what I knew about lab work at that time. You are also responsible for the fact I had to write this beast. Your enthusiasm and confidence in my abilities convinced me to apply for a PhD position way back in 2014. And look where we are now! Through the years you have become a great friend, and I will cherish all the fun moments we have had in the lab and during PhD dinners, movie nights, after-work events, …

Monsieur (!) Claude Mfossa, **Raghda Ramadan**, **Ali Muntasir**, **Valérie Van Eesbeeck**, **Emma Coninx**, **Noami Daems**, **Auchi Inalegwu**, **Eline Radstake**, **Magy Sallam**, **Charlotte Segers**, **Shari Wouters**, **Laurens Maertens**, **Tom Rogiers**, and **Merel Van Walleghem**, the other PhD students at SCK•CEN, I thank you for the wonderful times both in and outside the lab. I wish you all the best for what is to come.

I would also like to thank **Liese Gilles**, **Kristof Smeets**, and **Jonas Welkenhuysen**. Your contributions can be found all throughout this thesis. Without your help, I could not have accomplished the massive feat that is/was this PhD project. Furthermore, it was my great pleasure to guide you in your MSc/BSc theses. Special thanks is due to **Natalie Alderson** and **Isatou Sheriff**, who voluntarily (!) helped me out during the summer holidays. Thank you all for your assistance and all the fun we had in the lab. Kudos to all other students that were also responsible for the fun and great atmosphere in the lab (you know who you are ☺).

Ik wil uiteraard ook mijn vrienden en vriendinnen bedanken voor hun steun en de nodige afleidingen in de afgelopen vier jaar. Door jullie kon ik de nodige stoom aflaten en op tijd en stond mijn zinnen verzetten.

Daarnaast wil ik ook mijn **familie** bedanken. Eerst en vooral mijn **ouders**. Ik wil jullie bedanken voor jullie onvoorwaardelijke steun tijdens dit doctoraat en ook voor alles daarbuiten. Ik kan niet beschrijven hoeveel jullie hulp en steun voor mij betekenen. Ook **Jolien**, mijn jongere zusje, wil ik bedanken. Hoewel we soms bekvechten en nu al een tijdje niet meer in het ouderlijk huis wonen, weet ik dat ik altijd op jou kan rekenen als ik hulp nodig heb. Mijn **grootouders** wil ik ook bedanken voor hun onvoorwaardelijke steun. Va en moemoe, waar jullie ondertussen ook zijn, ik heb jullie steun op elk moment gevoeld.

Als laatste wil ik **Liese** bedanken. Woorden schieten te kort om te beschrijven hoeveel ik aan jou te danken heb. Jij kwam (terug?) in mijn leven halverwege mijn doctoraat. Sindsdien heb je mijn leven op ontelbare manieren positief beïnvloedt. Jouw liefde en steun gaven me de nodige energie om dit doctoraat succesvol af te ronden. Weet dat ik dit zonder jou niet had gekund!

P.S. For those who requested a copy of my thesis solely to check if they are mentioned in the 'Acknowledgements' section (I'm looking at you Randy), I strongly suggest you take some time to read the rest. There is some pretty interesting stuff in there ☺